Examining the biological consequences of DNA damage caused by irradiated J2-3T3 fibroblast feeder cells and HPV16

Characterisation of the biological functions of *Mll*

Yeong-Lih Hiew (Samantha)

Division of Virology

National Institute for Medical Research

Mill Hill

London

This thesis is submitted for the degree of Doctor of Philosophy (PhD)
at University College London 2011

This PhD thesis consists of two research projects that can be connected to form one title:

Examining the biological consequences of DNA damage caused by irradiated J2-3T3 fibroblast feeder cells, HPV16 and *Mll* proto-oncogene.

Acknowledgements

"*You will find as you look back upon your life that the moments when you truly live, are the moments when you have done things in the spirit of love.*"
Henry Drummond

This thesis is produced as a finale to two parts of work, in which I have carried out in the National Institute of Medical Research (2008-2010) and Institute of Child Health (2005-2008). Merging two lines of research in this thesis has proven to be challenging and thus, it is befitting for me to mention how grateful I am to some of the most wonderful people I am lucky to have met, who showed me important virtues in this journey.

I would like to thank Ken, who in many ways, have not only mentored me in life and science, but also to reinstall my spark for science. I owe it to him for his constructive criticisms, scientific advice, and honesty. I am deeply grateful to Joanna and Lietta, my conquest partners through thick and thin, for their friendship, encouragement, and lively conversations. Special thanks to two of my most devoted friends, Katya and Poh Choo, for providing a comforting shelter from the hardships I have encountered at the race to the light at the end of the tunnel.

I would like to reserve my most heartfelt gratitude to Jake, who has never failed to be there for me throughout the entire process. His profound love and support is irreplaceable – for it has shown me the boundless patience that I have never seen anyone have, for someone who is accompanying a PhD student in their writing up stages.

In quintessence, I would like to thank my family – Daddy, Mommy, Jarod, Hanny, Brenny, and Nicolai, who from thousands of miles away, have assured me of their unconditional love. I would like to dedicate this thesis to anyone who has carried on against all odds in order to do the things that they love.

Examining the biological consequences of DNA damage caused by irradiated J2-3T3 fibroblast feeder cells and HPV16

Division of Virology

National Institute for Medical Research

The Ridgeway

Mill Hill

London UK

Abstract

The study of human papillomavirus (HPV) utilises human keratinocytes as host cells that are co-cultured with lethally irradiated mouse fibroblasts. Although this co-culture system has been effective in recapitulating HPV's life cycle, it resembles studies whereby radiation-induced bystander effect (RIBE) has been identified. We considered the possibility that Normal Immortalised Keratinocytes (NIKs) that we used as host cell for HPV16 may be in receipt of DNA damaging agents from heavily irradiated J2-3T3 fibroblasts. We report that NIKs (+/ - HPV16) cells respond to the presence of feeders by increasing DNA damage response leading to H2AX phosphorylation. NIKs receive DNA damaging agents from irradiated feeder cells primarily through direct cell-to-cell contact and secondarily through the culture media. Although ATM, ATR, and DNA-PK were activated by RIBE in NIKs, we found that feeders inhibited ATM activation in NIKs (+HPV16). Moreover, we found that expression of HPV16 E6 and E7 oncoproteins activated ATM, ATR, and DNA-PK. HPV16 also activated H2AX, 53BP1, RPA32, and NBS-1. We considered that both feeder cells and HPV16 could induce DNA damage response in NIKs. This would change the interpretations of HPV16's interactions with host cell's DNA damage surveillance system in NIKs (+ HPV16) cells co-cultured with feeders.

We proceeded to enhance our understanding of how feeder cells and/ or HPV16 changed the way NIKs cells respond to direct DNA damage. We found that NIKs cells (+feeders or +HPV16) respond to direct gamma radiation in a broadly similar way, whereby activation of ATM was inhibited, increase in ATR was extremely small and delayed, while activation of DNA-PK was still generally responsive. We report that presence of HPV16 sensitised NIKs cells to direct gamma radiation and as such, the implications of these observations could be considered for radiotherapy of cancers with HPV. Our initial belief that feeder cells were essential in ensuring stable autonomous replication of HPV16 in NIKs cells was proven otherwise, as NIKs maintained HPV16 DNA episomal copies in the absence of feeders. Contrary to current accepted publication, ATM was found be unnecessary for maintenance of HPV16 DNA episomes and viral genome amplification.

Table of Contents

List of Figures

List of Tables

Abbreviations

^{137}Cs	Cesium-137
ATM	Ataxia telangiectasia mutated
ATR	ATM and Rad3-related
Bp	Base pairs
BSA	Bovine serum albumin
C8:O	N 1,2-dioctanoyl-sn-glycerol
CDK	Cyclin dependent kinase
ct	Cycle threshold
DAPI	4'-6' diamidino-2-phenylindol
DDR	DNA damage response
DH2O	Distilled water
DNA	Deoxyribonucleic acid
DNA-PK	DNA dependent protein kinase
DNA-PKcs	DNA dependent protein kinase catalytic subunit
DSB	Double-strand break
EGF	Epidermal Growth Factor
EdU	5-ethynyl-2'-deoxyuridine
g	Gram
GAPDH	Glyceraldehyde 3-phosphate dehydrogenase
GFP	Green Fluorescent Protein
Gy	Gray unit
HK	Human keratinocyte
HPV	Human Papillomavirus
HR	Homogous recombination
HRP	Horseradish Peroxidase
IR	Ionising radiation
L	Liter

LB	Luria-Bertani
LCR	Long control region
MAdCAM-1	Mucosal addressin cellular adhesion molecule-1
mg	Milligram
mL	Milliliter
mRNA	Messenger ribonucleic acid
NHEJ	Non-homogous end joining
NIKS	Normal Immortalised Human Keratinocytes
ORF	Open reading frame
PBS	Phosphate buffered saline
PCR	Polymerase Chain Reaction
PD	Population doubling
PIKK	Phosphoinositide 3-kinase-related protein kinases
PV	Papillomavirus
Q-PCR	Quantitative Polymerase Chain Reaction
RIBE	Radiation-induced bystander effect
RNA	Ribonucleic acid
ROS	Reactive oxygen species
rpm	Rotations per minute
RT	Real-Time
SCC	Squamous cell carcinoma
SDS	Sodium dodecyl sulfate
SSB	Single-strand break
TAE	Tris-acetate EDTA
TGF	Transforming growth factor
UV	Ultraviolet

Chapter 1: Introduction

1.1 Cervical cancer and Human Papillomavirus (HPV)

Every year, cervical cancer claims the lives of over 200,000 women worldwide, with approximately 80% of these cases occurring in the developing world. Human papillomavirus (HPV) infection is now recognized as the main cause for cervical cancer. More than thirty years ago, researchers started to postulate a possible association between HPV and cervical cancer, through isolation of HPV from genital warts (zur Hausen, 1977). The first cervical cancer-linked HPV types that were isolated from cancer biopsies of the cervix, HPV16 and HPV18, were cloned in 1983 and 1984, respectively (Durst et al., 1983; Boshart et al., 1984). Since then, more than 200 different types of HPVs have been identified and more than 120 putative novel types have been partially characterized (de Villiers, 1994; de Villiers et al., 2004; Bernard et al., 2010).

HPVs can be generally grouped into the cutaneous (those infecting the skin) and the mucosal (those infecting the mucosa) types based on their preferred tissue tropism (Mistry et al., 2008). The mucosal HPV types are known to infect anogenital epithelium and can be divided into two types, the low- and high-risk genotypes. The HPV types 16, 18, 31 and 45 (high risk HPVs) are found in almost 80% of cervical squamous cell carcinoma (SCC), whilst HPV types 6 and 11 (low risk HPVs) cause predominantly benign exophytic genital warts (condylomata acuminata) (Stoler, 2003; zur Hausen, 2009).

1.2 HPV's host cell and life cycle

HPVs are small, double-stranded DNA viruses with specific tropism to the squamous epithelium. Normal squamous epithelial cells grow as stratified epithelium, which consists of multiple layers of cells in various stages of growth and differentiation (Figure 1.1). HPV carries out its infectious cycle in five layers of the epithelium: basal, suprabasal, spinous, granular and cornified layer – all that make up the epidermis. Keratinocytes make up the majority of the cells in the basal epithelium. The basal keratinocytes are separated from fibroblast cells in the dermis by the basement membrane. Keratinocytes undergo differentiation as they move upward from basal to cornified layer in the epidermis.

The basal layer of the squamous epithelium contains basal cells, of which some of these cells are stem cells. Upon division, a stem cell in the basal layer gives rise to one daughter stem cell and another daughter amplifying cell. The latter undergoes several cell divisions, before exiting the basal layer and begins to undergo terminal differentiation. The daughter stem cells remain as the reservoir of the epithelium. On top of the basal layer, the suprabasal layer consists of cells that are non-proliferative and have committed to terminal differentiation. The successive stages of differentiation of the keratinocytes forming the epidermal layers are spinous, granular, and the cornified cells.

The HPV life cycle begins when the virus gains entry to the keratinocytes of the basal epithelium, possibly through site of wounding or lesion. HPV then uses the entire differentiation program of the host keratinocytes to carry out its life cycle. HPV first finds itself in the environment of a proliferating cell, which eventually ceases proliferation, and begins differentiation. This mixture of cell states, in which HPV will have to adapt to distinct host epithelial cell environments, has resulted in different modes of viral DNA replication. The viral lifecycle can be separated into two different stages: the non-productive and productive stages. The non-productive stage occurs in the proliferating basal layer of the epithelium. It is proposed that shortly after infection, the viral DNA copy number is amplified rapidly to approximately 50-400 copies per cell (Chow and Broker, 1994). This is known as the first amplification replication that is rapid and transient. As the cells

continue to proliferate, viral DNAs are maintained as stable episomes at low copy number in the basal cells. The replication of HPV DNA is thought to require an origin of replication and the two virally encoded proteins, HPV E1 and E2. HPV utilizes the host cell's DNA polymerase α, proliferating cell nuclear antigen (PCNA), replication protein A (RPA), and topoisomerase I and II (Topo I and II) to proceed with DNA replication (Chow and Broker, 1994). It is thought that there are at least two possible ways by which maintenance replication of HPV DNA is achieved. The first is an ordered process, where HPV DNA is replicated once-per-S-phase, similar to cellular DNA (Hoffman et al., 2006). The second is a relaxed random-choice viral DNA replication, whereby some DNAs replicate in S phase once, some several times, or not at all (Gilbert and Cohen, 1987; Hoffman et al., 2006). Following viral DNA replication and basal cell division, one of the daughter cells migrates away from the basal layer into the suprabasal layer and begins differentiation. In this differentiating compartment, the virus amplifies its DNA (second amplification replication) to about 1000 copies per cell (Flores and Lambert, 1997). In the very late stage of differentiation where keratinocytes reach the cornified layer, the viral genomes are packaged into capsids and shed from the cell as mature virions. Rarely, the DNA of oncogenic HPVs integrates into the host genome, thereby terminating the life cycle (zur Hausen, 2002).

Although HPV DNA replication is a common feature among all HPV types, a rising complexity of different modes of DNA replication have been proposed for certain HPV types. It has been suggested that the bidirectional theta mode of replication operates for HPV16 and BPV-1 in undifferentiated cells, while the unidirectional rolling circle mode of replication has been suggested for HPV16 in differentiated cells (Gilbert and Cohen, 1987; Flores and Lambert, 1997; Kusumoto-Matsuo et al., 2010). It has also been suggested that low-risk and high-risk HPV types are inherently different in their replication modes (Auborn et al., 1994; Flores and Lambert, 1997). Although there are growing speculations that HPV have different modes of DNA replication, there is little evidence to suggest that this is a constant feature. These results were formed by observations within the limits of experiments in different laboratories and have yet to achieve a consensus with all HPV types.

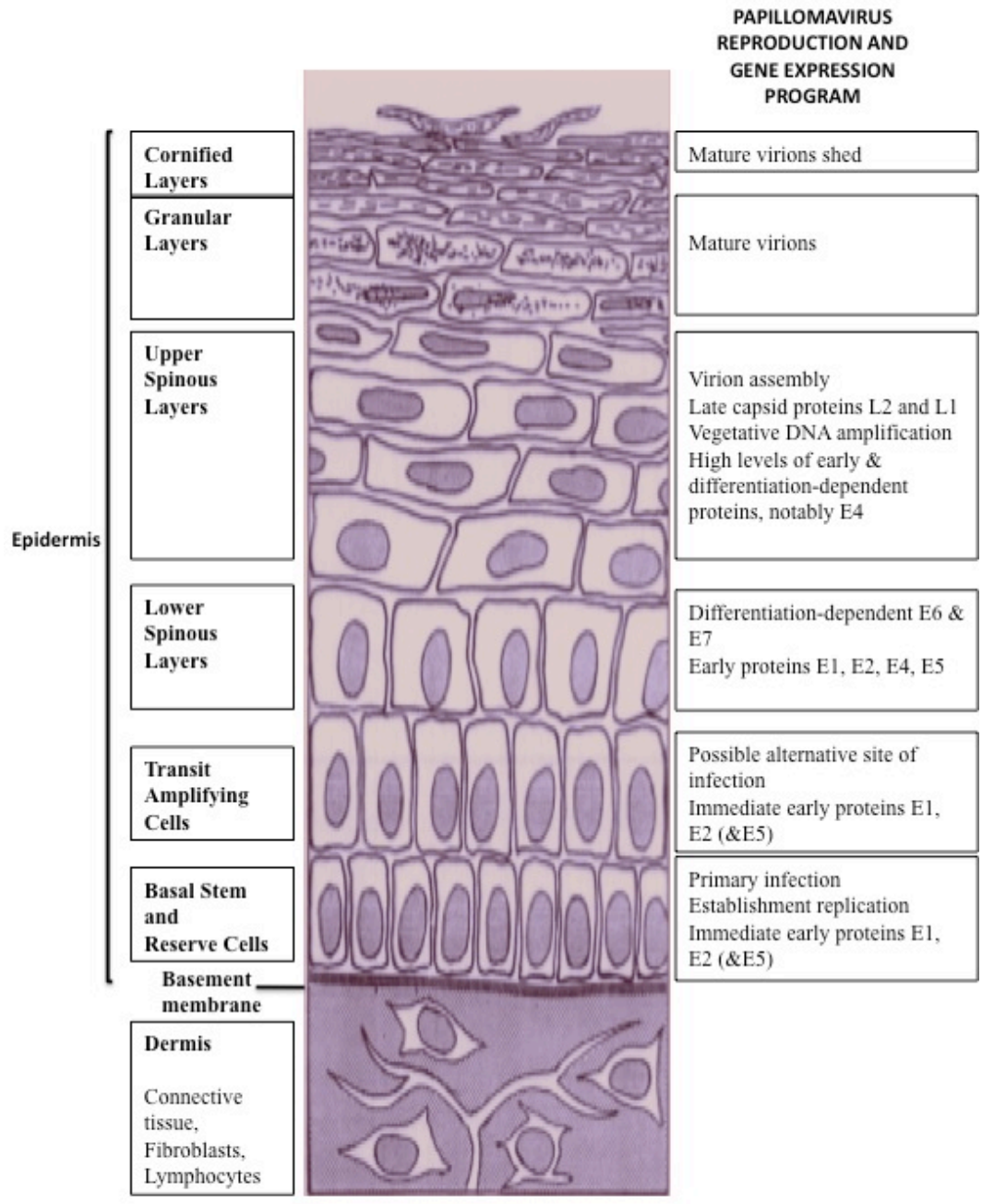

Figure 1.1 (Adapted from Chow and Broker, 1997)

Differentiation of normal cutaneous epithelium and HPV genetic activies in productively infected benign lesions.

The various epithelial strata in the keratinocyte differentiation programme is indicated on the left and center panels. Viral gene expression program in corresponding strata within the epithelium during productive infection are shown on the right. Virus infects keratinocytes in the basal layer of the epithelium but produce viral capsids proteins and viral particles only in terminally differentiated keratinocytes.

1.3 The HPV16 genome and the functions of HPV oncoproteins

HPVs contain covalently closed, circular double-stranded DNA genomes of approximately 8 kb (Seedorf *et al*., 1985) although the precise size of the genomes varies from one type to another. This viral genome encodes six "early" proteins- E1, E2, E4, E5, E6, and E7 and the transcripts encoding viral open reading frames (ORFs) are multi-cistronic (Figure 1.2) (Stanley et al., 2007). The "late" genes, L1 and L2, were expressed in the squamous layer of the epithelium.

The E1 and E2 proteins function as DNA replication factors in HPV. The E1 protein, a helicase, and E2 protein, a transcription factor, have been shown to be important for episomal DNA replication and maintenance (Piirsoo et al., 1996). In cervical cancer, integration of HPV sequences into the host genome is frequently accompanied by disruption of E1 and E2 ORFs (Baker et al., 1987; Kalantari et al., 2001). It has been suggested that repression of E2 protein allows an increase in the expression of viral oncoproteins E6 and E7 (Romanczuk et al., 1990). HPV E6 and E7 oncoproteins can reactivate cellular DNA synthesis in non-cycling cells, inhibit apoptosis and delay the differentiation programme of the infected keratinocyte (Moody and Laimins, 2010). Some of the most well-established functions of E6 and E7 are further discussed in Section 1.12.

The E4 protein is the most abundantly expressed HPV protein and accumulates in differentiating cells of the upper epithelial layers (Doorbar, 2006). It is synthesized from a spliced mRNA, E1^E4, which encodes five amino acids from the E1 ORF spliced to the protein encoded by the E4 ORF. Specific interactions between the HPV16 E1^E4 product and cytokeratins result in the collapse of the epithelial cell intermediate filament network, and thus may facilitate virion release. E4 is also thought to activate the productive phase of the HPV lifecycle (Peh et al., 2004).

The E5, E6 and E7 proteins are known to possess proliferation-stimulating activity (zur Hausen, 2002). Although E6 and E7 are still expressed following viral DNA integration into the host genome, the expression of E5 is abolished by deletion of the E5 coding sequence. However, E5 proteins have been implicated

to have cooperative transforming property with E6 and E7 (reviewed in Moody and Laimins 2010). Although E6 and E7 cannot transform cells, they are contributing factors by inducing additional oncogenic events such as genomic instability (Duensing and Munger, 2004; Moody and Laimins, 2010). The “late” proteins, L1 and L2, are required for the production of major and minor viral capsid proteins, respectively.

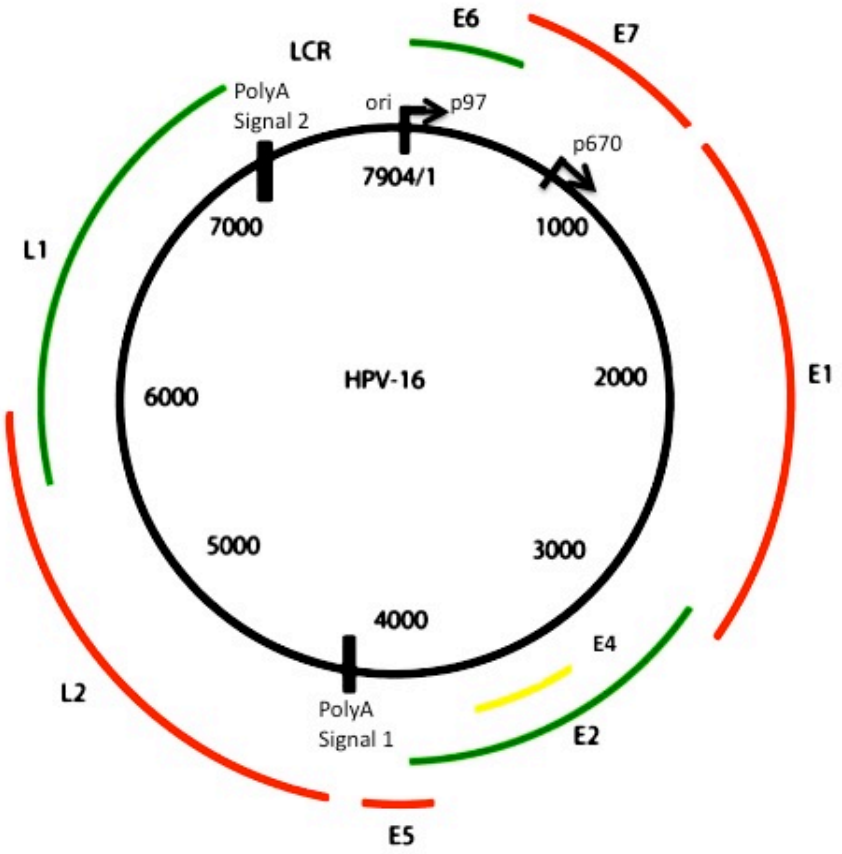

Figure 1.2: The organization of circular HPV16 genome.

The human papillomavirus (HPV) genome contains 8000 base pairs and is divided into eight open reading frames — E6, E7, E1, E2, E4, E5, and L2 and L1 — coding for 'early' (E) or 'late' (L) functions. Early genes are expressed from the early p97 promoter whereas a subset of early as well as the late genes are expressed from the differentiation-dependent late promoter, p670. The long control region (LCR) is situated upstream of the early region and contains cis-acting regulatory regions which are necessary for both viral replication and transcription.

1.4 Keratinocyte culture

The *in vivo* HPV life cycle is intimately linked to the differentiation program of the host keratinocyte. In order to study the biology of HPV and their interaction with host cell, an *in vitro* tissue culture system that can support HPV infectious cycle and reproduce the differentiation program of the keratinocyte is necessary. In 1975, Rheinwald and Green published a study that demonstrated the first successful serial cultivation of human keratinocytes (HKs) derived from the foreskin of an infant. Previously, studies of epidermal cells were carried out on cultures that were initiated by explanted epithelial fragments (Matoltsy, 1960). Although sheets of epithelial cells were obtained, serial cultivation was rarely successful and there was no means of controlling growth of contaminating fibroblast populations from connective tissues (Prose et al., 1967; Stanley, 2002). The technology that enhanced serial cultivation of keratinocytes revolved around the provision of connective tissue factors by an irradiated mouse feeder layer (Rheinwald and Green, 1975; Green et al., 1979). The mouse feeder layer is made up of lethally irradiated 3T3 cells that were able to stimulate keratinocyte growth and increase plating efficiency of these cells (Puck et al., 1956; Green et al., 1979). The irradiated 3T3 layer was also known to inhibit the growth of contaminating fibroblasts. Later, factors that enhanced keratinocyte growth rate and defer differentiation such as epidermal growth factor (EGF) and cholera toxin were also included in the culture medium (reviewed in Tenchini et al., 1992). The addition of hydrocortisone, triiodothyronine and insulin further increase the rate of proliferation. The monolayer culture of keratinocytes often exhibits features of squamous differentiation and full stratification can be created through the use of three-dimensional organotypic raft culture where keratinocytes are grown on top of collagen containing dermal fibroblasts (Fusenig et al., 1978; Fusenig, 1994). The basal cells account for all cell multiplication and the cells that leave the basal layer become terminally differentiated. This keratinocyte culture system formed the basis for the study of human epidermal biology.

The early studies of HPV in culture have been hampered owed to the lack of a cell culture system that is derived from the early stages of HPV infection. The first and most widely used cervical keratinocyte cell line, HeLa, was isolated from the

aggressive glandular cervical cancer of a young woman (Gey et al., 1952; reviewed in Masters, 2002). As HeLa was derived from a rare form of malignant adenocarcinoma and possessed integrated HPV18 genome, the use of this cell line was not suitable for studies of infection and establishment of HPV.

Some more suitable cell lines, W12 and CIN612E, were isolated from squamous intraepithelial lesions (SIL) where the viral DNA exists predominantly in the episomal form (Stanley et al., 1989; Bedell et al., 1991). W12 cells contained 100 copies of HPV16 DNA that could be maintained in episomal form up to 200 population doublings (PDs) (Stanley et al., 1989). Meanwhile, CIN612E contained approximately 50 copies of HPV31 DNA and provided a raft tissue culture system permissive for propagating HPVs (Bedell et al., 1991). These cell lines are excellent resources for studying the full HPV life cycle; examination of the biology of HPV in the early lesions; the factors that influence the progression of these lesions (Meyers et al., 1992; Flores and Lambert, 1997). The growth of these cell lines utilized the method from Rheinwald and Green (1975) that involved co-cultivation with non-proliferating feeder layer. Even though these cell lines (which are derived from cervical lesions with HPV genomes) allow the study of the non-productive and productive stage of HPV infection *in vitro*, they cannot be used to study the consequence of mutations in the viral genome on the HPV life cycle. To achieve this goal, a method using transfected recombinant HPV genomes into normal human foreskin keratinocytes was developed (Fratini et al., 1996; Chow and Broker, 1997; Meyers et al., 1997). The advantage of using this method is that it allows genetic manipulation of the HPV genome to study the biological functions of a particular HPV gene of interest. In addition, these cells were usable in the long term as cells transfected with HPV (e.g., HPV16 and 18) are immortalized through the expression of E6 and E7 oncoproteins (Hawley-Nelson et al., 1989; Kaur and MacDougall, 1989).

The study of HPV in tissue culture was further aided by the introduction of a spontaneously immortalized cell line, NIKs (Normal Immortal Keratinocytes), which arose from human neonatal foreskin keratinocytes (Figure 1.3) (Allen-Hoffmann et al., 2000). NIKs cells are primarily diploid but contain duplication in the long arm of chromosome 8 that can be the primary factor contributing to

spontaneous immortalisation of these cells. For example, spontaneously immortalized keratinocytes (SIK cells) exhibited chromosomal duplications and increased expression of cell cycle proteins, suggesting a possibility that these were important features for immortalisation (Rice et al., 1993). The NIKs cell line is non-tumorigenic, wild type for p53 and pRb, and can produce a complete stratification of squamous epithelium in organotypic culture. The use of this immortalized human foreskin keratinocyte (HFK) line that supports the full life cycle of HPV allowed investigation of wild-type or mutant papillomaviral genomes that do not confer immortalization, i.e., HPVs other than high-risk genotypes (Flores et al., 1999; Lambert et al., 2005). NIKs cells were grown as monolayer and induced to differentiate using organotypic raft culture. NIKs cells were able to maintain HPV16 and HPV31 DNA episomally in the monolayer culture, as observed in the non-productive stage of HPV life cycle. Following organotypic culture, NIKs containing HPV cells were also able to amplify viral DNA in the suprabasal layer and produce virus like particles (VLPs) in cell nuclei in the differentiated layer of the raft (Flores et al., 1999).

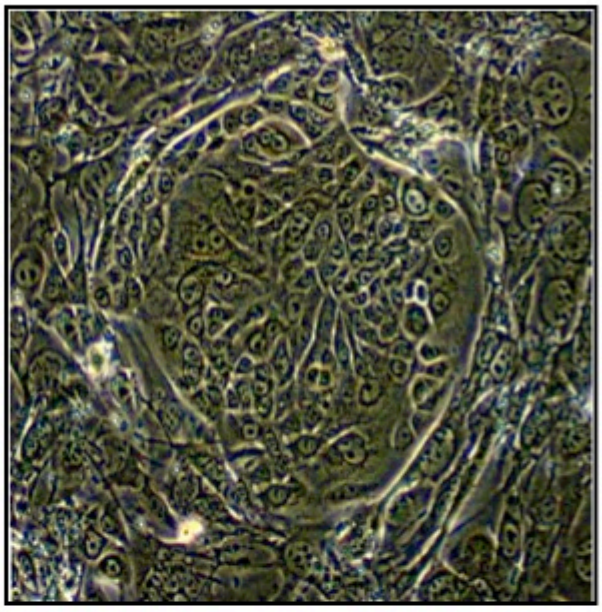

Figure 1.3: Immortalised keratinocyte culture on a fibroblast feeder layer. NIKs keratinocytes were grown and serially subcultured in standard keratinocyte growh media. NIKs cells form a colony on a J2-3T3 mouse fibroblast feeder layer at the periphery.

1.5 Effect of the feeder layer

Many studies on human keratinocytes have utilized lethally irradiated mouse feeder layer to support serial cultivation *in vitro.* Feeder cells are thought to stimulate the growth of primary human keratinocytes (HKs) and for reasons that are still not understood, inhibit the growth of human fibroblasts that are isolated along in the epithelial cell preparation (reviewed in Tenchini et al., 1992). Feeder cells were first used to stimulate the growth of colonies from single HeLa cells (Puck and Marcus, 1995; Puck et al., 1956). Before mouse fibroblasts were introduced as feeder layer (Rheinwald and Green, 1975), many experiments used lethally irradiated feeder layer that was derived from the same genetic background as test cells. Feeder cells are routinely irradiated before co-cultivation to avoid overgrowth of feeders on to test cells. In effect, feeder cells do not divide but remain metabolically active to synthesize proteins and release extracellular materials that are necessary to sustain colony formation (Stoker and Sussman, 1963; Prunieras, 1979). It has been shown that feeders transfer short-lived growth-promoting factors mostly through cell-to-cell contact, though some level of diffusible factors may also be involved (Stoker and Sussman, 1965; Borrelli et al., 1989).

Despite strong evidence that feeders provide growth-promoting effect to human keratinocytes (Rheinwald and Green, 1975), Peehl and Ham (1980) found that human keratinocytes could grow without feeders, by culturing them in medium 199 supplemented with 10 μg/ml hydrocortisone (HC) and 20% (v/v) whole fetal bovine serum (FBS), and 0.15 mg/ml each of two pituitary extracts. This modification involved increasing concentrations of HC, FBS, and pituitary extracts to permit efficient keratinocyte growth and stratification that did not depend on feeder cells (Peehl and Ham, 1980). However, the addition of epidermal growth factor (EGF) did not stimulate human keratinocyte growth, as the mitogenic activity of EGF required feeder cell activity. The absence of feeders negated the effect of EGF on either the clonal growth or cumulative multiplication potential of HK (Peehl and Ham, 1980).

Proper adhesion and growth of human keratinocytes require extracellular matrix proteins such as collagen type IV, laminin, fibronectin, and collagenous polypeptides that are produced by human epidermal keratinocytes themselves (Alitalo et al., 1982). It was thought that feeder cells play a role by synthesizing low amounts of laminin and collagen type IV. Therefore, feeders can be removed after the establishment of substrate-attached keratinocyte islands without any detrimental effects on keratinocyte growth.

Apart from promoting the growth of viable mammalian cells in culture, feeder cells have also been shown to increase clonogenic survival of tumour cells in response to *in vitro* irradiation, heat, or treatment with anti-metabolites (Hill et al., 1979; Weizsaecker and Deen, 1980; Wells et al., 1980; Borelli et al., 1989). The provision of diffusible factors by feeder cells was believed to be one of the contributing factors to increased plating efficiency of cells (Hill et al., 1980; Weizsaecker and Deen, 1980). However, other studies have also indicated that the role of feeder cells extend beyond mere growth-promoting effects; some substances produced by feeder cells could also suppress apoptosis induced in test cells by certain treatments, thereby increasing cell growth (Falk et al., 1993). This hints at a complex mechanism governing the effect of feeder layer on radiation response of target cells. Essentially, the use of a feeder layer alters the response of cells to radiation. In effect, the experimental results obtained using feeder cells may not reflect the intrinsic cellular sensitivity to radiation or chemicals (Deschavanne et al., 1996; Matsumoto et al., 2001). The biological consequences observed in non-irradiated test cells that are cultured with irradiated feeders may reflect the non-targeted effects of radiation (Waldren et al., 2004). In this study, we are interested in some of the phenomena that are associated with radiation exposure such as direct radiation-induced genomic instability and indirect radiation-induced bystander effect (RIBE) as well as adaptive response. To appreciate the effects of indirect radiation, we must first understand the biological effects of direct radiation exposure.

1.6 Biological effects of direct radiation exposure

Ionizing radiation (IR) produces a wide spectrum of DNA lesions including damage to nucleotide bases (base damage), cross-linking, single-, and double-strand breaks (DSBs) (Little, 2003; Lorimore et al., 2003). These DNA lesions induce a variety of processes in exposed cells such as chromatin changes, DNA damage recognition and repair, cell cycle arrest, changes in gene expression, disruption of mitochondrial processes, and apoptosis (reviewed in Suzuki et al., 2003; Szumiel, 2008). If DNA lesions are incorrectly repaired, e.g., misrepaired DSBs, it may cause genetic changes such as mutations at the initial sites of damage and induce chromosomal abnormalities (Little, 2000). This may be subsequently expressed in progenies of irradiated cells.

Eventually, accumulation of DNA damage in conjunction with disrupted cellular regulation processes can lead to carcinogenesis (Little, 2000; Lorimore et al., 2003; Suzuki et al., 2003; Valerie et al., 2007). Apart from intracellular factors that cause genomic instability, extracellular factors as by-products of radiation could also be transferred from irradiated cells to non-irradiated cells (Suzuki et al., 2003).

1.7 Cellular response to DNA damage caused by direct ionizing radiation

The genome of eukaryotic cells is constantly under attack by various exogenous and endogenous factors. From within, the genome is threatened by intrinsic factors such as by-products of oxidative metabolism (such as reactive oxygen species, ROS, i.e., superoxide anions, hydroxyl radicals, and hydrogen peroxide), DNA replication errors, and programmed double strand breaks (e.g., lymphocyte development) (Ito et al., 2007; Houtgraaf et al., 2006). Some of the environmental factors that can damage cellular DNA are sunlight (UV ray), ionizing radiation (X-ray and γ-ray), chemical agents, and numerous genotoxic drugs.

Ionizing radiation (IR) can generate ROS to cause a broad spectrum of DNA lesions, similar to those that rise from oxidative metabolism (Altieri et al., 2008).

IR damages DNA and ultimately affects the cellular outcome through two mechanisms, the direct and indirect effect. The direct effect of radiation occurs when IR interacts with the atoms of the DNA molecule (e.g, phosphodiester backbone of DNA) and leaves a gap in the DNA (Henner et al., 1982). The indirect effect of radiation is when radiation interacts with water and breaks the bond that holds the water molecule together, producing radicals such as hydrogen (H•) and hydroxyls (OH•). These fragments may recombine to form reactive radical species such as hydroxyl radical, singlet oxygen, hydrogen peroxide, peroxynitrite, and one electron oxidation that can cause a variety of DNA oxidation (Riley, 1994; Cooke et al., 2003; reviewed in Altieri et al., 2008). IR causes damage to purine (adenine or guanine) or pyrimidine (cytosine or thymine), base loss (to form apyrimidinic or apurinic sites, AP sites), single- or double-strand breaks. How the cell responds to DNA damage will determine whether or not it will develop genomic instability and with additional oncogenic events, could potentially lead to cancer (Kastan and Bartek, 2004). The molecular signalling events following DNA damage may lead to activation of cell cycle checkpoints.

Eukaryotic cell cycle checkpoints

The eukaryotic cell division cycle encompasses a series of coordinated events whereby cells continuously oscillate between replicating their DNA (in S phase) and dividing (Mitosis or M phase) (Kastan and Bartek, 2004; Houtgraaf et al., 2006; Ljungman, 2005; Altieri et al., 2008). Cells undergo lag phases or intervals that allow growth and reorganisation of components before the subsequent stage in the cell cycle. The lag phase or a gap in time between completion of mitosis and the subsequent DNA replication is termed G1 and the gap between completion of DNA replication and mitosis is termed G2. If errors arise in these cell cycle phases, the regulatory pathways that control the cellular events with high fidelity, i.e., cell cycle checkpoints, can arrest the cell cycle to provide time for cells to execute repair processes.

The G1 phase is the first phase within the interphase, from the end of mitosis and to the beginning of DNA synthesis. During the G1 phase, cells increase in size and undergo synthesis of various enzymes that are needed in S phase, mainly for DNA replication. There are subphases within the G1 phase, i.e., competence, entry, progression and assembly, which may be perturbed by limiting growth factors and nutrient supply. The G1/S checkpoint ensures that cells that are damaged do not enter S phase. In the subsequent S phase, DNA replication occurs. When DNA synthesis is finished, a duplicate copy of the genome is produced for the subsequent daughter cells. The intra-S checkpoint causes largely transient, reversible inhibition of the firing of the origin of DNA replication and as a result, slows down DNA replication. During the G2 phase, the cell continues to grow and synthesize proteins that are required in M phase. The G2/M checkpoint prevents cells with damaged DNA from initiating mitosis. The retention of cells in G2 may also reflect the presence of persistent DNA lesions from the previous S phase caused by incomplete DNA replication. The M phase is where mitosis occurs to give rise to two genetically identical daughter cells, after which the whole cell cycle division may begin again. Although eukaryotic cells can and do undergo consecutive cell cycles in a short period of time, the majority of cells in the body do not do so. This is because many cells cease division and undergo a process known as terminal differentiation and become quiescent in a state or phase that is called G0. Under certain conditions, such as that resulting from exposure to growth-stimulating signals, cells can exit the quiescent G0 state and re-enter the cell cycle.

Progression from one cell cycle phase to the next is controlled by phosphorylation or dephosphorylation of cyclin dependent kinases (Cdks). Control of Cdks is regulated by cyclins and their interactions are fundamental in being able to govern cell-cycle progression. This is because oscillating changes in the activity of Cdks determine the phosphorylation status of target proteins that affect the cell cycle.

Cellular DNA damage response

The cellular response to IR-induced DNA damage revolves around two interconnected chains of events that take place in the nucleus (Kastan and Bartek, 2004; Ljungman, 2005; Szumiel, 2008). One is connected to the activation of proteins that are responsible for sensing damage to DNA and repair them. The other is the DNA damage signalling pathways that halt cell cycle progression until repair is complete. This encompasses multiple signal transduction pathways that lead to expression of genes necessary for executing the programs for cell survival, cell cycle control or cell death (Figure 1.4) (Kastan and Bartek, 2004). There is mounting evidence that the damage recognition complexes that control cell cycle arrest also interact with the DNA repair machinery.

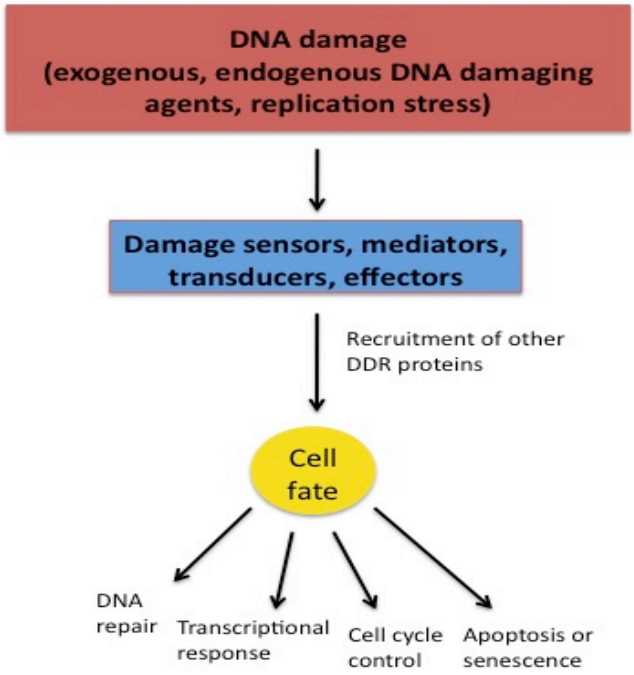

Figure 1.4 (Adapted from Sancar et al., 2004)

DNA damage response reactions in mammalian cells.

The four responses (DNA repair, transcriptional response, cell cycle control, and apoptosis) may function independently, but frequently a protein primarily involved in one response may participate in other responses.

Activation of DNA damage detection and DNA repair

IR produces many different types of lesions. Of these lesions, the DNA double strand break (DSB) is the most deleterious and can decrease propensity for cell survival if repair is not coordinated properly. One of the earliest responses following IR-induced DNA damage is the phosphorylation of histone H2AX protein at serine 139 residues in the carboxyl terminus (C-terminus) to form γH2AX (Bonner et al., 2008; Rothkamm and Horn, 2009). γH2AX is the core component of numerous signalling pathways in response to DSBs (Rogakou et al., 1998; Bonner et al., 2008; Podhorecka et al., 2010). Cells lacking H2AX display radiation sensitivity, growth retardation, and immune defects (Bonner et al., 2008; Ismail and Hendzel, 2008).

H2AX is a substrate of several phosphoinositide 3-kinase-related protein kinases (PIKKs) such as ataxia telangiectasia mutated (ATM), ATM and Rad3-related (ATR), or DNA-dependent protein kinase (DNA-PK) (Figure 1.5) (Collis et al., 2005; Lavin, 2008; Cimprich and Cortez, 2008). The nature of the DNA lesion determines which protein kinase phosphorylates H2AX (Ismail and Hendzel, 2008). H2AX is phosphorylated in a redundant manner by ATM and DNA-PK following IR (Stiff et al., 2004; Wang et al., 2005), and by ATR following DNA replication-associated or single-stranded DNA breaks (Furuta et al., 2003). These PIKK proteins are defined by their PI3K catalytic domains and are able to phosphorylate H2AX at an evolutionary conserved serine/glutamine (SQ) motif within the extended C-terminal tail of H2AX. All members of the PI3K family are activated by stress (e.g., inefficient DNA replication or IR-induced DNA damage). Another family member of PIKKs, hSMG-1 (human suppressor with morphogenic effect on genitalia) is involved in modification of histone H2AX phosphorylation in response to IR-induced DNA damage (Brumbaugh et al., 2004).

H2AX becomes phosphorylated over regions of several thousand base pairs surrounding the damage sites and appears as individual punctate foci in cell nuclei (Rogakou et al., 1999). The scoring of γH2AX foci using fluorescence

microscopy is currently the most sensitive method for DNA damage analysis. The formation of γH2AX foci occurs within minutes following IR and this process is cell-type dependent. Some studies have shown that maximum foci formation happens within 3-10 minutes, while others have reported maximum levels as late as 30 mins to an hour (reviewed in Rothkamm and Horn, 2009). One of the main functions of H2AX following IR is the concentration of DNA damage signalling and repair proteins at DSBs. One of the first proteins to be recruited to the site of DNA damage is the MRN complex that is composed of Mre11 (meiotic recombination 11), Rad50 (homolog of yeast radiation 50), and NBS1 (Nijmegen breakage syndrome). In addition, 53BP1 (p53 binding protein 1), MDC1 (mediator of DNA damage checkpoint protein 1), BRCA1 (breast cancer susceptibility gene 1) are relocalized to the nuclear foci where they recognize and interact with the phosphorylated C-terminus of H2AX (Podhorecka et al., 2010). These DNA repair foci promote chromatin remodelling to keep broken DNA ends together and facilitate rejoining of DNA ends (Podhorecka et al., 2010). Meanwhile, H2AX phosphorylation was found to be dispensable for the recruitment and maintenance of DNA repair foci following stalled replication forks but was shown to be required for the p53-/p21-mediated cell cycle arrest (Fragkos et al., 2009).

ATM kinase is a crucial mediator of H2AX phosphorylation in response to DSBs. In response to IR, the inactive ATM homodimer undergoes autophosphorylation on serine 1981 residue (Bakkenist and Kastan, 2003). This phosphorylation is required for dimer dissociation into single molecules that is needed for increased kinase activity toward other substrates (reviewed in Lavin, 2008). Apart from phosphorylating H2AX and activating other DNA repair proteins, ATM also functions to regulate cell cycle checkpoints and facilitate cell cycle arrest in the event of DNA damage.

ATR is predominantly activated by single-stranded regions of DNA arising at stalled replication forks or during processing of bulky lesions following UV-induced DNA damage (Hanasoge and Ljungman, 2007; reviewed in Cimprich and Cortez, 2008). Apart from single strand DNA (ssDNA) structures, ATR is activated following many different types of DNA damage, including DSBs, base

adducts, crosslinks, and stalled replication forks (Cimprich and Cortez, 2008; Fragkos et al., 2009). Unlike ATM, ATR does not undergo autophosphorylation. Instead, ATR expression is regulated by ATR-interacting protein (ATRIP). Binding of ssDNA by replication protein A (RPA) localizes the ATR-ATRIP complex to sites of DNA damage. However, activation of ATR requires colocalization of ATR-ATRIP complex with the RAD9-RAD1-HUS1 complex (also known as 9-1-1 complex).

Like ATM and ATR, DNA-PK is a nuclear serine/threonine kinase that comprises a catalytic subunit (DNA-PKcs) and a DNA binding Ku70/80 subunit. DNA-PK can be activated by autophosphorylation of DNA-PKcs in response to IR and UV exposure. Unlike ATM and ATR that seem to mediate both DNA repair and signalling to DNA damage checkpoints, DNA-PK have a specific role in phosphorylation of targets involved in DNA repair, i.e., non-homologous end-joining (NHEJ) repair, which is the mechanism by which most DSBs in mammalian cells are repaired (Yang et al., 2003; Collis et al., 2005; Dip and Naegeli, 2005). DNA-PK functions as a sensor of primary DNA damage. DNA-PK also has an important role to play as a scaffold to recruit NHEJ repair proteins to DSB sites (Lee and Kim, 2002). Recruitment of DNA-PKcs on a DNA end by Ku leads to conformational change that will activate its kinase activity (Jackson, 2002; Yang et al., 2003).

Depending on the source of DNA damage and DNA lesions involved, heterogenous γH2AX staining patterns is found. The H2AX phosphorylation following IR produces clear and punctate subnuclear foci that have been adopted as the main indicator of DNA DSBs (Ismail and Hendzel, 2008). It was found that ATM and DNA-PK both function redundantly to phosphorylate H2AX after IR (Stiff et al., 2004; Wang et al., 2005). UV irradiation induces pan-nuclear γH2AX staining and this activity was attributed to the ATR protein kinase (Marti et al., 2006; Hanasoge and Ljungman, 2007). Interestingly, it has been implicated that ATR may play an indirect role in H2AX phosphorylation through an effector kinase that diffuses in the nucleus and results in pan-nuclear type of H2AX phosphorylation (Fragkos et al., 2009).

Since DSBs represent the most biologically significant lesion following exposure to IR, the focus of the discussion will be on DNA damage response mechanisms triggered by DSBs. To repair DSBs, mammalian cells utilise two major recombination pathways, the NHEJ and error-free homologous recombination (HR) (reviewed in Valerie and Povirk, 2003; Shrivastav et al., 2008). The fundamental difference between these two pathways is the dependence on DNA homology in HR repair.

The main characteristic of NHEJ is its ability to join non-complementary DNA ends. NHEJ is believed to repair most of the DSBs in G0 and G1 stages of the cell cycle. Although a minor role, its participation in repair of damage induced in other cell cycle phases, such as S phase, also exists (Valerie and Povirk, 2003). Important components in NHEJ are Ku70/Ku 80, DNA-PKcs, DNA ligase IV and its cofactor XRCC4 (reviewed in Jackson, 2002; Valerie and Povirk, 2003). Apart from DSBs, other types of DNA breaks and base damages can also be repaired by NHEJ with the help of additional components such as Werner syndrome protein (WRN), MRE11 and Artemis that are all nucleases implicated in DNA end-joining (Valerie and Povirk, 2003; Collis et al., 2005). WRN is a helicase that possesses both ATP-dependent helicase activity and together with MRE11, which possesses a 3'–5' exonuclease activity. WRN is stimulated by Ku and is required to remove 3' phosphate or 3' phosphoglycolate groups, produced by IR. Artemis has 5'–3' exonuclease activity upon phosphorylation by DNA-PK, has the ability to open hairpin loops, removes 5' overhangs and shortens 3' overhangs.

HR repair is most active in late S/G2 cells and it is a high-fidelity mechanism to repair DNA DSBs by utilizing the information on the undamaged sister chromatid or homologous chromosome (Valerie and Povirk, 2003). DSBs generated from replication fork collapse are primarily repaired by HR repair (Shrivastav et al., 2008). Central components in HR repair are Rad51, 52, 54, BRCA1, BRCA2, and the MRN complex. Apart from these molecules that are involved directly in DNA repair mechanisms, the "sensors" for damage, such as ATM, ATR, and DNA-PK, are required to trigger DNA damage responses that are also important in cell cycle regulation and DNA repair themselves.

It is thought that NHEJ is primarily responsible for rejoining the majority of radiation-induced DSBs. One of the reasons for this may be that NHEJ repair is active all throughout the cell cycle, while HR repair is more enhanced in late S/G2 phases. In addition, NHEJ can repair most of the DSBs that usually arise from multiple ionization and oxidation events, e.g., ROS-mediated oxidation of DNA sugar residues (Ward, 1988; Regulus et al., 2007). However, there are subsets of DSBs that cannot be repaired by NHEJ and require HR repair. This is because additional processing of the damaged DNA might be necessary (Valerie and Povirk, 2003). For example, DSBs may need to undergo a process known as DNA resection, whereby the 5' strand of the DSB is degraded to produce a 3' single-stranded DNA overhang, to facilitate subsequent DNA repair. While this process initiates HR recombination pathways, it makes the DSB refractory to repair by the NHEJ pathway.

One protein that could potentially regulate the cell's choice of using NHEJ or HR repair following DNA-damage is p53. p53 has been implicated to play a direct role in sensing DNA damage, interact with proteins that play a direct role in HR, bind to Holliday junctions to facilitate their cleavage, or coordinate the resolution of secondary structures back to wild type conformation or signal for its repair (Gebow et al., 2000; Restle et al., 2008). Although the exact role that p53 plays in regulating DNA repair is not known (especially in NHEJ repair), cells without p53 may exhibit unregulated recombination that could lead to DNA deletions.

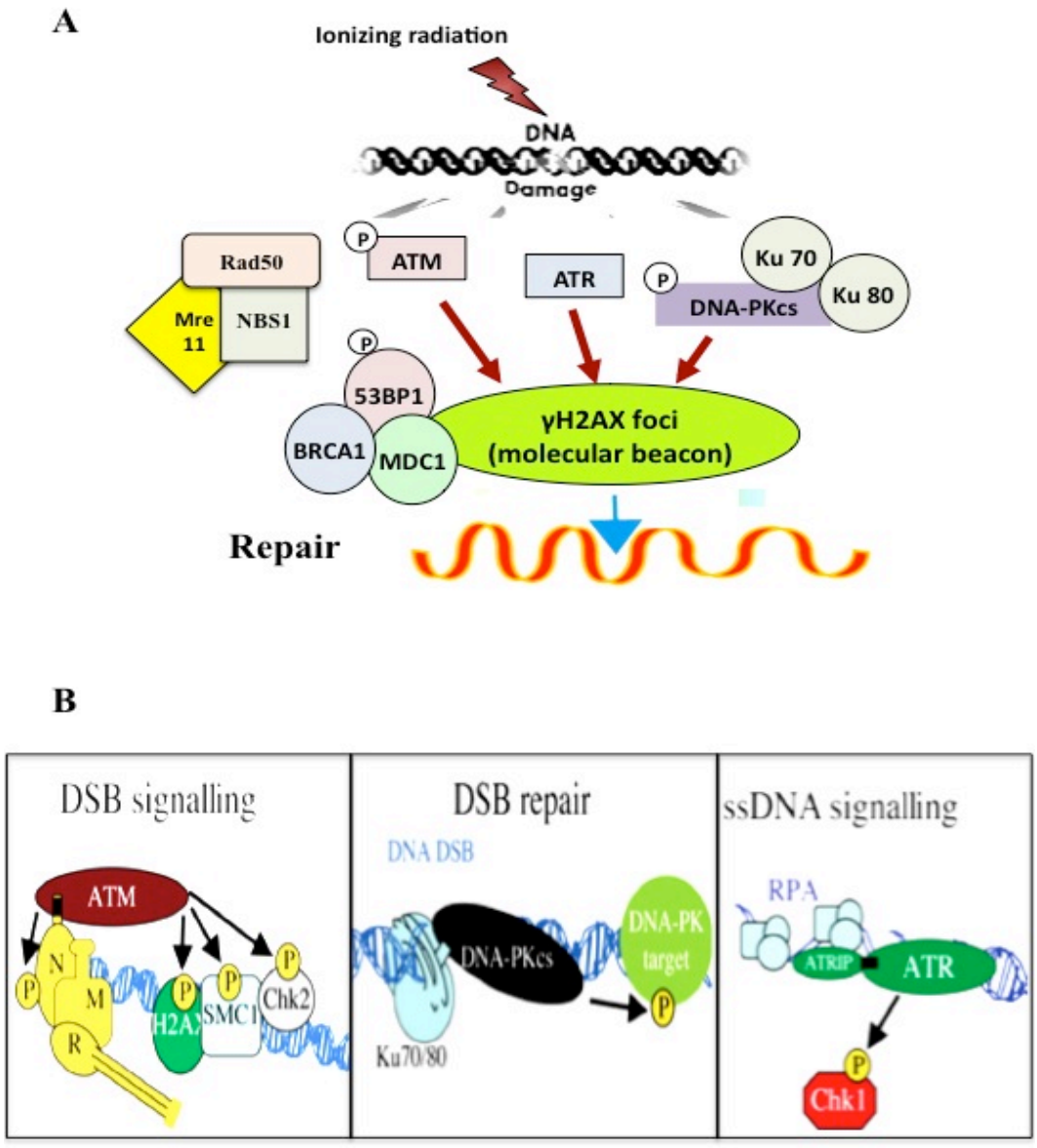

Figure 1.5: DNA damage signalling and repair following IR.

(A) A simplified model of recruitment of DNA repair proteins following DNA damage induced by IR. IR-induced DNA breaks are repaired by the DSB repair proteins such as Mre11/Rad50/Nbs1, H2AX, Mdc1, 53BP1, and components of the NHEJ apparatus (Ku70, Ku80, DNA-PK.), (B) Models depicting how ATM, DNA-PKcs and ATR are recruited to sites of DNA damage by analogous mechanisms, but possess different functions. SMC1, structural maintenance of chromosomes 1 [Reproduced with permission from Jackson SP. **The DNA-damage response: new molecular insights and new approaches to cancer therapy.** Biochem Soc Trans. 2009 Jun; 37(Pt 3): 483-94.]

Induction of DNA damage-sensitive cell cycle checkpoints

The other arm of DNA damage response is the signalling cascade leading to activation of cell cycle arrest (Figure 1.6). The cellular response to IR starts with the detection of the DNA damage. Activation of PIKK proteins occurs via mediator proteins and chromatin modifications. Ultimately, transducers amplify DNA damage signals and facilitate effector kinase activation. The execution of cell cycle checkpoints provide extended time for DNA repair enzymes to complete repair before entering the critical cell cycle stages of S phase and mitosis (Lukas et al., 2004; Ljungman, 2005, Altieri et al., 2008).

To allow correct localization of DNA repair proteins to damaged sites in proper timing and velocity, the PIKK proteins ATM, ATR and DNA-PK must cooperate closely with two other classes of checkpoint regulators, the mediators and transducers. The appropriate localization of ATM to sites of DSBs is mediated by MRN complex, MDC1, 53BP1 and BRCA1 whereby upon relocalisation, ATM can phopshorylate its substrates (Kastan and Bartek, 2004). ATR phosphorylation of Chk1 relies on the mediator protein claspin, which selectively interacts with chromatin structures that are created by active replication forks (Kastan and Bartek, 2004; Gottifredi and Prives, 2005).

While the role of DNA-PK appears to be restricted to DNA repair and apoptosis, ATM and ATR are the main regulators of the cell cycle checkpoints in response to DNA damage. Some of the most prominent substrates of ATM and ATR are the checkpoint transducer serine/threonine kinases Chk2 and Chk1. Essentially, ATM- and ATR-mediated phosphorylation triggers the activation of Chk2 and Chk1, respectively. Aside from this, one of the key transcription regulators in cell cycle checkpoints is p53. One of the main controllers of p53 activity is its negative regulator, MDM2. MDM2 binds to p53 and targets it for ubiquitination and subsequent degradation. The role of p53 in response to IR-induced damage is complex since it affects some aspects of DNA repair, cell cycle checkpoint arrest and the onset of apoptosis (reviewed in El-Deiry, 2003; Kastan and Berkovich, 2007).

The spatio-temporal coordination of cell cycle proteins reflects that checkpoint responses following DNA damage operate through post-translational modification of proteins, re-localization, dynamic interactions, and changes of chromatin conformation and/or stability of pre-existing proteins (reviewed in Kastan and Bartek, 2004; Szumiel, 2008).

The main arm of the G1/S arrest is the ATM (ATR)/ Chk2 (Chk1)-p53/MDM2-p21 pathway (reviewed in Kastan and Bartek, 2004). The G1 checkpoint response targets two critical tumour suppressor pathways, regulated by p53 and pRb (retinoblastoma tumour suppressor). ATM regulates G1 checkpoint by directly phosphorylating p53 at serine (Ser) 15 and by phosphorylation of Chk2 at threonine (Thr) 68 (reviewed in Valerie and Povirk, 2003). A parallel regulator of G1 checkpoint, ATR also directly phosphorylates p53 Ser15 and phosphorylates Chk1 at Ser345. Activated Chk1 phosphorylates p53 at Ser20, which serves as a backup for ATM-Chk2 signalling. ATM also phopshorylates the p53 inhibitor, MDM2, at Ser395 and thereby prevents MDM2 from degrading p53. Following phosphorylations on p53 and release of its inhibition by phosphorylation of MDM2, p53 is stabilised and able to activate its downstream target p21WAF1/Cip1, which is an inhibitor of cyclin dependent kinases. p21WAF1/Cip1 plays its major role in G1/S arrest by binding to the cyclin D/Cdk6 complex. This inhibits cyclin cdk's ability to phosphorylate pRb, which in turn inhibits the release of pRb from E2F. This is an essential step that triggers S phase progression. In cells that have activated DNA damage response caused by stalled replication forks, H2AX is required to stabilise p21 levels to elicit an effective cell cycle arrest (Fragkos et al., 2009).

The S phase cell cycle checkpoint pathways are complex in that the DNA damage sensors will have to coordinate both DNA replication and DNA repair. While ATM may only sense damaged DNA, ATR, which is the primary S phase checkpoint kinase, can play roles in both damage sensing and DNA replication (Gottifredi and Prives, 2005). In the absence of DNA damage, ATR is able to regulate DNA replication through these functions: associate with replication forks and regulate the timing of origin firing, detect changes in the processivity of polymerases, or monitor the extent of ssDNA accumulation at the replication fork

(Gottifredi and Prives, 2005). There are at least two parallel pathways whereby ATM or ATR can regulate S phase checkpoints in response to IR. In the first instant after IR exposure, ATM phoshorylates Chk2, which in turn phosphorylate CDC25A that is a phosphatase acting on cyclin E/A-Cdk2 complex. The inhibition of Cdk2 activity will block the loading of Cdc45 onto chromatin, which prevents the initiation of replication origin firing and slows down DNA synthesis (Kastan and Bartek, 2004; Gottifredi and Prives, 2005). ATM also phosphorylates NBS1 and SMC1 (Structural maintenance of chromosomes 1) (Houtgraaf et al., 2006). This pathway requires BRCA1, 53BP1, FANCD2 (Fanconi anaemia, complementation group D2) proteins, as cells lacking these proteins exhibited defective intra-S-phase checkpoint (reviewed in Lukas et al., 2004).

The G2/M checkpoint prevents damaged cells from initiating mitosis. Additionally, cells with DNA lesions that arise from inappropriately replicated DNA in S phase also accumulates in G2 (Kastan and Bartek, 2004; Lukas et al., 2004). When cells are irradiated in G2, ATM regulates the G2 checkpoint by phosphorylating Chk2, which in turn inhibits Cdc25c phosphatase. This prevents the mitosis-promoting activity of cyclin B-Cdc2 kinase, resulting in G2/M arrest. Apart from this, checkpoint mediators such as 53BP1 and BRCA1 have been implicated in contributing to G2 checkpoint arrest (Xu et al., 2001; Abraham, 2002).

It is possible that the maintenance phase of the G2/M checkpoint partly relies on the transcriptional programmes that are regulated by p53 (Kastan and Bartek, 2004; Lukas et al., 2004). It has been shown that wild-type p53 cells exhibit a prolonged G2 arrest, possibly through stimulating expression of cell cycle inhibitors such as p21, GADD45a (growth arrest and DNA damage-inducible 45 alpha) and 14-3-3 sigma proteins (Taylor and Stark, 2001; Nyberg et al., 2002). The success of regulating cell cycle checkpoint will determine the outcome of cells after IR. Depending on the severity of the lesion, the cell may be able to repair it, survive and resume cycling. However, cells that have mutations in signalling pathways that halt cell cycle progression or apoptosis may sustain genomic instabilities that lead to cancer.

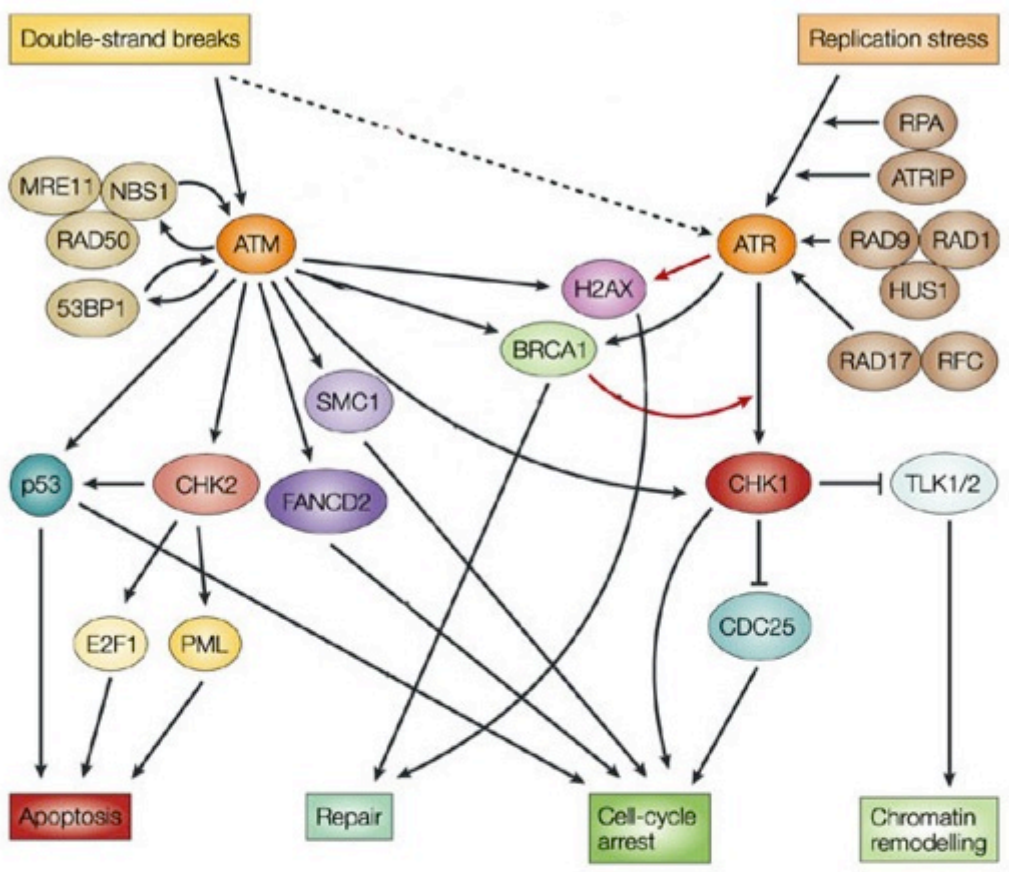

Figure 1.6: DNA damage response signal transduction network.

The DNA-damage-response network consists of two parallel pathways that respond to different types of DNA damage. The ATM pathway responds to the presence of double-strand breaks (DSBs), and acts during all phases of the cell cycle. It can activate many of the downstream components of the ATR pathway, which also responds to DSBs, but more slowly than ATM. In addition, the ATR pathway can respond to agents that interfere with the function of DNA replication forks, such as ultraviolet light and hydroxyurea. ATM and ATR are proximal kinases that are central to the entire DNA-damage response, including checkpoints, DNA repair and apoptosis. Other proteins lie both upstream, to detect the damage, and downstream, to effect the response. Dashed lines represent less strong interactions. Red lines represent interactions that are supported by only limited data**.** Adapted by permission from Macmillan Publishers Ltd: Nature Reviews Cancer (Zhou and Bartek, 2004).

1.8 Radiation-induced bystander effect (RIBE)

In recent years, there has been an increase of studies on the indirect effects of radiation, termed the radiation-induced bystander effect (RIBE). RIBE is a phenomenon whereby irradiated cells can elicit increased levels of mutations, DNA damage, and genomic instability in neighbouring cells that have never been exposed to irradiation (Mothersill and Seymour, 2001 and 2004; Prise and Sullivan, 2009). Many studies on bystander responses were performed on different cell culture and irradiation conditions *in vitro*. The first approach involves irradiation of a small fraction of cells in monolayer cultures to very low fluences of α particles or exposure of cell cultures to partially shielded radiation (reviewed in Little, 2003). Another approach involved co-cultivation of irradiated cells with non-irradiated cells (Gerashchenko and Howell, 2003a). In these approaches, the biological effects were subsequently measured in non-irradiated cells. A parallel protocol involved harvesting of conditioned medium from irradiated cultures and transferring it to culture of non-irradiated cells (Mothersill et al., 2006). This method is unique as bystander cells were not in direct physical contact with irradiated cells. In confluent monolayer cultures, it is thought that RIBE involves gap-junction mediated cell-to-cell communication (Mothersill and Seymour, 2001; Azzam et al., 1998; Prise and Sullivan, 2009). In experiments that involved transfer of conditioned medium on to non-irradiated cells, RIBE may be mediated by diffusible factors that are secreted into the medium by irradiated cells (Mothersill and Seymour, 2006; Prise and Sullivan, 2009).

Apart from this, bystander effect has also been observed in three-dimensional (3D) system where 3D cell-to-cell interaction between irradiated cells and non-irradiated cells affect radiation resistance of test cells (Djordjevic and Lange, 2006). Research on bystander effects has also been demonstrated *in vivo*, whereby studies with tissue explant models and mouse bone marrow stem cell transplant system demonstrated bystander effect may occur *in vivo* (Watson et al., 2000; Morgan, 2003; Koturbash et al., 2006). For example, Watson et al. (2000) have demonstrated that bone marrow cells that were irradiated *in vitro* that were mixed with non-irradiated cells and transplanted *in vivo* induced chromosomal instability in non-irradiated haematopoietic stem cells, using a cytogenetic marker.

Some of the endpoints that are manifested in RIBE are reduced colony formation, induction of apoptosis, changes in gene expression, cell cycle regulation and proliferation, which affect cell growth in culture (reviewed in Chaudhry, 2006; Burdak-Rothkamm et al., 2008). Some of the bystander responses that have implications in carcinogenesis include gene mutations, production of ROS, chromosome aberrations, sister chromatid exchanges, micronuclei production, induction of DNA breaks, and increase in expression of genes involved in DNA damage response and repair (Azzam et al., 2003; Lorimore et al., 2003; Burdak-Rothkamm et al., 2007; Burdak-Rothkamm et al., 2008; Dickey et al., 2009).

One of the most prominent markers of DSBs is used as indicator of bystander effect, the phosphorylation of histone 2A variant X (γH2AX) foci that arise as a result of cellular responses to DNA damage (Sokolov et al., 2005; Sokolov et al., 2007; Dickey et al., 2009). The signalling leading to bystander-induced γH2AX focus formation was found to be dependent on ataxia-telangiectasia and Rad3 related (ATR) kinase (Burdak-Rothkamm et al., 2007; Burdak-Rothkamm et al., 2008). The formation of bystander foci is accompanied by co-localisation of ATR, 53BP1, ATM-S-1981P (ATM phosphorylated at serine 1981 residue that is indicative of ATM activation), p21 (WAF1/CIP1), and BRCA1 foci in non-targeted cells.

1.9 Implication of irradiated fibroblasts in bystander effect

In this study, the J2-3T3 mouse feeder layer was used to promote serial cultivation of immortalised NIKs cells. In recent years, irradiated fibroblast layer has been shown to be capable of inducing bystander effects in non-irradiated human cells. One of the examples was shown in 3D culture constructs of hybrid spheroids (HeLa and fibroblasts) that mimicked *in vivo* environment and suited for measurement of radiation effects (Djordjevic and Lange, 2006). In this study, the use of irradiated fibroblasts as feeders induced bystander effect in non-irradiated HeLa cells, which was assessed as significant growth reduction in the

latter (Djordjevic and Lange, 2006). This study provides insight into survival of cells that are in contact with irradiated neighbouring cells during multi-fraction radiotherapy, thereby raising the prospect of devising more effective treatment.

In a separate study, irradiation of mouse NIH3T3 fibroblasts also induced non-targeted effects of radiation on squamous cell carcinoma (SCC) cells (Kamochi et al., 2008). Irradiation of fibroblasts was found to enhance the expression of molecules involved in promoting growth, motility, and invasion of SCC cells. The irradiated fibroblasts-induced phenomenon above is elicited through bystander mechanisms, because the SCC cells are not irradiated. Although the precise mechanism of irradiated fibroblasts-induced bystander effect remains unclear, both irradiated fibroblasts and SCC cells formed 53BP1 irradiation-induced foci (IRIF). Irradiated fibroblasts enhanced the induction of 53BP1 IRIF formation more extensively than non-irradiated fibroblasts. This indicates that irradiated fibroblasts elicited more DNA damage in SCC cells under cancer-fibroblast interaction, as a consequence of indirect exposure to IR. In turn, it was suggested that irradiated fibroblasts promoted the invasion of SCC cells through expression of MMP-1 and 9 and filamin A in a bystander manner. This study showed that irradiated fibroblasts-induced bystander effect is a powerful player in determining the biological behaviour of SCC cells under cancer-fibroblasts interactions.

1.10 DNA damage response in non-targeted bystander cells

It was demonstrated that more than 90% of the bystander-induced mutations are point mutations, through studies of biological endpoints such as sister chromatid exchange (SCE) and HPRT mutations (Huo et al., 2001; Nagasawa et al., 2002). While most bystander-induced mutations occur on a smaller scale, direct IR-induced mutations are present on larger scale varying from partial to total gene deletions (Nagasawa et al., 2002; Prise et al., 2007). It was suggested that the increased occurrence of point mutations in bystander cells compared to directly irradiated cells was possibly owed to oxidative base damage by ROS (Huo et al., 2001; Hamada et al., 2007). In a separate study, DNA base damage and SSBs were found to be the primary driving factors that cause chromatid-type aberrations

in bystander cells (Nagasawa et al., 2005). It is also thought that some DSBs occur in bystander cells are converted from unrepaired SSBs, upon collision of replication fork with SSBs (Wiseman and Halliwell, 1999; Zheng et al., 2005). Meanwhile in directly irradiated cells, DNA DSBs are primarily responsible for chromosome-type aberrations (Nagasawa et al., 2005). Chromatid-type aberrations occur when the DNA breaks and rejoining affects only one of the sister chromatids at any one locus, while chromosome-type aberrations occurs when DNA breaks and rejoining affects both sister chromatids at any one locus. It is thus conceivable that SSBs and base damage are the primary lesions induced in bystander cells, while DSBs are the main lesions induced in directly irradiated cells. The induction of genetic damage occurs on a larger scale in directly irradiated cells compared to bystander cells.

Of primary importance to us in this study is the activation of DNA damage detection and repair genes in bystander cells. The staining for DSB marker, γH2AX, indicates that DNA DSBs exist in bystander as well as in irradiated cells (Sokolov et al., 2005; Hu et al., 2006; Dickey et al., 2009). However, the origins of γH2AX foci may be different in irradiated and bystander cells and may be expected to have different kinetics. In most irradiated cells, induction of γH2AX foci increase to the maximum at 30 mins post-IR and resolve to pre-IR amounts by 18 hr (Rogakou et al., 1998; Rogakou et al., 1999). Meanwhile, the induction of γH2AX foci in bystander cells is prolonged up to 48 hour after irradiation, which suggests the continuous production of DNA damaging agents by irradiated cells (Sokolov et al., 2005; Burdak-Rothkamm et al., 2007). Some factors that can damage DNA (e.g., ROS) are produced by the irradiated cell and can be passed through the medium to the bystander cells, through induction of a secondary factor. Secondary factors such as some cytokines can be induced by ROS (Bellocq et al., 1999; Ayache et al., 2002). Some of these cytokines (e.g., transforming growth factor beta, TGF-β or cyclooxygenase-2, COX-2) can also induce ROS production and further induce γH2AX in non-irradiated bystander cells (Burdak-Rothkamm et al., 2007; Prise et al., 2007; Burdak-Rothkamm et al., 2008; Dickey et al., 2009). For example, Zhou et al. (2005) has demonstrated that the COX-2 signalling cascade, which is essential in cellular inflammatory response, may be a

critical event in mediating bystander responses. The cellular inflammatory response is a non-specific defence mechanism of the body to invasion of foreign pathogens. The inflammatory-type response that is activated in cells that exhibit bystander effect may reflect the cellular response to radiation injury (Lorimore et al., 2001).

Recruitment of DNA repair proteins to γH2AX foci is an indication that DNA DSB formation is a major event in manifesting bystander phenotype. Sokolov et al. (2005) was the first to report the co-localization of γH2AX and DDR effectors such as ATM-S-1981-P, 53BP1 and components of the MRN complex (Mre11, Rad50 and NBS1) in bystander cells. The three PIKK proteins, ATM, ATR, and DNA-PK, are known to phosphorylate H2AX in directly irradiated cells. However, inhibition of ATM and DNA-PK did not abolish γH2AX induction in bystander cells (Burdak-Rothkamm et al., 2007). Instead, ATR was found to be the primary mediator of bystander γH2AX induction that is restricted to S phase cells. This indicates that the observed DNA damage response presumably arises from stalled replication forks in S phase (Burdak-Rothkamm et al., 2007). Since there is now evidence suggesting the involvement of long-lived ROS in bystander mechanisms (Azzam et al., 2002; Azzam et al., 2003), it is likely that the accumulation of oxidative damage at stalled replication forks in S phase may lead to activation of DNA damage signalling in bystander cells. An updated model of ATR-dependent bystander signalling was proposed following the findings of Burdak-Rothkamm et al. (2008). In this model, ATR is recruited at replication forks through binding of ssDNA by RPA and ATRIP. Following this, a DNA damage response is initiated which leads to the recruitment of DNA repair factors such as γH2AX, 53BP1, and BRCA1. Subsequently, ATM is activated in an ATR-dependent pathway and it is thought that ATR and ATM phosphorylate Chk1 and Chk2, respectively (Burdak-Rothkamm et al., 2008). Although p21WAF1/Cip1 was induced in bystander foci, it is still unknown which protein is responsible for its activation in bystander cells. In directly irradiated cells, ATM/p53 phosphorylation activates p21 and this leads to activation of cell cycle arrest or apoptosis (Valerie and Povirk, 2003).

Bystander cells generally require NHEJ to repair most of the bystander-induced DSBs, as NHEJ-deficient cells display increase bystander phenotypes such as sister chromatid exchange, micronucleus formation, chromosome-type aberrations, and gene deletions (reviewed in Hamada et al., 2007). There has been evidence for induction of the proteins that are involved in base excision repair (BER) pathways in bystander cells, such as RPA, proliferating cell nuclear antigen (PCNA), and AP endonuclease (Iyer et al., 2000; Balajee et al., 2004; Hill et al., 2005). The activation of BER pathway is presumably attributed to the DNA base lesions and SSBs in bystander cells (Hamada et al., 2007). These lesions in bystander cells may arise from ROS that are generated by exposure to irradiated cells. In addition to producing oxidative damage, sites of base loss (abasic sites) and AP sites, ROS can generate SSBs with modified 5' and/or 3' ends (Dianov and Parsons, 2007). SSBs containing 3'-end phosphate or phosphoglycolate can also be generated from oxidative damage to the sugar residue of DNA. The complexity of the DNA lesions generated by ROS may require individual subsets of BER proteins to repair.

Aside from that, p53 might play a role in DNA damage response in bystander cells. After being exposed to very low doses of α-particles, isolated clusters of bystander cells exhibited increased levels of p53, p21WAF1/Cip1 and decreased Cdc2, Cyclin B1, and Rad51 (Azzam et al., 1998). In effect, these bystander cells exhibit a transient but not permanent G1 arrest. On the contrary, bystander cells that are in receipt of conditioned medium from irradiated cells exhibit an enhanced proliferation following decreased p53 and p21WAF1/Cip1 levels (Iyer et al., 2000). These differences in growth effects in bystander cells may be owed to the net amount of DNA damaging agents (ROS) that are received by these cells from irradiated cells. It is possible that low level of ROS (transmitted via media) stimulate growth, while higher level of ROS (transmitted via cell-to-cell contact) is inhibitory to growth (Geraschenko and Howell, 2003b). It has been thought that the responses in bystander cells, e.g., proliferative or cell cycle arrest, may vary depending on the genetic background of the recipient (Mothersill and Seymour, 2006). Many studies of bystander effect used deleterious endpoints for cells such as increased mutation levels, chromosomal instability, and apoptosis. On the other hand, bystander effect can also be advantageous by inducing high fidelity repair,

preventing the growth of cancer cells, or eliminating damaged cells from the populations (Matsumoto et al., 2004; Waldren et al., 2004).

Since signal production by irradiated cells and response of bystander cells to this DNA damaging signals are separate processes (Mothersill and Seymour, 2006), it is believed that there is no simple relationship between exposure and effect of cells to radiation. Especially in cells that sustained bystander effect from exposure to low dose radiation, the outcome may not be a linear dose-effect relationship (Mothersill and Seymour, 2006). Bystander cells that are exposed to low dose radiation may elicit apoptosis, proliferation or differentiation and which response predominates in bystander cells appear to depend on the genetic background of the cell and not necessarily the dose. The induction of bystander responses may require a certain level of the DNA damage signals to be reached before it can be elicited (Mothersill and Seymour, 2006). For example, bystander cells that are exposed to low dose radiation can elicit either a proliferation or death response. The induction of a particular bystander response, whether they are protective or detrimental), could rely on the net amount of ROS within the cells. The balance between ROS generation and scavenging in bystander cells may depend on the cellular physiological processes that can result in either more or less ROS production. If there is more ROS production, the bystander response may lean toward a detrimental effect.

There are also reports for “protective” bystander responses, whereby bystander cells exhibited increased radioresistance (Matsumoto et al., 2001). A protective bystander response is similar to another phenomenon in radiobiology known as adaptive response.

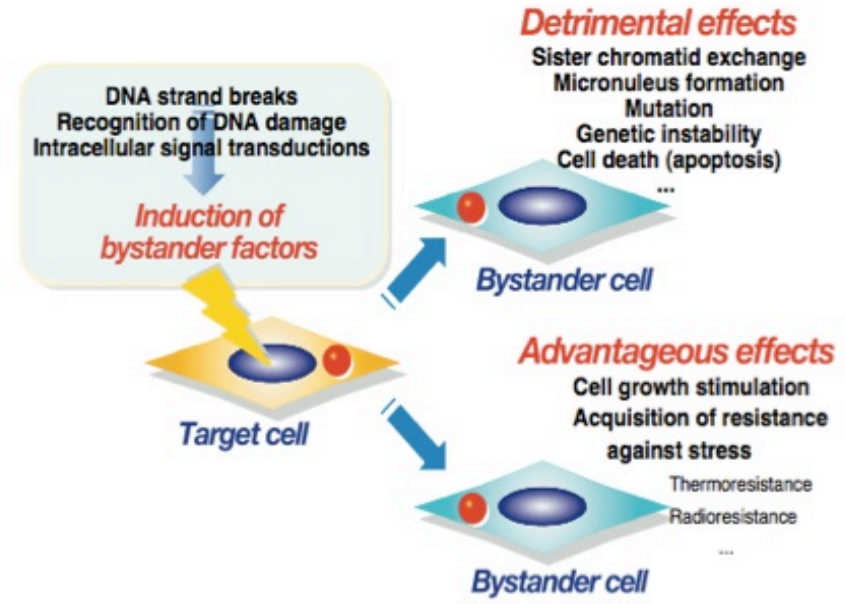

Figure 1.7: Radiation-induced bystander effects lead to advantageous as well as detrimental effects.

[Reproduced with permission from Matsumoto H. **Radiation-induced adaptive responses and bystander effects.** Biol Sci Space. 2004. 18(4): 247-254.

1.11 Adaptive response

Adaptive response is a phenomenon whereby exposure to a mild priming or conditioning dose of radiation before a larger challenging dose of irradiation reduces the damage induced by the second dose of radiation (Wolff, 1998; Szumiel, 2005; Tapio and Jacob, 2007). Adaptive response can be divided into three successive processes following irradiation – the intracellular response, extracellular signal and maintenance (Tapio and Jacob, 2007). The intracellular responses that lead to adaptation of a cell to irradiation is a complex process that includes induction or suppression of groups of gene; particularly those involved in the DNA damage response and repair pathways (Wolff, 1992; Sasaki et al., 2002; Kadhim et al., 2004; Szumiel, 2008). An extracellular signal, the nature of which is presently unknown, may be sent from affected cell to neighbouring cells to cause them to adapt as well (Tapio and Jacob, 2007). It was thought that this occurs through release of diffusible signalling molecules or cell-to-cell communication, (Tapio and Jacob, 2007). Adaptive response can be maintained from a few hours to several months. The signals that are generated by components of adaptive response pathways are targeted at DNA repair, nuclear import of repair enzymes, cell cycle checkpoints, and apoptosis (Szumiel, 2005).

Since treatment with DNA-damaging agents (e.g., α-particles, β-ray, γ-ray, X-ray, bleomycin, hydrogen peroxide, ROS) can induce adaptive response, it was thought that the "priming" event is DNA damage (Szumiel, 2005). An essential part in the development of adaptive response is the transmission of DNA damage signal to initiate a DNA repair process. In the adaptive repair pathway, p53 was found to be the central component and cells lacking p53 do not exhibit adaptive response (Sasaki et al., 2002). The adaptive repair pathway is inducible at a narrow dose range; its optimal priming dose is believed to vary between different cell types and experimental conditions (Sasaki et al., 2002; Matsumoto et al., 2004). At low doses, the DNA damage signal can be transduced by the protein kinase C (PKC)-p38 mitogen-activated protein kinase (p38 MAPK)-phospholipase C (PLC) signalling pathway that act to phosphorylate p53 at Ser15, 33, and 46 (reviewed in Matsumoto et al., 2004; Szumiel, 2005). It is believed that p53 plays a critical role to channel radiation-induced DNA DSBs into a high-

fidelity repair pathway (Lee et al., 1995; Reed et al., 1995; Schultz et al., 2000). At high dose exposures, extracellular signal-regulated protein kinase (ERK), Jun N-terminal kinase (JNK) and wild-type p53-induced phosphatase (Wip1) dominantly activate p53. p53 is able to bind to either p38MAPK or ERK to form p53-p38MAPK or p53-ERK complexes and these associations are competitive. Binding of ERK to p53 can inhibit activation of PKC-p38MAPK-PLC signalling pathway. Such feedback regulatory system could be the molecular basis of cellular mechanism to recognise the cellular effect to a particular dose, whether to induce adaptive or death pathway following recognition of certain doses.

It is believed that p53-associated adaptive repair system is most probably mediated by NHEJ, since the adaptive repair is executed in G1 phase of the cell cycle. However, this NHEJ repair may not be dependent on DNA-PK as cells that are defective in the catalytic activity of this protein can still elicit an adaptive response. Another component in the adaptive repair pathway, poly (ADP-ribose) polymerase (PARP), is activated to prevent illegitimate recombination (Szumiel, 2005).

Activation of adaptive responses may reduce damaging effects of IR by increasing capacity for DNA repair, decreasing transformation efficiency, reducing sister chromatid changes and micronucleus frequency – shown as increased cloning efficiency following the challenging dose of radiation (Kadhim et al., 2004; Jeggo and Lavin, 2009). Since non-targeted cells were able to adapt to subsequent irradiation after being grown in medium transferred from irradiated cells, adaptive response is likely to be mediated through diffusible extracellular signals (Iyer et al., 2002a, b). The nature of this extracellular signal is unknown, but some studies have suggested the involvement of long-lived radicals or ROS that release peroxides into the medium (Azzam et al., 2002; Azzam et al., 2003).

Adaptive response and bystander effect are both phenomenon related to non-direct effects of irradiation and are able to be maintained for a long time. This has lead to speculations that adaptive response is a subgroup of bystander effect – the protective bystander effect (Matsumoto et al., 2004; Tapio and Jacob, 2007). For example, bystander effect mediated by nitric oxide (NO) that was secreted by

irradiated cells may contribute to increased radioresistance in these cells following exposure to radiation (Matsumoto et al., 2001, 2004). It is likely that both adaptive response and bystander effect are defined by the experimental procedures that are used to study them (Kadhim et al., 2004). These indirect responses to radiation should be considered as cellular homeostatic responses that recognise when the cellular equilibrium is distorted (i.e., in the event of DNA damage) and facilitate cellular response aimed toward restoration of the equilibrium. The induction of these responses can cause either repair or removal of cells following exposure to DNA damage.

1.12 Manipulation of cell cycle control and DNA damage response by HPV16

Apart from non-targeted effects of radiation, this thesis also studies the effects of HPV16 infection on keratinocyte proliferation, cellular DNA damage response signalling, and survival. The cellular DNA damage surveillance system is robustly attuned to recognising aberrant DNA structures. Some triggers for this response could be incoming viral DNA or virally encoded proteins, which could bind to DNA or themselves modify cellular DNA repair proteins (Lilley et al., 2007; Weitzman et al., 2010). Hence, it is not surprising that this system would be employed as an anti-viral defence. While the host cell elicits a DNA damage response to limit HPV infection and protect its genome (Kadaja et al., 2009; Moody and Laimins, 2009), the virus has evolved numerous strategies to counteract host defence mechanisms.

HPV avoids undergoing a productive replication cycle (leading to synthesis and packaging of virions) in proliferating cells. Instead, the HPV has chosen to replicate in the differentiating compartment of the epithelium where cells have exited the cell cycle (Moody and Laimins, 2010). HPVs require cellular DNA polymerases and replication factors that are only produced in mitotically active host cells (Stanley et al., 2007). Therefore, the viruses will need to disconnect keratinocyte differentiation from cell cycle arrest, reactivate cellular DNA synthesis to re-establish replication competent state and inhibit apoptosis to create a suitable milieu for viral DNA replication (Stanley et al., 2007; Kadaja et al., 2009). The primary HPV proteins that are responsible for disrupting these signalling pathways are the E6 and E7 oncoproteins. E7 binds to Rb family members, consisting of p105 (Rb), p107, and p130, targeting them for degradation and result in their release from E2F transcription factors (reviewed in McLaughlin-Drubin and Munger, 2009). This action abrogates the G1/S checkpoint and facilitates entry of cells into S phase. However, E7 degradation of Rb also stabilizes p53, which inhibits proliferation and increases the probability of E7-expressing cells to apoptosis (Jones et al., 1997). To counteract this, E6 binds to p53 and promote its degradation, preventing p53-mediated apoptosis in infected cells (reviewed in Howie et al., 2009). The expression of E6 and E7 give HPV-

infected cells a selective growth advantage over normal cells through increased cell immortalisation (Hawley-Nelson et al., 1989; Romanczuk and Howley, 1992; Jeon et al., 1995). It is thought that HPV's cellular immortalization capability is achieved through activation of human telomerase reverse transcriptase (hTERT) by E6 together with pRb destruction by E7 (Moody and Laimins, 2010).

To increase the proliferative ability of infected cells, HPV also interact with cyclins and Cdk inhibitors (p21 and p27) and abrogate their inhibitory effects on Cdk2. Cdk2 is important for G1 to S phase entry (Deshpande et al., 2005). Hence, E7-expressing cells maintains high levels of Cdk2 activity, which promotes S phase entry. HPV16 E7 has also been shown to attenuate DNA damage checkpoint control by accelerating the proteolytic turnover of claspin (Spardy et al., 2009). The degradation of claspin abolished the G2/M cell cycle checkpoint and allowed aberrant entry of cells into mitosis. Thus, the combined actions of E6 and E7 stimulate differentiated cells to re-enter the S phase and promote an S-phase-like milieu suitable for viral genome replication (Longworth and Laimins, 2004).

The manipulation of host cell's machineries to create an environment to suit HPV propagation does not go unnoticed. In fact, it is probable that the consequence of this is cancer, a state of continued proliferation and a resistance to cell death. One of the consequences of aberrant entry into the mitosis can lead to numerous mitotic defects, which is a driving factor for induction of genomic instability. For example, it has been reported that the expression of E6 and E7 oncoproteins caused multipolar mitoses that can lead to chromosome missegregation and aneuploidy (reviewed in McLaughlin-Drubin and Munger, 2009; Moody and Laimins, 2010). These abnormalities are believed to arise from centrosome duplication errors, which presumably occur owed to cell division errors. Although cells with abnormal mitoses are more susceptible to cell death, E6 and E7 cooperatively allow cells with abnormal centrosomes to accumulate. This could possibly occur through relaxation of G2/M checkpoint or inhibition of apoptotic signalling (Moody and Laimins, 2010).

One of the mechanisms by which HPV16 E6 and E7 contribute to genomic instability is through induction of DNA damage. Both E6 and E7 have been shown to independently induce numerical and structural abnormalities (Duensing and Munger, 2002). Although expression of both E6 and E7 induced DNA breaks, only E7-expressing cells have been shown to display increased H2AX phosphorylation and activation of a DNA repair protein, PARP. This was further accompanied by increase in phosphorylated p53 at serine 15 (p53-Ser15-P) and cdc2, which could represent the activation of cell cycle checkpoint controls to facilitate cell cycle arrest while DNA is repaired in HPV-infected cells. Studies have shown that one of the reasons for HPV to utilise cellular DNA damage response and repair proteins is for execution of efficient productive phase of the viral life cycle (Moody and Laimins, 2009). In this study, HPV was thought to utilise DNA damage response and repair proteins to aid viral genome amplification in differentiating cells. The MRN-ATM pathway was thought to be important for HPV genome amplification, as NBS-1, ATM, Chk2, BRCA1, were detected in differentiated HPV positive cells.

Another way by which HPV proteins could induce genomic instability is through disruption of host cell's DNA repair activity. While HPV16 E6 and E7 can impair nucleotide excision repair activity in human oral keratinocytes (Liu et al., 1997), HPV16 E6 can subvert DNA DSB repair activity through binding with XRCC1 in CHO cell lines (Iftner et al., 2002). Another branch of DNA repair, the DNA end-joining repair, has also been targeted for disruption by HPV16 E6 protein through p53-dependent or independent pathway (Shin et al., 2006).

The exploitation of host cell DNA damage responses by HPV have been shown to induce genotoxic stress that leads to activation of the Fanconi Anemia (FA) pathway (Spardy et al., 2008). The activation of FA by HPV16 E7 restores telomere length through the alternative lengthening of telomeres (ALT) pathway in an ATR-dependent manner. This activity of HPV16 E7 can promote extension of HKs lifespan, and ultimately, immortalization. It is noteworthy that although E6 has been shown to induce hTERT expression, it has been shown that HPV E7 can promote telomere length maintenance in the absence of E6 (Stoppler et al.,

1997). This study has shown that activation of telomerase did not necessarily result in maintenance of telomere length.

Collectively, HPV targets multiple signalling pathways to maintain cells in a continuous proliferative state that permit viral replication. However, the consequences of this interference of normal cellular process results in accumulation of mutations, cell division errors, and insufficient DNA repair that lead to increased genomic instability and progression to cancer (Duensing et al., 2001; reviewed in Moody and Laimins, 2010).

1.13 Maintenance of HPV16 copy number in keratinocyte culture

Examination of the early stages of HPV infection and transformation relies on the establishment of viral replication *in vitro*. One of the important factors that permit such studies is the stable HPV episomal replication in culture (Flores et al., 1999; Fratini et al., 1996, 1997; Allen-Hoffman et al., 2000). In the routine cultivation of human keratinocytes, the presence of irradiated 3T3 feeder cells is needed (Rheinwald and Green, 1975). It has been shown that episomal replication of HPV16 in W12 cells is quite stable when cultured with irradiated feeder fibroblast (Sprague et al., 2002). Human keratinocytes that are grown with feeders have been shown to grow up to approximately 50 PDs, while HKs that are cultured in serum-free medium have a replicative lifespan of less than 20 PDs (Green et al., 1977; Stoppler et al., 1997). This differences highlight that feeders increase the proliferative lifespan of HKs. However, it is still not entirely clear whether feeder cells are actually necessary for the episomal maintenance of HPV16 in HKs.

The use of feeder fibroblasts has been shown to prolong the E6 and E7 mRNA expression in keratinocytes by approximately 50 PDs longer than when these cells were grown on plastic (Fu et al., 2003). While there is no direct evidence that shows feeders importance in maintenance of HPV16 episomes, both HPV31 E6 and E7 oncoproteins have been demonstrated to be necessary for episomal maintenance (Thomas et al., 1999). A separate study by Park and Androphy (2002) demonstrated that E6 and E7 activities (p53 degradation and Rb binding)

were necessary for maintenance of HPV16/31 chimeric genomes in primary keratinocytes. On the contrary, it has been reported that HPV16-E7 deficient genomes were maintained as stable episomes after transfection into an immortalised keratinocyte cell line (Flores et al., 2000). Similar to this study, the work carried out in our laboratory has shown that while HPV16 E7 is not necessary for episomal maintenance of immortalised keratinocyte cell line, NIKs cells, HPV16 E6 is necessary (Ken Raj, personal communications). This discrepancy in E7's necessity in promoting episomal maintenance between primary and immortalised keratinocytes could be owed to the immortalisation or anti-apoptotic activity of E7. In primary cells, HPV may have evolved to require E7 predominantly to keep these cells alive and as a secondary effect, to maintain HPV genomes. However, after keratinocytes have achieved immortalisation, the immortalisation function of E7 is no longer needed, which could explain how immortalised cell lines did not require E7 for maintenance of HPV genomes. Collectively, the HPV16 E6 and E7 oncoproteins were thought to provide a suitable environment for HPV maintenance by attenuating the cell cycle checkpoints that block long-term retention of extrachromosomal DNA (Thomas et al., 1999; Garner-Hamrick et al., 2004). It has also been shown that the long-term maintenance of HPV episomes in culture could eventually lead to integration over time (Jeon et al., 2005).

Aside from this, one of the DNA damage response protein, ATM, has been shown to be necessary for HPV viral genome amplification in calcium-induced differentiated keratinocytes (Moody and Laimins, 2009). However, in monolayer culture of undifferentiated cells, lack of ATM activity did not affect HPV episomal maintenance.

1.14 Radiosensitivity of cervical cancer cells

For the interests of determining response of cervical cancer cells to radiotherapy, many studies have been carried out with the attempt to elucidate the mechanisms underlying a radiosensitive or radioresistant phenotype using HPV-positive cell lines (Eastham et al., 2001; Vozenin et al., 2010). Most *in vivo* data of cervical

carcinoma patients implied good prognosis of cervical cancer patients to radiotherapy. Settle et al. (2009) reported one of the most prominent finding that correlated HPV infections with an excellent prognosis of squamous cell carcinoma head and neck cancer (SCCHN) in response to radiotherapy. The finding suggested that the presence of HPV strongly sensitises head and neck tumours to chemoradiation and parallels with the increased treatment sensitivity of patients with cervical cancer (Eifel et al., 2004; Fakhry et al., 2006; Settle et al., 2009). In support of this finding, an *in vitro* study showed increased radiosensitivity of head and neck cancer cell lines (Gupta et al., 2009). These HPV-positive cells contained integrated HPV genome to match clinical tumours and was found to have activation of PI3-K-Akt signalling pathway and possibly increased E6-mediated p53 degradation (Gupta et al., 2009). The latter was also found in cervical cancer cell lines that expressed HPV16 E6, where the combined degradation of p53 and activation of aurora A led to increased radiosensitivity (Shin et al., 2010).

Although there are increasing evidences from *in vitro* data whereby HPV-positive cells lines were found to be more sensitive to radiation, there has been considerable controversy regarding the outcome of cells to radiation. For example, HPV16- or 18-positive cells were found to be resistant to cisplatin, 5-fluorouracil and radiation treatments (Saxena et al., 2005). In addition, HPV16 E6-expressing tumours were radioresistant and have been found with an increase in the DNA repair enzyme, excision repair cross-complementing rodent repair deficiency, complementation group 1 (ERCC1) (Hampson et al. 2001). The variability in radiation response of HPV-positive cells may be owed to the status of p53 mutations in the cells (Rantanen et al., 1998; Sionov and Haupt, 1999; Komarova et al., 2004). The radiation response in these cells was shown to be more sensitive especially when HPV16 E6 is present (Shin et al., 2010). One of the explanations for this is that E6 is able to abrogate radiation-induced cell cycle arrest through a p53-dependent pathway to a certain level (Song et al., 1998). In addition, the discrepancies between the *in vivo* and *in vitro* data can also be explained by the integration of HPV genome into cellular genome in the former that will enhance chromosomal and genomic instability (Pett et al., 2004; Kadaja et al., 2009).

There are many other factors that play a role in determining the outcome of cells to radiation, such as competence of the DSB repair and efficiency in induction of cell cycle checkpoints (Eastham et al., 2001). Cell signalling pathways such as epidermal growth factor receptor (EGFR) and PI3K/Akt pathways have also been implicated in signalling to radiation response (Gupta et al., 2009; Vozenin et al., 2010). Cells that expressed HPV16 E7 markedly activate Akt/PKB, thereby inhibiting apoptosis in these cells and potentially increase the oncogenic potential of the virus (Pim et al., 2005)**.** The increased expression of Akt has been associated with resistance to radiation in cervical cancer (Kim et al., 2006). HPV18 E6 variants has also been shown to increase phospho-PI3K-proteins, suggesting that HPV18 differentially activate cell-signalling pathways such as Akt/PKB and MAPKs that are directly involved in cell survival and proliferation (Contreras-Paredes et al., 2009).

In addition, p73 protein, which is a family member of p53, is resistant to degradation by E6 and has been implicated in cellular response to radiation-induced damage (Liu et al., 2006). p73 induces apoptosis in a manner similar to p53, is able to activate p53-responsive genes. p73 expression has been found to be prominent in p53-impaired cervical cancer cells and may be the determinant of cellular radiosensitivity (Liu et al., 2006; Vozenin et al., 2010). The complex molecular mechanisms revolved around radiation response of cervical cancer cells remains to be elucidated.

As adjuvant to radiotherapy, targeting specific molecules to inhibit genes that are involved in radiation response could increase radiosensitivity of cancer cells. Some molecular markers that are frequently found in HPV-positive cells that could be inhibited are E6/E7, p53, p73, p16, VEGF, EGFR, and COX-2. For example, the inhibition of E6 and E7 using Cidofovir or glucocorticoid inhibitors can modulate radiosensitivity of cervical cancer cells (reviewed in Vozenin et al., 2010). In particular, treatment of a PI3K inhibitor known as LY294002 has been shown to have radiosensitising effects on cervical cancer cells, through inhibition of DSB repair (Lee et al., 2006; Fuhrman et al., 2008). LY294002 is a broad inhibitor across all major classes of PI3Ks and PIKKs (targeting ATM, ATR, and DNA-PK) (Salles et al., 2006).

Thesis Aims

The introduction covers inter-related disciplines in biology since the aims of this thesis were derived from parallel observations in wide areas of research. Our main interest lies in the co-culture system of keratinocytes-irradiated feeder cells that is routinely used to recapitulate HPV's life cycle *in vitro*. As the culture condition involves plating non-irradiated keratinocytes (NIKs) over a feeder layer of irradiated fibroblasts, it bears similarities to studies in which radiation-induced bystander effects (RIBE) have been identified. It was our interest to characterise the alterations inflicted on NIKs as a result of co-culture with feeder cells, as this ought to influence interpretations of any DNA damage studies utilising NIKs cells.

1) To ascertain if NIKs (+/ - HPV16) display DNA damage phenotypes as a result of co-culture with irradiated fibroblasts.

A comparison was made between NIKs (+/ - HPV16) cells cultured with or without irradiated fibroblasts. The aim was to ascertain if keratinocytes were in receipt of DNA damaging agents as a result from being in co-culture with the feeder cells. This knowledge is important to help us consider the actual DNA damage responses that occur from interaction of HPV with the host cell's DNA damage surveillance system.

2) To investigate if HPV16 can activate the DNA damage signalling in NIKs.

The levels of DNA damage response proteins were assessed in NIKs containing HPV16 cells. To investigate if HPV16 E6 and/ or E7 oncoproteins are able to activate cellular DNA damage signalling, we also assessed the levels of DNA damage response proteins in NIKs cells expressing E6 and/ or E7 proteins.

3) To investigate if the presence of feeders affects the way by which NIKs (+/ - HPV16) cells respond to direct gamma radiation.

Following direct gamma radiation, the abilities of NIKs (+/ - HPV16) cells in different culture conditions (+/ - feeders) to activate their DNA damage-response

proteins were assessed. To ascertain if feeders altered the way NIKs cells respond to direct DNA damage, a comparison was made between NIKs with and without feeders. To assess if the presence of HPV16 and/ or feeders altered the way NIKs cells respond to direct DNA damage, a comparison was made between NIKs (+/ - HPV16) with and without feeders.

4) To assess the cellular consequences of subjecting HPV16-containing cells to direct gamma radiation.

To assess the consequences of HPV16-induced DNA damage on survival of NIKs cells after direct gamma radiation, the clonogenic capacities of NIKs (+/ - HPV16) cells were analysed thereafter.

5) To investigate if feeder cells were necessary for the maintenance of HPV16 DNA episomes in NIKs.

The necessity of feeders to maintain HPV16 DNA in NIKs cells was assessed through measurements of HPV DNA copies per cell throughout ten passages (or 30 population doublings). The necessity of irradiation of feeders or direct cell-to-cell contact between feeders and keratinocytes was also ascertained.

6) To investigate if ATM was necessary for the maintenance of HPV16 DNA episomes and viral genome amplification in NIKs.

The effect of ATM knockdown on maintenance of HPV16 DNA was assessed in NIKs (+/ - HPV16) monolayer cells, through quantification of the HPV DNA copies per cell throughout ten passages (or 30 population doublings). To ascertain the effects of ATM knockdown on HPV16 genome amplification in differentiating cells, an organotypic raft culture was established, whereby the HPV DNA copies were quantified prior to and after cellular differentiation.

Chapter 2: Materials and Methods

2.1 Materials, Chemicals, Reagents and Kits

All reagents and chemicals, except where specified, were purchased from Sigma-Aldrich Company Ltd. (UK), BDH Laboratory Supplies (UK), Invitrogen, Fisher Scientific (UK) and VWR (UK).

Table 2.1: Chemicals and Reagents

Chemicals and Reagents	Supplier
Acrylamide	National Diagnostics
Agarose	Bio-Rad (UK)
Ammonium persulfate (APS)	Bio-Rad (UK)
Benzonase	Novagen
DAPI 4',6-diamidino-2-phenylindole	Molecular Probes
Dulbecco's modified Eagle's medium (DMEM)	PAA
Ethidium bromide	Bio-Rad (UK)
F-12 Ham medium	PAA
Fetal calf serum (FCS)	Perbio Science Ltd. (UK)
Precision Plus protein Dual colour marker	Bio-Rad
Protease inhibitor tablet	Roche
QPCR SYBR Green ROX mix	Thermo Fischer Scientific
Skimmed milk (Marvel)	Premier International Foods
TEMED (N,N,N',N'-Tetramethylethylenediamine)	Bio-Rad (UK)

2.2 Growth media, Buffers, Solutions, and Antibodies

2.2.1 Growth media

NIKs cells were cultured in F-medium (3 parts F-12 Ham: 1 part DMEM) supplemented with 5% FCS, 1% penicillin/streptomycin (stock of 10,000 units penicillin and 10 mg of streptomycin/ml), 24 μg/ml adenine, 8.4 ng/ml cholera toxin, 5 μg/ml insulin, 0.4 μg/ml hydrocortisone, and 10 ng/ml EGF. J2-3T3 cells were cultured in DMEM supplemented with 10% FCS. For freezing of cell lines, freeze media containing 50% FCS, 40% F-medium, and 10% DMSO was used.

2.2.2 Buffers and Solutions

Table 2.2: Buffers and reagents

5 x denaturing loading buffer	5% SDS, 50% glycerol, 0.1 M DTT, 0.25 M Tris (pH 6.8), 0.5% bromophenol blue
10 x loading buffer	50% glycerol, 0.5% bromophenol blue, 0.4% xylene cyanol
Luria Bertani (LB) medium	1% Tryptone, 0.5% Yeast extract, 1% NaCl
LB agar	LB broth plus 2% Bacto agar
Penicillin/streptomycin stock (antibiotics for cell culture)	0.6% penicillin, 1% streptomycin
Phosphate buffered saline (PBS)	0.17 M NaCl, 3.3 mM KCl, 10 mM Na_2HPO_4, 1.8 mM KH_2PO_4, pH7.4
SDS electrophoresis buffer	25 mM Tris base, 192 mM glycine, 0.1% sodium dodecyl sulfate (SDS)
Transfer buffer	30 mM Tris base, 240 mM glycine, 10% methanol
Trypsin-EDTA	0.14 M NaCl, 2.7 mM KCl, 8.5 mM Na_2HPO_4, 1.5 mM KH_2PO_4, 0.27 mM EDTA, 0.13% trypsin, 0.001% phenol red, pH 7.6 - 7.8
Tris acetate EDTA (TAE)	0.04 M Tris-acetate, 0.001 M EDTA
Tris Buffered Saline (TBS)	50 mM Tris, 150 mM NaCl, pH 7.4

2.2.3 Antibodies

The primary and secondary antibodies that were used in western blotting and/or immunofluorescence are listed below.

Table 2.3: Primary and secondary antibody supplier information

Antibody	Supplier	Catalogue number	Dilution
ATM	Abcam	2C1(1A1) ab78-100	1:2000
ATM-S-1981	Rockland	600-401-398	1:1500
ATR	Abcam Pl	ab10312	1:20000
DNA-PKcs	BD pharmingen	556456	1:1500
γH2AX (serine 139) for immunofluorescence	Millipore	#05-636	1:200
γH2AX (serine 139) for western	Bethyl Lab	A300-081A	1:1500
H2AX for western	Bethyl Lab	A300-082A	1:1500
p53	Santa Cruz	DO-1	1:1500
Phospho-p53 (serine 15)	NEB	9284	1:1500

Antibody	Supplier	Catalogue number	Dilution
Phospho-53BP1	NEB	2674s	1:800
NBS1	Novus	NB100-277A	1:1000
RPA32 serine 33-P	Bethyl Labs	BL744#A300-246A	1:1000
Phospho-Akt (serine 473)	NEB	4058	1:1000
MAdCAM-1	Serotec	MCA1551	1:500
Hsp70 (W27)	Santa Cruz	SC-24#D2604	1:3000
Actin	Santa Cruz	SC-1616(1-9)	1:1000

HRP conjugated secondary antibodies used for western blotting were purchased from GE Healthcare, UK. Secondary Alexa conjugated antibodies used for immunofluorescence were purchased from Molecular Probes, UK.

2.3 Keratinocyte cell culture techniques

2.3.1 Maintenance of cells in monolayer culture

J2-3T3 cells

The J2-3T3 cells, an immortalised fibroblast cell line, are used as a feeder layer to support the growth of keratinocytes in this study. These cells were originally recovered from Swiss albino mouse embryos (Todaro and Green, 1963). The 3T3 cells were maintained at 37°C in a 5 % CO_2 and grown to about 80% confluence, after which they were passed at a splitting ratio of 1:10 to 1:20. To harvest these cells, they were washed with 5 ml of PBS and added with trypsin-EDTA to be incubated at 37°C for 1 minute. When fibroblasts are lifted off the surface, the trypsinisation reaction was neutralized by DMEM. The usage of these cells was continued up till passage 20 (P20), after which the cells were replaced by a new stock of early passage 3T3. The early passage 3T3s were frozen (by adding 1 ml freeze media) down at -70°C overnight and transferred to liquid nitrogen.

NIKs and NIKs HPV (wild type HPV16 cell lines)

In this study, **N**ormal **I**mmortalised **H**uman **K**eratinocytes **(**NIKs) cells were used on their own and as host cells for HPV16. NIKs cells are spontaneously

immortalised keratinocytes isolated from human neonatal foreskin following successive passages of their parental Bc-1-Ep cell line (Allen-Hoffman et al., 2000). NIKs cells that contain wild type episomal HPV16 DNA were established following co-transfections with 0.8 μg recircularised W12-HPV16 DNA (Section 2.5.4) and 0.2 μg of pCDNA6A vector that contained a Blasticidin resistance gene (Invitrogen, Carlsbad, CA) (courtesy of Kenneth Raj; NIMR, London, UK). Cells were plated at clonal density and were subjected to blasticidin selection (6 μg/ml) for several days. When blasticidin-resistant colonies became visible, they are expanded into 6-well plates.

NIKs and NIKs HPV cells were maintained in 10 cm tissue culture dishes (Nunc) in F-medium as described above at 37°C in a 5 % CO_2 incubator. NIKs and NIKs HPV cells were maintained on 2 x 10^6 J2-3T3 (denoted as Irr 3T3) cells that have been lethally irradiated with 60 Gy. Following their attachments, NIKs and NIKs HPV cells were passed on to a feeder layer of Irr3T3 and grown to 80 – 90% confluence, with media change every two days. The feeder layer was renewed every 4 days. To pass NIKs and NIKs HPV cells, the cells were washed with PBS and 1 ml of trypsin was used to detach the feeder layer. The detached feeders were removed and the keratinocytes were detached by fresh trypsin for 5 min incubation at 37°C. The trypsin was neutralised with F12 media and the cells were plated on a dish containing fresh Irr 3T3. The cells were counted on a haemocytometer using a phase contrast light microscope (Nikon Eclipse TS100, UK).

2.3.2 Weaning keratinocytes off feeder cells

To study NIKs and NIKs HPV in the absence of feeders, it was required to culture the cells without feeders for 3-4 passages. Thereafter the cells were plated onto plate A with no feeders, and plate B with feeders (Figure 2.1) for experimental use. The former was used as a comparison to assess the effects of feeder cells. These keratinocytes were used and cultured until Passage 10.

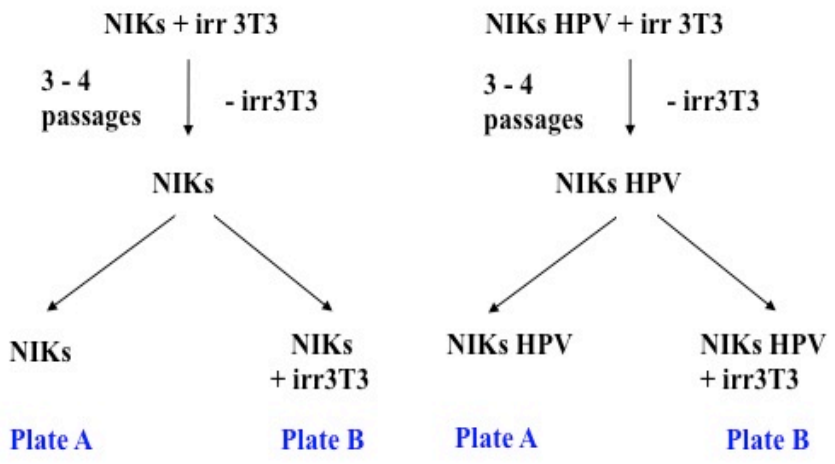

Figure 2.1: Preparation of cells for studying the effects of feeder

2.3.3 Culture of cells on 6-well transwell plates

In order to assess the necessity of (1) cell-to-cell contact between keratinocytes and feeders or (2) irradiation of feeders to elicit biological effects on keratinocytes, several culture conditions were designed. Keratinocytes and feeder cells were co-cultured in Transwell plates (Fischer), which consists of 6 inserts that are pre-loaded in a 6 well cluster plate. The insert contains a 0.4 μm permeable polyster membrane, which allows exchange of factors between two different cells that are cultured on two different surfaces – the surface of the well or membrane of the transwell insert (Figure 2.2). 3.5 x 10^5 keratinocytes that were resuspended in 4 ml of F-medium were plated on the surface of the well and allowed to adhere overnight at 37°C. The next day, overnight medium was replaced. 3 x 10^5 feeder cells resuspended in 1 ml medium were plated either on to the surface of the well or transwell membrane, the exact experimental set-ups and their purposes are described in Figure 2.2. Where no feeders were grown on a transwell membrane, an insert was still added on top of a well to control for any potential cytotoxic effect caused by inserts. Whenever necessary, the keratinocytes were harvested by trypsinisation (as described in Section 2.3.1) and subjected to western blotting or immunofluorescence analysis.

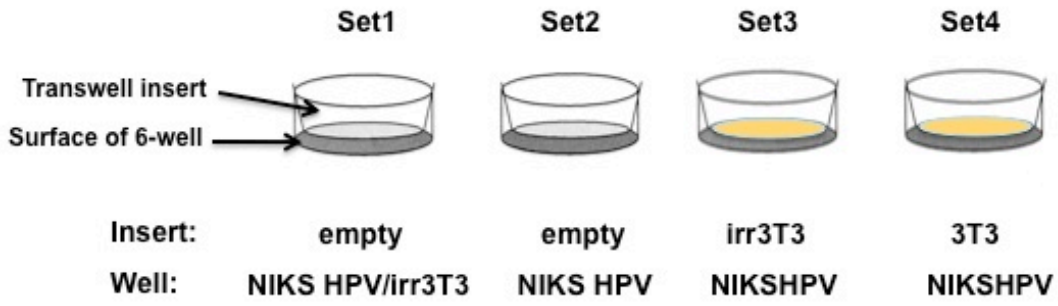

Set 1	NIKs HPV in direct contact with feeders - standard culture as control
Set 2	NIKs HPV grown without feeders - Test the necessity/effect of feeders
Set 3	NIKs HPV co-cultured with irradiated feeders, separated by insert - Test the necessity of cell-to-cell contact
Set 4	NIKs HPV co-cultured with non-irradiated feeders, separated by insert - Test the necessity of irradiation of feeders

Figure 2.2: Figure illustrating the keratinocyte-feeder culture conditions in Transwells and their purposes.

2.3.4 Keratinocyte organotypic raft culture

Table 2.4: Materials and reagents for raft culture

Materials	Supplier	Catalogue number
Collagen 1, Rat tail (10X 100mg)	BD (VWR)	734-1097
Deep well plate (BDBioCoat) 6-well (3X)	BD (VWR)	734-1095
Transwell Permeable Supports (3X)	Costar (Fisher)	TKT526-010M
Thick cotton pads	Schleicher & Schuell Bio Science Inc.	740-E
C8:0 – 1,2-dioctanoyl-sn-glycerol	Sigma	D5156-10mg
10X DMEM	Promocell	C-71190

Table 2.5: Media for raft culture

Organotypic raft culture media and supplements	
Media name	**Components**
J2-3T3 media	10% FCS/DMEM
F-medium (keratinocyte plating media)	3 parts DMEM: 1 part F-12 Ham, 5% FCS, 24 μg/ml adenine, 5 μg/ml insulin, 8.4 ng/ml cholera toxin, 0.4 μg/ml hydrocortisone
Cornification media	F-medium with 10 μM C8:0

i) Preparation of dermal equivalent for rafts

To prepare dermal equivalents (collagen matrix) for growing raft cultures, 20 ml collagen was mixed with 2.5 ml 10x DMEM, 60 μl 10 M NaOH, and 2.5 ml reconstitution buffer (containing 6 x 10^6 J2-3T3 fibroblasts) on ice. 3.6 ml of the collagen matrix solution was pipetted into the centre of each insert, in the 6 well plate provided with the inserts. The 6 well plate was left in 37ºC for 30 min to allow the collagen to solidify. After this, the inserts were transferred into deep well plates containing 20 ml of F-medium (with EGF) per well and equilibrated overnight at 37ºC.

ii) Seeding and differentiation of keratinocytes

Once the collagen has solidified, any medium was removed before 1 x 10^6 keratinocytes was mixed with 1 ml of F-medium and added dropwise onto each insert. The collagen was submerged in medium and incubated at 37ºC. The cells were grown to confluence in this submerged culture for 3 to 4 days, with media change every two days. On the fourth day, the medium was removed and 3 pieces of sterilized cotton pads (1 x 1 inch) were loaded on to the outer well (under the transwell inserts). 12 ml of cornification media (10 μM C8:0, no EGF) was added and the whole setup was incubated at 37ºC 5 % CO_2 and this was considered as Day 1. Exposure to air allows cornification to begin and is necessary to establish the epithelial architecture of the raft culture (Wilson and Laimins, 2005). At Day 3, medium from the outer well and any medium from the insert was removed and 9.5 ml of F-medium was added into the outer well, ensuring that no medium was left in the insert at all time after the lifting of the raft from Day 1 onwards. The

medium change for the outer well was carried out every two days while the raft cultures were left to differentiate for a total of 10 to 12 days post lifting. When the rafts were ready to be harvested for protein and DNA, the raft was peeled away from the semi-permeable transwell membrane, removing any excess collagen using a sterile scalpel. The raft consisting of intact keratinocyte layers is then subjected to total DNA extraction using QIAamp DNA mini kit according to the manufacturer's instruction (Section 2.5.3). Protein lysates were also prepared from the rafts as described in Section 2.9.

2.4 Manipulation of keratinocytes

2.4.1 Production of retrovirus

For production of retrovirus, plasmid DNA was initially transfected into Phoenix A cells using the polyethylinimine (PEI) method. Briefly, reagent A (655 μl plain DMEM, 45 μl of 1 mg/ml PEI) and B (15μg plasmid DNA, 700 μl with plain DMEM) were mixed by vortexing and incubated at room temperature for 15-30 min. 3.6 ml of plain medium was added to A and B mixture before gently pipetting it in to the plate containing Phoenix cells. The transfection mix was removed after 5-7 hours and replaced with 10 ml of F-medium. On the third day, the medium that contained retroviruses were filter sterilized through 0.2 μm filters and used for infection. An infection mixture was prepared by mixing 1 ml of virus, 3 ml F12, 10 μl of 4 mg /ml polybrene stock, along with supplements and EGF that were required for keratinocyte culture. This mixture was used to infect 0.5 x 10^6 NIKs cells per well on a 6-well plate. The plate was then incubated at 37ºC for at least 6 hr and then the medium was replaced with F-medium. The next day, infected cells were passed from 6 well plate into 10 cm plate with Irr 3T3. Antibiotic selection was carried for sufficient time until the cells in control-uninfected plate were all dead. For selection of *pRETROSUPER shATM and shGFP plasmids (kindly given by Yosef Shiloh, Biton et al., 2006), antibiotic selection was carried out using 0.75 μg/μl puromycin for 4 days. For selection of **LXSN plasmids (kindly given by Denise Galloway) (Halbert et al., 1992), 250

μg/ml of neomycin was added to cells for 6 days. After selection was completed, the cells were passed in to a new plate with Irr 3T3.

* For shRNA expression silencing of ATM and GFP, the sequences were:
ATM: 5′-
gatccccGACTTTGGCTGTCAACTTTCGttcaagagaCGAAAGTTGACAGCCAAAG
TCtttttggaaa-3′

GFP: 5′-
gatccccGGAGCGCACCATCTTCTTCttcaagagaGAAGAAGATGGTGCGCTCCtttt
tggaaa-3′

** Sequences of LXSNE6, LXSNE7, and LXSNE6/E7 obtained from Halbert et al. (1992):

LXSNE6	Nucleotide sequence 56-562[a]
LXSNE7	Nucleotide sequence 551-875[a]
LXSNE6/E7	Nucleotide sequence 56-875[a]

[a]Nucleotide sequences are designed according to Seedorf et al. (1985).

2.5 Molecular biology techniques

2.5.1 Bacterial transformation

50 ng plasmid DNA was added to the XL-1 Blue supercompetent *E. coli* cells on ice for 30 min. Cells were then heat shocked to 42ºC for 45 seconds and placed in ice for 2 min. The *E. coli* cells were then added to 1ml SOC medium in a 1.5 ml ependorf tube and incubated in an orbital shaker at 37ºC for 90 min. 250 μl of transformed *E. coli* was then added to an LB agar plate containing 0.1 mg/ml ampicillin, incubated at 37ºC overnight. The colonies that arose on the LB plate were picked and transferred into 3 -5 ml of LB broth with 0.1 mg/ml ampicillin. The seed culture was shaken at approximately 300 rpm at 37ºC for 6 hr. The expanded culture was subjected to mini-prep DNA extraction using the QIAprep spin mini-prep kit (Qiagen, UK). For large-scale DNA extraction, 250 μl from the seed culture was transferred in to 250 ml of LB broth with 0.1 mg/ml ampicillin at

37ºC overnight and shaken at 220 rpm. DNA was extracted using the HiSpeed Maxi Kit (Qiagen, UK) according to the manufacturer's instructions. DNA was eluted in 500 µl of dH2O.

2.5.2 DNA Restriction Digest and TAE Agarose gel electrophoresis

All plasmid DNA preparations were examined by restriction endonuclease (RE) digestion to ensure that the insert was correct. 0.3 µg plasmid DNA was incubated with 10 units of RE and their RE buffers. The DNA was digested at 37ºC overnight. Agarose gel electrophoresis was used to determine the size of digested products. 1% agarose was dissolved in TAE, containing 1 µg/ml ethidium bromide. Samples were mixed with 10 x loading buffer and DNA was electrophoresed for 1 hr at 100V. DNA bands were visualized by UV light and compared to DNA markers (Invitrogen, UK) of known sizes.

2.5.3 Extraction of total genomic DNA from keratinocytes

Cells were washed in PBS and centrifuged at 3000 rpm for 5 min. The supernatant was aspirated and the resultant cell pellet was immediately placed on ice to prepare for removal of RNA. Next, 200 µl PBS-RNAseA (2mg/ml) and this mixture were incubated at 37^{o}C for 5 min. The total DNA extraction was carried using the QIAamp DNA mini kit following the manufacturer's instructions. DNA was eluted from columns using 100 µl Buffer AE. DNA was quantified using a Nano-drop 8000 spectrophotometer.

2.5.4 Recircularisation of W12-HPV16 DNA

To produce recircularised HPV16 DNA, the W12-HPV16 DNA sequence was excised from pSPW12 plasmid through restriction enzyme digestion comprising the following reaction mixture: 5 µg pSPW12 plasmid, 2 µl of BamHI (10U/ µl), 3 µl of 10X reaction buffer in a volume of 30µl for 2.5 hours at 37^{o}C. Next, BamHI is inactivated at 75°C for 20 minutes and the DNA was cooled to room temperature. Following this, the digested DNA was then recircularised by ligation using T4 DNA ligase (NEB) at 16°C overnight. The ligated DNA products were mixed with 10 ml PB buffer from Qiagen mini-prep kit and the mixture was

passed through a column using the Vac-Man Jr. Laboratory Vacuum Manifold. When all the solution has gone through the column, 0.75 ml PE buffer (from the Qiagen mini-prep kit) was added into the column. The DNA was then eluted with 55μl of elution buffer (from the Qiagen mini-prep kit) and analysed by agarose gel electrophoresis. Successful recircularisation of the viral DNA should yield a supercoiled band at about 7kb.

2.5.5 Quantitative PCR (Q-PCR)

Quantitative real-time (RT) polymerase chain reaction was performed to determine the HPV DNA copy number per cell in NIKs HPV. The amplification of HPV16 E6 and GAPDH sequences were carried out using the forward and reverse primers as depicted in Table 2.6. The region of the GAPDH gene that the primers span contains human GAPDH DNA sequence, with the least amount of homology to the mouse GAPDH DNA sequence. Therefore, any contamination by mouse J2-3T3 fibroblasts would not be reflected in the readout. The Q-PCR reaction was carried out using a SYBR Green ROX mix reagent that contained a Thermo Start DNA polymerase in 96 well plates using an ABI 7000 sequence detector system.

Table 2.6: Q-PCR primer sequences

Target DNA	Primer sequence
HPV16 E6 (Forward)	5'-AGCGACCCAGAAAGTTACCA-3'
HPV16 E6 (Reverse)	5'-GCATAAATCCCGAAAAGCAA-3'
GAPDH (Forward)	5'-CGAGATCCCTCCAAAATCAA-3'
GAPDH (Reverse)	5'-CATGAGTCCTTCCACGATACCAA-3'

To produce statistical significance, each sample was tested in triplicate wells. In one reaction, the volumes of each reagent are 12.5 μl of 2X Sybergreen Mix, 1.75 μl of forward primer (1μM), 1.75 μl of reverse primer (1μM), 7.75 μl of dH_2O, and 3.0 μl of DNA. The DNA concentrations were diluted to 4 ng/μl for every sample. To prepare the reaction mix, 9 μl of each DNA sample was mixed with 66 μl of master mix was transferred into a 0.5 ml eppendorf tube. Following this, 25 μl of the mixture was loaded into each well of the 96-well plate and a Q-PCR

reaction was carried out using the cycling parameters that are shown in Table 2.7 and 2.8.

Table 2.7: Q-PCR cycling parameters
1) 50°C for 2 minutes x1
2) 95°C for 15 minutes x1
3) 95°C for 15 seconds x40
4) 60°C for 1 minutes x1
Table 2.8: Dissociation parameters
1) 95°C for 15 seconds x1
2) 60°C for 20 seconds x1
3) 95°C for 15 seconds x1

GAPDH was used as a normalizing gene and the HPV DNA copy numbers were calculated using the standard curve equations for HPV16 and GAPDH primer pairs:

Standard curve equation for HPV16 E6: y = -3.3871logx + 36.577

Standard curve equation for GAPDH: y = -3.473logx + 35.932

For evaluation of maintenance of HPV16 DNA copy number in cells grown in monolayer or raft culture, Q-PCR was performed on DNA extracted from keratinocytes from passage 1 (P1) to passage 10 (P10). The total genomic DNA was extracted by using QIAamp DNA mini kit. In addition, Southern blotting was carried out to evaluate the physical state of HPV DNA.

2.5.6 Southern blotting

For analysis of whether HPV16 DNA existed as integrated or un-integrated form in NIKs, Southern blotting was performed. To cut high molecular weight DNA strands into smaller fragments, DNA was first digested using the restriction endonuclease (RE), HindIII (Roche, UK) in a 40 µl reaction mix as follows: 5 µg genomic DNA, 4 µl of 10x restriction buffer, 2 µl HindIII, and remaining volume with dH_2O. The RE digests were incubated at 37ºC overnight. The following day, the digested DNA samples were loaded in to the wells of 1% TAE agarose gel that contained 40 µl (10 mg/ml) ethidium bromide. The samples were then

separated by gel electrophoresis at 100V for 2 hr. After that, the gel was pre-soaked in denaturation solution (0.5 M NaOH, 1.5 M NaCl) for 45 min, washed briefly with dH_2O and then soaked in a neutralization solution (1 M Tris-HCl, 1.5 M NaCl pH 8.0) for 30 min. DNA from the gel was then transferred to nylon membrane (Millipore) via capillary action, using 20x SSC overnight. After the transfer, the membrane was dried completely before DNA was cross-linked to membrane using 5,000 $\mu J/cm^2$ UV. The membrane was then pre-wet before it was blocked with 10 ml of pre-hybridisation solution (0.5 ml of 100X Denhardt, 0.25 ml of 20% SDS, 0.2 ml of 5 mg/ml Herring sperm DNA, 2.5 ml of 20X SSPE) for 4 hr. To generate radiolabelled probes, random-priming DNA-labelling method was used. Briefly, 50 ng of pSPW12 was labeled with 5 µl of alpha-^{32}P-dCTP using the Ready to Go labeling system (GE; UK) and cleaned using a G50 Sephadex column (GE, UK) in accordance of the manufacturer's instructions. The radiolabelled probes were resuspended in 10 ml of hybridisation solution (with the same contents as pre-hybridisation solution) and incubated with membrane at 68ºC overnight in a rotator oven. The following day, the membrane was washed at room temperature with wash solution I (2x SSC, 0.1% SDS) for 15 min interval twice. Subsequent washing step was performed at 68ºC using wash solution II (0.2x SSC, 0.1% SDS). The membrane was then exposed to phosphorimager cassette and analysed on Storm 860 phosphorimager scanner overnight. Alternatively, membrane can also be exposed to Kodak MXB X-ray film. Films can also be developed using a Fujifilm FPM-2800A processor (UK).

2.6 DNA damage assay (comet assay)

Comet Assay (Adapted from Olive and Banath, 2006)

i) Preparation of stock solutions

1. 0.5 M Na_2EDTA (Add 55.8g EDTA and 6.4 g NaOH to 270 ml distilled water). Stir for approx 1 hour (pH should be ~7.4) and adjust pH to 8.0 with additional 5M NaOH
2. 5 M NaOH (add NaOH slowly to ice-cold distilled water)
3. 5 M NaCl
4. 2 mg/ml of Propidium Iodide (PI)

ii) Preparation of comet assay solutions

1. Alkaline lysis solution for single-strand break detection
   Make cold alkaline lysis solution (1.2 M NaCl, 100 mM Na2EDTA, 0.1% sodium lauryl sarcosinate, 0.26 M NaOH: pH more than 13). Pre-chill in cold room for 4 hours. Prepare fresh on day of experiment.

2. Alkaline rinse and electrophoresis solution
   0.03 M NaOH, 2 mM Na2EDTA (pH approximately 12.3)

iii) Sample preparation, Lysis and Electrophoresis

To prepare samples for comet assay, cells were embedded in a single layer of agarose on a plain glass slide pre-coated with agarose and dried. To prepare the cell suspensions, cells were suspended in Ca^{2+}- and Mg^{2+}-free phosphate-buffered saline (PBS), then mixed with low-melting-point agarose (Type VII; Sigma), in order to obtain a final concentration of 0.5% agarose and 2 x 10^4 cells/ml. To lay the cell suspension on pre-coated slides: 400 µl of the solution containing cells were mixed with 5 ml of agarose, after which 1.2 ml of this cell suspensions were loaded on a pre-coated slide and kept for 5 min on ice. To lyse the embedded cells, the slides were submerged in freshly prepared lysis buffer overnight at 4°C. After overnight lysis, slides were then transferred into the alkaline rinse solution for three washes at 20 min each. Slides were then transferred to a horizontal electrophoresis unit filled with fresh alkaline electrophoresis solution at 4°C. To

drive the migration of damaged DNA away from the body of the cell (cell nucleus), electrophoresis was performed for 20 min at 15 V and 50 mA. After electrophoresis, the slides were drained and rinsed twice with distilled water. To stain DNA, the slides were submerged in staining solution containing 2.5 μg/ml PI for 20 min, rinsed with distilled water, and air-dried for 30 mins before analysis. Comets were observed at 400x magnification using a fluorescence microscope (LEICA) and the distribution of DNA between the tail (damaged DNA) and the head (DNA within the body of the cell that were not damaged) were scored.

2.7 Irradiation of NIKs and NIKs HPV cells with Cesium-137 gamma rays

To check the cellular DNA damage response following direct ionizing radiation, NIKs or NIKs HPV cells were irradiated with 10 Gy of Cesium-137 (^{137}Cs) gamma rays in Gammacell 40 Exactor (MDS Nordion) under conditions of ambient oxygen. The dose rate was 0.81525 Gy/min. Prior to irradiation, keratinocytes were plated on feeder layer of irradiated 3T3 and incubated for 2 days. For each cell type, protein lysates were collected at 0 hr and after irradiation at 0.5, 2, and 4 hrs.

2.8 Clonogenic cell survival assay

2.8.1 Clonogenic assay setup

The clonogenic cell survival assay performed in our study was adapted from Franken et al. (2006). 2 x 10^5 NIKs and NIKs HPV cells were plated on a feeder layer and cultured overnight. The following day, the cells were subjected to 0, 2.5, 5, or 10 Gy of ^{137}Cs gamma-irradiation (Figure 2.3). Immediately after irradiation, these cells were trypsinised and resuspended to generate single cell suspensions. Next, these cells were serially diluted and counted. To assess the clonogenic survival of NIKs and NIKs HPV following irradiation, these cells were plated at the same seeding density. 160 cells were plated on individual dishes containing

feeders. The clonogenic survival of these cells was examined by allowing the cells to form colonies. After 14 to 21 days, staining with methylene blue was performed so the colonies were visible.

2.8.2 Methylene blue staining of tissue culture monolayers

Prior to staining of keratinocytes with methylene blue, the feeder cells were removed by squirting PBS on them. The cells were washed twice with PBS and then a solution of 1% methylene blue in 50% methanol/PBS was pipetted onto them to cover the entire surface of the plate. The plates were incubated at room temperature for 1 hr. Staining solution was decanted from the plates and cells were washed extensively with PBS. Plates were air-dried in the dark and the number of colonies was evaluated in each plate.

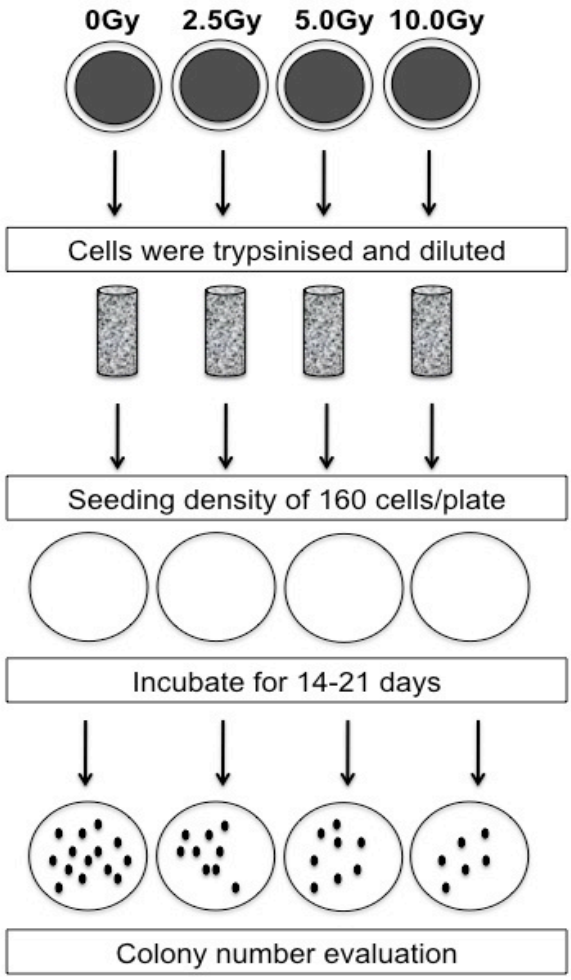

Figure 2.3: Steps involved in setting up a clonogenic survival assay.

2.9 Protein analysis

2.9.1 Protein extraction

Prior to harvesting cells for protein, the irradiated J2-3T3 cells on the plate were dislodged by squirting PBS on them. After ensuring that all feeders were removed by inverted microscopy, the remaining keratinocytes were then scraped off the plate into a tube and centrifuged at 6000 rpm for 5 min. The supernatant was aspirated and the cell pellets were resuspended in 200 μl ice-cold RIPA lysis buffer (1.5 ml 5M NaCl, 0.5 ml 10% Triton X-100, 0.25 g sodium deoxycholate, 0.5 ml 10% SDS, 2.5 ml 1M Tris pH 8.0, 0.5 ml 0.5 mM EDTA pH8.0) supplemented with protease inhibitor cocktail (Bio-Rad). The pellet resuspended in RIPA buffer is kept on ice for 20 min and vortexed every 5 min after which the cells were spun at 13,000 rpm at 4°C for 15 min. The clarified cell lysate was collected and the concentration was measured by the Bradford method and stored at -70°C before analysis.

For histone protein extraction, cells were subjected to the acid method. The acid extraction method is an efficient way to obtain proteins that may not be soluble in RIPA, which are proteins that are of neutral or alkaline pH. The pellet from the final centrifugation step of the RIPA lysis above is resuspended in 0.1 M HCl in PBS and left on ice for 10 to 15 min, with pulse vortex every 5 min. The cells were centrifuged at 13,000 rpm at 4°C for 15 mins and the supernatant that contain the acid-soluble proteins was collected. The acid lysates were aliquoted and the protein concentration was determined by Bradford assay according to the manufacturer's instructions (Bio-Rad). The aliquots were then stored at -70°C before analysis.

For protein extraction from rafts, the raft is first peeled away from the collagen and placed into a 1.5 ml tube with 100 μl PBS. The raft was centrifuged to the bottom of the tube at 6000 rpm for 5 mins and the PBS was aspirated from the tube. At this point, the raft pellet can be stored at -70°C. To continue with lysis, DNA elimination was first performed by addition of 2-3μl benzonase to the raft

pellet for 20 min on ice. The raft suspension was taken off ice, added with 200 µl of 10% SDS, and pipetted repeatedly to avoid precipitation. The suspension was added with 100 µl of raft lysis buffer (6% SDS, 0.03 M DTT, 1.7 M urea) and pulse vortexed. Following this, 50 µl of 5 M urea was added to the raft lysis solution and was heated at 95°C for 20 min with vortexing every now and then. After 20 min, the raft suspension was put on ice for 5 min. This step was repeated twice and then subjected to centrifugation at 13,000 rpm at 4°C for 15 mins. The supernatant, the raft protein lysates, was collected and the concentration was measured by the Bradford method and stored at -70°C before analysis.

2.9.2 Sodium dodecyl sulphate-polyacrylamide gel electrophoresis (SDS-PAGE)

Proteins from cell lysates were analysed by SDS-PAGE using the NUPAGE 4-12% Bis-tris gradient gel with 1.5 mm wells (Invitrogen). Protein samples were prepared by mixing a 5x SDS-PAGE denaturing sample loading buffer (see Table 2.2 for recipe) and boiled at 100°C for 5 minutes. Boiled samples and protein standards (dual colour marker, Bio-Rad, UK) were then loaded into the wells of the gel apparatus (Mini Protean II apparatus, Bio-Rad). The gel was then subjected to electrophoresis at a constant voltage of 130V in 1 x SDS-PAGE running buffer.

2.9.3 Western Blotting

To detect proteins that have been separated on SDS gels, western blotting was performed. To prepare for western blotting, a sheet of PVDF blotting membrane (Immobilon^{TM}, Millipore) was pre-soaked in 100% methanol for 10 sec and then washed in Western blot transfer buffer (see Table 2.2 for recipe). The separated proteins from the SDS gels were transferred to a PVDF membrane using a wet transfer system, Mini Transfer Blot (Bio-Rad, UK; filled with transfer buffer), at a constant voltage of 100 V overnight at 4°C. For western blotting of H2AX, the transfer time was shorten to 1 hr.

The membrane was incubated in blocking solution consisting of 5% Marvel skimmed milk powder in 1 x TBS/0.1% Tween 20. The membrane was then

incubated with primary antibody (see Table 2.3 for a list of antibodies) in 5% skimmed milk and 0.1% Tween 20, overnight at 4°C with gentle shaking. After the incubation, the membrane was washed with 1 x TBS/ 0.1% Tween 20 three times at 15 min interval. The membrane was then incubated for 1 hour at RT with secondary antibody solution containing HRP-conjugated secondary antibody from the relevant host (GE Healthcare, UK) diluted to 1:3000 in 5% skimmed milk/ 1 x TBS and 0.1% Tween 20. After an hour, the membrane was washed five times at 15 min intervals. Protein bands were visualised by chemiluminescence reagent (Immobilon Western Chemiluminescent HRP S, Millipore) and exposed to light sensitive Kodak MXB X-ray film (X-ograph imaging systems, UK).

2.10 Staining and imaging techniques

2.10.1 Immunofluorescence labelling of γH2AX

A day before the experiment, coverslips were placed in 10 cm dishes. The following day, Irr 3T3 cells were seeded onto plates containing coverslips and 1 x 10^6 keratinocytes were plated. For analysis of keratinocytes grown without feeders, no prior plating of feeder cells was done. Cells were stained with an anti-Phospho-Histone H2A.X (Ser 139) (clone JBW301) antibody. The cells were first fixed with cold methanol for 10 min at RT and permeabilised with ice-cold acetone for 1 min. Cells were blocked with 10% FCS in TBS-0.1% Tween-20 for 15 minutes at RT, and then washed in the same buffer 3 times for 5 mins each. Anti-γ-H2AX antibody was added at 1:200 dilution in TBS-0.1% Tween-20 2% BSA for 2 hr. Cells were then washed three times with TBS-0.1% Tween-20 and then incubated for 1 hr with 1:200 dilution of Alexa Fluor 488 in TBS-0.1% Tween-20 2% BSA. Next, cells were washed and DNA was stained with 1% μg/ml DAPI for 10 min, followed by washing three times. The coverslips were mounted 1-2 μl with Vectashield (Vector Labs). At least 10 random fields from each coverslip were imaged using a fluorescent microscope at 400x magnification or a Delta Vision imaging system.

2.10.2 Cell imaging

For high-resolution images, cells were scanned using a DeltaVision imaging system (Applied Precision DeltaVision Core) fitted with an Olympus IX 70 inverted microscope that employs a 100W mercury lamp. Deconvolution and image analysis began by taking a Z series, which is a series of images with the same X and Y coordinates but varying up and down the vertical focus (the Z axis). As a result, optical sections of the nucleus of cells that have punctate or pan-nuclear γH2AX staining can be obtained, which will allow us to determine the actual pattern of γH2AX phosphorylation at high resolution. Samples were observed using a 40x objective lens and were scanned using the following excitation (ex) filters and their emission (em) wavelengths: DAPI ex 359 nm, em 395-520 nm; Alexa 488 ex 488, em 505-685 nm. To scan through many sections of one nucleus, the upper and lower limits of the vertical focus (Z-axis) was set so that the desired number of sections was obtained at a particular depth. Each specimen was scanned with 10 sections. An image projection was produced by stacking each of the individual Z sections of both fluorescent probes into one image.

2.10.3 EdU cell proliferation assay for measurement of cell proliferation

For detection of cells that were undergoing DNA synthesis, keratinocytes were examined by using the Click-iT® EdU cell proliferation assays. The methods used were in accordance of the manufacturers instructions. EdU (5-ethynyl-2'-deoxyuridine) is a modified nucleoside that is incorporated during DNA synthesis. Detection of EdU molecules is based on a copper-catalyzed covalent reaction between an azide and an alkyne, which is an efficient reaction utilizing functional groups that do not occur naturally in biological systems. Incorporated EdU molecules has alkyne that can be detected with the Alexa Fluor 594 azide and visualised by immunofluorescence microscopy.

2.11 Synchronisation of cells in G1 phase of the cell cycle

2.11.1 G1 synchronisation

For growth in FCS- and EGF-deprived medium, the feeder cells and keratinocytes were previously trypsinised and washed to remove nutrient residues. To synchronize cell cultures in G1 phase, keratinocytes were grown in medium that was not supplemented with FCS or EGF for 4 days. For G1 block, the media in test plates were replaced with FCS- and EGF-free media. After 4 days, the test plates were nourished with media containing FCS and EGF to release cells from G1 block. The control for this experiment was a plate containing 5 x 10^5 NIKs cells that were grown on 3 x 10^5 J2-3T3 cells in complete F-medium. The test plates for this experiment included: plate with predominantly G1 NIKs following 4 days of nutrient deprivation, plate with NIKs that have been released (through medium replenishment) for 6 hr after G1 block, plate NIKs that have been released (through medium replenishment) for 24 hr after G1 block.

2.11.2 Propidium iodide staining of DNA for cell cycle analysis

To assess the proportion of cells in each phase of the cell cycle, the cells were stained with propidium iodide (PI). Feeders were removed by trypsinisation and squirting with PBS. NIKs cells were trypsinised, resuspended in PBS, and centrifuged at 2000 rpm. The supernatant was removed and the cell pellet was vortexed in their residual fluid. Cells were fixed with 1 ml of ice-cold 70% ethanol that was added drop wise during continuous agitation with vortex. The cell suspension at this stage was either stored at -20 or 4'C. Otherwise, cells suspension was centrifuged at 2000 rpm for 5 min and the supernatant was aspirated. The cells were then resuspended in 0.1 mg/ml RNAse and incubated at 37ºC for 15 min. Cells that were resuspended in RNAse-PBS were transferred in to FACs tubes containing 0.02 mg/ml PI and ready for flow cytometry analysis. DNA content was analysed using CellQuest software on FACSCalibur flow cytometer (Becton Dickinson). By plotting the cell counts versus FL2A, a histogram, which depicts four distinct phases of the cell cycle: the G0/G1-, S-, G2-, and M-phase. To discriminate G1 doublet from a G2/M single, FL2W was plotted versus FL2A in a dot plot graph. The data for DNA content was analysed using Win MD1 software.

Chapter 3: Biological consequences of culturing keratinocytes with irradiated J2-3T3 murine fibroblast feeder layer

Introduction

Investigation into the persistence of human papillomavirus (HPV) in keratinocytes is carried out by introducing HPV DNA into human foreskin keratinocytes. As such the keratinocyte cell line NIKs, is very useful because it is a spontaneously immortalised foreskin keratinocyte line (Allen-Hoffmann et al., 2000). Hence it is an inexhaustible source of foreskin cells. NIKs cells are cultured in the presence of lethally-irradiated murine fibroblast (J2-3T3) (Allen-Hoffman et al., 2000; Wise-Draper et al., 2009). This method of culture is not new and has been advocated for keratinocytes since the 1970s (Rheinwald and Green, 1975; Green et al., 1979). Although the introduction of feeder cells markedly improved the ability to keep primary keratinocytes proliferating in culture, little is known about what the exact contributions are from feeder cells. It was observed that a direct transfer of fibroblasts media to the keratinocytes were only partially effective in supporting the growth of the latter (Stoker and Sussman, 1965; Borrelli et al., 1989), prompting the suggestion that feeder cells will only produce the required growth factors upon receiving stimuli from the keratinocytes. If this "cross-talk" were to be achieved by a straight-forward co-culture of these two cell types within the same vessel, it would lead to the fibroblasts out-competing the keratinocytes, as the former proliferate at a far greater speed. To overcome this problem, fibroblasts were either irradiated by X-ray of Gamma rays up to 60Gy (Wise-Draper et al., 2009), or treated with mitomycin C (Allen-Hoffman et al., 2000), prior to culturing them with keratinocytes. Both these treatments damage the DNA of the fibroblasts. Improvements in culture media in the recent past have resulted in the production of culture media that can support growth of primary keratinocytes extremely well without the need of feeder cells (Peehl and Ham, 1980). Keratinocytes grown in these media proliferate very rapidly and do not grow in colonies as they do when cultured with feeder cells.

Developments in the culture of human keratinocytes have a profound impact on research into the human papillomavirus (HPV). This is because the host of human papillomavirus is the keratinocytes of the epithelium. Since the beginning of HPV research, attempts were made to generate a culture system that can stably harbor HPV DNA as non-integrated and replicating episomes within the nucleus of keratinocytes. It was hoped that such a culture would recapitulate the maintenance phase of the virus, which takes place in proliferating keratinocytes of the basal layer. Initial attempts were made by using keratinocyte lines that grew well in culture without the need of feeder cells (Matoltsy, 1960). These attempts invariably ended in the failure to generate cell lines that harbor the viral DNA as episomes. Either no HPV DNA was harboured in the cells, or the HPV DNA was integrated into the cellular DNA, a situation which is not part of the viral life cycle. It was not until primary keratinocytes cultured with feeder cells were used (Rheinwald and Green, 1975), that the attempts were met with success. As such, it became accepted in the field that in order to maintain HPV DNA as replicating episomes in keratinocytes, these cells must be cultured together with feeder cells that were either pre-irradiated or treated with mitomycin.

The notion that DNA-damaged feeder cells are essential for the maintenance of viral genome is particularly interesting in view of numerous reports that have emerged about a phenomenon that is referred to as radiation-induced bystander effect (RIBE) (Gerashchenko and Howell, 2003a,b; Kamochi et al., 2008). In essence, un-irradiated cells can receive DNA-damaging agents from neighbouring cells that were irradiated. This causes the former to exhibit characteristics of post-irradiated cells. RIBE has been demonstrated in non-irradiated cells that were cultured in close proximity with cells that have been directly irradiated (Gerashchenko and Howell, 2003a,b; Little, 2006). Of particular relevance to our interest, irradiated fibroblasts have been shown to induce bystander effect in SCC cells under cancer-stromal interactions (Kamochi et al., 2008). The transmission of DNA damaging agents appear to happen directly via gap junctions between adjacent cells and indirectly via autocrine or paracrine factors secreted into the medium (Stenerlow, 2006). Following direct gamma irradiation, a variety of DNA lesions could arise as a consequence of direct or indirect damage caused by ionizing radiation. Ionizing radiation such as gamma rays (γ rays) has high photon

energies and is able to interact directly with DNA to cause breaks on the phosphodiester backbone of DNA (Jeggo and Lavin, 2009). In addition, the electronic excitation of γ rays is sufficient to cause ionization of water (H_2O) molecules to produce hydroxyl and hydrated electrons (H atom) and hydroxyl radicals (.OH) (Riley, 1994; Jeggo and Lavin, 2009). Free radicals, also known as reactive oxygen species (ROS), that are formed from radiolysis of water molecules can interact with and cause damage to DNA. There is increasing evidence that unirradiated cells receive ROS and cytokines from neighbouring irradiated cells (Prise and Sullivan, 2009), that can induce DNA damage.

Since the standard keratinocyte culture condition for HPV research is very similar to those in which bystander effects have been identified, we wanted to know whether keratinocytes are recipients of RIBE from the irradiated fibroblasts. Obtaining an understanding of this is extremely important because we are interested in studying the interaction between HPV and DNA damage surveillance, signaling and repair processes in the host cell. This area of research is gaining interest as virologists are beginning to appreciate that viruses have to interact with these cellular processes in order to replicate their genomes in the hosts' cells (Lilley et al., 2007; Weitzman et al., 2010). As such it is very important to first identify whether, and if so how, the culture conditions of the system that we are using affect these cellular processes so that we will not mistakenly ascribe culture-induced changes to those induced by the virus.

In the laboratory, we have introduced circularised HPV16 into NIKs cells and have successfully generated lines of these cells that support the long-term persistence of the viral DNA as replicating episomes (Hoffmann et al., 2006). These NIKs cells that contain wild-type HPV16 DNA are denoted as NIKs HPV cells. As this study is based on analysing effects caused by irradiated feeder cells on NIKs (+/- HPV16), it was essential that we first obtain NIKS that were grown without feeder cells. This would then allow us to study the effect of introducing irradiated feeders to NIKs. To do this, NIKs and NIKs HPV cells were weaned off feeder cells for three to four passages to produce keratinocytes that were devoid of feeder cells (Figure 3.1). Although we mentioned above that feeder cells were thought to be necessary for the long-term maintenance of HPV episomes in

keratinocytes, we know from past experience that short-term removal of feeder cells, together with high-density culture of the keratinocytes, does not result in any detectable loss of viral episomes. Following this, the keratinocytes that were free from feeder cells were seeded into two duplicate plates, one that did not contain feeders (Plate A) and another one where irradiated feeder cells were added (Plate B). Experiments were carried out with keratinocytes Plate A and Plate B, using the former as a comparison to assess the effects of feeder cells.

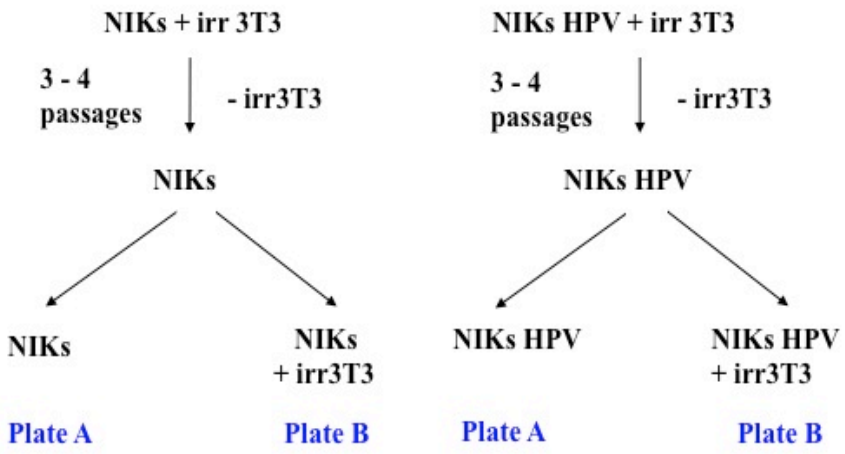

Figure 3.1: Strategy for producing NIKs and NIKs HPV cells that were grown in the absence or presence of feeders. NIKs and NIKs HPV (HPV16 DNA-containing keratinocyte derived from transfection of NIKs with HPV16 wild type DNA).

Results

Feeder cells induced signs of DNA damage in NIKs cells

To assess whether feeder cells (which were pre-irradiated) affects the physical integrity of NIKs cells' DNA, we stained NIKs cells (+/- feeder cells) and NIKs HPV cells (+/- feeder cells) for phosphorylated histone H2AX, a central regulator of the signaling of DNA damage. This histone protein has a serine at position 139 (Ser139), which can be phosphorylated by members of the phosphoinositide-3-Kinase-related protein kinases **(**PIKK) family members (ATM, ATR and DNA-PK) to generate γH2AX foci following activation of DNA damage response (DDR) (Yang et al., 2003). Each γH2AX focus functions as a docking site for the recruitment of DNA repair proteins (Rogakou et al., 1999; Podhorecka et al., 2010), generating domains that can be visualized by fluorescence microscopy.

The cells were stained with γH2AX antibody twenty-four hours following plating (with or without irradiated 3T3-J2 cells) onto coverslips. The average proportion of cells with γH2AX formation was calculated from five independent fields. Interestingly, we noticed two distinct staining patterns of γH2AX in NIKs and NIKs HPV cells. The γH2AX staining observed were of either clear, punctate pattern within the nucleus or diffused throughout the nucleus (Figure 3.2A and 3.3). We enumerated the proportion of cells with γH2AX by assessing both γH2AX foci and non-foci/pan-nuclear formation. NIKs cells by themselves (- feeder cells) exhibited γH2AX-positivity in 29% of the population (Figure 3.2B). Co-culturing these cells with irradiated feeder cells significantly increased this percentage to 55% (Figure 3.2B). Similarly, feeder cells also increased the proportion of NIKs HPV cells with activated H2AX by 33% (Figure 3.2B). Therefore, it appears that these keratinocytes, although un-irradiated, sustained DNA damage as a result of their proximity to irradiated feeder cells. This would imply that the keratinocytes were in receipt of DNA damaging agents that were produced by irradiated feeder cells.

However, we cannot ignore the observation stated above, which is that the γH2AX staining produced two types of positive results; punctate foci and pan -

nuclear staining (Figure 3.2A). This might indicate that more than one type of event caused H2AX phosphorylation in NIKs and NIKs HPV cells that were cultured with feeder cells. In this context, it must be remembered that apart from being a marker for DNA double-strand breaks (DSB), phosphorylated H2AX also serves as an indicator of DNA replication stress within the cell (Gagou et al., 2010). DNA replication stress is caused by inefficient DNA replication that results in stalling or slow progression of replication forks (Burhans and Weinberger, 2007). It has been proposed that pan-nuclear γH2AX could represent a nuclear-wide conformational change that exposes H2AX to kinase activity during DNA replication arrest (Marti et al., 2006). Hence the heterogeneous γH2AX staining patterns might reflect H2AX phosphorylation that arises from a mixture of different events such as DNA damage and DNA replication stress (Marti et al., 2006; Bonner et al., 2008).

NIKs (-feeder cells) displayed approximately equal proportions of γH2AX foci and pan-nuclear staining at 11 and 15%, respectively (Figure 3.2C). In the presence of feeder cells, the percentage of cells with pan-nuclear staining increased by 26%, to 41% (Figure 3.2C). However, the percentage of NIKS cells with γH2AX foci staining remained generally unchanged. Hence, it is clear that whatever the feeder cells are doing to NIKs cells, they are only increasing phosphorylated H2AX that do not form foci.

This situation is quite different for NIKs HPV cells, where feeder cells augmented the levels of γH2AX foci from 13% to 53% with very minimal affect on pan-nuclear γH2AX (Figure 3.2C). This indicates that the kind of effect that feeder cells impose on NIKs cells is influenced by the presence of HPV16 DNA in the cells. In this respect, it is important to point out that even without the contribution of feeder cells, NIKs HPV cells already have elevated percentages of pan-nuclear γH2AX. In fact, the contribution of HPV16 to the rise in pan-nuclear γH2AX was similar in magnitude to that caused by feeder cells (Figure 3.2C). This observation is interesting and is consistent with other studies showing that other viruses, such as adenovirus, adeno-associated virus and simian virus 40 (Fragkos et al., 2009; Boichuk et al., 2010; Weitzman et al., 2010), also induce phosphorylation of H2AX protein.

If one were to take H2AX foci as indication of double-strand breaks, then we can formally deduce that feeder cells do not induce double-strand breaks in NIKs cells, but they do if HPV16 DNA is present. It is intuitive to think that this is owed to the already heightened level of γH2AX present in NIKs HPV cells. This however remains a hypothesis at this stage. While many interesting questions were raised and could be addressed with these observations, we were intent on keeping to our attention on the initial question of bystander effect. The results above show that there is indeed radiation-induced bystander effect (RIBE) that is contributed by feeder cells to NIKs cells (+/- HPV). As such, we were interested to know the routes by which feeder cells transmit these DNA-damaging agents to keratinocytes.

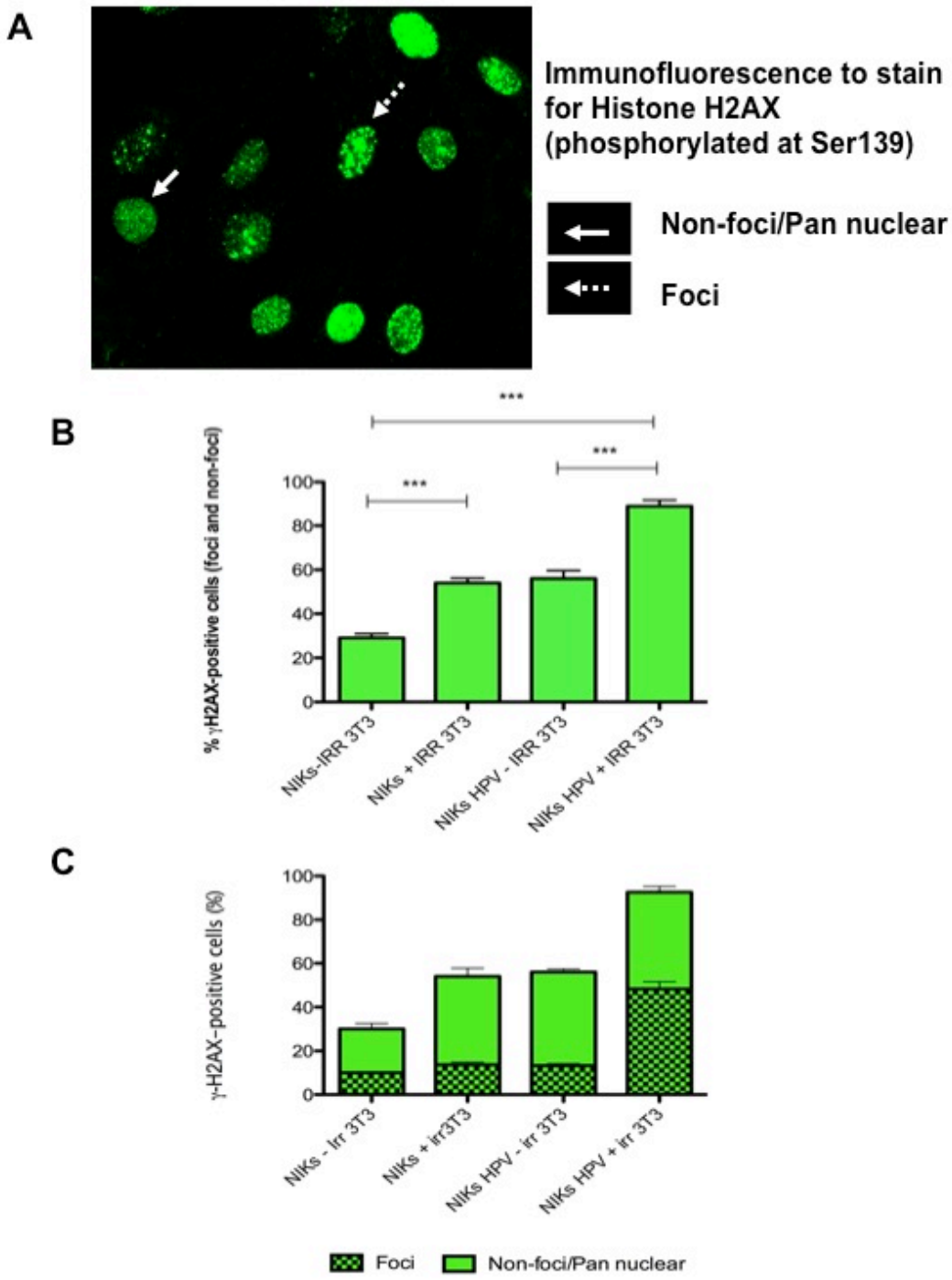

Figure 3.2: Feeder cells and HPV16 increased γH2AX-positivity in NIKs.

(A) Immunofluorescence analysis displayed two distinct staining patterns in NIKs, foci and non-foci/pan nuclear appearances. (B) Feeder cells increased γH2AX-positivity in NIKs and NIKs HPV; HPV16 also increased γH2AX-positivity in NIKs. (C) Total γH2AX-positivity enumerated with two different staining patterns. ***$p < 0.05$, student's t-test, n=5 per group, average of three experiments.

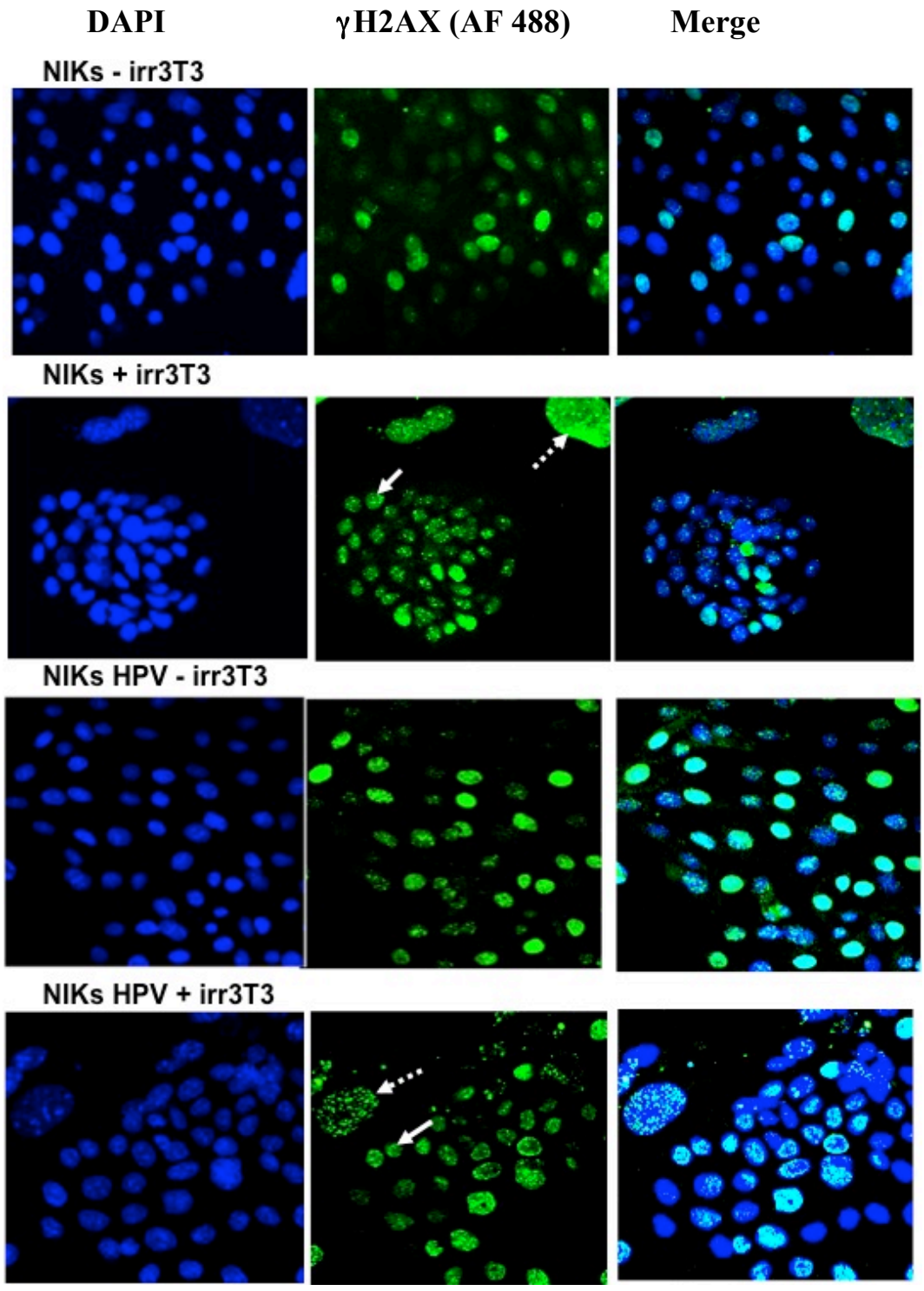

Figure 3.3: Immunofluorescence staining of γH2AX in NIKs and NIKs HPV. Cells were stained for γH2AX (AF488, Alexa Fluor 488 green) and DNA was stained by DAPI (blue). White dotted arrow indicated irradiated feeder cells, while white block arrow indicated keratinocytes.

Routes of transmission of DNA damaging agents to bystander cells

The primary route of radiation-induced bystander effect (RIBE) is through direct cell-to-cell contact that is often mediated by gap junctions (Gerashchenko and Howell, 2003b). The second route is by means of soluble factors secreted by the irradiated cells into the surrounding medium and entering neighboring cells (Prise and Sullivan, 2009). Regardless of the route, the soluble factors that are generated from the directly irradiated cells are likely to be DNA-damaging agents, such as reactive oxygen species (ROS) or its derivatives. ROS has been implicated in many medium-mediated bystander responses (Azzam et al., 1998, 2002) and have been shown to generate secondary long-lived organic radicals that can cause damage to DNA (Koyama et al., 1998; Kumagai et al., 2003).

Experiments were carried out to address (a) whether feeder cells need to be in direct contact with keratinocytes to tranduce DNA damaging signals (b) whether feeder cells need to be irradiated to tranduce DNA damage signals, and (c) the duration of the bystander effect (Figure 3.4). To do so, the following keratinocyte culture systems were utilised:

Set 1 – NIKs cells (+/- HPV16) cultured in direct contact with irradiated feeder cells.
Set 2 – NIKs cells (+/- HPV16) co-cultured with irradiated feeders that were plated on transwell inserts,
Set 3 – NIKs cells (+/- HPV16) co-cultured with non-irradiated feeders that were plated on transwell inserts, and
Set 4 – NIKs cells (+/- HPV16) grown without feeders (Figure 3.4).

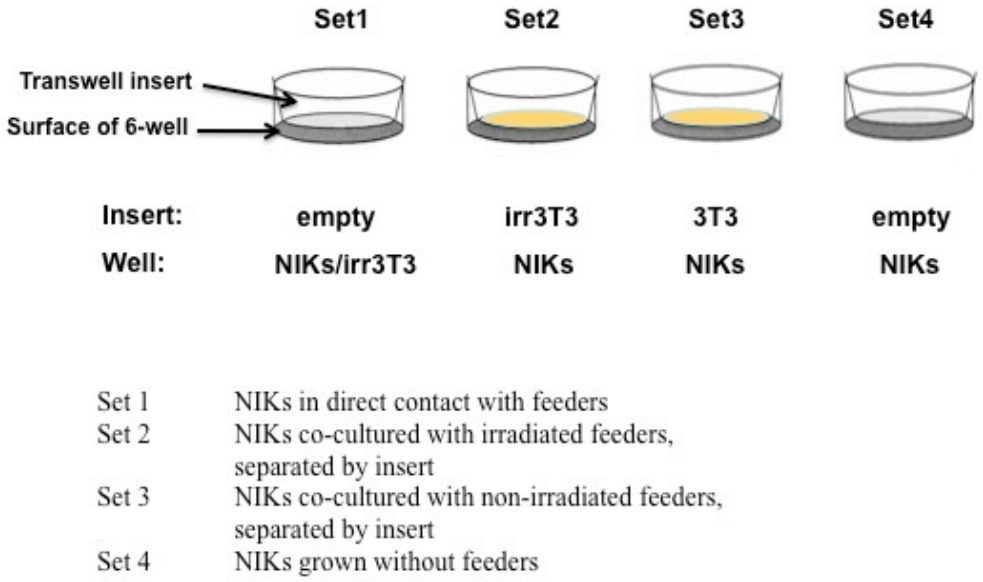

Figure 3.4: The keratinocytes culture systems that were utilized to examine the routes of transmissions of DNA damaging agents from feeder cells to keratinocytes. Figure shows the example of co-culturing NIKs and feeder cells through three different ways of feeder interaction: feeders and keratinocytes in direct contact, separated by transwells, and non-irradiated feeders separated from keratinocytes. NIKs grown without feeders were used as the benchmark comparison to determine the effects of feeder cells.

At the appropriate time points after addition of feeder cells, the keratinocytes were harvested for protein lysate. Feeder cells, which attached very weakly on the culture surface, were first removed with PBS washes and squirting. This procedure is very effective and is controlled for each time by using mouse-specific antibodies to detect mouse proteins in the protein lysate of NIKs cells, which are human cells. A representative of such a control is shown later in Figure 3.12. Protein lysates were tested by western blotting for ATM-S-1981P and γH2AX. NIKs and NIKs HPV cells grown without feeders exhibited the lowest level of these proteins, which indicated the basal level of DNA damage when there is no induction of bystander effect (Figure 3.5 and 3.6).

Within 4 hours of addition of irradiated feeder cells, NIKs cells that were co-cultured with irradiated feeders (Set 1) exhibited the highest level of γH2AX induction out of all the culture conditions (Figure 3.5). In comparison, the ATM-

S1981-P and γH2AX levels in all other culture conditions of NIKs cells were unchanged. However 24 hours later, γH2AX level increase in NIKs that were cultured separately from irradiated and non-irradiated 3T3 cells in the transwell insert. The magnitude of increase of this protein is much greater in NIKs that were cultured either together with irradiated feeder or with the irradiated feeders in the transwell insert, suggesting that irradiated feeders are far more capable of inducing activation of H2AX in NIKs cells than non-irradiated feeder cells. Furthermore it also demonstrates that cell-cell contact is very much more effective in mediating this effect. Interestingly, the ATM protein was not visibly increased in NIKs that were cultured separately from the 3T3 cells (irradiated or not). Even in NIKs that were cultured together with feeder cells, the rise in phosphorylated ATM was minimal unlike the marked increase in γH2AX (Figure 3.5).

Meanwhile, a very different result was obtained with NIKs cells that harboured the viral DNA (NIKs HPV cells). Within 4 hours of adding 3T3 cells, the level of γH2AX increased in NIKs HPV, with the greatest increase in cells that were cultured in direct contact with irradiated 3T3, followed by cells that were grown with irradiated feeder in the transwell insert, and non-irradiated feeder cells in the transwell insert (Figure 3.6). The levels of activated ATM did not correlate at all with the changes in γH2AX levels. After 24 hours, there were very great rises in the level of γH2AX across all the culture conditions, with similar relative magnitude differences as the 4-hour time point (see Hsp70 of bottom Figure 3.6). Although there were rises in active ATM in NIKs HPV cells cultured with feeders (irradiated or not) these rises did not fully reflect the change of γH2AX in these cells.

Collectively, the transfer of DNA damaging agents from feeders to NIKs and NIKs HPV occur primarily through direct cell-to-cell contact. Separating feeders from these cells reduced DNA damage signaling, as indicated by decreased γH2AX levels (Figure 3.5 and 3.6). When cells were separated from feeders, the exchange of components was still allowed through the porous membrane of the inserts. The γH2AX levels continued to persist from 4 to 24 hr, indicating that the DNA damaging agents that were transferred from irradiated feeders to non-irradiated keratinocytes were continuously generated and / or were relatively

long-lived. In summary, irradiated feeders were able to channel their DNA damaging agents to keratinocytes through two different routes of transmission and this fitted in with the currently understood physical mechanisms of bystander effect. Since γH2AX is a sensitive indicator for DNA damage as well as DNA replication stress, this suggests to us that feeders could be inducing H2AX phosphorylation in keratinocytes through these events. Further experiments were carried out to elucidate the events that occur in keratinocytes as a result of co-culture with feeder cells, leading to H2AX phosphorylation.

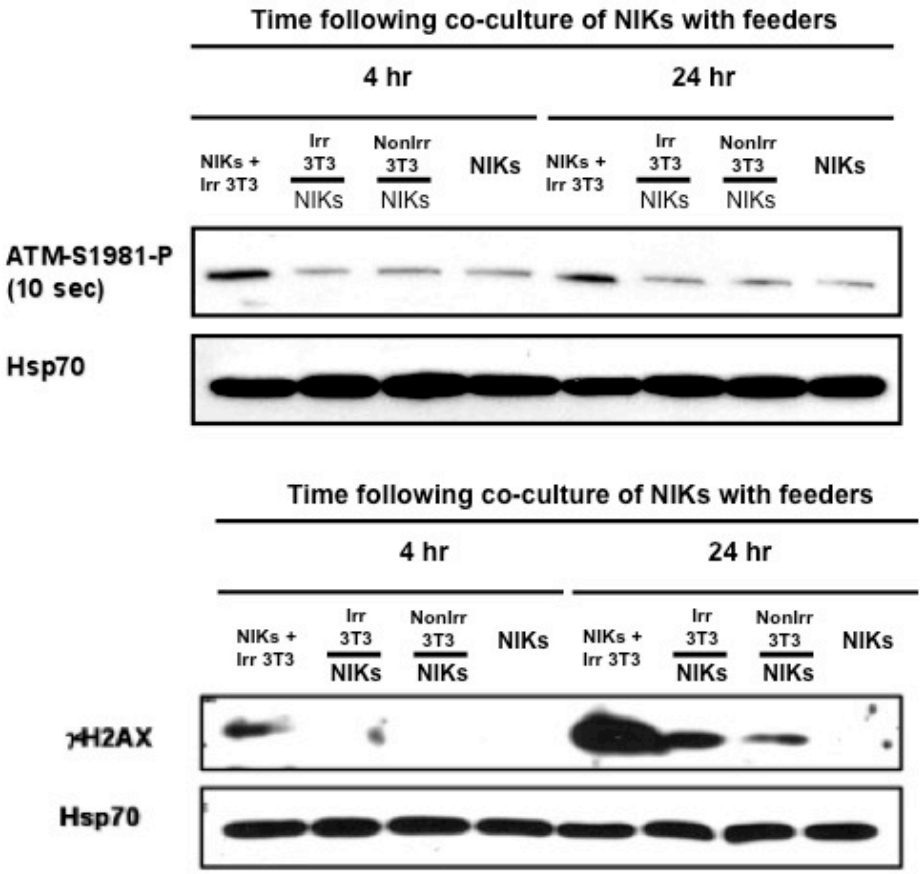

Figure 3.5: Direct contact with and irradiation of feeders increased DNA damage signaling in NIKs.

Protein lysates were prepared from NIKs from all culture conditions at 4 and 24 hrs following putting feeders/inserts with feeders and non-irradiated feeders with the keratinocytes. ATM-S1981-P and γH2AX protein levels were assessed.

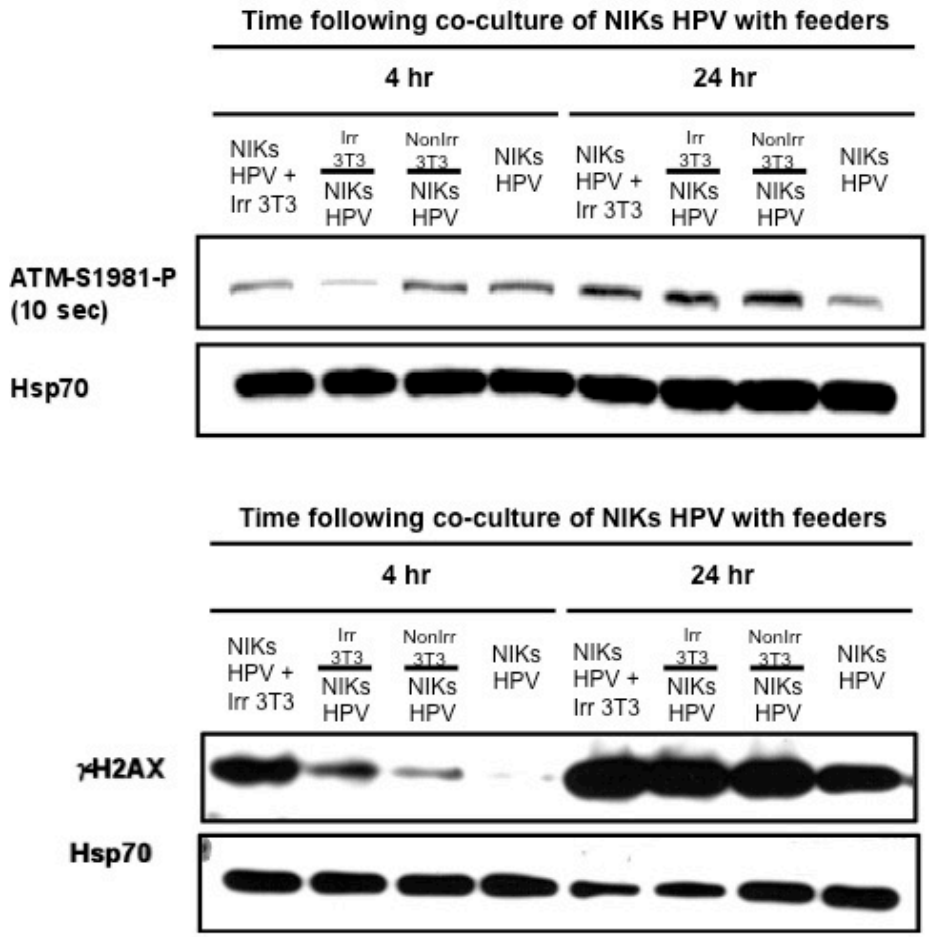

Figure 3.6: Direct contact with and irradiation of feeders increased DNA damage signaling in NIKs HPV.

Protein lysates were prepared from NIKs HPV from all culture conditions at 4 and 24 hrs following putting feeders/inserts with feeders and non-irradiated feeders with the keratinocytes. ATM-S1981-P and γH2AX protein levels were assessed.

Elucidation of events that lead to H2AX phosphorylation

A) DNA replication

The appearance of different staining patterns and variable intensity of γH2AX formation indicates that there is more than a single type of event that led to H2AX phosphorylation (Marti et al., 2006; Ismail and Hendzel, 2008). H2AX has been shown to be a sensitive marker of both DNA damage and DNA replication stress. H2AX is believed to play a role in repairing double-strand breaks (DSBs) generated during DNA replication. These so-called "endogenous" DSBs are derived from replication termination at single-strand breaks (SSBs) that arise as a result of oxidative damage by ROS that are produced from normal cellular metabolic processes (Podhorecka et al., 2010). ROS may also cause DSBs as well as genome rearrangements at the sites of DNA replication fork, contributing to replication fork stalling or DNA replication stress (Burhans and Weinberger, 2007). Therefore, it was our aim to ascertain whether the increased γH2AX formation in keratinocytes that were grown with feeders was contributed by DNA replication stress. A step towards knowing this is to first find out whether cells that stained positive for γH2AX were in S-phase.

The most straightforward method to identify S-phase cells is by incubating cells with BrdU and then staining with antibodies to visualise cells that have incorporated this thymidine analog in their DNA during S-phase. Attempts to double stain cells for γH2AX and BrdU were unsuccessful due to the denaturing of the γH2AX epitope during the HCl treatment step for BrdU staining. Next, we attempted to synchronise cells in S phase and stain for γH2AX. Although aphidicolin or thymidine (2 mM) can arrest cells in the S-phase, these treatments were not suitable for our purpose as they would cause damage to the cellular DNA, due to stalled replication forks. Hence we chose to arrest cells in G1 instead, by serum and EGF starvation. The release of these G1 cells from the block (by introduction of serum and EGF) would allow us to intercept the cells several hours later when they are in S phase, and to stain them for γH2AX. While deprivation of serum and EGF were able to cause some build up of NIKs cells in

G1 (85% from 75% of untreated cells), they were absolutely ineffective with NIKs that contain HPV16 DNA (Appendix 1 and 2). This is consistent with the fact that E6 and E7 proteins of the virus, by binding and destroying p53 and pRb proteins of the cell, abrogate the G1/S checkpoint.

We then decided to look at percentage of cells within the test population that is in S phase and compare that to the percentage of cells that were positive for γH2AX. Although this would not reveal cells that are both in S phase and are γH2AX positive, their respective percentage would provide a clue as to the likelihood that the feeder effect is due to aberrant DNA replication of the keratinocytes.

The following keratinocyte culture systems were utilised:
Set 1 – NIKs and NIKs HPV cultured in direct contact with irradiated 3T3s,
Set 2 – NIKs and NIKs HPV co-cultured with irradiated feeders that were plated on inserts,
Set 3 – NIKs and NIKs HPV co-cultured with non-irradiated feeders that were plated on inserts, and
Set 4 – NIKs and NIKs HPV grown without feeders (Figure 3.4).

Using Click-iT® EdU cell proliferation assays, S phase cells were detected by incorporation of a modified nucleoside, EdU (5-ethynyl-2'-deoxyuridine), that is incorporated during DNA synthesis. Detection of EdU molecules is based on a click reaction that is a copper catalyzed covalent reaction between an azide and an alkyne. Incorporated EdU molecules have alkyne that can be detected with the Alexa Fluor 594 azide and visualised by immunofluorescence microscopy. NIKs and NIKs HPV were labeled for 5.5 and 4 hrs, respectively.

Keratinocytes that were in direct contact with irradiated feeders exhibited marginal increases in the percentage of Edu-positive cells, i.e., 48% in NIKs and 55% in NIKs HPV, in comparison to keratinocytes that were cultured on their own without any feeders (NIKs and NIKs HPV were 43 and 47%, respectively) (Figure 3.7). Therefore, irradiated feeders affected only a very minor increase in the percentage of cells in S-phase. Likewise, separating irradiated feeders from keratinocytes only marginally decreased the proportion of EdU-positive cells by

1% in NIKs and 6% in NIKs HPV, respectively.

Interestingly, the proportion of NIKs and NIKs HPV cells in S-phase was actually decreased when they were co-cultured with non-irradiated feeders (Set 3) (Figure 3.7, 3.8, and 3.9). This is probably due to competition for nutrients with the non-irradiated feeder cells.

Essentially, we found that the proportion of cells that were stained positive for EdU (S phase cells) remained almost unchanged between all the four culture conditions of NIKs and NIKs HPV, (with the exception when NIKs HPV cells were co-cultured with non-irradiated feeders, where there was a significant decrease in EdU-positive cells) (Figure 3.7). This lies in stark contrast with the 26% increase in γH2AX positivity of NIKs when co-cultured with irradiated feeders, and 20% increase of γH2AX positivity of NIKs + HPV16 cells induced by irradiated feeder cells. It is therefore unlikely that RIBE induced by irradiated 3T3 cells to these keratinocytes caused aberrant DNA replication, which induced γH2AX. Instead the increased γH2AX induced by RIBE is independent of DNA replication of the recipient keratinocytes.

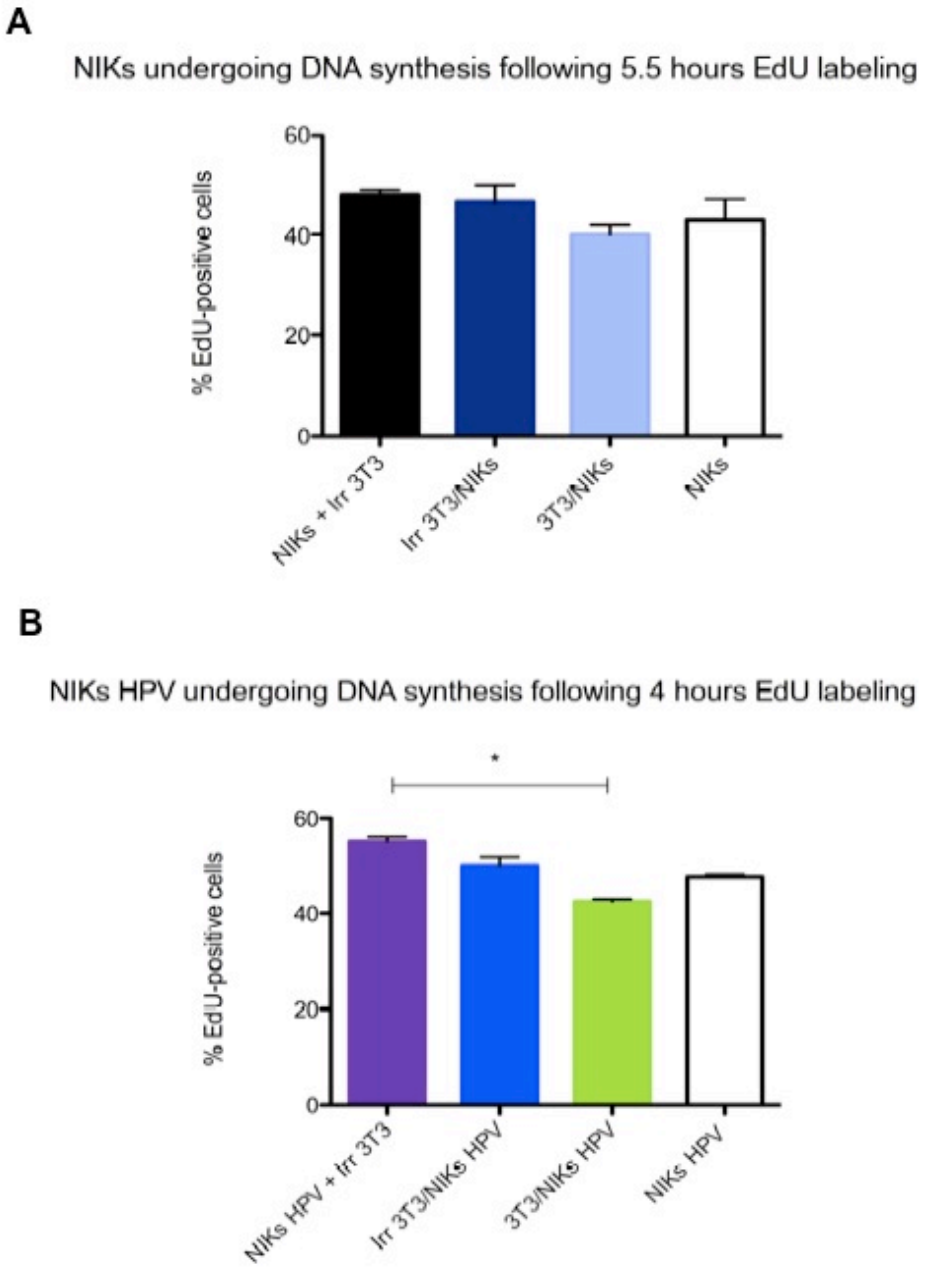

Figure 3.7: Proportion of cells that were undergoing DNA synthesis in NIKs and NIKs HPV. Experiment repeated in triplicate, statistical analysis was carried out using a 1-way ANOVA with a Bonferroni post test, * $p < 0.05$.

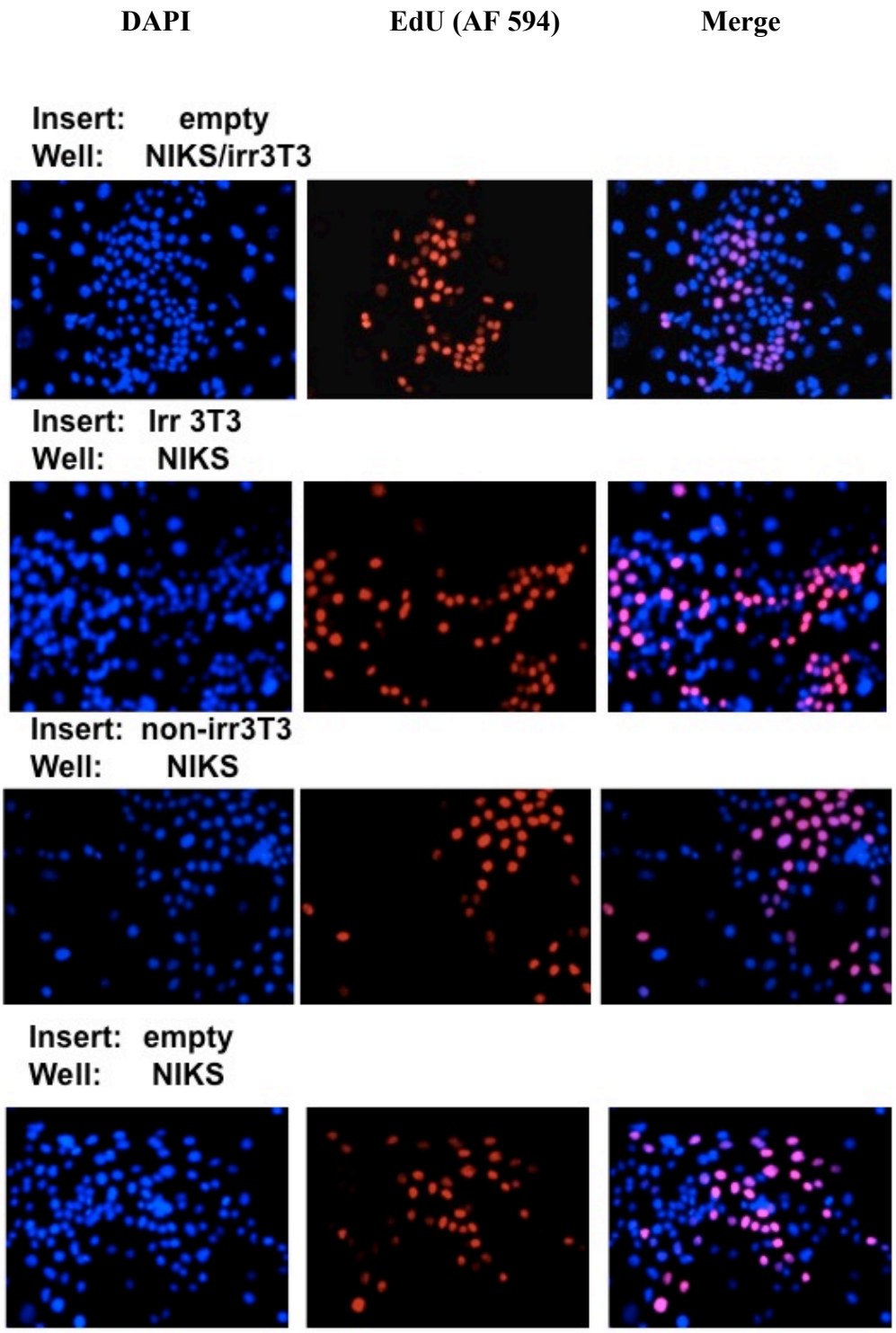

Figure 3.8: EdU-positive NIKs cells.

Cells that were stained with EdU (Alexa Fluor 594) and DNA was stained with DAPI.

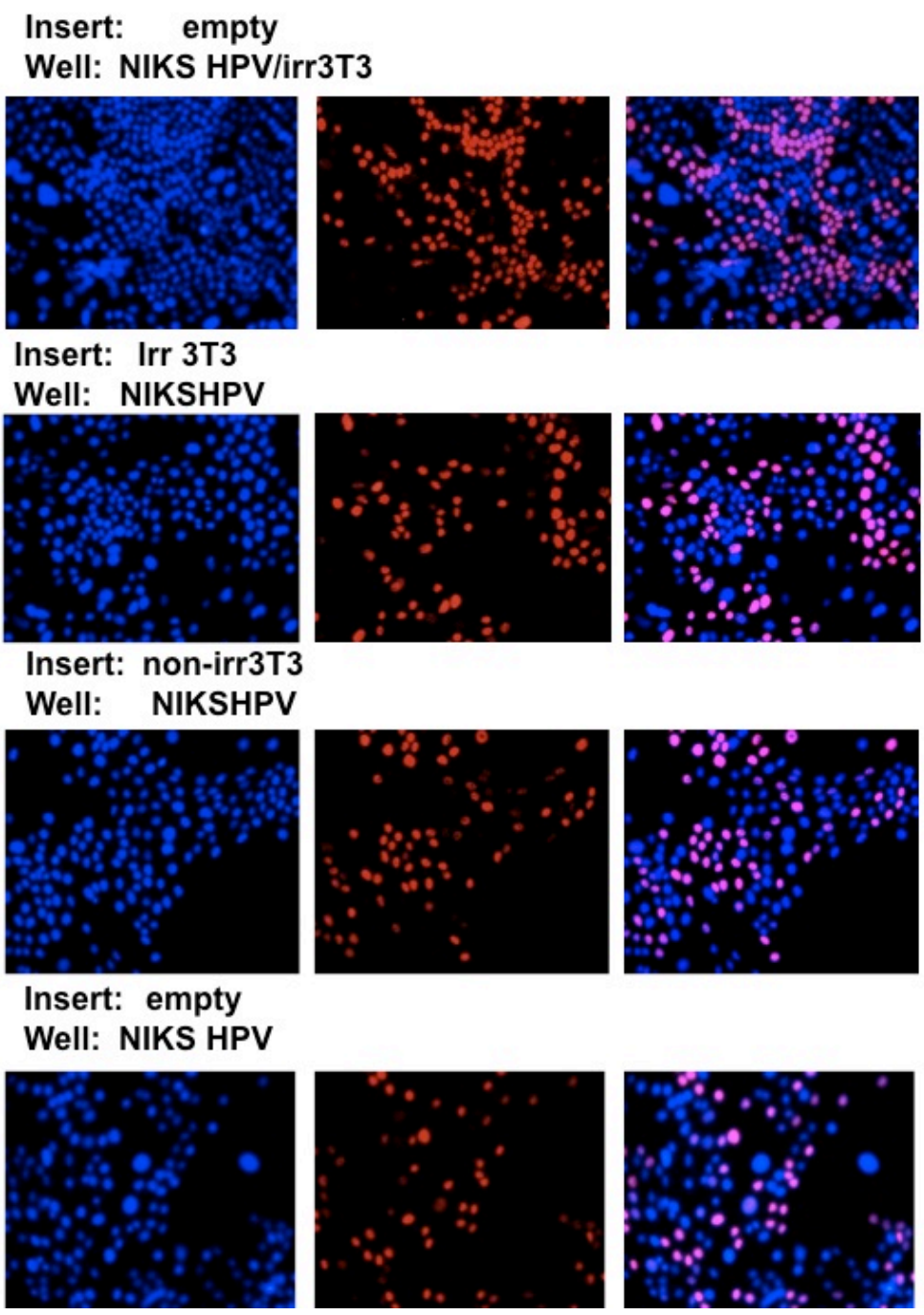

Figure 3.9: EdU-positive NIKs HPV cells.

Cells that were stained with EdU (Alexa Fluor 594) and DNA was stained with DAPI.

B) DNA damage

The results described above effectively removed the likelihood that DNA replication stress was the cause of γH2AX increase in cells co-cultured with irradiated feeder cells. We proceeded to address the possibility that RIBE on these keratinocytes resulted instead in actual damage to their DNA. To determine if this was indeed the case, we employed comet assays (single-cell gel electrophoresis) on NIKs and NIKs HPV cells that were cultured in the presence or absence of irradiated feeder cells. We used an alkaline lysis solution, which would unwind the double helix of DNA so that DNA fragments resulting from single strand breaks can also be detected in the comet tail (Olive, 2009). This method can directly determine the state of DNA damage by revealing the totality of DNA breaks in cells. Cells were embedded in low-melting point agarose, lysed and subjected to an electric field that caused broken DNA to migrate away from the cell. Subsequent staining with propidium iodide allowed visualization of DNA through fluorescence microscopy. Each cell has the appearance of a "comet" with a bright fluorescent head, which consists of intact DNA in the cell nucleus, and a tail of broken DNA that migrated out of the cell body (Figure 3.10A).

Cells with increased fluorescence intensity in the tail compared to that of the head indicated that they have sustained vast amount of DNA damage (Figure 3.10A). The intensity of tail fluorescence was observed to range from category 1 (no DNA in tail) to 4 (almost all DNA in tail) (Figure 3.10B). Figure 3.11A and 3.11B show that NIKs grown without feeders exhibited the basal level of DNA breaks in 10% of the population. The presence of irradiated feeders significantly increased the proportion of NIKs cells with damaged DNA from 10% to 24%, with the majority of cells exhibiting comets of class 1, 2, and 3 (Figure 3.11B). NIKs cells harbouring HPV16 DNA were also similarly affected, with 7% increase in cells with damaged DNA when cultured with irradiated feeder cells; the majority of these cells exhibited comets of category 3 and 4.

Although the percentage increases in NIKs and NIKs + HPV16 cells were not as large as the percentage increases of γH2AX positive cells in these two lines, this

does not undermine the fact that there is significant increase in NIKs and NIKs + HPV16 cells with damaged DNA when they were cultured with irradiated feeder cells. This provides us with an idea of the series of events that were occurring: Irradiated feeder cells released DNA damaging factors (yet to be identified) to the neighbouring keratinocytes via (a) communication junctions which required cell-cell contact and (b) through the culture medium. Upon entering the recipient cells, these factors caused damage to the DNA of the cells, resulting in the activation of ATM and H2AX proteins. We are satisfied that these observations have provided the answer to our question of whether the co-culture of irradiated feeder cells and keratinocytes, which is the standard culture system in HPV research, is affected by bystander effect or not.

In addition to revealing that irradiated feeder cells induce significant damage to the DNA of NIKs cells, these results also show that HPV16 also induce DNA damage of these cells (Figure 3.11B). In fact, the amount of damage caused by HPV16 is even greater than that caused by irradiated 3T3-induced bystander effect (Figure 3.11C). This is consistent with our earlier data, which demonstrated that NIKs harbouring HPV16 DNA had a greater percentage of γH2AX-positive cells (Figure 3.2). Collectively, throughout all the experiments, NIKs + HPV16 exhibited more DNA damage (comet assay) and γH2AX staining (immunofluorescence and western blotting) than NIKs. It is therefore without doubt that HPV16 induces damage to the DNA of its host cells; a feature of HPV that is of particular interest to us.

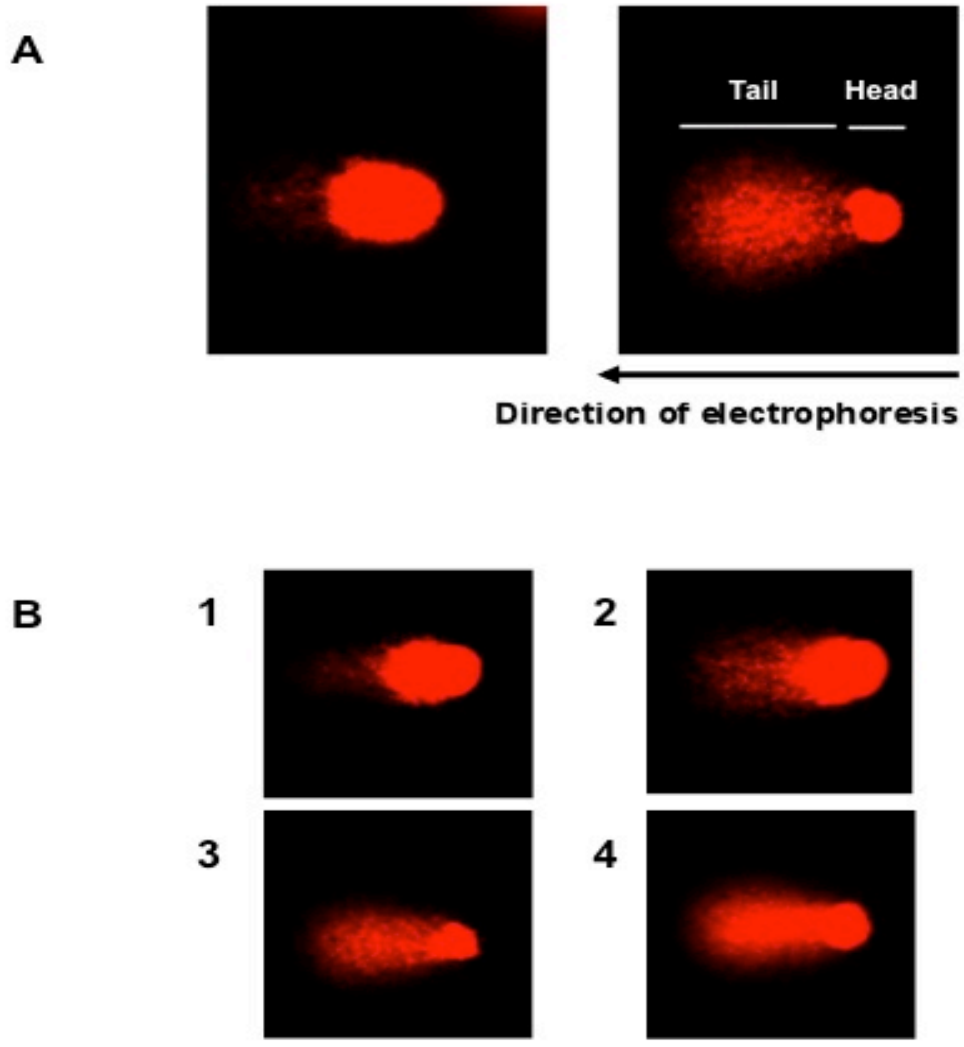

Figure 3.10: Images of comets (from keratinocytes), stained with propidium iodide in this study.

(A) *right*, the appearance of a comet – Head (body of the cell) and Tail (damaged DNA that migrates from the body of the cell), *left*, a cell with no or minute damage where unbroken DNA remains in the cell nucleus as head of the comet. (B) Classes 1-4 that were used for visual scoring where increasing tail intensity represented increasing levels of DNA damage.

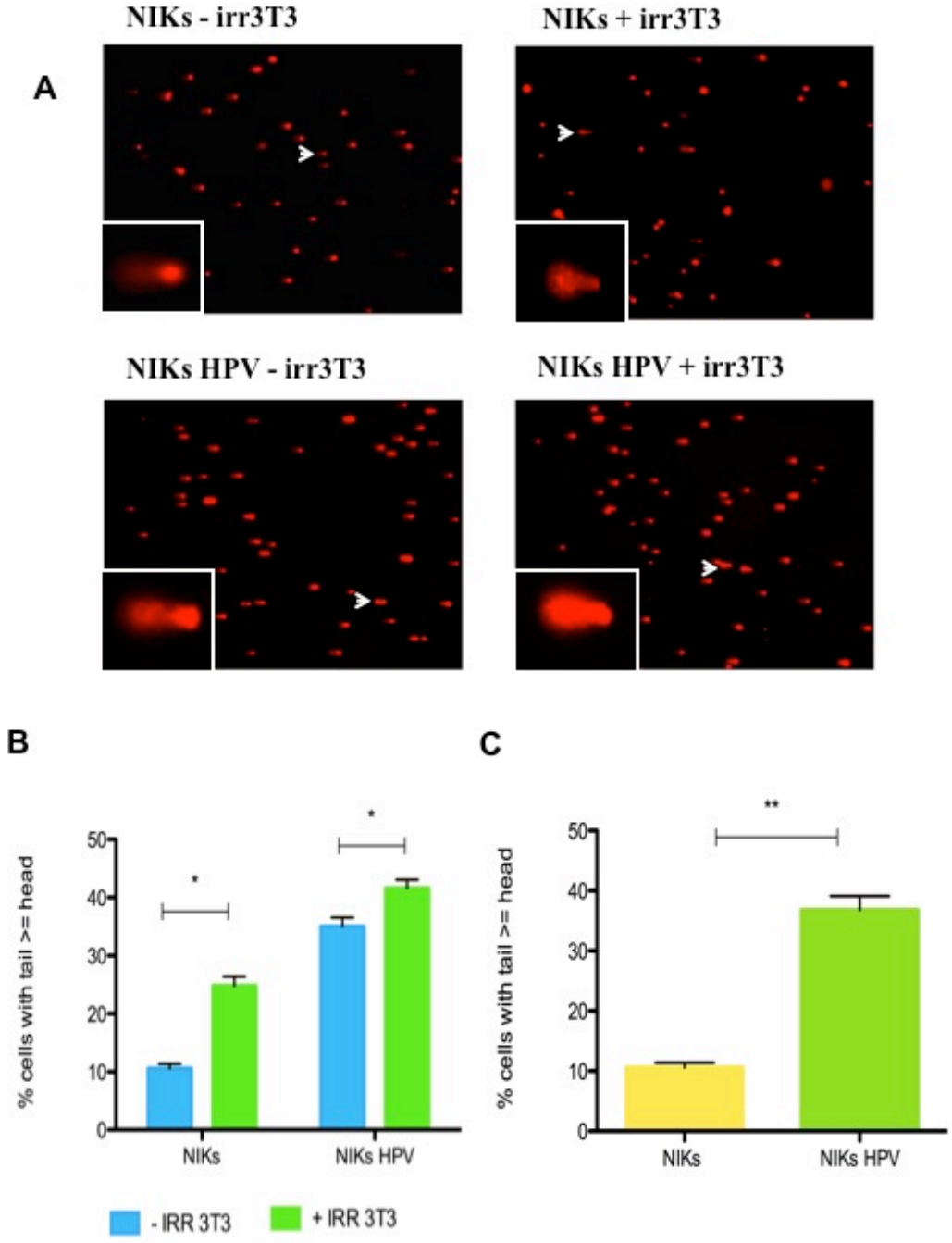

Figure 3.11: Presence of feeders and HPV16 increased DNA breakages in NIKs as analysied by comet assay. (A) Comet assay in NIKs and NIKs HPV grown with or without feeders. (B) Quantitation of cells with increased tail fluorescence intensity equal or bigger than head fluorescence intensity. * Statistical analysis was carried out using a 2-way ANOVA with a Bonferoni post test, $p < 0.0001$. (C) DNA breakages are more pronounced in HPV16-containing cells. **$p < 0.05$, student's t-test, n=5 per group, average of three experiments.

Further examination of how bystander effect changes ATM, ATR and DNA-PKcs levels in NIKS cells with or without HPV16 DNA

Thus far, we have established that the only cell culture system available that can continuously harbour HPV16 DNA in a non-integrated state, in a stable copy number per cell, also experiences radiation-induced bystander effect from the irradiated feeder cells. It is immediately obvious that this knowledge is extremely important if we were to investigate how HPV interacts with its host cell's DNA, DNA damage signaling pathway and DNA repair processes. As such we decided to analyse in greater molecular detail, the effects of irradiated feeder cells on the major DNA damage signaling proteins in NIKs cells (with or without HPV16 DNA), that were cultured in the absence or presence of feeders for 36 hrs. The three major PIKK family of proteins; ATM, ATR and DNA-PK were the major focus of these analyses. All these three proteins are able to phosphorylate the H2AX proteins (Yang et al., 2003).

Feeder cells were removed from the culture dishes before harvesting for protein lysates. To control for any contamination of feeders in NIKs lysates, mouse MAdCAM-1 antibody that is mouse-specific and does not have any cross-reactivity with human proteins was used to signal any inadvertent cross-contamination of feeder cells in the harvest of NIKS cells.

ATM is catalytically activated upon DNA damage, whereby this protein undergoes auto-phosphorylation at serine residue 1981 (ATM-S1981-P) (Lavin, 1998, 2008). In other words, ATM-S1981-P levels increase when there is DNA damage within the cell (especially DSB). We did indeed observe increase of ATM-S1981-P in NIKs cells cultured with feeders compared to NIKs alone (Figure 3.12). Unlike ATM, ATR is not maintained in a catalytically inactive state and activates its partner proteins, such as ATR-interacting protein (ATRIP) and replication protein A (RPA) (Cimprich and Cortez, 2008). ATR associates with ATRIP which has been proposed to localize ATR to sites of DNA damage through an interaction with single-stranded DNA (ssDNA) coated with RPA. In this study, presence of feeder cells appeared to marginally increase the levels of ATR in NIKs cells (Figure 3.12). Interestingly, we observed a big increase in

DNA-PKcs (DNA-PK catalytic subunit) when NIKs cells were cultured with feeder cells (Figure 3.12). NIKs cells displayed a marked increase in γH2AX levels, compared to NIKs that have been weaned off feeder cells (Figure 3.12). This result further substantiated the γH2AX induction that was observed through immunofluorescence staining, a method that is at best more qualitative than quantitative (Figure 3.2). Collectively, our results demonstrate that irradiated feeder cells activated all the PIKK proteins of the DNA damage-signalling pathway – ATM, ATR, and DNA-PK.

Interestingly, similar experiments with NIKs cells that harbour HPV16 DNA yielded very different results (Figure 3.13). While the level of ATR protein was marginally increased and the level of DNA-PKcs strongly increased in NIKs + HPV16 cells (as were the case in NIKs cells), irradiated feeder cells actually caused a decrease in the levels of ATM-S1981-P in these cells (compare Figure 3.13 with Figure 3.12). As NIKs and NIKs + HPV16 cells are isogenic partners with the exception of HPV16 DNA in the latter, it is clear that the different outcome of RIBE on NIKs + HPV16 cells is greatly influenced by the resident viral DNA. Importantly, in spite of this, irradiated feeder cells did increase the level of γH2AX (Figure 3.13), suggesting that phosphorylation of H2AX in these cells, in response to RIBE was probably carried out by ATR or/and DNA-PKcs.

It has been reported that the sensing of DNA damage and phosphorylation of H2AX can occur through the DNA-PKcs pathway in cells lacking ATM (Shrivastav et al., 2008). In NIKs cells, where ATM-S1981-P levels were increased by RIBE, ATM might participate in phosphorylating H2AX. This notion is supported by the report that DNA-PKcs pathway is normally inactive in cells that have active ATM pathway (Shrivastav et al., 2008). However, we cannot ignore the increase of DNA-PKcs levels in NIKs cells cultured with feeder cells; especially when the magnitude of the increase is so great (Figure 3.12). Hence, in spite of the fact that ATM is also activated in NIKs cells cultured with feeder cells, we are inclined to think that H2AX in these cells could be phosphorylated predominantly by DNA-PKcs. This is somewhat different from a report that shows that H2AX phosphorylation generation of bystander effect is ATR-dependent, and that ATM activation occurred downstream of ATR (Burdak-

Rothkamm et al., 2007; Burdak-Rothkamm et al., 2008). It is plausible that any role that ATM plays in the DNA damage signaling of bystander NIKs cells could be minor or secondary to DNA-PKcs or ATR.

In summary, we have substantial evidence to suggest that feeder cells induced bystander effect in NIKs and NIKs HPV cells. Our studies have come to the conclusion that these bystander cells displayed induction of γH2AX, DNA breaks, and activation of DNA damage signaling when grown in the presence of irradiated feeders. While culture with feeder cells increased levels of phosphorylated / active ATM in NIKs cells, they have an opposite effect in NIKs cells containing HPV16. This demonstrates that the presence of HPV16 influences the way bystander effect impinges on NIKs cells.

To allow for direct comparison of the levels of the various proteins in NIKs and NIKs HPV cells (+/- feeder cells), we analysed these proteins in parallel, on a single gel/western blot. From Figure 3.14, it is clear that HPV16 and irradiated feeder cells augmented the levels of ATM-S1981-P, ATR, DNA-PKcs, γH2AX, and 53BP1, but only HPV16 increased the levels of NBS-1 and RPA. This suggests that although HPV16 and RIBE from irradiated feeder cells share the ability to induce DNA damage on NIKs cells, the means or mechanisms employed by them are not identical. It is also worth noting that HPV16 together with feeder cells decreased the levels of 53BP1, in parallel with ATM-S1981-P. While RIBE is reported to be mediated by ROS or its derivatives that are longer living, or even by cytokines, it is particularly perplexing how HPV can induce DNA damage. Hence having answered the question of whether RIBE is present in the standard culture for HPV maintenance, we decided to turn our attention to addressing how HPV induces DNA damage in its host cell.

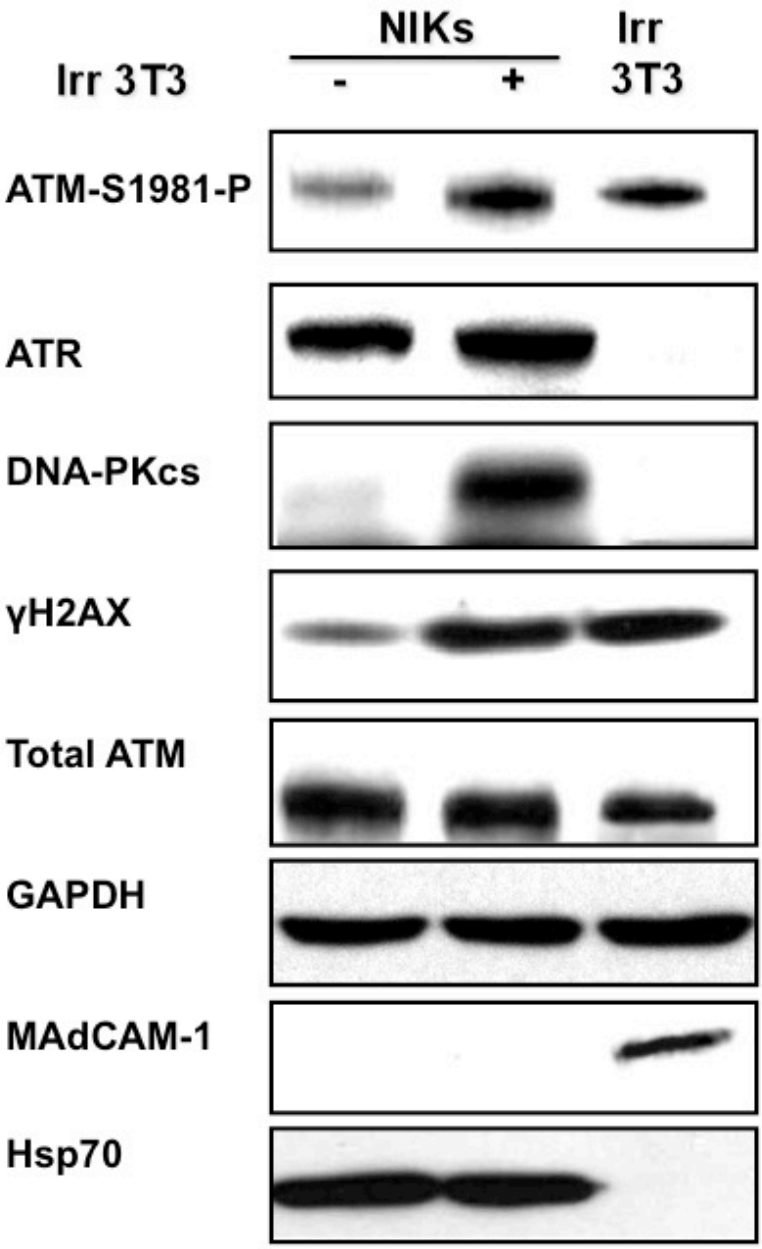

Figure 3.12: Feeder cells activated DNA damage signaling that led to H2AX phosphorylation in NIKs.

Levels of ATM-S1981-P (the activated form of ATM), ATR, DNA-PKcs, γH2AX, and total ATM were assessed in NIKs grown with or without feeders. Cell lysates were prepared from NIKs at 36 hr following passaging on a new dish that is with or without feeders.

MAdCAM-1 is a mouse-specific antibody that does not crossreact with human proteins and used to verify the absence of contamination from mouse 3T3 fibroblasts feeders in th e preparation of human NIKs lysates. GAPDH and Hsp70 were used as loading controls.

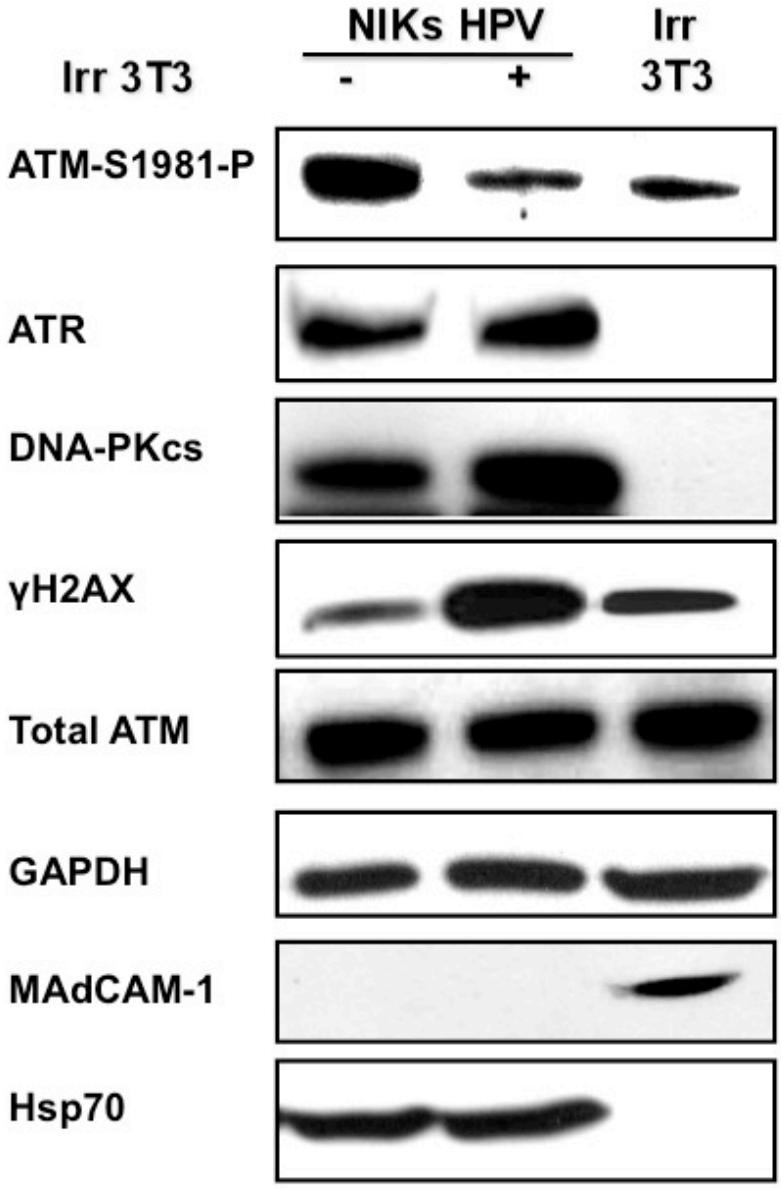

Figure 3.13: Feeder cells activated H2AX signaling in NIKs HPV.

Levels of ATM-S1981-P (the activated form of ATM), ATR, DNA-PKcs, γH2AX, and total ATM were assessed in NIKs HPV grown with or without feeders. Cell lysates were prepared from NIKs HPV at 36 hr following passaging on a new dish that is with or without feeders.

MAdCAM-1 is a mouse-specific antibody that does not crossreact with human proteins and used to verify the absence of contamination from mouse 3T3 fibroblasts feeders in th e preparation of human NIKs lysates. GAPDH and Hsp70 were used as loading controls.

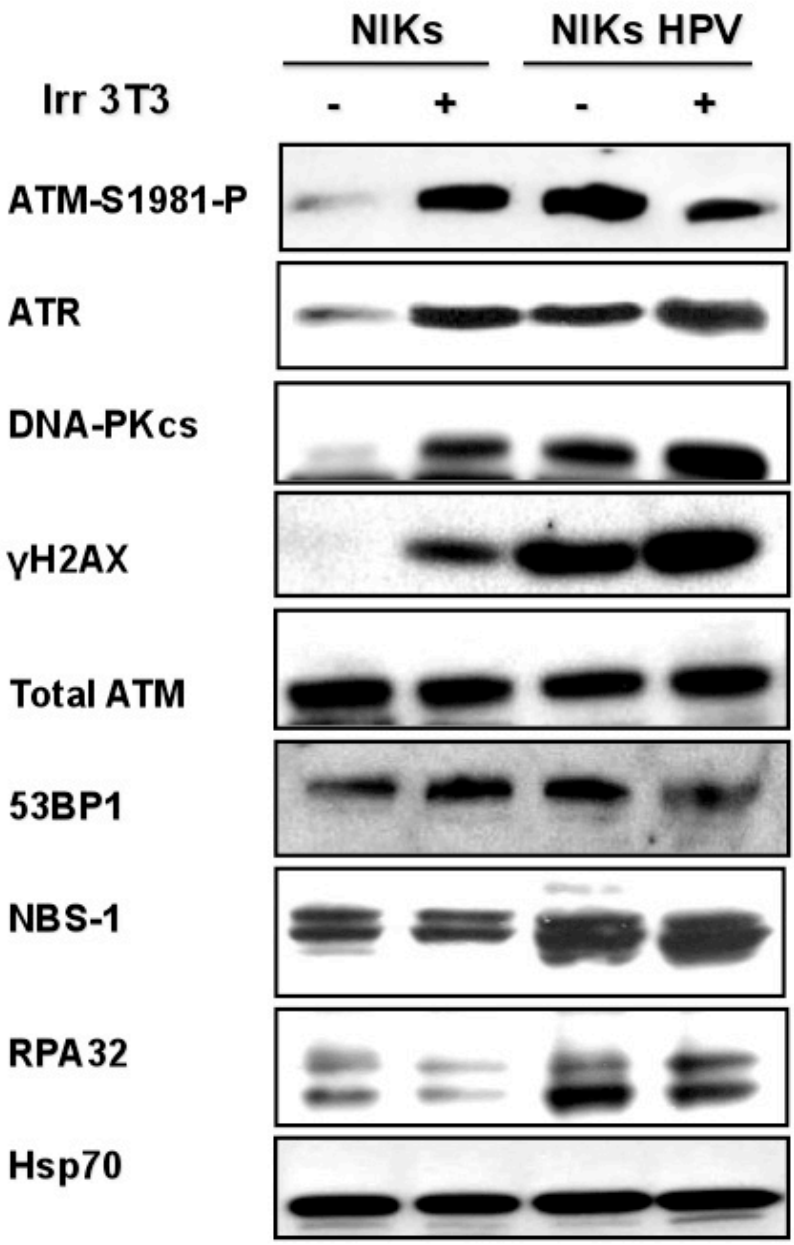

Figure 3.14: HPV16 activated DNA damage signaling.

Levels of ATM-S1981-P (the activated form of ATM), ATR, DNA-PKcs, γH2AX, 53BP1, NBS-1, and RPA32 were assessed in NIKs and NIKs HPV grown with or without feeders. Cell lysates were prepared from NIKs HPV at 36 hr following passaging on a new dish that is with or without feeders.

Hsp70 was used as a loading control.

Investigation into HPV-induced DNA damage in NIKS cells

We know that feeder cells activate DNA damage signaling leading to γH2AX induction in NIKs via bystander effect. However, we have not fully explored how HPV16 does this. Although HPV might elicit this purely by activating the DNA damage pathway, this scenario is unlikely as the comet assay showed that NIKs HPV cells displayed significantly ($p<0.05$) elevated amount of DNA breaks and their comet tail intensities were much greater compared to that of NIKs cells, even in the absence of feeders. Without any indication of how this occurs, we began by testing whether the viral oncoproteins were involved.

We generated NIKs cells that expressed HPV16 E6, HPV16 E7 or both HPV16 E6 and E7 oncoproteins. Retroviral packaging cell line, Phoenix A, were transfected with LXSN empty vector, LXSN E6, LXSN E7, or LXSN E6/E7 plasmids that contain the neomycin resistance gene. Following production of retroviruses, NIKs cells were infected with these viruses. The infected cells were grown for 3 days after which neomycin was added to the culture media to kill uninfected NIKs cells. This selection was carried out for 4 days; by which time all the un-infected control NIKs cells were dead. The surviving NIKs infectants were grown and expanded in the presence of irradiated feeder cells, as they grew less well in the absence of feeders in the long term.

Expression of either HPV16 E6 or E7 triggered a strong γH2AX induction. γH2AX levels were elevated even more when both HPV16 E6 and E7 were expressed together in the cells (Figure 3.15). In line with this, ATM-S1981-P levels were also increased in cell expressing either E6 or E7 alone. The combined expression of E6 and E7 caused even a greater increase of ATM-S1981-P in these cells (Figure 3.15). Interestingly, there is a marginal increase in ATR levels in NIKs expressing E6 or/and E7 (Figure 3.15). Similarly, the levels of DNA-PKcs were also increased in HPV16 E6- or/and E7-expressing NIKs cells (Figure 3.15). The combined expressions of HPV16 E6/E7 did not further increase ATR or DNA-PK, compared to when these viral oncoproteins were expressed alone.

In summary, our results demonstrate that both the oncoproteins of HPV16 are able to activate ATM and marginally increase ATR and DNAPKcs protein levels in cells. Since the biggest increase induced by the E6 and E7 proteins is active ATM, it is very likely that this kinase is predominantly responsible for the rise in the level of phosphorylated H2AX. It is particularly intriguing how the E6 and E7 proteins, which are very different in terms of their activities, are both able to activate ATM with cumulative effect. Numerous interesting scenarios can be conjured to explain this, but in view of the fact that our previous experiments demonstrated that HPV16 caused real physical damage to DNA of NIKs, it is perhaps through this common event that E6 and E7 induces activation of ATM. This could be verified by performing comet assays on NIKs expressing E6 or E7 proteins alone; an important experiment that could not be carried out due to time constraints.

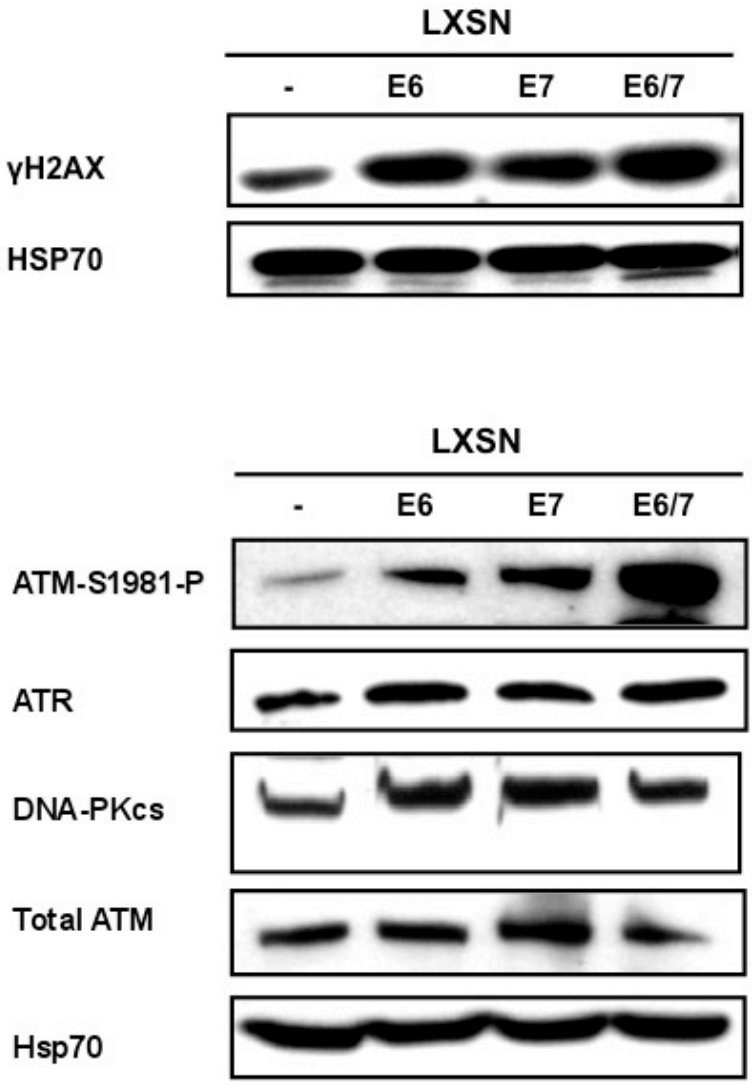

Figure 3.15: Expression of HPV16 E6 and E7 activated DNA damage signaling cascade leading to H2AX phosphorylation.

Levels of γH2AX, ATM-S1981-P (the activated form of ATM), ATR, DNA-PKcs, and total ATM were assessed in NIKs expressing LXSN (control vector), HPV16 E6 or/and E7 proteins. Cell lysates were prepared from NIKs cells that have been cultured with feeders for 36 hr. Hsp70 were used as loading controls.

Discussion

Even though co-culture with feeder cells is the optimum method for growth of keratinocytes at clonal density, other effects of feeder cells on the keratinocytes have not been thoroughly examined. In this chapter, we have addressed the consequences of culturing keratinocytes with feeder cells, within the context of DNA damage. Feeder cells provide growth-promoting factors to keratinocytes by transferring these factors through points of cell-to-cell contact or by diffusion through the culture medium (Rheinwald and Green, 1975; Borelli et al., 1989). However, there have been a number of publications on the "feeder effect" on test cells, which suggested that the effect of feeder cells may extend beyond growth-promotion. For example, human Burkitt Lymphoma cells benefited of protection from apoptosis, when they were co-cultured with feeder cells (Falk et al., 1993). It was suggested that the prolonged lifespan of some cells co-cultured with irradiated feeder cells could be due to mutagens or carcinogens produced from the feeder cells (Gerashchenko and Howell, 2003a,b; Little, 2006).

Specifically relevant to our interest is the fact that "feeder effect" has been observed in a co-culture system of which the providers of RIBE were irradiated fibroblasts (Wright and Coates, 2006; Hamada et al., 2007). Irradiated feeder cells are capable of inducing DNA breaks in non-irradiated cells that are as far as 7.5 mm away (Hu et al., 2006). This sparked our interest to investigate if the irradiated feeder cells we used in our culture system induce bystander effect in NIKs and NIKs HPV cells. This is particularly important given that this method of cell culture is the only way by which HPV16 DNA can exist stably as autonomous replicating circular DNA in the nucleus of dividing cells in culture.

Since induction of γH2AX foci has been shown to be an early step in bystander effect (Sokolov et al., 2005; Sokolov et al., 2007; Koturbash et al., 2006), we stained NIKs and NIKs HPV cells with γH2AX antibody to see if presence of feeders has any effect on H2AX phosphorylation. Although H2AX antibody stained both keratinocyte and feeder cells, there is no risk of mistaking any

residual feeder cells that were not removed in the PBS wash that was performed before staining because it is very easy to tell these two cell types apart. NIKs cells grow as very distinct colonies and have smaller nuclei than the irradiated fibroblasts, which have swollen nuclei because they were irradiated. Also, feeder cells do not grow as colonies and they are "sick-looking" and are easily identified under brightfield channel of the fluorescence microscope. The feeder cells adhere very weakly onto the culture surface and are easily removed by washing and squirting of the surface with PBS. This culture system is actually a great advantage over many other co-culture system which utilised two cell types that are difficult to tell apart; necessitating the use of markers that are only present in one cell type and not the other. Figure 3.2A shows γH2AX staining in NIKs cells whereby two different staining patterns are apparent – foci and non-foci/pan-nuclear staining, suggesting that there may be more than one event leading to phosphorylation of H2AX in NIKs cells. While punctate γH2AX foci staining is widely associated with double-strand breaks after ionising radiation (Marti et al., 2006; Sokolov et al., 2007; Burdak-Rothkamm et al., 2009; Dickey et al., 2009), the cause of diffused γH2AX staining is less clear. One possibility is that diffuse, even, and nuclear-wide (pan nuclear) γH2AX staining is triggered by DNA repair intermediates and is independent of DSBs as has been observed in human fibroblasts after UV exposure (Marti et al., 2006; Hanasoge and Ljungman, 2007; de Feraudy et al., 2010). It is also possible that many single-strand breaks across the DNA result in pan-nuclear distribution of γH2AX. Alternatively, the PIKK proteins were activated in the absence of damage to the cellular DNA as was reported by Fragkos et al. (2009). Yet another factor that may cause the mixed type of staining that was observed in NIKs is DNA replication. It is possible that while punctate γH2AX is triggered by double-strand breaks, the pan-nuclear staining is caused by DNA replication itself. The latter is particularly interesting as DNA replication stress has manifestation that are akin to DNA damage including H2AX activation (Gagou et al., 2010). However, our measurements revealed that the proportion of DNA-replicating NIKs cells was unchanged after the introduction of irradiated feeders, while the proportion of NIKs that activated γH2AX was increased markedly. This result, combined with that of the comet

assay, suggest strongly that the increased activation of H2AX is due, if not entirely, at least in large part, to real physical damage of the cellular DNA.

While we still do not know for certain, the types of DNA damage that caused the two types of γH2AX staining, we have clear results that show that the causative agents are transmitted from irradiated feeder cell to the keratinocytes through two routes. The major route requires cell-cell contact and the minor route is via the culture media. This is consistent with previous reports that demonstrated that the cell-cell contact route involves gap junctions (Sokolov et al., 2007) and that non-irradiated cells may also exhibit bystander effect following transfer of "conditioned medium" from culture of directly irradiated cells (Dickey et al., 2009; Prise and Sullivan, 2009). Irradiated cells can secrete cytokines, e.g., transforming growth factor-beta (TGFβ) or tumour necrosis factor-alpha (TNF-α), nitric oxide (NO), or cyclooxygenase-2 (COX-2), that serve to increase intracellular levels of ROS in non-irradiated cells (Lorimore et al., 2003; Sokolov et al., 2007; Hei et al., 2008).

Analyses of γH2AX levels by western blotting revealed an interesting feature of RIBE in NIKs cells. They show γH2AX levels to increase between 4 to 24 hr after addition of irradiated feeders (Figure 3.5 and 3.6), suggesting that γH2AX persist in these keratinocytes for a long time; unlike directly-irradiated cells that normally remove γH2AX by dephosphorylation through protein phosphatases very rapidly (within 3-4 hours) after repair has been completed (Chowdhury et al., 2005). Cells that are directly irradiated activate H2AX very swiftly and by 24 hours, the quantity of this protein is greatly diminished to near the basal level. The persistence of γH2AX induction is one of the characteristics of bystander effect and it has been suggested that this could be attributed to a continuous production of DNA damaging agents and insufficient DNA repair (Burdak-Rothkamm et al., 2007; Sokolov et al., 2007). In addition, this also suggests the possible generation of secondary long-lived radicals that presumably arose from ROS that were generated from irradiated feeders. It has been shown that ROS, which has been implicated frequently in medium-mediated bystander responses, were short-lived but could generate long-lived radical species that can damage DNA (Azzam et al.,

2002; Koyama et al., 1998; Kumagai et al., 2003). This point is particularly important for the field of RIBE to address, given that ROS, by its very nature is very active and hence have a very short half-life. As such the suggestion that RIBE may be mediated by the secretion of cytokines from the irradiated cells to the non-irradiated bystander cell is attractive as it provides an explanation of a continuous and long-lived supply of the causative agent, which itself is not able to damage DNA but can do so indirectly by generating a high level of ROS in the bystander cell. It would have been interesting to delve deeper into this area but we did not do so as our purpose at this point in time was to determine whether or not NIKs cells that are cultured beside irradiated feeder cells, experience RIBE from the latter. The results thus far satisfy the physical criteria of RIBE; i.e. persistent DNA damage and predominantly mediated via cell-cell contact (with a minor route through the medium). In this regard, it is important to emphasise that although the definition of bystander effect covers the phenomenon of transmission of DNA damaging agents from one cell to the other, the outcome of bystander effects can be very different (reviewed in Chaudhry, 2006; Burdak-Rothkamm et al., 2008). For some recipient cells, death ensues. In others, transformation occurs or in some cases, cells develop radioresistance or hyper radiosensitivity. Bystander studies done on irradiated fibroblasts showed enhanced growth-, invasion-, and motility-related molecules in squamous cell carcinoma (SCC) cells that are not irradiated and likely to be elicited through bystander effect (Kamochi et al., 2008). It is clear that outcome of bystander responses vary between different cell types and state of the cell (whether they are normal or immortalised or transformed). It may also be dependent on the recipient cells' DNA repair capacity (Mothersill and Seymour, 2006; Burdak-Rothkamm et al., 2008).

In the case of NIKs, no apparent detrimental effects on viability or proliferation are observed. Instead the cells appear to grow better with feeder cells especially during clonal density growth. Clearly, NIKs cells are able to manage and repair the damage inflicted on their DNA by RIBE from feeder cells. This could be viewed from the perspective of a trade-off between NIKs cells receiving growth-promoting factors from feeders cells and at the same time having to endure RIBE as well, and the success of NIKs (and keratinocytes in general) in such a system is owed to their ability to keep up with the repair of the damaged DNA. On the other

hand, it is possible that the low level of DNA damage may be the very feature that is beneficial to NIKs. This notion, at first consideration appears illogical, but if the numerous reports that show the apparent benefits of very low doses of radiation are to be believed (Matsumoto et al., 2001; Zhou et al., 2003; Mothersill and Seymour, 2006), it is possible that NIKs cells (or keratinocytes in general) might be benefiting from what is equivalent to low-doses of radiation, but indirectly through RIBE from the irradiated feeder cells. However, it must be pointed out that the reports (close to 2000 publications), on the benefits of low dose radiation, are not accepted by many in the field and it remains a controversial subject. It is raised here only as a formal possibility of the effect of irradiated feeder cell on NIKs cells.

On the other hand, a real and important implication of bystander effect in the co-culture system for keratinocytes is the question of genomic stability of these cells. As they experience continuous DNA damage from feeder cells, it is curious how these cells maintain the stability of their genome. Would not such a growth environment result in great number of mutations, mis-repair, deletions and a whole host of cytogenetic abnormalities that eventually result in the death, immortalisation or transformation of the keratinocytes? Apparently this is not the case. Spontaneous immortalisation of primary keratinocytes (most often from foreskin tissues) from growth with feeder cells is extremely rare, and transformation of these cells has never been reported. Hence it is clear that the keratinocytes have a very efficient way of dealing with the damage inflicted on their DNA. How this achieved is not known but it would not be unusual since prokaryotic organism such as *Deinococcus radiodurans*, can live in environment with extremely high level of radiation and still survive very well (Blasius et al., 2008). It would be interesting to elucidate how keratinocytes deal with the continuous damage to their DNA as this will surely reveal fascinating features that will teach us new things about cellular management of damaged DNA.

Analyses of the RIBE on NIKs cells at the protein level showed that all three protein members of the PIKK family; ATM, ATR and DNA-PKcs were affected by RIBE. ATM was phosphorylated at serine 1981, and the levels of ATR and DNA-PKcs proteins were increased. Although ATM was clearly activated, the

increase in DNA-PKcs protein level is even more dramatic in terms of magnitude of change, and ATR protein exhibited only a very modest increase. Interestingly, ATR has been implicated as the main sensor kinase in bystander signalling leading to γH2AX induction in human glioma cells, a process that is mediated by ATM and 53BP1 (Burdak-Rothkamm et al., 2007; Burdak-Rothkamm et al., 2008). We cannot be certain that this is not also the case with NIKs cells since we have not ascertained whether ATRIP level is increased significantly in response to RIBE. However, the startling increase of DNA-PKcs protein level cannot be ignored and it would not be unlikely that in contrast to glioma cells, the NIKs cells respond to RIBE predominantly through DNA-PKcs. If time had permitted, we could resolve this uncertainty by inhibiting DNA-PKcs activity with drugs and testing whether this affects H2AX phosphorylation when NIKs are co-cultured with irradiated feeder cells. Alternatively, siRNA against ATR could also be used to the same effect.

Up to this point, the cellular events caused by RIBE on NIKs cells were also seen (qualitatively) in NIKs cells that harboured HPV16 DNA in their nucleus (NIKs HPV). However, when we looked at the molecular events in response to RIBE, an interesting difference became very apparent. Unexpectedly, the level of phosphorylated (activated) ATM was reduced in NIKs HPV cells, when feeder cells are added to them. This is in stark contrast to the rise in phosphorylated ATM in NIKs cells (+ feeder cells) devoid of the virus. As NIKs and NIKs HPV are an isogenic pair of cell lines, with the exception of HPV16 DNA being present in the latter, it is clear that it is the HPV16 DNA that has caused this change in the way NIKs cells respond to RIBE. This difference brings to fore the other observations, namely; immunofluorescence of γH2AX, western blotting of γH2AX protein, comet assay and western blot analyses of phosphorylated (activated) ATM. All these analyses indicated that independently of feeders, NIKs HPV cells exhibited greater amount of damaged DNA than its isogenic partner devoid of the virus. The likelihood that HPV can generate all these without damaging the genome of the cells, as reported for AAV (Fragkos et al., 2009), is low since the comet assay revealed that the DNA of the cells were truly broken. The comet tails are not viral DNA as the quantity of HPV16 DNA in these cells

(approximately 300 copies per cell on average) are too low to be visualised by ethidium bromide (personal observation). These data point to the inescapable conclusion that HPV16 DNA causes damage to the cellular DNA. It follows that by doing so ATM is more activated in NIKs HPV16 than NIKs devoid of this virus. Strangely, RIBE from feeder cells, which normally activates ATM in NIKs cells, causes reduction of pre-elevated levels of active ATM. It is possible that a negative feedback loop exist whereby if activated ATM level reaches a certain level, an inactivation process is triggered. However, such system has not been identified or reported thus far. At present we do not know how this fascinating antagonistic effect is mediated.

In spite of the reduction of active ATM levels in NIKs HPV cells grown with feeders, the H2AX protein is still very efficiently activated (Figure 3.13). This suggests that either ATR or/and DNA-PKcs are responsible for the phosphorylation of the H2AX. ATR has been shown to mediate bystander γH2AX induction and this process occur upstream of ATM (Burdak-Rothkamm et al., 2007; Burdak-Rothkamm et al., 2008). Does this mean that ATM is not the major kinase or not at all involved in RIBE-induced H2AX induction? This may indeed be the case, at least when HPV is present in the cell. We are unable to rule out the possibility that H2AX is differently activated in NIKs depending on whether HPV is present or not.

To return to the fact that HPV can induce DNA damage of NIKs, it is interesting that we observed both the oncoproteins (E6 and E7) of HPV to be able to increase the level of active ATM, ATR and DNA-PKcs in NIKs. This increase is mirrored by activation of H2AX. This is consistent with the observations by Duensing and Munger (2002) who reported that HPV16 E6 and E7 could independently induce DNA breaks in primary human keratinocytes. This observation is particularly intriguing because the E6 and E7 proteins have very different activities. The HPV16 E6 protein can degrade p53 while the E7 protein can bind to the p21 protein and degrade the pRb protein. The common denominator between all these activities is the p53-p21-cyclin/CDK-pRb pathway that controls the G1/S checkpoint (Garner et al., 2007; Moody and Laimins, 2010). Does it suggest that abrogation of the G1/S checkpoint results in damage of DNA? This notion is

given credence by reports showing that over-expressed oncogenes do indeed induce DNA damage (Duensing and Munger, 2002; Moody and Laimins, 2009). This is thought to be owed to unregulated DNA replication (Funk et al., 1997; Day and Vaziri, 2009; Chen et al., 2009). In addition, HPV16 E7 weakens cellular DNA damage checkpoint control at the G2 phase of cell cycle by facilitating the proteolysis of claspin that is a critical mediator of the ATR/Chk1 signalling cascade and allows mitotic entry (Spardy et al., 2009). However, HPV16 E6 and E7 cause DNA damage of NIKs cells through a mechanism that is clearly different from that induced by RIBE. This is evident from the fact that, while HPV16 increased the level of NBS-1 and RPA32, RIBE did not (Figure 3.14).

Previously, we have observed that NIKs HPV cycle faster than NIKs, owed to the faster rate of EdU incorporation in NIKs HPV (Figure 3.7). The increase in cellular proliferation rate of NIKs HPV could potentially contribute to errors and stalling of DNA replication fork that induces γH2AX formation, along with the dramatic activation of the proteins involved in recognition of DNA single strand breaks, DNA double strand breaks and DNA repair, e.g., ATM, ATR, DNA-PK, H2AX, 53BP1, RPA32, NBS-1 (Figure 3.14). Therefore, the presence of HPV16 elicited DNA damage that might encompass a wide spectrum of DNA lesions. Expressing HPV16 E6 and/or E7 oncoproteins in NIKs also activated ATM, ATR, DNA-PK, and H2AX (Figure 3.15), suggesting that HPV oncoproteins might play a major role in regulation of the activated DNA damage signalling in host cells. In support of the notion that HPV16 induces vast DNA damage in NIKs, NIKs HPV cells exhibited a dramatic increase in category 3 and 4 comets (Figure 3.10B, 3.11A and 3.11C). Our results are broadly in agreement with the work of Spardy et al. (2008), where they found HPV16 E7-expressing cells stalled DNA replication forks at the alternative lengthening of telomeres (ALT)-associated promyelocytic leukaemia bodies (APBs), which may ultimately lead to enhanced DNA breakage. It is likely that HPV16-containing cells were able to inhibit cellular death- or senescence-response, through functions of E6 and E7 oncoproteins, to allow continued proliferation (Moody and Laimins, 2010).

Chapter 4: Investigation into how feeder cells and HPV16 influence the way NIKs cells respond to gamma-irradiation

Introduction

Following exposure to ionizing radiation, numerous types of DNA damage occur within the cell such as base and nucleotide alterations, single- and double-strand DNA breaks (Jackson, 2002; Houtgraaf et al., 2006). One of the most lethal forms of DNA damage sustained by radiation-damaged cells is DNA double-strand break (DSB) (Khanna and Jackson, 2001; Jackson, 2002). Recent work has highlighted the importance of early cellular DNA damage detection mechanisms in eliciting the necessary responses that lead to eventual repair of DNA double-stranded breaks. Failure to detect or repair DSBs will lead to cellular consequences such as chromosomal aberrations, increased genomic instability, and decreased cell survival (Khanna and Jackson, 2001; Natarajan and Palitti, 2008).

The earliest cellular detection of DNA damage following exposure to ionising radiation (IR) involved the activation of ATM, which is believed to require interaction with the MRN (Mre11, Rad50, and NBS1) complex to recruit it to DNA double strand lesions (Lavin, 2008). Following ATM's binding to a double-strand break, this lesion is converted to a structure that attracts and activates ATR (Jazayeri et al., 2005; Cimprich and Cortez, 2008). Apart from ATM and ATR, DNA-PKcs is also involved in sensing and repair of damage DNA following ionising radiation. Binding of DNA-PKcs to free DNA ends causes activation of DNA-PKcs to facilitate non-homologous end joining repair (NHEJ) of radiation-induced breaks (Yang et al., 2003; Collis et al., 2005). It is thought that DNA-PKcs serves as a scaffold protein to assist in the localisation of DNA repair proteins to the site of damage (Park et al., 2003; An et al., 2010). All the three PI3K-like protein kinase (PIKK) family members, ATM, ATR, and DNA-PKcs, can phosphorylate H2AX in response to DNA damage (Redon et al., 2002). The activation of these kinases will in turn lead to activation of independent and overlapping downstream targets such as Chk1, Chk2, and p53, to kick-start

myriad DNA repair activities and cell-cycle arrests. The primary response to DSBs requires the activation of ATM, however because there are overlapping functions between ATM and ATR, these downstream targets can be sufficiently activated by either kinases in the absence of the other (Collis et al., 2004; Myers and Cortez, 2006). Defects in these DNA damage response and repair signalling pathways could lead to failure to elicit cell cycle arrests, resulting in replication of damaged DNA, mitosis of damaged cells, and hypersensitivity to radiation (Kastan and Bartek, 2004). We hypothesised that some of the biological processes that we discussed previously, e.g., bystander effect caused by feeder cells and DNA damage caused by HPV16, could alter the way keratinocytes respond to gamma-irradiation as these cells have pre-activated DNA damage signalling.

Bystander NIKs and NIKs HPV cells already possessed pre-activated DNA damage signalling from co-cultivation with irradiated feeder cells. Therefore, treating these cells to a subsequent dose of radiation may alter the expression of genes that are involved in the DNA damage response pathway. This can either diminish or increase the effects of DNA damage (Tapio and Jacob, 2007; Mothersill et al., 2006) on these cells grown with feeders. Increased radio-resistance is associated with a phenomenon known as adaptive response, which is defined as the acquisition of resistance against subsequent dose of radiation as a result of adaptation to an initial lower dose of radiation (Matsumoto et al., 2004; Tapio and Jacob, 2007). Pre-exposing cells to a low “priming” or “conditioning” dose of radiation can protect these cells from the effects of a second larger dose (Mothersill and Seymour, 2001; Kadhim et al., 2004). On the contrary, prior exposure to an initial dose of radiation could also enhance cell death after a subsequent treatment with gamma-irradiation (Joiner et al., 2001; Mothersill et al., 2002). The determining factor that controls cellular radiation response, whether it is increased radio-resistance or radio-sensitivity, appeared to be the genetic background of the cell and not necessarily the radiation dose (Mothersill and Seymour, 2006). In the case of NIKs cells, culturing them with feeder cells or having them harbour HPV16 DNA causes increased DNA damage. Hence we wanted to know how RIBE or / and HPV16, influences the way by which NIKs cells respond to a direct dose of ionising radiation.

Results

Activation of DNA damage response in NIKs cells grown with or without feeders following exposure to gamma-irradiation

To investigate whether the presence of feeders affects the way by which NIKs cells respond to direct gamma radiation, we treated NIKs cells (+/- feeder cells) to 10 Gy of ^{137}Cs gamma-irradiation. Over a period of four hours after irradiation, individual dishes of NIKs cells were harvested at 0 (unirradiated), 0.5, 2, and 4 hr. The levels of ATM-S1981-P, ATR, DNA-PKcs, p53Ser15-P, and γH2AX proteins in the lysates of these cells were analysed by immuno-blotting.

In the absence of feeder cells, all the three PIKK proteins ATM, ATR and DNA-PKcs were activated within 30 minutes of radiation (Figure 4.1). Equally rapid and robust in being activated, were two proteins, H2AX and p53, which are substrates of the three PIKK proteins. Not surprisingly, the rise and fall in the levels of activated H2AX and p53 were very similar to the levels of the three PIKK proteins (Figure 4.1). Collectively, this study reveals that NIKs cells (without feeders or HPV16) are exquisitely sensitive to the effects of ionising radiation, and are very efficient in activating all the three PIKK family members, ATM, ATR, and DNA-PKcs, in a manner that is consistent with the current understanding of how cells would normally respond to DNA damage.

However, when NIKs cells were grown with feeders cells, two of the three PIKK proteins; ATM and ATR, failed to respond to ionising radiation, while DNA-PKcs level rose rapidly within 30 minutes and remained so up to at least 4 hr following irradiation (Figure 4.1). Although the p53 protein was activated within 30 minutes of irradiation, it did not achieve maximum phosphorylation until 2 hours after irradiation. This is in contrast to the situation when NIKs were grown without feeders, where p53 was maximally phosphorylated within 30 minutes of irradiation. Interestingly, in spite of the apparent lack of response from ATM and ATR proteins,

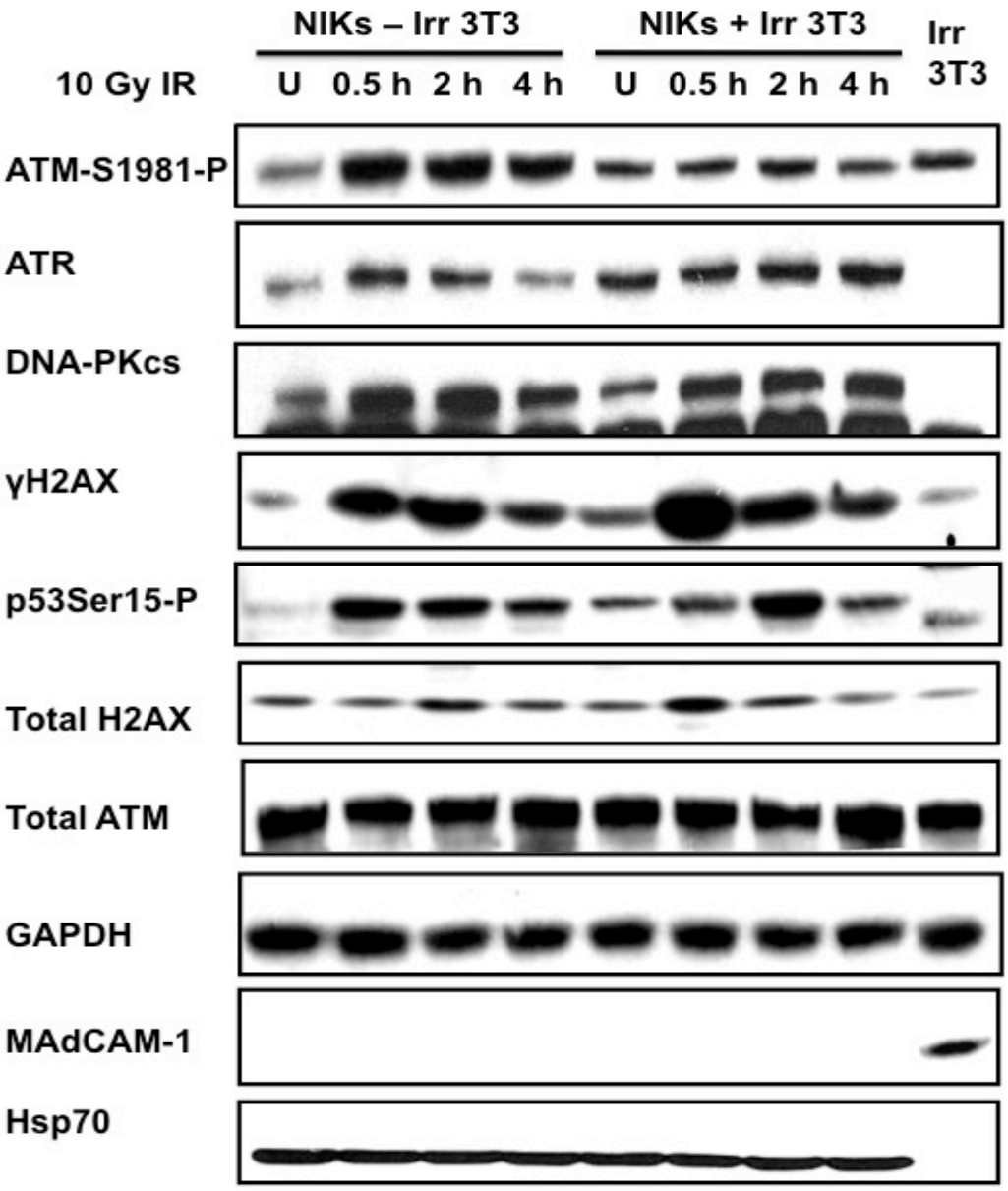

Figure 4.1: Expression levels of DNA damage checkpoint proteins in NIKs grown with and without feeders at 0.5, 2, and 4 hr following 10 Gy IR. U is lysates isolated from unirradiated cells. Levels of ATM-S1981-P, ATR, DNA-PK, γH2AX, p53 Ser15-P, Total H2AX, Total ATM, GAPDH, MAdCAM-1 and Hsp70. MAdCAM-1 is a mouse-specific antibody that does not cross-react with human proteins and used to verify the absence of contamination from mouse 3T3 fibroblasts feeders in the preparation of human NIKs lysates. GAPDH and Hsp70 were used as loading controls. These blots are representative of several consistent experiments.

the phosphorylation of H2AX was not impeded or even delayed. In fact the dynamics of H2AX activation was largely similar to that in NIKs cells grown without feeders.

In conclusion, NIKs cells on their own are able to activate ATM, ATR, and DNA-PKcs very efficiently (leading to activation of H2AX and p53) following ionising radiation. However, when NIKs cells are cultured with feeder cells, only DNA-PKcs appear to respond to ionising radiation. Notwithstanding this change, H2AX can still be as efficiently activated and p53 can still be activated albeit with less efficiency.

Activation of DNA damage response in NIKs HPV cells grown with or without feeders following exposure to gamma-irradiation

Having observed that feeder cells exert a profound effect on the way by which NIKs cells respond to ionizing radiation, we tested the effect of HPV16 (which also induces DNA damage) on NIKs's cells response to irradiation. We irradiated NIKs HPV cells (+/- feeder cells) with 10 Gy of gamma-irradiation and monitored the cellular DNA damage response at the protein level.

When NIKs HPV cells (- feeder cells) were irradiated, the level of active ATM in the cells did not rise as expected (Figure 4.2). Although the amounts of ATR and DNA-PKcs proteins did increase, there was a significant delay. ATR took 4 hours and DNA-PKcs took 2 hours after irradiation to rise, in contrast to NIKs cells without HPV and feeders, whereby all three PIKK proteins were activated within 30 minutes. In spite of this slow response, there was no apparent compromise in the phosphorylation of H2AX; the implication of which is addressed in the discussion section. The phosphorylation of the p53 protein was also severely affected, in that there was only a very slight perceptible rise 2 hours after irradiation. It is difficult to interpret this particular result as HPV16 E6 protein, which we know are expressed in these cells, actively shuttles the p53 protein for degradation. Hence the dynamics of p53 phosphorylation cannot be easily compared to that of NIKs cells without the virus.

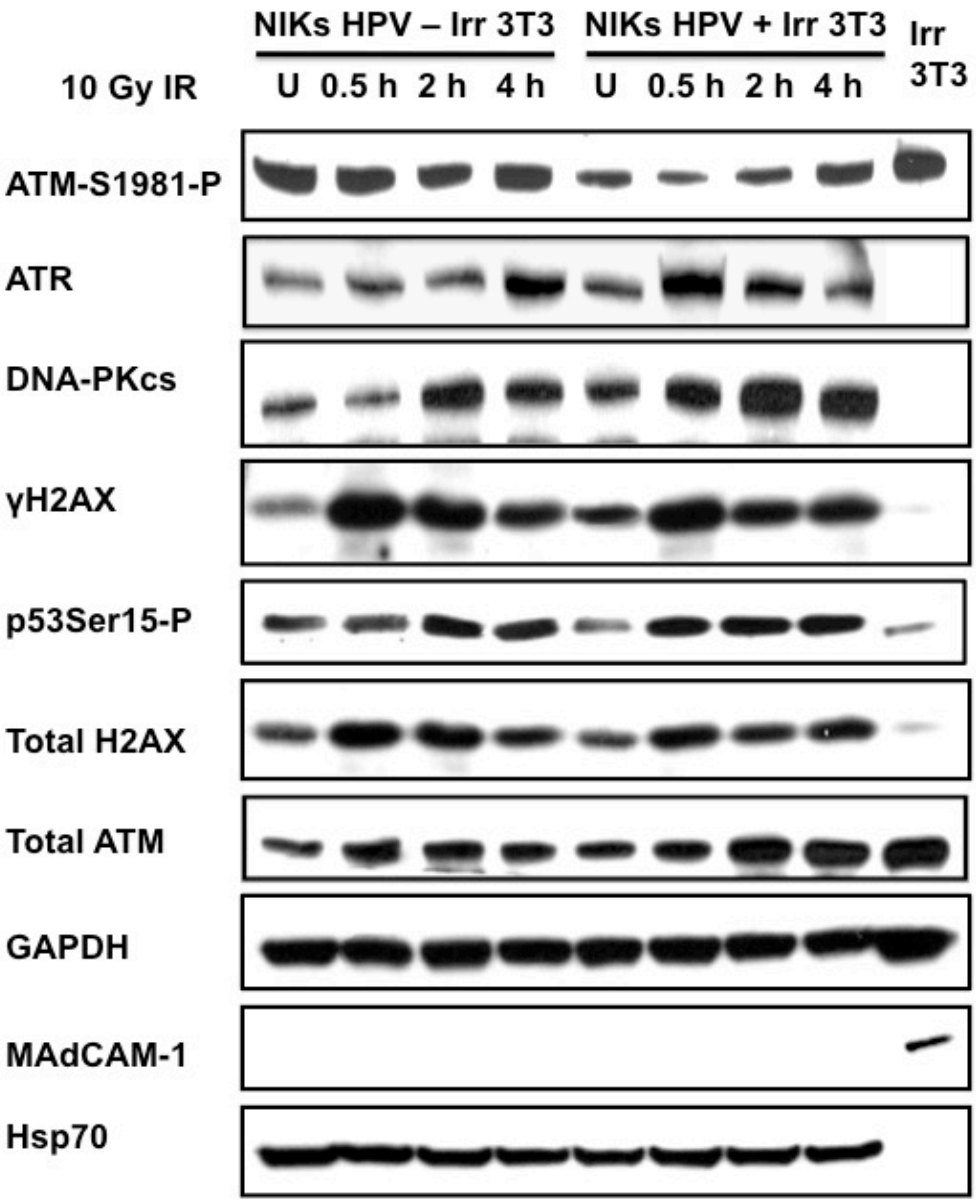

Figure 4.2: Expression levels of DNA damage checkpoint proteins in NIKs HPV grown with and without feeders at 0.5, 2, and 4 hr following 10 Gy IR. U is lysates isolated from unirradiated cells.

Levels of ATM-S1981-P, ATR, DNA-PK, γH2AX, p53 Ser15-P, Total H2AX, Total ATM, GAPDH, MAdCAM-1 and Hsp70. MAdCAM-1 is a mouse-specific antibody that does not cross-react with human proteins and used to verify the absence of contamination from mouse 3T3 fibroblasts feeders in the preparation of human NIKs HPV lysates. GAPDH and Hsp70 were used as loading controls. These blots are representative of several consistent experiments.

When NIKs HPV cells were grown with feeders, we observed that the basal level of activated ATM was significantly lower than when feeder cell were absent

(Figure 4.2). Following exposure to 10 Gy of gamma rays, ATM activation was not seen until 4 hours later (Figure 4.2). Surprisingly, the levels of ATR and DNA-PKcs protein increased rapidly within 30 minutes, in a fashion that is akin to that of NIKs cells without feeders and HPV16 (compare Figure 4.1 and 4.2). Yet again, the rise in γH2AX levels was not at all affected by the changes in the response of PIKK proteins to radiation. We observed that NIKs HPV cells grown on feeders have already a lower basal level of p53Ser15-P. Following irradiation, the level of this protein increased rapidly within 30 minutes and remained high even up to 4 hours after irradiation (Figure 4.2). As mentioned above, p53 levels in these cells are influenced by HPV16 E6 proteins. As such, the interpretation of this result is not straightforward and will be addressed in the discussion section.

Collectively, it is clear that feeder cells and HPV16 influence the way by which NIKs cells respond to ionising radiation. Although both feeder cells and HPV16 appear to cause broadly similar changes to the responsiveness of ATM, ATR and DNA-PKcs to radiation, the resultant consequence of both of these factors on NIKs cells were not additive. Instead, feeder cells reduced the basal level of active ATM in NIKs HPV cells, and from this reduced level, ATM was able to respond to radiation by being activated, albeit very gradually. Feeder cells also attenuated the effects that HPV alone have on the responsiveness of ATR and DNA-PKcs proteins following radiation. Interestingly, amidst all the changes in levels and dynamics of PIKK proteins, caused by either HPV or feeder cells, or both; the H2AX protein was always efficiently phosphorylated within 30 minutes of irradiation. This phenomenon highlights the difficulty in predicting the outcome of DNA damage on cells merely by the state of the three PIKK proteins. It is undeniable that the absence of a single protein such as ATM has an adverse effect on cells, but the resultant changes in all three PIKK proteins, by HPV16 as a case in point, cannot be predicted. In this regard, and for reasons that will be detailed below, we wanted to know the long-term outcome of cells bearing HPV16 DNA, following ionising irradiation, compared to cells devoid of this virus.

Consequence of gamma-irradiation on the survival of NIKs and NIKs HPV cells grown with feeders

The observations that we made in the sections above raised many exciting questions that could and should be answered. Among them is the question of whether HPV influences the survival of NIKs cells following ionising radiation. We chose to address this particular question because of its potential relevance in terms of radiotherapy of cervical cancer, and head and neck cancer. These cancers are common and are treated with radiation and/ or DNA-damaging chemotherapy drugs. Hence understanding how HPV affects the cell's response to DNA damage is important and relevant. In this section, we present results from experiments that measured the long-term effects of irradiation of these cells (i.e., cell viability).

To determine if HPV16-induced DNA damage causes increased or reduced sensitivity of NIKs cells to radiation, NIKs and NIKs HPV cells that were grown with feeders were irradiated at 0, 2.5, 5, or 10 Gy and then plated for clonogenic cell survival assay. Clonogenic survival assay assesses the long-term survival of cells by measuring the ability of cells to proliferate and form large colonies or clones (Munshi et al., 2005). Although long-drawn, this assay is the only reliable measurement of cell survival, as opposed to short and quick cell death (apoptosis) assays, which only measure the *rate* of cell death, and do not show the true survival of cells (Munshi et al., 2005; Franken et al., 2006). The nature of clonogenic assay requires that the cells be seeded at clonal density (very sparsely) and cultured for long periods of time. This limited us to doing the experiment with the presence feeder cells, because NIKs and NIKs HPV cells cannot grow well when seeded sparsely without the aid of feeder cells.

NIKs and NIKs HPV cells were subjected to gamma-irradiation at 0, 2.5, 5, or 10 Gy (Figure 4.3). Immediately after irradiation, these cells were trypsinised, resuspended to generate single cell suspensions, counted, serially diluted, plated on feeder cells and cultured for 14 to 21 days. Prior to this, we carried out experiments to determine the suitable number of cells to plate in order to obtain colony numbers that are amenable to counting (Table 4.1). This we ascertained to

be 160 cells per plate, and is suitable for both, NIKs and NIKs HPV cells, in spite of them having different plating efficiencies. NIKs HPV have a higher plating efficiency at 45% compared to NIKs at 12.5% (Figure 4.4A). As expected, the number of NIKs and NIKs HPV colonies decreased with increasing dose of radiation. To determine the percentage of survival in NIKs and NIKs HPV cells following irradiation, the number of colonies in the non-irradiated control plate were first counted and set as 100% survival. The percentage survival of these cells was determined by dividing the number of colonies that arose after irradiation with the number of colonies in the non-irradiated plate. The results are tabulated in Figure 4.4A and plotted in Figure 4.4B, which shows that NIKs cells are more radio-resistant than NIKs HPV cells following gamma-irradiation at 2.5Gy and 5 Gy. Not surprisingly, exposure to 10 Gy of ^{137}Cs gamma rays killed all the cells in these experiments. In conclusion, the presence of HPV16 significantly sensitised NIKs cells to gamma-irradiation. This result is particularly interesting as HPV16 was also observed to hyper-sensitise NIKs to Camptothecin-induced DNA damage (Ken Raj; personal communication). The viral proteins responsible and the pathways involved in the sensitisation were subjects of a parallel research programme in the laboratory, and will be addressed in the discussion.

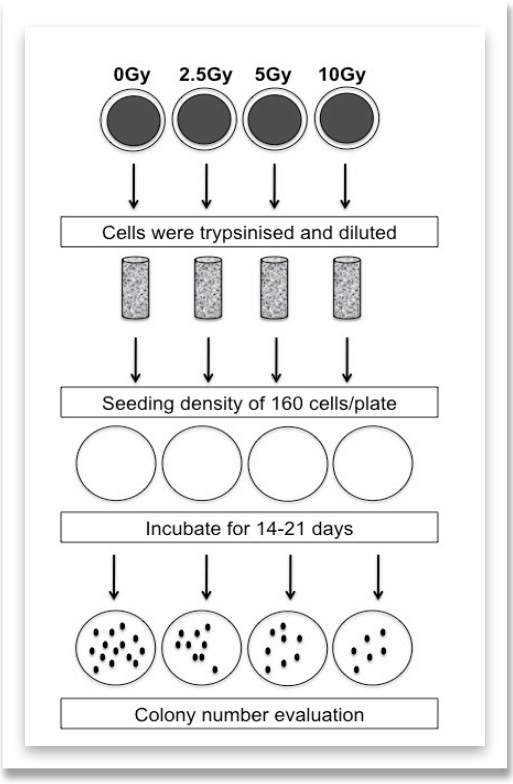

Figure 4.3: Steps involved in the setup of clonogenic cell survival assay. 10^5 NIKs cells were plated on feeders and allowed to grow overnight. Individual dishes of cells were then subjected to 0, 2.5, 5.0, and 10.0 Gy of ^{137}Cs gamma-irradiation. Following IR, cells were trypsinised, resuspended to produce single cell suspensions, and serially diluted. 160 cells were plated on individual dishes containing feeders, followed by incubation for 14-21 days. The dishes were then stained with methylene blue to visualise colonies and evaluate colony numbers.

NIKs

Dose (Gy)	No. cells plated	No. Colonies	Mean colony number	% Plating efficiency	% of survival
0	100	15, 14	14.5	14.5	100
	160	25, 20	22.5	14.1	100
2.5	160	15, 19	17	10.6	75
	320	20, 30	25	7.8	55.3
5	160	8, 6	7	4.4	31
	320	10, 12	11	3.4	24
	480	20, 15	17.5	3.6	26
10	160	0	0	0	0
	320	0	0	0	0
	480	0	0	0	0

NIKs HPV

Dose (Gy)	No. cells plated	No. Colonies	Mean colony number	% Plating efficiency	% of survival
0	40	18, 20	19	47.5	100
	80	36, 42	39	48.8	100
	160	70, 80	75	46.9	100
2.5	80	18, 25	21.5	26.9	55
	160	33, 30	31.5	19.7	42
5	160	6, 10	8	5	10.7
	240	17, 13	15	6.3	13.4
	320	18, 21	19.5	6.1	13
10	160	0	0	0	0
	320	6, 8	7	2.2	4.6
	480	2, 5	3.5	0.7	1.5

Table 4.1: Setup of dilution sheet used during optimisation of the seeding density for clonogenic cell survival assay.

A portion of NIKs and NIKs HPV cells were plated at a seeding density of 40 to 480 cells in duplicate after subjected to 0, 2.5, 5.0, 10.0 Gy of ^{137}Cs gamma-irradiation. Plates were stained and colonies were counted after incubation for 14-21 days. Counts from the two plates were averaged, and surviving fraction was calculated as the ratio of the plating efficiency of the treated cells divided by the plating efficiency of the control cells (0 Gy).

A

NIKs	From plating of 160 cells		
	Mean colony number	% Plating efficiency	% of survival
Control 0Gy	20	12.5	100
2.5Gy	19	11.9	95
5.0Gy	6	3.8	30
10.0Gy	0	0	0

NIKs HPV	From plating of 160 cells		
	Mean colony number	% Plating efficiency	% of survival
Control 0Gy	72	45	100
2.5Gy	33	20.6	45.8
5.0Gy	9	5.6	12.5
10.0Gy	0	0	0

B

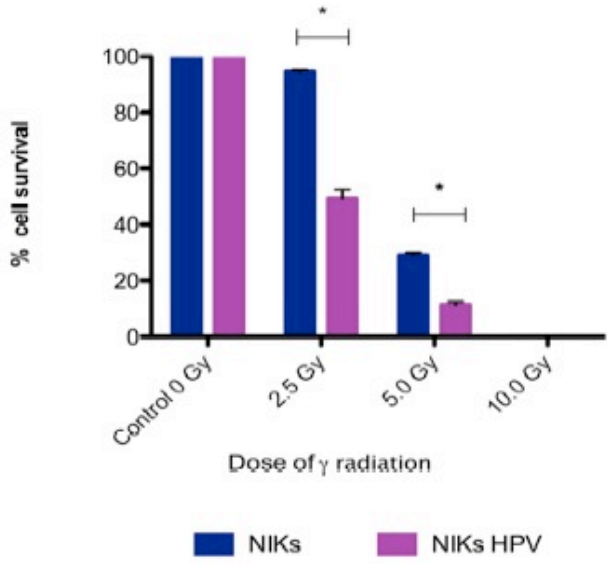

Figure 4.4: Clonogenic survival assay of NIKs and NIKs HPV cells irradiated with ^{137}Cs gamma rays.

(A) Clonogenic survival data consisting mean colony number of 3 different experiments, plating efficiency and percentage of cell survival. (B) Graphic representation of the results, with each bar representing the mean ± SEM of 3 different experiments. Statistical analysis was carried out using a 2-way ANOVA with a Bonferroni post test, * $p < 0.001$.

Discussion

The experiments described in chapter 3 established that both irradiated feeder cells and HPV16 DNA cause damage to the DNA of NIKs cells – the former by radiation-induced bystander effect and the latter through the HPV16 E6 and E7 proteins. The experiments described in this chapter were carried out to ascertain how NIKs cells, by being in a DNA damage-primed state, would respond to a dose of direct irradiation. Knowing this is particularly important for several reasons. Firstly, this system of co-culture is the only *in vitro* system that can support the HPV DNA as replicating episomes. With the increasing interest in how viruses interact with their host cells' DNA damage surveillance systems (Lilley et al., 2007; Weitzman et al., 2010), it is crucial, that we understand how the co-culture system itself influences our observations. Secondly, knowing that HPV16 induces damage to the host's DNA, it is important to determine whether this environment of perpetual low-level DNA damage influences the way by which the host cell respond to a direct dose of irradiation. The implications of this are obviously relevant in the context of radiotherapy of cancers with HPV compared to those that are devoid of the virus.

Our experiments revealed that NIKs cells (- feeder cells) were fully competent in mounting a rapid DNA damage response by activating ATM, ATR and DNA-PK within half an hour (Figure 4.1). This is in contrast to NIKs cells that were grown with feeders, where activation of ATM and ATR in response to direct ionizing radiation was not observed. However, the basal levels of active ATM and ATR proteins in NIKs cells were already augmented by feeder cells prior to irradiation (as shown and discussed in chapter 3 and seen in Figure 4.1). It would appear that this prevented further increases in their levels following a direct dose of ionizing radiation. However, this does not apply to DNA-PKcs, as even though its level was also augmented by feeder cells (Figure 3.12 and Figure 4.1), DNA-PK responded equally well to ionizing radiation whether or not feeder cells were present.

It is interesting that HPV16 also influenced NIKs response to ionizing radiation in much the same way as feeder cells did. We found that upon direct irradiation of NIKs HPV cells, further activation of ATM did not occur and there was a severe delay in the rise of ATR protein level, and also a delay in the increase of DNA-PKcs (albeit less severely than that of ATR) (Figure 4.2). Hence it appears that whether the "priming" DNA damage of NIKs cells prior to direct irradiation was elicited by feeder cells or HPV16, the outcome is rather similar in that, active ATM and ATR levels did not rise significantly with further DNA damage, while DNA-PKcs was still responsive to subsequent assault on the DNA.

The similarity between the effects generated by HPV16 DNA and feeder cells in NIKs might suggest that the types of damage inflicted on NIKs DNA by these two agents are quite similar. This notion however, is challenged when we consider the combined effects of HPV16 and feeder cells on NIKs cells. Here we do not see additive changes to the levels of ATM, ATR or DNA-PKcs, as would be expected if the types of DNA lesions inflicted by HPV16 and feeder cells were the same. Instead we see that the basal level of active ATM in NIKs HPV cells was lowered when feeders were added to them; as was described and seen in Figure 3.17, and also apparent in Figure 4.2. From this level, active ATM increased upon direct radiation of these cells, albeit very gradually. However, ATR and DNA-PKcs levels in NIKs HPV cells grown with feeders rose swiftly as it did in NIKs cells devoid of virus or neighboring feeder cells. It would appear that the inability to activate ATR and DNA-PKcs proteins efficiently in NIKs cells, due to either feeder cells or HPV16, was obliterated when both these agents were present together. These observations do not lend credence to the suggestion that RIBE and HPV16 inflict the same types of lesions on NIKs DNA.

It is interesting that regardless of the condition of NIKs culture (+/- feeders, +/- HPV16 DNA) and irrespective of whether all or only one or two of the PIKK proteins responded to direct ionizing irradiation, H2AX was efficiently phosphorylated. The simplest interpretation of this is that since at least one of the PIKK proteins was activated in all the different NIKs culture, this is sufficient to ensure that H2AX is efficiently activated. Furthermore, feeder cells and HPV16 individually augmented the level of active ATM in NIKs cells, and this

heightened level of active ATM may be sufficient to respond to additional DNA breaks (from IR) without the need for further activation of ATM. As a case in point, NIKs HPV cells (-feeder cells) did not increase the levels of any of the PIKK proteins, until 2 hours (DNA-PKcs) to 4 hours (ATR) after irradiation, yet a clear and robust activation of H2AX was evident within 30 minutes (Figure 4.2). It is however very clear that the level of active ATM in these cells were extremely high (Figure 4.2 and 3.14) even before irradiation. As such it is not surprising that subsequent double-strand breaks inflicted by gamma irradiation were very swiftly responded to (in the form of phosphorylation of H2AX) by the ever-present active ATM in these cells.

In the case of NIKs HPVs cells grown with feeders, the basal level of active ATM levels was not heightened before irradiation and its increase after irradiation was very sluggish; taking up to 4 hours. Yet, the H2AX was swiftly and maximally phosphorylated within 30 minutes. In these cell, the ATR and DNA-PKcs levels rose sharply within 30 minutes of irradiation and they were almost certainly responsible for the rapid phosphorylation of H2AX. This highlights an interesting fact, which is that although ATM, ATR and DNA-PKcs can phosphorylate similar substrates, and hence seem to be redundant (Stiff et al., 2004; Wang et al., 2005; Hanasoge and Ljungman, 2007), the means by which they are regulated (activated / inhibited) are very different. It would appear that this is a great advantage for the cell, so as to be able to still activate the appropriate DNA damage response when one or the other PIKK protein is indisposed for one reason or another.

As for the p53 protein, the situation is more complicated because the E6 protein of HPV16 actively targets p53 for degradation and direct comparisons should not be made between NIKs cells (+/- feeders) and NIKs HPV cells (+/- feeders). In NIKs cells (-feeders), the p53 protein was very rapidly phosphorylated, to the maximum within 30 minutes after irradiation. However, with feeders, this peak is delayed to 2 hours. Since active ATM is the only PIKK protein that did not rise in response to irradiation, this delay in p53 phosphorylation may be due to the lack of or deficiency in ATM activation. Interestingly, H2AX phosphorylation peaked at 30 minutes, suggesting that it is phosphorylated by DNA-PKcs (whose level rose to maximum in 30 minutes as well) and possibly by ATR as well (whose level rose

very modestly after irradiation). As such, it seems that H2AX is a better substrate of DNA-PKcs than p53 is.

It is very clear from these sets of experiments that great care must be taken when this co-culture system is used to study the interaction between HPV and DNA damage surveillance, signaling and repair systems within the cell. Without the benefit of this information one would have performed such experiments with feeder cells in NIKs and NIKs HPV cultures, and encountered the curious fact that NIKs cells are not able to activate ATM when irradiated (even at 10 Gy) and that HPV16 sensitised (albeit modestly) NIKs to the presence of damaged DNA (compare the levels of active ATM in right hand sections of Figure 4.1 and 4.2). One would also conclude that ATR in NIKs cells was also not raised in response to irradiation and yet again, HPV16 appears to provide NIKs cells with the ability to increase ATR when irradiated. These two conclusions would have been accompanied by the observation that DNA-PK activity was unchanged by HPV16. All these three anomalous observations are in stark contrast to the real effect of HPV16 on NIKs cells, which is that (a) HPV16 increases the basal level of active ATM in the cells, and upon subsequent DNA damage (by ionizing radiation), this level is refractive to further increase, and (b) HPV16 delays severely, the rise of ATR and DNA-PKcs protein levels when the host cells are irradiated. How these effects could be induced by HPV16 was discussed in the previous chapter, and will not be addressed here. Instead, we must not digress from the main conclusion of these results, which is that the co-culture system exerts a profound effect on the DNA damage response of NIKs cells, and this must be seriously considered when this system is used to investigate the interaction between HPV and cellular processes involved in DNA damage surveillance.

An obvious follow-up question from this is; does the presence of pre-damaged DNA in NIKs cells, generated either by feeder cells or HPV16, compromise NIKs ability to deal with direct irradiation? One could propose that since H2AX proteins (and presumably other substrates as well) could still be activated; changes caused by feeder cells or HPV16 in NIKs cells response to ionizing radiation is irrelevant as long as a DNA damage signal is triggered (as represented

by γH2AX). This proposition assumes that all necessary downstream proteins would be equally well activated as H2AX. This assumption may be correct but it remains an assumption until proven. There are however, a couple of possibilities in addition to this one. They involve the consideration of the fact that low-level DNA damage in cells can either adapt the cells to cope better with a second dose of irradiation, or hyper-sensitise the cells to the second dose of irradiation instead (Szumiel, 2005, 2008). In the case of NIKs cells, whether they would benefit from the low level of DNA damage induced by HPV16 (or feeder cells), by being better poised to deal with ionising radiation, or instead become even more susceptible, cannot be predicted, and must be tested empirically.

Experiments to test this fascinating question may appear simple, but is actually very complex. The best way to ascertain the true outcome of irradiated NIKs and NIKs HPV cells is the clonogenic assay, which was explained in detail in the result section. As this assay relies on counting colonies of cells derived from single cells, it is essential that the test cells be seeded very sparsely. This is a particularly difficult thing to do with NIKs because while NIKs can be weaned off feeders and cultured without feeder support, they have to be seeded at high density at each passing. Attempts to seed these cells at low density without feeder cells resulted in adverse effect on their survival and growth. This restricted us to testing the effect of HPV16 on the radio-sensitivity of NIKs cells in the presence of feeder cells. In spite of this less-than-ideal situation, the results were very interesting indeed.

The clonogenic experiment showed that HPV16-containing cells were more sensitive to radiation than control NIKs cells (Figure 4.4). Since we are comparing NIKs with NIKs HPV that were both grown with feeders, this brings us back to the observation that NIKs HPV cells grown with feeders have an impediment in ATM activation following IR. It is possible that this is one of the contributing factors to decreased survival in these cells after treatment with IR, as ATM-deficient cells have been known to display increased radiosensitivity (Lavin, 1999, 2008). It is also likely that NIKs HPV cells grown with feeders display increased radiosensitivity owed to the increased level of DNA damage

contributed jointly by HPV16 and feeders, as is evident from the γH2AX level seen in Figure 3.14. This might sensitize the cell to further DNA damage from irradiation.

Although the above proposals may well be correct, there are reasons to think that HPV16 itself (independently of feeder cells) can sensitise cells to irradiation. Similar to our findings, two naturally occurring HPV16-containing head and neck (H & N) cancer cell lines that were grown without feeder cells were reported to also exhibited increased radiosensitivity (Gupta et al., 2009). It was noted that the increased radiosensitivity of these cell lines matches the increased survival of cancer patients to radiation treatment (Settle et al. 2009). This was also observed for cervical cancers, where the presence of HPV in the tumour cells increased the sensitivity of the tumours to DNA-damaging treatment (Eifel et al., 2004; Fakhry et al., 2006; Settle et al., 2009). Furthermore, in cervical cancer cell lines that expressed HPV16 E6, it was reported that the combined degradation of p53 and activation of aurora A led to increased radiosensitivity (Shin et al., 2010).

The notion that HPV16 E6, or the loss of p53 activity can sensitise cells to dying when they are irradiated, is still surprising to many, although this has been observed and reported since 1995, when Xu, C et al. showed that HPV16 E6 sensitised human mammary cells to apoptosis induced by DNA damage. A year later the group of Galloway showed that inactivation of p53 enhanced the sensitivity of cells to being killed by multiple chemotherapeutic agents (Wahl et al., 1996). This observation was further supported by work from numerous other groups, including that of Vogelstein and O'Connor (Wang et al., 1996; Polyak et al., 1997). More recently work from Raj et al. (2001), and Garner et al. (2007), provided more evidence for this and uncovered one possible way by which the loss of p53 can sensitise cells to radiation-induced death (Garner and Raj, 2008).

As mentioned in the results section, during the period in which this work was done, a separate on-going project (headed by K. Raj) in the lab also revealed that NIKs HPV cells were far more sensitive to Camptothecin than NIKs cells were. Interestingly, they observed that this sensitivity was conferred by E6 and E7 individually and also together. Mutants of E6 that cannot degrade p53 and

mutants of E7 that cannot degrade pRb failed to sensitise NIKs to ionising radiation-induced death. This suggests that the disruption of the p53-p21-cyclin/Cdk-pRb pathway was responsible for the sensitisation of the NIKs cells. It was observed that NIKs HPV cells, which have this pathway disrupted, failed to arrest the cell cycle when treated with Camptothecin and this resulted in the conversion of single-stranded DNA breaks to double-stranded breaks, which are lethal to cells. Although this is not the subject of this thesis, these results provide plausible explanations as to why NIKs HPV cells are more sensitive to radiation than NIKs cells are.

However, it must be mentioned that, several other reports have shown that cell lines containing HPV16 or expressing E6 oncoproteins alone exhibited increased radio-resistance (Tsang et al., 1995; Hampson et al., 2001; Saxena et al., 2005). These studies attributed the radio-resistance to E6-mediated degradation of p53, and the lack of p53-dependent apoptosis following IR. It is not clear why different results are obtained, but it is possible that the effects of p53 status on radiation response depend on the system studied and the radiation dose (Sionov and Haupt, 1999; Komarova et al., 2004; Szumiel, 2008). Whatever the case may be *in vitro*, it is unequivocal that in the clinical setting (*in vivo*), HPV does indeed sensitize tumours to radiotherapy and chemotherapy. Hence it is of great importance to delineate how this occurs as it might lead us to exploit the knowledge to induce or increase the sensitivity of other tumours to such treatments.

Chapter 5: Investigation into the persistence and maintenance of HPV16 episomal copy numbers in NIKs cells

Introduction

We have observed that irradiated feeder cells that were used to support the growth of NIKs cells caused radiation-induced bystander effect on the latter. This information is particularly interesting in view of the failure of several groups to generate keratinocytes that can harbour episomal HPV DNA without the use of feeder cells (Dall et al., 2008). It raises the question that we address here, which is; whether the non-published accounts of the need of feeder cells to support HPV episome maintenance are true and if so, could it be due to the radiation-induced bystander effect that keratinocytes receive from the feeder cells. This notion is based on the numerous reports of how many other viruses benefit from the DNA damage response of their hosts cells. Some of these are briefly described below.

Simian Virus 40 (SV40)

When SV40 infects primate cells, its large T protein induces damage to the cellular DNA. This in turn activates a DNA damage response which is accompanied by the phosphorylation of ATM. The activation of ATM is beneficial to SV40 because this activity is required for the phosphorylation of the SV40 large T protein, which cannot function in viral DNA replication if it is not phosphorylated. Besides this, the ATM protein also forms a complex with MRN complex, SV40 large T protein and a host of other proteins in centres within the nucleus where SV40 DNA is replicated. Interestingly, during replication, the protein level of MRN actually declines and this is mediated by active ATM as well. Perturbation of this process cripples the replication of the viral DNA (Boichuk et al., 2010 Zhao et al., 2008, Shi et al., 2005).

Polyomavirus (PyV)

Another virus that is related to the SV40, the polyoma virus also activates the ATM protein, when it infects mouse cells. This activation is crucial for PyV

replication as inhibition of ATM activity reduces the yield of viral DNA replication by many folds. There is some indication that a substrate of ATM, cohesin, is the route through which active ATM helps to prolong the S phase of the cells, allowing more PyV DNA replication to occur (Dahl et al., 2005).

Herpes Simplex Virus -1 (HSV-1)

The HSV-1 is the alpha member of the herpes virus family. When HSV-1 DNA (linear, double-stranded) replicates in the cell, ATM becomes activated. This is thought to be caused by the structures of the replicative intermediates of the viral DNA. However, in addition to this, the ICP0 protein of the HSV-1 can also activate ATM, resulting in activation of Chk2. This in turn prevents the cell from traversing G2. As such the cell remains in a perpetual DNA replication-competent state, which greatly benefits the virus (Iwahori et al., 2007, Li et al, 2008).

Epstein-Barr Virus (EBV)

EBV is also a member of the herpes virus family but of the gamma group. However, its genome is a circular double-stranded DNA. One of its proteins, EBNA-1 promotes the generation of reactive oxygen species in the host cell. This causes DNA damage and as a result, ATM is activated (Gruhne et al., 2009). One of the consequences of this is the phosphorylation of RPA, which converts RPA from a replicative form to a DNA repair one. This RPA, Rad51, Rad52 and MRN proteins form a complex, in which is loaded onto newly replicated EBV DNA, which appears to have double-stranded breaks. It is thought that the recruitment of this complex aids in the repair of the newly replicated DNA (Kudoh et al., 2009). Although the active ATM activates p53 during the replication of this virus, signalling downstream of p53 is inhibited by EBV. Hence EBV is able to benefit from features of ATM activation that is positive for its replication but at the same time it is able to prevent other activities of ATM that are detrimental to its replication.

Adenovirus

While the viruses described above benefit from the cellular DNA damage response, other viruses are actually inhibited by DNA damage response of the cell. A case in point is the adenovirus, whose genome is a linear double-stranded

DNA. When adenovirus infects, the flushed ends of its DNA is sensed as double-strand breaks and this elicits a DNA repair mechanism (via the MRN complex) that actively ligates the ends of the viral DNA together. This is detrimental to adenovirus, whose replication mode and life cycle is dependent on its genome being linear. To prevent this from happening, adenoviral proteins E4orf3 and E4orf 6 inhibit the MRN complex. The absence of these proteins prevents a productive infection of this virus (Stracker et al., 2002). From this perspective, one could view the cellular processes involved in sensing damaged DNA, signalling the presence of damage and repair of the damage as part of the cellular defence which viruses have to contend with if they were to be successful.

Human Cytomegalovirus (HCMV)

Another virus that seeks to prevent activation of the cellular DNA damage signalling is the Human Cytomegalovirus, which is a member of the beta family of herpes virus. The replication of HCMV DNA (linear, double-stranded) induces a DNA damage response in the host cells. Specifically, the ATM protein is very efficiently phosphorylated. However, this does not lead to activation of the usual down-stream proteins. Instead the Chk2 protein, which normally resides in the nucleus, is re-localised to the cytoplasm by the virus (Gaspar and Shenk, 2006, Luo et al., 2007).

Some of the viruses mentioned above can induce DNA damage response indirectly merely by the DNA replication intermediates that form during their replication; while other viruses elicit DNA damage response by the actions of their proteins. This feature is not restricted to DNA viruses. Instead RNA viruses can also be affected by the cellular DNA damage response.

Hepatitis C Virus (HCV)

The non-structural protein of HCV, NS3 elicits double-strand breaks to the host cell's DNA. This activates ATM, and in turn Chk2. Several of HCV proteins physically interact with activated ATM and Chk2, and this interaction appears to be necessary for the virus because inhibition of ATM or Chk2 activity severely reduces the replication of HCV RNA (Ariumi et al., 2008).

Human Immunodeficiency Virus (HIV)

HIV-1 is a member of the retrovirus family, which upon infection of immune cells converts its single-stranded RNA into double stranded DNA. An essential step in HIV-1 life cycle is integration of its DNA into the host genome to form provirus, upon which viral DNA can be transcribed along with the host's own DNA. HIV-1 integration activates ATM-associated DNA damage response. This activation is beneficial for facilitating efficient retroviral infection by increasing the survival of host cells in response to integrase-induced DNA damage (Lau et al., 2005). In the later stage of infection, another HIV-1 gene product, viral protein R (Vpr), triggers cell cycle arrest in G2 that is followed by apoptosis (Roshal et al., 2003; Andersen et al., 2005; Lai et al., 2005). This leads to induction of ATR-mediated DNA damage signalling, increased death of HIV-1-infected cells and ultimately, CD4+ lymphocyte depletion (Andersen and Planelles, 2005; Skalka and Katz, 2005; Andersen et al., 2008). The HIV-1 envelope glycoprotein complex (Env) causes syncitia (cell fusion) that activates the ATM-DNA damage response and induce bystander cell killing by fusion of the interacting cells (Perfettini et al., 2008). In such cases, HIV-1 Vpr- and Env-driven activation of the cellular DNA damage responses appear to be crucial for the disease pathogenesis.

Adeno-associated Virus (AAV)

AAV is a human parvovirus or dependovirus with single stranded DNA genome flanked by inverted terminal repeats (ITRs) on either ends. To establish a productive infection, AAV relies on a helper virus (e.g., adenovirus, herpes simplex virus, or human papillomavirus). On its own, wild type or UV-inactivated AAV2 is capable of mounting a modest DNA damage response and cell cycle arrest (Raj et al., 2001; Berthet et al., 2005; Fragkos et al., 2008, 2009). In the former, wild type AAV2 replication (Rep) proteins nick cellular chromatin; induce ATM-DNA damage response and cell cycle arrest (Berthet et al., 2005). UV-inactivated AAV2, which presents itself as foreign DNA structure that resembles stalled replication forks to the host, activates an ATR-DNA damage response that lead to mitotic catastrophe (Fragkos et al., 2008, 2009; Ingemarsdotter et al., 2010). Although AAV replication can occur without a helper virus, it is normally at a low level or limited to certain parts of the viral life cycle. In addition to this, AAV replication activates ATM- and DNA-PK-DNA

damage signalling and some of the DNA repair proteins in these pathways can limit AAV infection (Sanlioglu et al., 2000; Choi et al., 2006; Collaco et al., 2009; Schwartz et al., 2009). In such cases, presence of a helper virus can increase AAV replication and dismantle certain aspects of DNA damage response caused by AAV replication. For example, the MRN (Mre11-Rad50-NBS1) complex targets AAV and impedes its replication (Schwartz et al., 2007). However, in AAV/Ad co-infections, no inhibition of AAV replication would be observed because Ad is able to suppress MRN functions (Stracker et al., 2002). Although AAV has to protect its genome from processing by certain DNA repair factors, the virus also benefits from the activation of cellular DNA damage response. Since AAV/Ad co-infections present the cell with a wide array of viral proteins and replicative intermediates, it is unsurprising that the DNA damage response induced is more robust (Schwartz et al., 2009). DNA-PK and to a lesser extent, ATM, co-localize with AAV Rep proteins that are expressed during AAV DNA replication (Collaco et al., 2009). DNA-PK has also been shown to phosphorylate AAV Rep proteins, which suggests that these DNA damage kinases may play a crucial role in AAV replication and assembly (Schwartz et al., 2009). AAV also utilises the host DNA damage response (ATM, DNA-PK, MRE11, NBS1, and the helicases BLM and WRN) to maintain its genome in a circular form, which is important for establishing persistent AAV infection (Duan et al., 1998; Choi et al., 2006).

As can be seen from the numerous examples described above, many viruses (DNA, RNA and retroviruses) either activate the cellular DNA damage response as a strategy to replicate their own genetic material (RNA or DNA), or they may inadvertently activate the cellular DNA damage signalling mechanism during their replication and as a consequence evolved various means to inhibit the detrimental effects of the signalling. While viruses such as HBV appear to activate the ATR pathway (Zhao et al., 2008) and others such as AAV activates the ATR (Jurvansuu et al., 2005) and DNA-PK (Schwartz et al., 2009) pathways, an over-whelming majority of the viruses tested thus far, activate the ATM protein instead.

In the context of HPV replication, Moody and Laimins (2009) reported that HPV31 activates ATM when the host cell of the virus is in the state of terminal

differentiation, and the inability to do so, results in very poor replication of the viral DNA. It is important to recall that during the life cycle of the HPV, the viral DNA undergoes two types of replication; amplification-replication, which occurs in terminally-differentiating cells, and maintenance-replication, which occurs in basal cells of the epithelium. In the former, the viral DNA replicates to very high numbers in the cell and these are eventually packaged into virions. In the latter, the viral DNA is replicated in a restrained fashion whereby the copies of the viral DNA are stably retained at a low number. It is clear that the mechanisms that control both these two types of replication are different. The report by Moody and Laimins (2009), demonstrates the need for ATM in the amplification-replication of HPV31, but not for its maintenance-replication.

Although we can assume that the conclusion from the report above is correct and can be extrapolated to other HPV types, it is not safe to do so, on the account of the following points. Firstly, HPV16 and HPV31 can have very different modes of maintenance-replication, which is dependent on the host cell that they reside in (Hoffmann et al., 2006). So what is observed for one virus type cannot immediately be assumed to be valid for another. Secondly, the authors inhibited ATM activity with a drug, KU-55933, which may have unknown non-targeted effects that could influence the results, and lastly but perhaps more importantly, is the means by which the host cells of the HPV31 were induced to differentiate. Calcium levels in the media of these cells were raised to very high levels and the DNA harvested for analyses within 48 to 96 hours. This crude method can induce keratinocytes to express differentiation markers, but it does not induce differentiation of the keratinocyte in the slow, ordered and careful way that naturally takes two weeks *in vivo*.

For the reasons cited above, in addition to testing whether feeder cells are essential for the maintenance of HPV DNA in NIKs cells, we were equally intent on testing whether ATM has any effect on this process.

Results

Feeders are not necessary for maintenance of HPV16 episomal copy number in NIKs

To compare NIKs HPV cells that were grown without feeders with those that were co-cultured with feeders. NIKs HPV cells were first weaned off feeder cells for three to four passages to produce keratinocytes that were devoid of feeder cells (Figure 5.1).

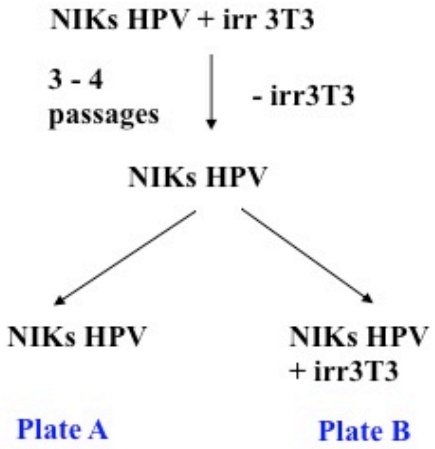

Figure 5.1: Strategy for producing NIKs HPV cells grown in the absence or presence of feeders (irradiated 3T3s, denoted as "Irr 3T3").
Experiments were carried out using keratinocytes Plate A. NIKs HPV (HPV16 DNA - containing keratinocyte derived from transfection of NIKs with HPV16 wild type DNA).

Following the weaning of feeder cells from NIKs HPV, the experiment was carried out in 6-well cluster plates with a Transwell insert in each well (Figure 5.2). This experimental design allowed us to compare the effect of growing NIKs HPV cells in various combinations with feeder cells. These include:

Set 1 – NIKs HPV cultured in direct contact with irradiated 3T3s,

Set 2 – NIKs HPV cultured without feeders,

Set 3 – NIKs HPV cultured separately with irradiated feeder cells (in inserts)

Set 4 – NIKs HPV cultured separately with non-irradiated feeder cells (in inserts)

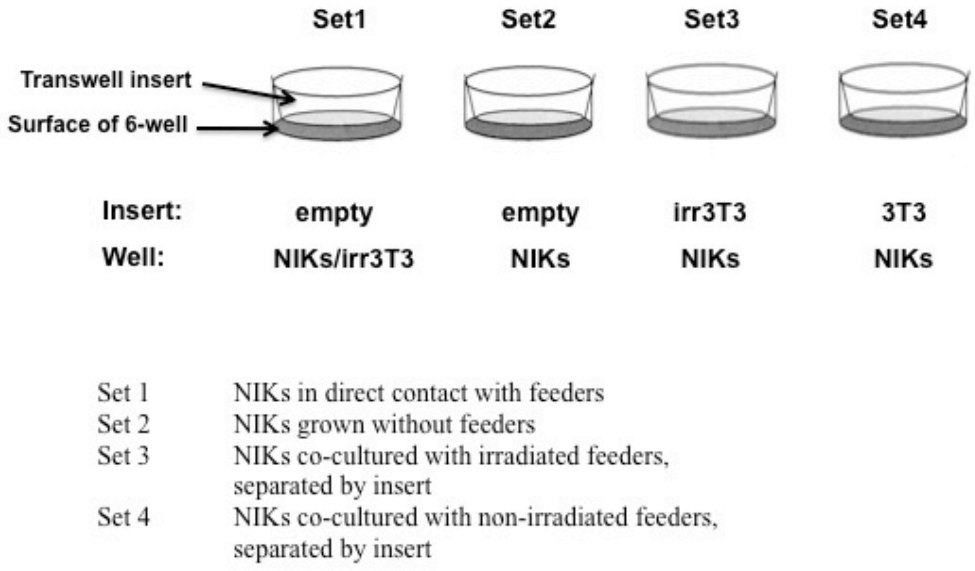

Figure 5.2: NIKs HPV culture conditions for assessment of the role of feeder cells in maintaining HPV16 DNA episomes.

3.5 x 10^5 NIKs HPV cells were seeded on the surface of the 6-well cluster plate and depending on the culture conditions, feeder cells were either seeded on the same surface of the 6-well plate or in the membrane of the Transwell insert.

The cells were cultured for 10 passages, which is equivalent to 30 population doublings (PDLs) as one passage equates to 3 PDLs. At each passage, DNA was extracted from the cells, and NIKs DNA and HPV DNA were measured by quantitative PCR (Q-PCR) to determine the HPV copy number per cell. Meanwhile, the qualitative assessment of whether the DNA existed as episomal or integrated forms was done through Southern blotting. Normally, HPV16 DNA exists as episomes in keratinocytes. The integration of the viral genome into cellular genome terminates the HPV lifecycle and this accidental event is often seen in cervical cancer (Pett et al., 2004).

Ten passages (30 PDLs) after NIKs HPV cells were grown in the different culture conditions mentioned in Figure 5.2, the assessment of HPV16 DNA copy numbers were carried out by Q-PCR. On first assessment, HPV16 DNA appeared to be maintained in a range of approximately 100 to 500 copies per cell in all culture conditions. HPV16 DNA copy number was maintained in the positive control in this experiment, i.e., NIKs HPV cells that were in direct contact with irradiated feeders. The copy numbers fluctuated throughout the passages, which was a phenomenon routinely seen in our laboratory and could be owed to the influence of culture confluency that may vary in each passage (Ken Raj, personal communication). Interestingly, the absence of feeders in the culture of NIKs HPV cells did not diminish HPV16 DNA copy numbers (Figure 5.3). In addition to seeing if presence of feeders were necessary for maintenance of HPV16 copy numbers, we also tested whether NIKs HPV needed to be in direct contact with feeders or irradiation of feeder cells were necessary. NIKs HPV that were co-cultured with irradiated feeders but that were not in direct contact also maintained HPV16 DNA copy numbers. Similarly, NIKs HPV cells that were co-cultured with non-irradiated feeders also maintained HPV16 DNA copy numbers in approximately similar quantity.

Regardless of whether feeder cells were present or not, HPV16 DNA copy numbers were still maintained in NIKs HPV cells (Figure 5.3). This is somewhat unexpected as attempts by others to generate keratinocyte lines that can support HPV DNA as episomes, have not been successful without the use of irradiated feeder cells. As such it was imperative to examine whether these HPV16 DNAs were maintained in an episomal state through Southern blotting. We utilised early passage NIKs HPV that contained the episomal form of HPV16 DNA as the positive control. A linearised 8 kb viral genome fragment was radioactively labelled with ^{32}P and used as a probe that hybridizes with HPV16 genomic DNA. DNA was extracted from the Set 1 to 4 cultures and digested with *Hind*III, which does not cut within the HPV16 genome and generate the uncut supercoiled and open circular forms. The bands that are visualised on a Southern blot are the uncut supercoiled, linear and open circular bands. The uncut supercoiled bands migrate the fastest and represent the intact viral episome. The open circular and linear bands are possibly generated via spontaneous DNA strand breakage during the

DNA extraction procedure. As *Hind*III does not cut within the HPV16 genome, any integrants would possibly include additional sequences from the cellular DNA and represented as other bands on top of the gel.

Southern blot analysis showed that in all culture conditions, HPV16 DNA existed as un-integrated episomes (uncut supercoiled, linear, or open circular) in NIKs HPV cells, whether or not feeders were present (Figure 5.4). However, it is noteworthy that the upper panel of the Southern blot for NIKs HPV in direct contact with feeders was contaminated with radioactivity, which caused difficulty in observing the presence of any bands above the uncut supercoiled DNA band. NIKs HPV that were co-cultured with but were not in direct contact with irradiated feeders also maintained HPV16 DNA episomally (Figure 5.5). The absence of irradiation also did not compromise the episomal maintenance of NIKs HPV. The analysis was meant to be qualitative and cannot be used to assess the levels of HPV16 copy number, owed to the fact that equal loading of DNA in our Southern blots were not quantified by a GAPDH genomic probe as loading control. Although feeders do not appear to be necessary for maintenance of HPV copy number after ten passages, it is possible that continuous culture of NIKs HPV without feeders may eventually lead to further decrease in copy numbers.

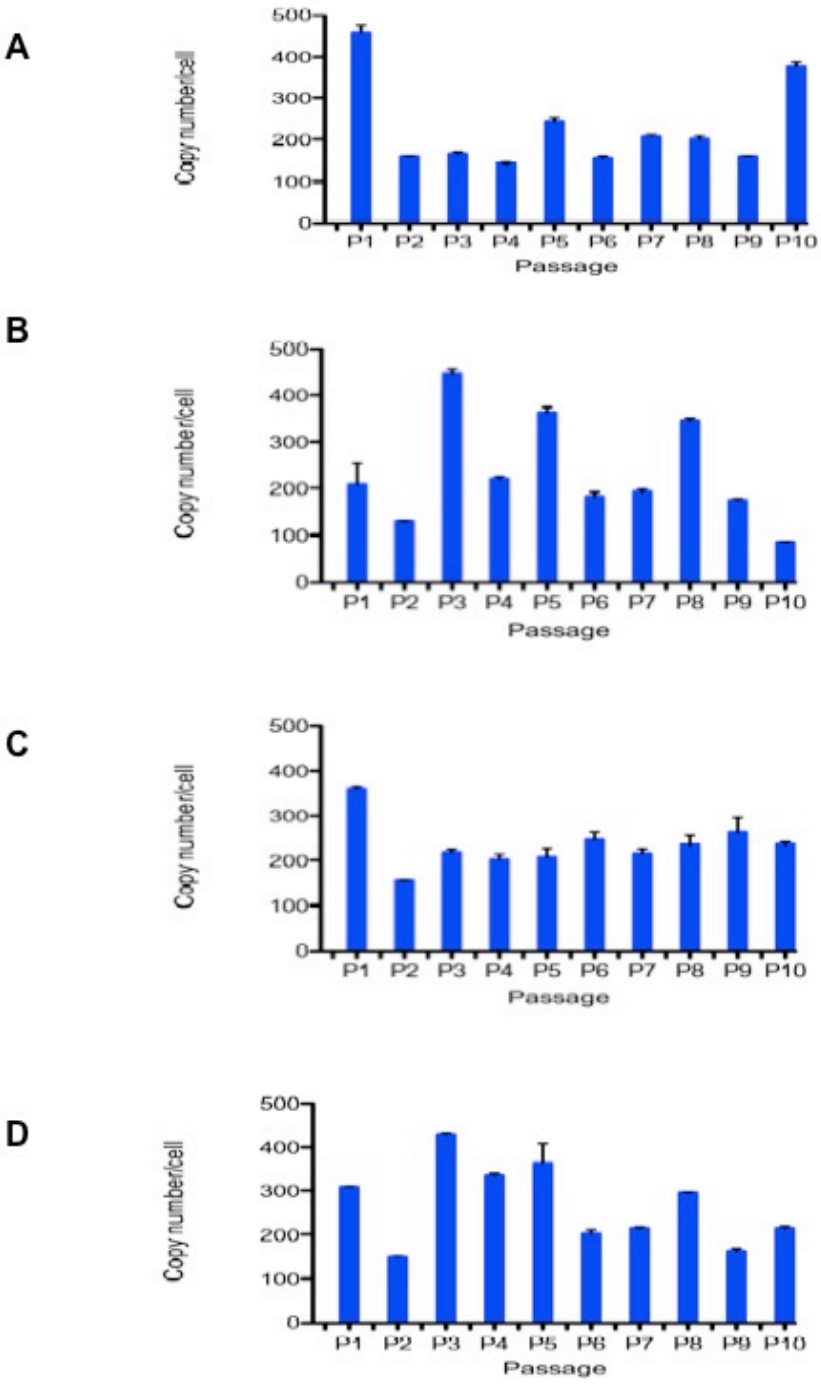

Figure 5.3: Q-PCR showing HPV16 DNA copy numbers in NIKs containing HPV16 cells from passage 1 to 10. (A) NIKs cultured in direct contact with irradiated 3T3s, (B) NIKs HPV grown without feeders, (C) NIKs HPV co-cultured with irradiated feeders, separated by inserts and (D) NIKs HPV co-cultured with non-irradiated feeders, separated by inserts.

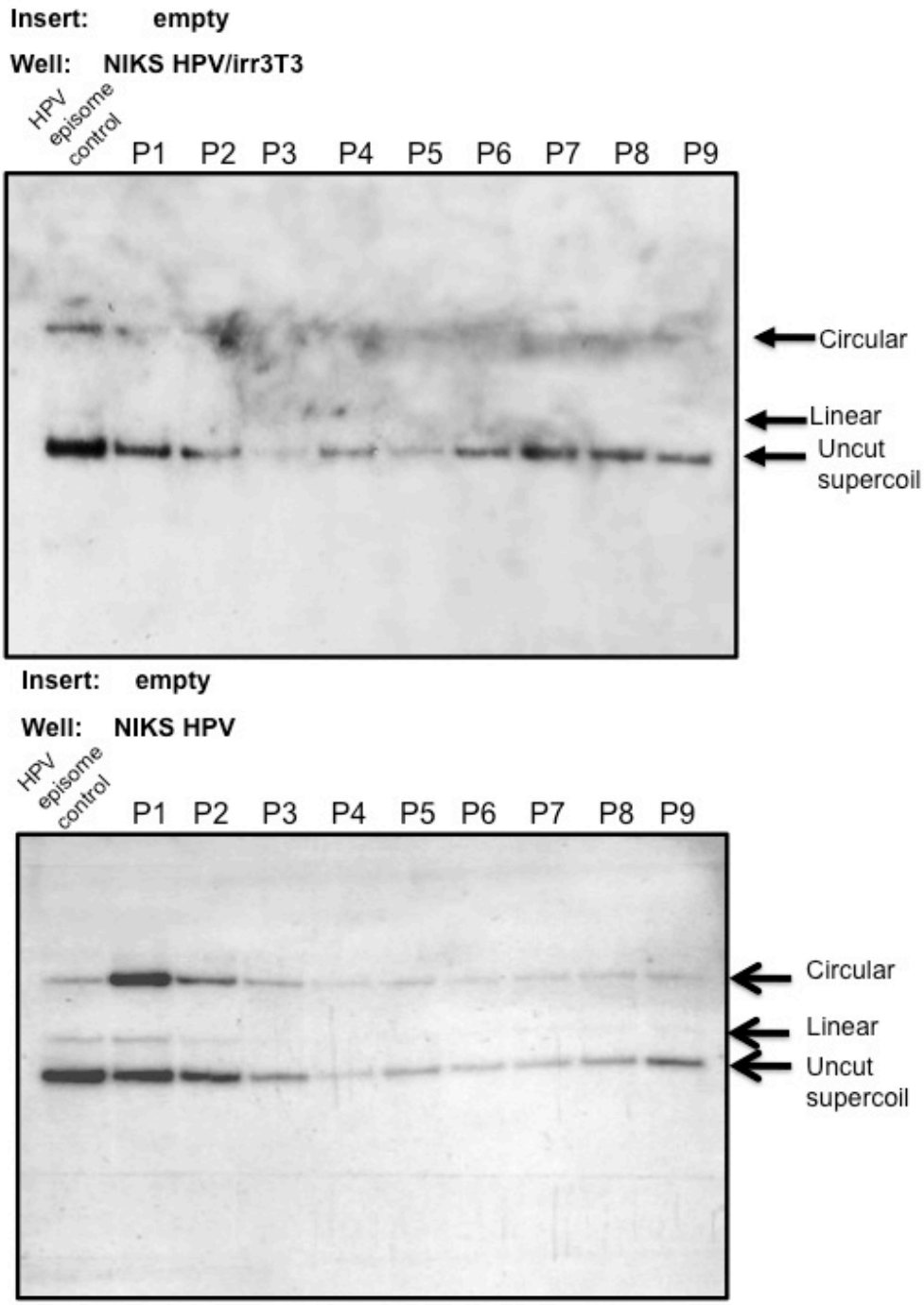

Figure 5.4: Southern blot analysis to verify the episomal state of HPV16 DNA from passage 1 to 10. *Hind* III, which does not cut within the HPV genome, resulted in mostly uncut supercoil and some circular and 8kb linear forms. Early passage NIKs HPV that contained the episomal form of HPV16 DNA was used as HPV episome control. Any integration events (if any) would be represented by other bands on the gel.

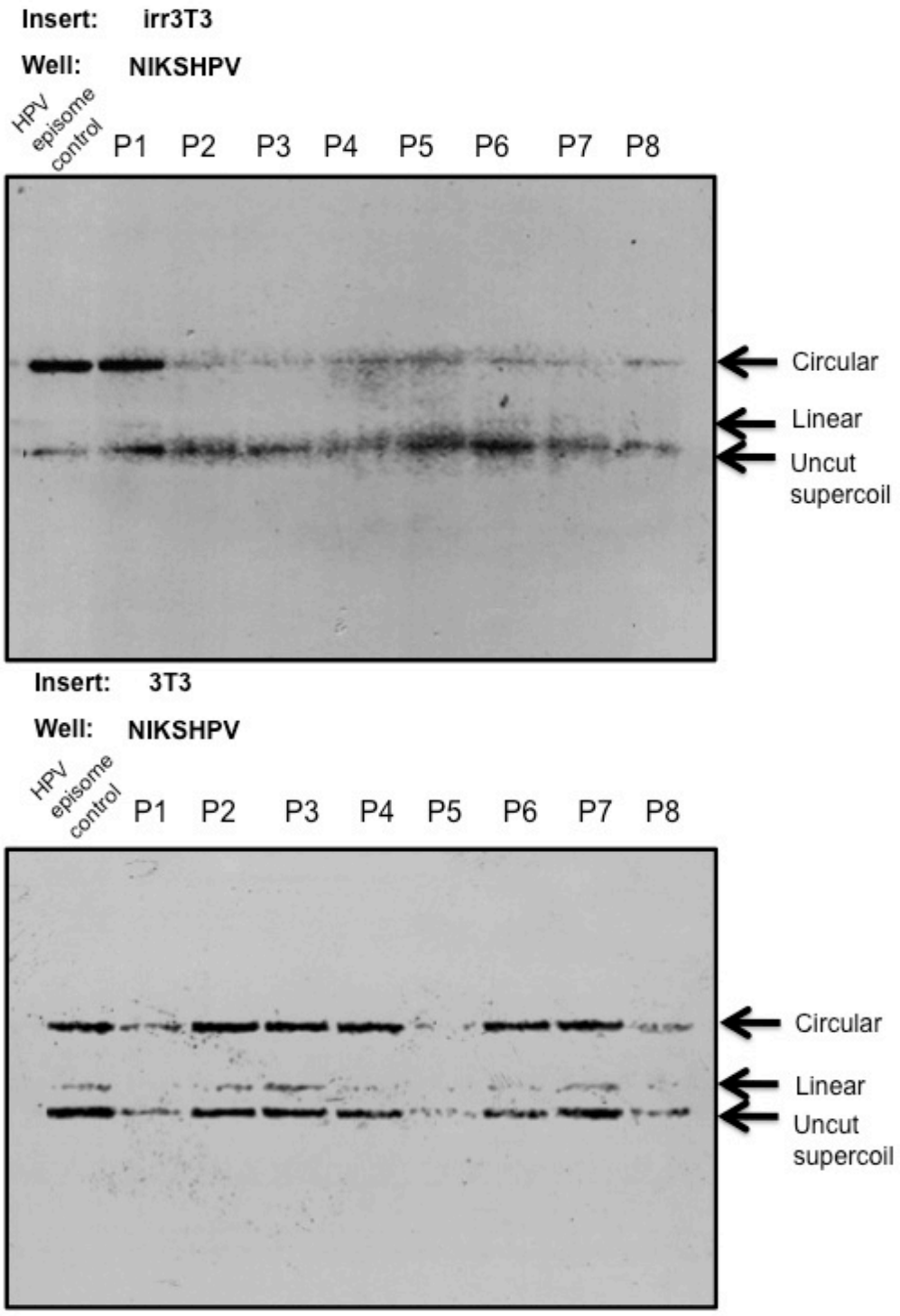

Figure 5.5: Southern blot analysis to verify the episomal state of HPV16 DNA from passage 1 to 10. *Hind* III, which does not cut within the HPV genome, resulted in mostly uncut supercoil and some circular and 8kb linear forms. Early passage NIKs HPV that contained the episomal form of HPV16 DNA was used as HPV episome control. Any integration events would be represented by other bands on the gel.

Effect of ATM on Maintenance-Replication of HPV16 DNA

As explained in the introduction to this chapter, in addition to the testing of the need of feeder cells to maintain HPV16 episomes in NIKs cells, we were equally intent on testing the role, if any, of ATM in maintenance of HPV episomes. To do this we first produced NIKs HPV cells with severely reduced levels of ATM. A retroviral packaging cell line, Phoenix A, was transfected with pRetroSuper shATM and shGFP plasmids (a gift from Yosef Shiloh). Following production of retroviruses, NIKs HPV cells were infected with retroviruses expressing shGFP or shATM and selected by puromycin. Through western blotting, the levels of ATM in the infectants were assessed. Control NIKs HPV shGFP cells maintained expression of ATM-S1981-P and ATM, while NIKs HPV shATM cells have severely reduced ATM protein levels in comparison (Figure 5.6).

These cells were cultivated for ten passages in the presence of feeder cells. In each passage, DNA was extracted from these cells and the measurement of HPV16 DNA quantity was done through Q-PCR. In addition, the qualitative assessment of whether the HPV16 DNA existed in episomal or integrated form was done through Southern blotting. As shown in Figure 5.6B, HPV16 copy number in NIKs HPV shGFP cells were reduced from P1 to P2, and maintained at similar levels thereafter until P10. We also observed that NIKs HPV shATM cells exhibited small fluctuation of copy numbers over time and gradually decreased from P8 to P10 (Figure 5.6C). However, the fluctuations of HPV16 copy number in the different passages of cells do not permit us to assume that the trend would continue in a downward way after P10. Southern blotting result also showed that HPV16 DNA was maintained as episomes overtime in NIKs HPV shGFP and shATM in uncut supercoiled, linear and circular forms (Figure 5.7A and B). This analysis was meant to be qualitative and cannot be used to assess the levels of HPV16 copy number, owed to the fact that equal loading of DNA in our Southern blots were not quantified by a separate genomic probe as loading control. These experiments were repeated several times with similar results. Collectively, the knockdown of ATM could not be said to diminish in any significant level, the episomal maintenance of HPV16 copy numbers over time in NIKs HPV cells.

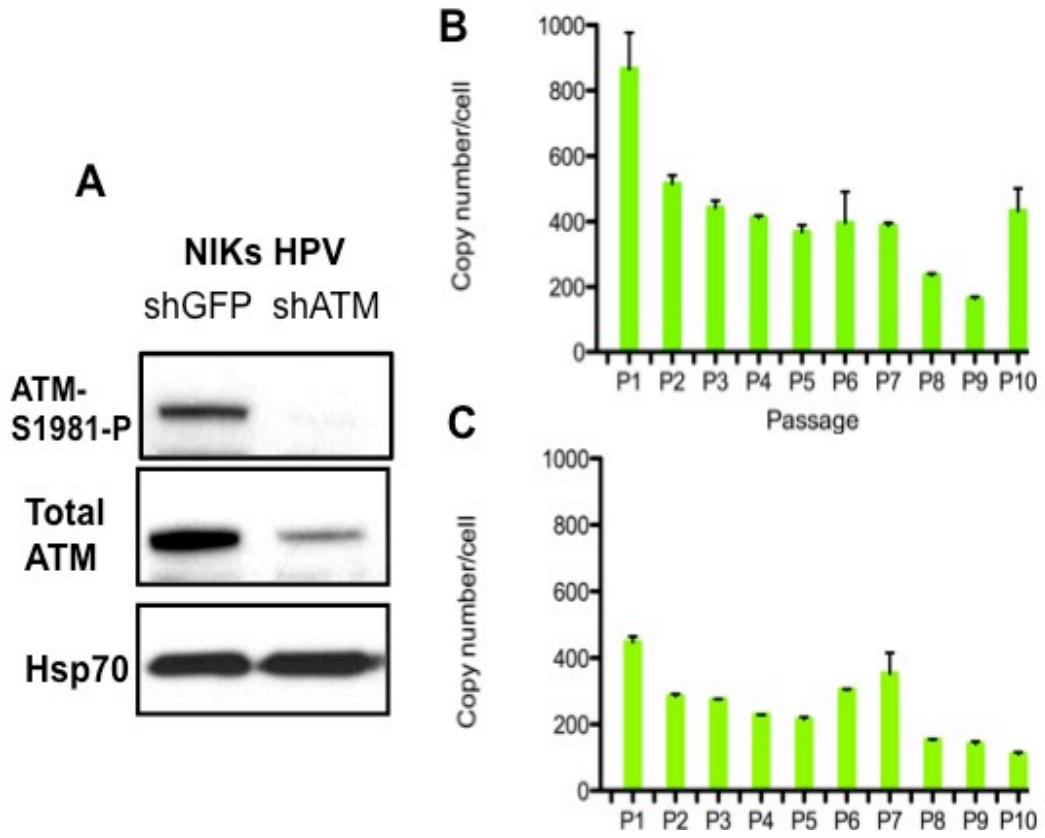

Figure 5.6: Assessment of the role of ATM in maintenance of HPV16 DNA copy numbers in monolayers.

(A) Western blot showing the reduction of ATM protein levels following ATM knockdown; Q-PCR analysis showing HPV16 DNA copy numbers for ten passages in (B) NIKs HPV shGFP cells and (C) NIKs HPV shATM cells.

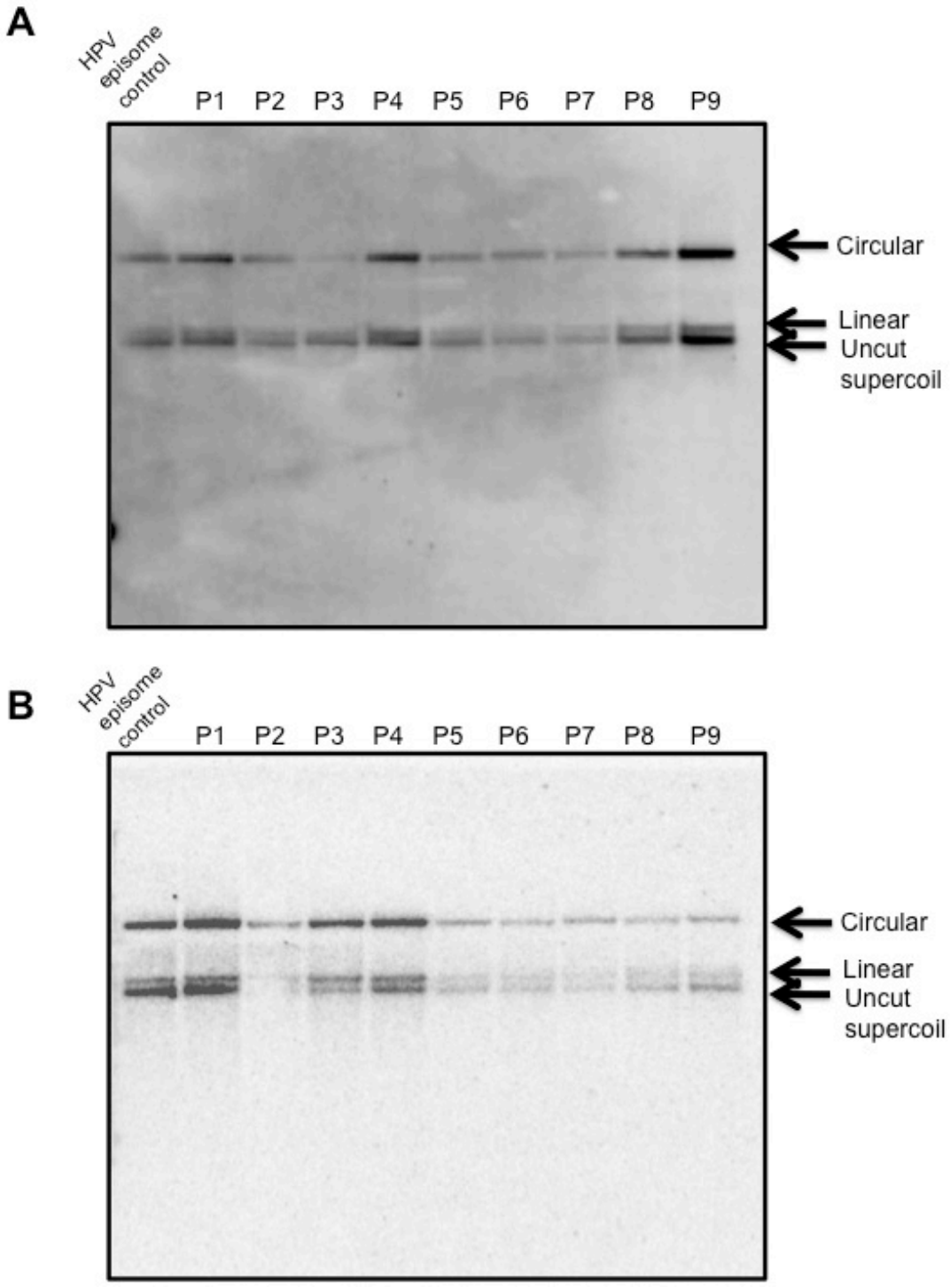

Figure 5.7: Southern blot analysis to verify the episomal state of HPV16 DNA in control and ATM knockdown cells. Southern blot showing episomal state of viral DNA in (A) NIKs HPV shGFP and (B) NIKs HPV shATM. Early passage NIKs HPV that contained the episomal form of HPV16 DNA was used as HPV episome control. Any integration events would be represented by other bands on the gel.

Effect of ATM on Amplification-Replication of HPV16 DNA

During epithelial differentiation, HPV episomes are amplified to thousands of copies per cell (Ruesch et al., 1998; Galloway, 2009). Therefore, this may be a crucial stage to investigate if the reduction in ATM protein levels would affect viral genome amplification in NIKs HPV cells. As mentioned before, the process of keratinocyte differentiation is slow, highly organised and results in a tissue with stratified layers of keratinocytes at different stages of terminal differentiation. Such an organisation is not induced merely by supplying high levels of calcium to the cells. The best method to generate in vitro differentiation of keratinocytes is by using an organotypic culture system. Briefly, keratinocytes are seeded on a collagen layer. When confluence is reached, the collagen (with keratinocytes on it) is raised from the medium and placed in a position that exposes the top part of the collagen, which contains the keratinocyte monolayer to air, while the bottom part of the collagen rests in liquid (medium). This air-liquid interface efficiently stimulates the differentiation programme of the cells in a way that is very reminiscent of terminal differentiation of epithelium *in vivo*. This culture method has been established for these cells in our laboratory by K. Raj and has been characterised by workers in the laboratory of J. Doorbar. Two sets of NIKs HPV cells that were stably infected by retroviruses expressing either shGFP or shATM were differentiated in these organotypic cultures (also referred to as raft cultures) for 14 days, after which the cells were harvested for protein lysates and DNA at two time points, Day 0 pre-differentiation and Day 14 post-differentiation in collagen rafts.

Figure 5.8 shows that NIKs HPV shGFP control cells from Set 1and 2 possessed high ATM-S1981-P and ATM protein levels at Day 0 pre-differentiation. However, the levels of these proteins decreased severely by Day 14 post-differentiation. Meanwhile, NIKs HPV shATM cells already have reduced levels of ATM and phosphorylated ATM at Day 0 before differentiation. Following differentiation, there was even a greater decline in the levels of these proteins (Figure 5.8A). To assess the effects of ATM knockdown on HPV16

amplification-replication, we performed Q-PCR analysis to measure viral copy numbers in cells that were harvested pre- and post-differentiation.

In both sets of cells (NIKs HPV expressing either shGFP or shATM) HPV16 DNA was augmented after differentiation on Day 14 (Figure 5.8B and 5.9). It is very clear from both sets of experiment that NIKs HPV shATM cells exhibiting a marked increase in HPV16 copy number from pre-rafting (Day 0) to post-rafting (Day 14), compared to NIKs HPV shGFP cells (Figure 5.8A and B). In addition, Southern blotting result showed that HPV16 DNA existed as episomes in NIKs HPV shGFP and shATM pre-rafting (Day 0) and post-rafting (Day 14) (Figure 5.9). In conclusion, the reduced level of ATM in NIKs HPV cells not only did not prevent HPV genome amplification in differentiating cells, but it actually increased the replication of the viral DNA in differentiating cells instead.

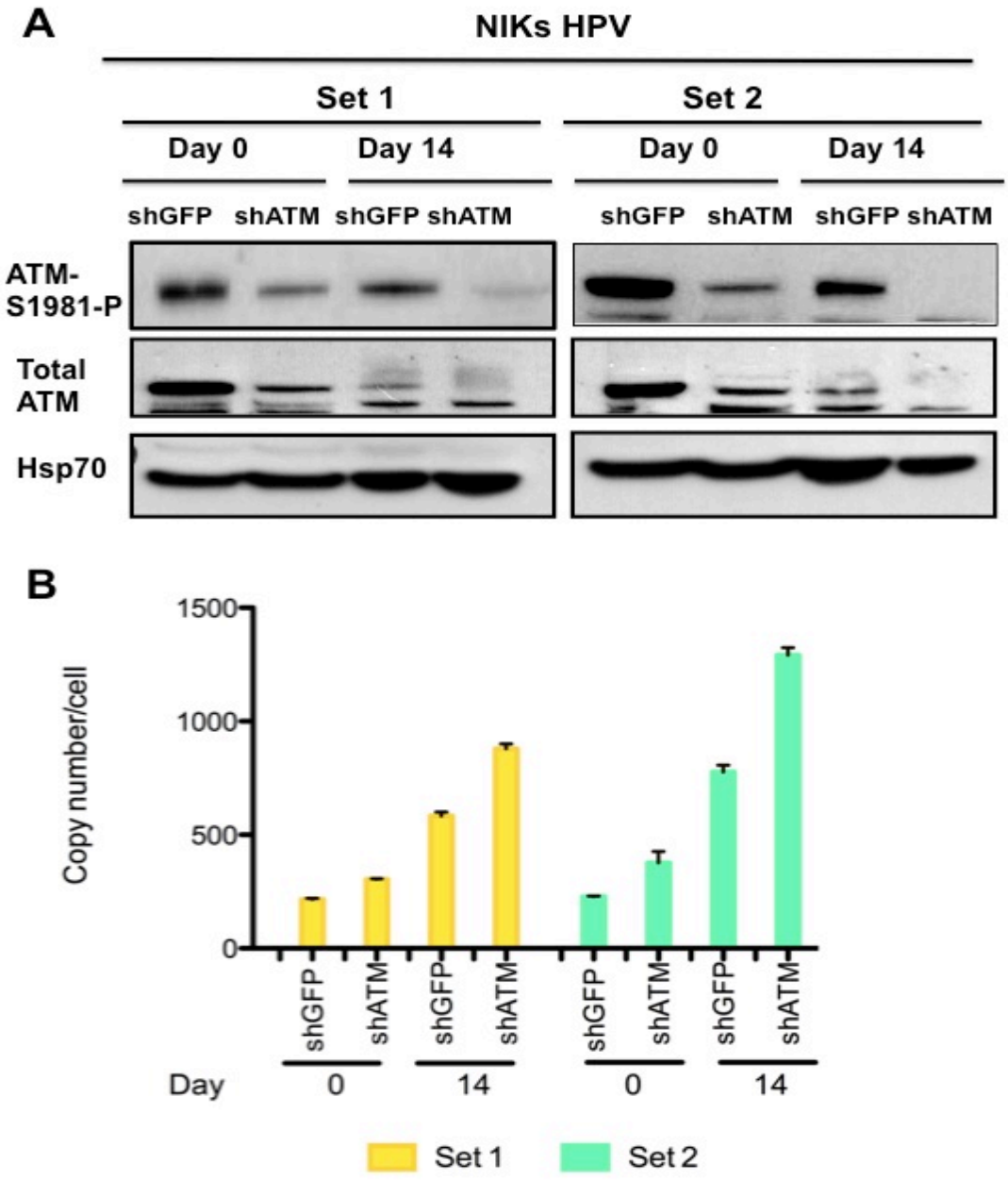

Figure 5.8: Assessment of the role of ATM in HPV16 genome amplification in pre- and post-differentiated cells.

(A) Western blots showing two sets of NIKs HPV shGFP and shATM cells (Set 1 and 2) that were harvested for protein lysates at day 0 pre-differentiation and day 14 post-differentiation, (B) Q-PCR analysis showing HPV16 DNA copy numbers in NIKs HPV shGFP and NIKs HPV shATM cells. DNA was extracted from two sets of NIKs HPV shGFP and shATM cells (Set 1 and 2) at Day 0 pre-differentiation and Day 14 post-differentiation.

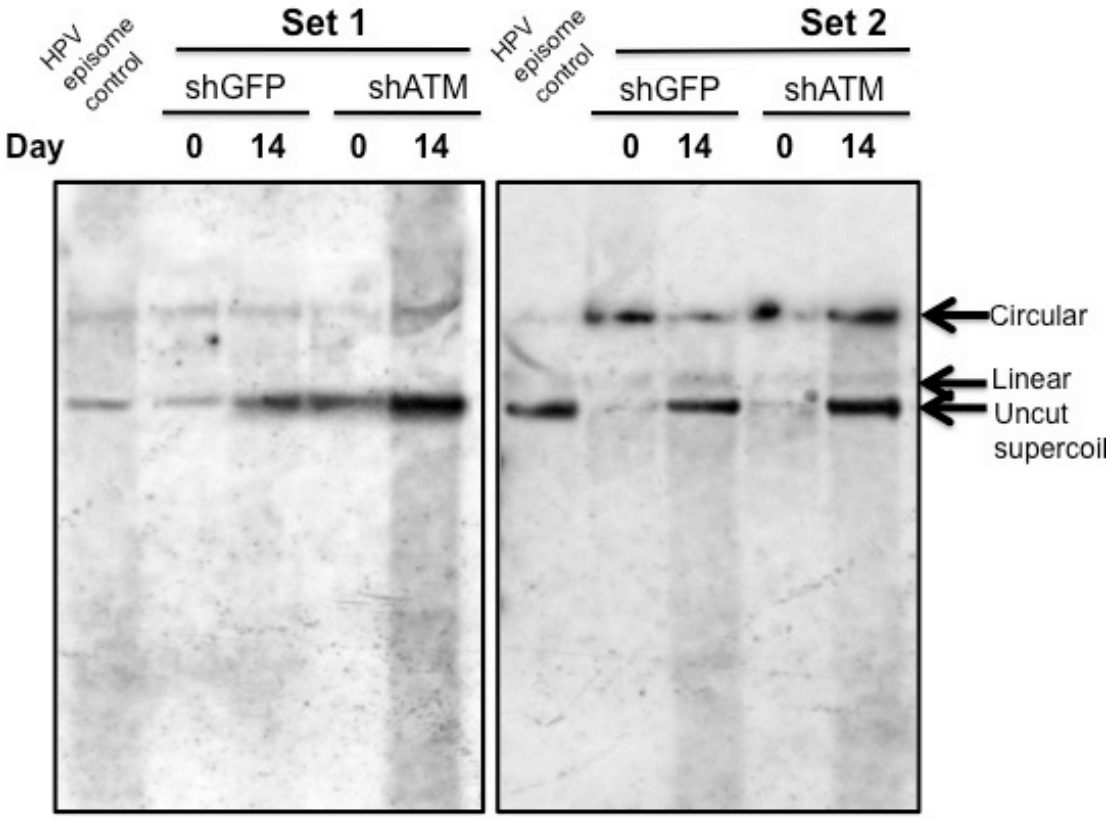

Figure 5.9: Southern blots showing episomal state of HPV16 DNA.

DNA was extracted from two sets of NIKs HPV shGFP and shATM cells (Set 1 and 2) at Day 0 pre-differentiation and Day 14 post-differentiation. Early passage NIKs HPV that contained the episomal form of HPV16 DNA was used as HPV episome control. Any integration events would be represented by other bands on the gel.

Discussion

When we withdrew feeders from the culture of NIKs containing HPV16 cells, HPV16 copy number were maintained episomally throughout the duration of its growth (up to 10 passages/ 30 PDs). Although HPV16 episomes were maintained, we observed a fluctuation of viral copy number throughout the ten passages, including those of NIKs HPV cells cultured in direct contact with feeder cells (positive control). The reason for such fluctuations is not known, but it has been observed by several co-workers in the laboratory on many occasions. As such, it is not possible to predict what would happen to the copy number of the cells beyond passage 10 (30 PDs). There is a possibility that further long-term passaging of NIKs HPV cells without feeder cells could eventually lead to loss of HPV16 DNA copy number. However, within the limits of our experiment, it is not possible to state that feeder cells are necessary for the maintenance of HPV16 episomes in NIKs cells. Following this, it is not surprising that other experimental conditions that we tested where NIKs HPV cells were separated from irradiated or non-irradiated feeders showed that HPV16 DNA copy numbers were still maintained. Even though eventual loss of episomes might be caused by integration of HPV16 DNA into the cellular genome (Pett et al., 2004; Stanley et al., 2007), our analyses of the physical state of HPV genome showed that HPV16 DNA existed as episomes. This result is surprising, given the accepted wisdom in this matter, which is that feeder cells are essential for the maintenance of HPV episomes in keratinocytes. It is not known how others attempted to do this in the past. It is possible that if keratinocytes were cultured at low densities in the absence of feeder cells, episomes might be loss due to the adverse effects on the growth and well-being of the keratinocytes themselves. As mentioned above, keratinocytes do not grow well at all when seeded sparsely in the absence of feeder cells, which is why during the process of weaning them of feeders; they were passaged at a high density. It would be interesting to test this possibility. Equally, it would have been ideal if time permitted the experiments above to be extended well beyond 30 population doublings of these cells.

Although these results appear not to support the initial hypothesis of why feeder cells might be needed, they have nevertheless showed us an important point. Since NIKs HPV cells can be cultured without feeders for at least ten passages without losing the viral episomes, such culture condition will allow us to study the effects of HPV on the DNA damage surveillance mechanisms of the cell without interference from feeder cells.

As we have seen in the previous section, when NIKs HPV were cultured without feeders, the level of activated ATM was extremely high but addition of feeders to these cells severely attenuated this. Hence in view of the fact that feeders appear not to be important for HPV maintenance, it would follow that ATM is also not important for HPV16 episome maintenance. This deduction appears to be supported by our experiments that were conducted to test the effect of ATM on HPV16 episome maintenance. This result is in agreement with the findings of Moody and Laimins (2009), who inhibited ATM activity with KU-55933.

Using KU-55933, Moody and Laimins (2009) went on to demonstrate that inhibition of ATM prevented the amplification-replication of HPV16 DNA when the cells were stimulated by high calcium level to differentiate. This result is very different from ours. We observed that severely reduced levels of ATM not only did not compromise HPV DNA replication in differentiating cell; it actually caused a greater increase in the amount of HPV16 DNA in differentiating NIKs cells. This is reproducibly seen in both sets of cultures in Figure 5.8B. It is likely that this difference could be partly explained by the difference in the method of differentiation that was used. The organotypic raft cultures that we used allow a very gradual and ordered differentiation of the keratinocytes as they migrate upwards to the top strata; akin to epithelium dynamics *in vivo* (Chow and Broker, 1997; Klumpp and Laimins, 1999). Calcium induction of keratinocyte differentiation on the other hand is a very crude method that pushes the cells into a rapid, disorganised and in-complete differentiation. In the experiments, of Moody and Laimins (2009), cells were treated with calcium for 48 and 96 hours prior to harvesting for analyses of their copy number. This is in stark contrast to the raft culture that we used, which stretched for 14 days from the moment the monolayer cells on the collagen were raised into the air-liquid inter-phase. While

we do not dispute the results of Moody and Laimins (2009) to be true within the system that was employed, we are confident that two features of our system inspire greater confidence in the real influence of ATM. The first is that, we used shRNA to stably knock down ATM levels. This avoids the possible non-targeted effects of drugs such as KU-55933. Secondly, the organotypic (raft) cultures that we employed are undoubtedly physiologically superior and closer to real epithelium than the use of high concentration of calcium to induce differentiation. Furthermore, our results is supported by the fact that ATM levels in the control cells, NIKs HPV shGFP, decreased naturally when these cells were differentiated, and this decrease was accompanied by increased amount of viral DNA, as was expected from differentiating cells. This is consistent with the lack of requirement of ATM for HPV DNA replication in differentiating cells (Moody and Laimins, 2009). From this, one could hazard a guess that perhaps reducing ATM levels is necessary for increased HPV DNA replication. The fact that shATM cells exhibited even greater HPV16 replication than shGFP-expressing cells when differentiated, lends credence (albeit not proof) to this possibility.

However, the possibility that ATM might have an inhibitory effect on the maintenance-replication of HPV16 DNA in proliferating keratinocytes is not supported by the observations we made where severely reduced ATM levels did not augment HPV DNA replication in monolayer cultures of NIKs HPV cells. Hence is there a beneficial role of HPV-induced DNA damage in NIKs cells for the viral DNA replication? While it is almost certain that ATM is not necessary for this, we have to bear in mind that it is not the only PIKK protein that was activated by HPV16. ATR and DNA-PKcs were also activated and in addition to this NBS1-1and RPA32 were also greatly increased (Figure 3.18). It would be very interesting to test whether any of these affect HPV16 DNA maintenance-replication and amplification-replication.

It is of significance that EBV, whose genome is circular and double-stranded, and which also exist in the nucleus of the host cell as episomes, also promotes the activation of ATM (Gruhne et al., 2009). However, this does not appear to be of any benefit to EBV, instead, it is the phosphorylation of RPA32, which converts RPA32 from a replicative form to a DNA repair one that is important for EBV.

The RPA32, Rad51, Rad 52 and MRN proteins are found to be attached to newly replicated EBV DNA, and this is consistent with the observation that the newly-replicated DNA possess double-strand breaks. It is thought that the recruitment of this complex aids in the repair of the newly-replicated DNA (Kudoh et al., 2009). Although the raised activity of ATM stimulates the phosphorylation and activation of p53, EBV inhibits the further downstream effects of this. It is quite exciting that many features of EBV's interaction with the cellular DNA damage signalling and repair mechanisms are also observed in HPV-infected cells. It would have been ideal if time permitted the testing of this hypothesis in NIKs HPV cells.

Final Discussion and Future Work

In this thesis we have shown that the co-culture system of NIKs grown with irradiated fibroblasts feeders has a wider spectrum of characteristics than we have previously envisioned. Irradiation of feeder cells not only inhibits growth of fibroblasts and provides growth-promoting factors for NIKs (Puck et al., 1956; Green et al., 1979), but our investigations showed that it has side effects of inducing radiation-induced bystander effect (RIBE) in NIKs. We report that feeder cells increased DNA breaks and H2AX phosphorylation in NIKs (+/ - HPV16), which indicate that feeder cells inflicted physical damage to DNA of these cells. Interestingly, dual γH2AX staining patterns was observed in these cells, indicating that H2AX could arise from more than one event, e.g., physical damage to the DNA and DNA replication stress (Gagou et al., 2010). Although the actual DNA damaging agents have yet to be identified, we have elucidated the routes that could transmit them from irradiated fibroblasts to NIKs (+/ - HPV16). The major route was through cell-to-cell contact and the minor route was through the cell media. Based on our observations that γH2AX expression persisted over 24 hrs, we hypothesised that the causative agents of RIBE were long-lived ROS that may be generated by cytokines (Koyama et al., 1998; Kumagai et al., 2003; Dickey et al., 2009). This possibility could be assessed by measurement of cytokines (e.g., transforming growth factor beta, TGF-β or cyclooxygenase-2, COX-2) or ROS (e.g., nitric oxide, NO) levels in cell medium of NIKs grown with irradiated feeder cells compared to NIKs grown without feeders.

Understanding the caveat of NIKs-feeder cells co-culture system is crucial because many groups, including ours, have utilised human keratinocytes in such a system to study the interactions of HPV16 with the host cell's DNA damage surveillance system *in vitro* (Moody and Laimins, 2009). We found that the presence of feeders activated all three DNA damage response proteins, ATM, ATR, and DNA-PK in NIKs cells and presence of HPV16 also caused similar activation of DNA damage response proteins in NIKs. Although presence of feeders or HPV16 induced similar cellular events in NIKs cells, an interesting

difference was observed when NIKs containing HPV16 cells respond to RIBE. Presence of feeders inhibited ATM activation but activated ATR and DNA-PK in NIKs containing HPV16 cells, which lent credence to our hypothesis that feeder cells could mask the actual DNA damage response that is inflicted by HPV16. These studies also add to the current knowledge in the field of RIBE, whereby ATR is thought to be the primary mediator of bystander signaling cascade leading to γH2AX formation in glioma cells (Burdak-Rothkamm et al., 2008). Unlike glioma cells, our system showed that whether or not HPV16 is present, bystander-signaling cascade is likely to be primarily mediated by DNA-PK and possibly a smaller contribution by ATR. This possibility can be investigated by adding inhibitor of DNA-PK activity (e.g., LY294002) and monitoring the ability of bystander cells to phosphorylate H2AX. Alternatively, inhibition of ATR activation can also be performed using shRNA against ATR for the same purpose; assessment of levels of ATR's downstream target, Chk1 phosphorylation (Ser317) to evaluate ATR activity. On the other hand, an unresolved question is how NIKs cells can grow in a state of continuous damage to their DNA in the presence of feeders with no detrimental effects on cell viability. This question can be investigated through assessment of NIKs cells' DNA repair capacity, as well as whether there is a potential cell death-evasion mechanism. These results suggest that the use of feeders in studies to understand host cell's DNA damage response needs to be considered.

Omitting the influence of feeder cells, we were able to ascertain that interactions of HPV16 with NIKs activated a wide spectrum of DNA damage response proteins, such as ATM, ATR, DNA-PK, H2AX, 53BP1, RPA32, and NBS-1. It became apparent that RIBE and HPV16 operated through different signaling cascades, as the former did not increase RPA and NBS-1 in NIKs. It has been shown that HPV16 E6 and E7 can abrogate host's cell cycle controls and enhance DNA synthesis, potentially leading to stalled replication forks and the activation of DNA damage responses (Day and Vaziri, 2009; Spardy et al., 2008, 2009). In addition to this, expression of HPV16 E6 and E7 has also been shown to induce mitotic abnormalities; DNA breaks and activates DNA damage response (Duensing and Munger, 2002). Therefore, we hypothesized that HPV16

exacerbated DNA replication in NIKs cells that cause accumulation of stalled replication forks and caused the activation of DNA damage response. It is likely that some, if not most of these functions, are mediated by HPV16 E6 and E7 oncoproteins. Further assessment of whether HPV16 E6 and E7 induce physical DNA damage in NIKs could be done through measurement of DNA breaks in cells expressing E6 and/ or E7 through comet assay.

We examined if the DNA damage-primed state of NIKs caused by presence of feeders or/ and HPV16 will alter the way these cells respond to direct DNA damage. Interestingly, we found that the responsiveness of NIKs to gamma radiation is largely similar when either feeder cells or HPV16 was present, whereby activation of ATM was inhibited, increase in ATR was delayed, but activation of DNA-PK is generally responsive. These studies showed that the presence of feeders would change the intrinsic molecular signaling of NIKs in response to gamma radiation.

Furthermore, we tested the susceptibility of HPV16-containing cells to direct gamma radiation and found that the virus sensitizes NIKs to radiation. As this experiment was performed with NIKs (+/ - HPV16) grown with feeders, there are several possibilities for the increased radiosensitivity of HPV16-containing cells. The net amount of DNA damage contributed by presence of HPV16 and feeder cells could emanate signals that result in cell death after gamma radiation. However, the possibility that the radiosensitivity of NIKs (+ HPV16) cells is ascribed to the viral effect itself is high, owed to the convincing *in vitro* and *in vivo* evidence for the increased radiosensitivity of squamous cell carcinoma head and neck cancers (SCCHN) that have accompanying HPV infections (Eifel et al., 2004; Fakhry et al., 2006; Gupta et al., 2009; Settle et al., 2009). These results could be useful in predicting the outcomes of HPV16-containing cells to radiotherapy. To clarify if HPV16 itself can sensitise NIKs cells to radiation, future work could utilise human keratinocytes as host cell of HPV16 without feeders. The production of such keratinocytes, as mentioned before, may require optimisation but could be an immense value for study of survival of epidermal cells to radiation, which mimics the cells in which HPV16 resides *in vivo*.

On the other hand, our parallel study also tested whether HPV16 benefit from activated DNA damage signaling. This was based on findings of how other viruses such as Simian Virus 40 (SV40), Polyomavirus (PyV), Herpes Simplex Virus-1 (HSV-1), Epstein-Barr Virus (EBV), Adenovirus (Ad), Human Cytomegalovirus (HCMV), Hepatitis C Virus (HCV), Human Immunodeficiency Virus (HIV), and Adeno-associated Virus (AAV) utilize the host DNA damage response proteins to aid in replication of their genetic material (RNA or DNA). We speculated that since feeder cells increased DNA damage response in NIKs, this DNA damage-primed cell milieu could be beneficial for maintenance of HPV16 DNA episomes. However, we found that NIKs without feeders could still maintain HPV16 DNA episomes up to 10 passages (30 PDs). Thus feeders were not necessary for the non-productive phase of HPV16 life cycle. On the other hand, it is possible that feeders may be needed to promote robust keratinocytes growth as shown by Alitalo et al. (1982) and it has also been proven to help overcome cell-culture induced senescence (Fu et al., 2003).

HPV31 has been shown to utilise ATM for the productive phase of the viral life cycle (Moody and Laimins, 2009). In contrast to that study, we report that ATM is not needed for either the productive or the non-productive phase of the viral life cycle. One could pursue this line of enquiry further by inhibiting DNA-PK or ATR, which would reveal the contribution (if any) of either of these proteins to HPV16 life cycle. Alternatively, the localization of these DNA damage response proteins in the nucleus could also be assessed, to observe whether they co-localise with HPV DNA replication centres. Altogether, these approaches will allow one to explicitly address if HPV16 benefits from interaction with its host cell DNA damage surveillance system.

Appendix 1

To identify cells that are undergoing DNA synthesis, i.e., S phase cells, without the use of any S phase marker, we used serum (FCS) and epidermal growth factor (EGF) deprivation, a method that is routinely used to enrich and block proliferating cells in G1 phase of the cell cycle (Pietenpol et al., 1990). Following this, the idea was to lift the G1 block by putting FCS and EGF back into the culture medium to monitor entry of cells back into S phase. The proportion of γH2AX-positive cells when the cells are entering into S phase is indicative of the amount of H2AX phosphorylation in NIKs cells that would be owed to DNA replication.

To optimise the conditions that were necessary for cells to maintain a G1 block, both NIKs and NIKs HPV cells were cultured in medium without FCS and EGF for five days. The blocked and their control unblocked cells were stained with propidium iodide and analysed for their cell cycle components by flow cytometric analysis. By plotting the FL2-width versus FL2-area in a dot plot graph, the proportion of cells that are in G0/G1, S, and G2/M were demarcated.

NIKs without FCS and EGF exhibited a G1 block with approx. 75.7% in G1, 12.9% in S, and 12.0% in G2/M phase of the cell cycle, compared to NIKs control cells with approx. 57.3% in G1, 22.2% in S, and 20.6% in G2/M. The proportion of G1 cells increased by 18.4% in NIKs cells that were starved of FCS and EGF.

Surprisingly, removal of FCS and EGF from culture medium of NIKs HPV did not retain sufficient cells in G1 phase with approx. 41.0% in G1, 28.7% in S, and 30.3% in G2/M, compared to control unblocked NIKs HPV cells with 38.4% in G1, 34.2% in S, and 27.6% in G2/M. NIKs cells containing HPV appeared to overcome the G1 block by abrogating the G1/S arrest to go back into the cell cycle.

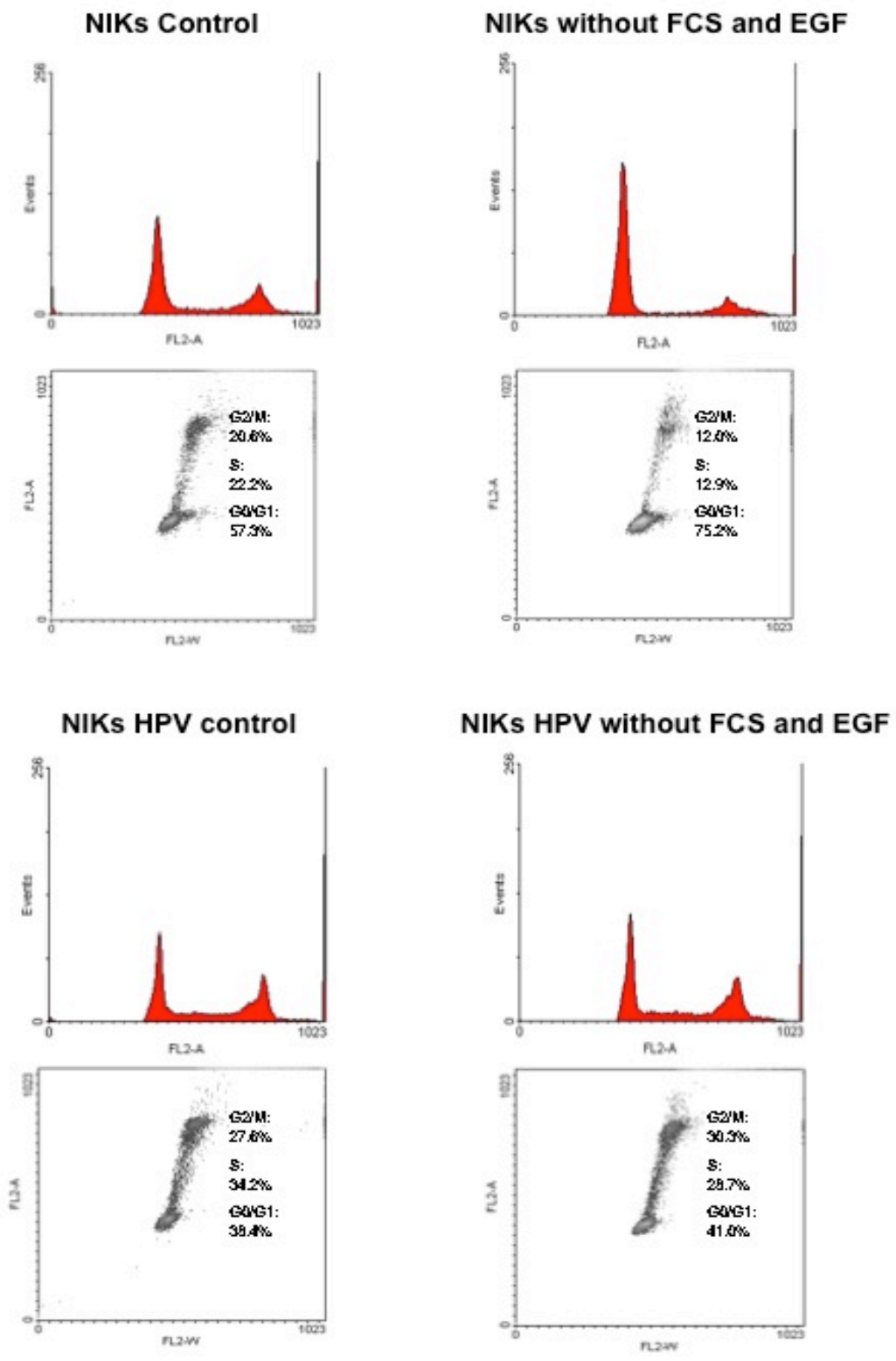

Cell cycle analysis of propidium-iodide stained NIKs and NIKs HPV cells following FCS and EGF withdrawal compared to untreated cells.

Appendix 2

The proportions of cells in G1, S, and G2/M phases were enumerated in each culture condition for NIKs, i.e., control/ no cell cycle block, G1 block, released for 6 hours, and released for 24 hours. In control cells where there were normal proliferating cells in these proportions: 75.5% in G1, 10.9% in S, and 11.3% in G2/M. Compared to control cells, G1 block cells formed smaller colonies and exhibited an increase in G1 cells at 85.1% and decrease in both S and G2 phase cells at 4.7% and 9.0%, respectively. Compared to G1 block cells, cells released for 6 hrs exhibited an increase in S phase cells at 1.3% that suggested it was the beginning of the release from G1 phase.

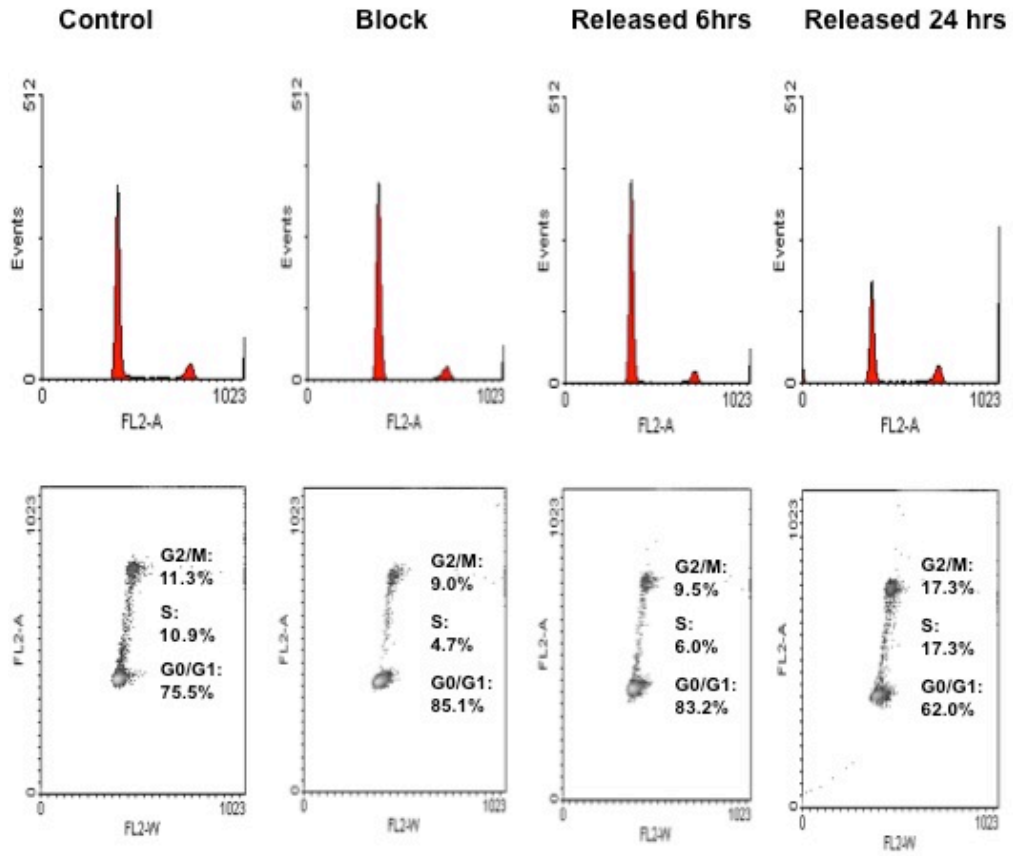

Cell cycle analysis following G1-synchronisation of NIKs cells.

The proportion of cells that were in G1, S, and G2/M were demarcated in each of these conditions: (Control) Cells that were in proliferating conditions (G1 block) Cells after 96 hr FCS and EGF withdrawal. (Released 6 and 24 hrs) After the block treatment, cells were analysed at 6 and 24 hr upon re-addition of FCS and EGF.

References

Abraham, R. T. (2002). "Checkpoint signalling: focusing on 53BP1." Nat Cell Biol 4(12): E277-279.

Alitalo, K., E. Kuismanen, et al. (1982). "Extracellular matrix proteins of human epidermal keratinocytes and feeder 3T3 cells." J Cell Biol 94(3): 497-505.

Allen-Hoffmann, B. L., S. J. Schlosser, et al. (2000). "Normal growth and differentiation in a spontaneously immortalized near-diploid human keratinocyte cell line, NIKS." J Invest Dermatol 114(3): 444-455.

Altieri, F., C. Grillo, et al. (2008). "DNA damage and repair: from molecular mechanisms to health implications." Antioxid Redox Signal 10(5): 891-937.

An, J., Y. C. Huang, et al. (2010). "DNA-PKcs plays a dominant role in the regulation of H2AX phosphorylation in response to DNA damage and cell cycle progression." BMC Mol Biol 11: 18.

Andersen, J. L. and V. Planelles (2005). "The role of Vpr in HIV-1 pathogenesis." Curr HIV Res 3(1): 43-51.

Andersen, J. L., E. S. Zimmerman, et al. (2005). "ATR and GADD45alpha mediate HIV-1 Vpr-induced apoptosis." Cell Death Differ 12(4): 326-334.

Ariumi, Y., M. Kuroki, et al. (2008). "The DNA damage sensors ataxia-telangiectasia mutated kinase and checkpoint kinase 2 are required for hepatitis C virus RNA replication." J Virol 82(19): 9639-9646.

Ayache, N., K. Boumediene, et al. (2002). "Expression of TGF-betas and their receptors is differentially modulated by reactive oxygen species and nitric oxide in human articular chondrocytes." Osteoarthritis Cartilage 10(5): 344-352.

Azzam, E. I., S. M. de Toledo, et al. (1998). "Intercellular communication is involved in the bystander regulation of gene expression in human cells exposed to very low fluences of alpha particles." Radiat Res 150(5): 497-504.

Azzam, E. I., S. M. De Toledo, et al. (2002). "Oxidative metabolism modulates signal transduction and micronucleus formation in bystander cells from alpha-particle-irradiated normal human fibroblast cultures." Cancer Res 62(19): 5436-5442.

Azzam, E. I., S. M. de Toledo, et al. (2003). "Oxidative metabolism, gap junctions and the ionizing radiation-induced bystander effect." Oncogene 22(45): 7050-7057.

Azzam, E. I. and J. B. Little (2004). "The radiation-induced bystander effect: evidence and significance." Hum Exp Toxicol 23(2): 61-65.

Backsch, C., N. Wagenbach, et al. (2001). "Microcell-mediated transfer of chromosome 4 into HeLa cells suppresses telomerase activity." Genes Chromosomes Cancer 31(2): 196-198.

Baker, C. C., W. C. Phelps, et al. (1987). "Structural and transcriptional analysis of human papillomavirus type 16 sequences in cervical carcinoma cell lines." J Virol 61(4): 962-971.

Bakkenist, C. J. and M. B. Kastan (2003). "DNA damage activates ATM through intermolecular autophosphorylation and dimer dissociation." Nature 421(6922): 499-506.

Balajee, A. S., B. Ponnaiya, et al. (2004). "Induction of replication protein A in bystander cells." Radiat Res 162(6): 677-686.

Bedell, M. A., J. B. Hudson, et al. (1991). "Amplification of human papillomavirus genomes in vitro is dependent on epithelial differentiation." J Virol 65(5): 2254-2260.

Bellocq, A., E. Azoulay, et al. (1999). "Reactive oxygen and nitrogen intermediates increase transforming growth factor-beta1 release from human epithelial alveolar cells through two different mechanisms." Am J Respir Cell Mol Biol 21(1): 128-136.

Bernard, H. U., R. D. Burk, et al. (2010). "Classification of papillomaviruses (PVs) based on 189 PV types and proposal of taxonomic amendments." Virology 401(1): 70-79.

Berthet, C., K. Raj, et al. (2005). "How adeno-associated virus Rep78 protein arrests cells completely in S phase." Proc Natl Acad Sci U S A 102(38): 13634-13639.

Biton, S., I. Dar, et al. (2006). "Nuclear ataxia-telangiectasia mutated (ATM) mediates the cellular response to DNA double strand breaks in human neuron-like cells." J Biol Chem 281(25): 17482-17491.

Blackford, A. N., R. N. Patel, et al. (2010). "Adenovirus 12 E4orf6 inhibits ATR activation by promoting TOPBP1 degradation." Proc Natl Acad Sci U S A 107(27): 12251-12256.

Blasius, M., S. Sommer, et al. (2008). "Deinococcus radiodurans: what belongs to the survival kit?" Crit Rev Biochem Mol Biol 43(3): 221-238.

Boehme, K. A., R. Kulikov, et al. (2008). "p53 stabilization in response to DNA damage requires Akt/PKB and DNA-PK." Proc Natl Acad Sci U S A 105(22): 7785-7790.

Boichuk, S., L. Hu, et al. (2010). "Multiple DNA damage signaling and repair pathways deregulated by simian virus 40 large T antigen." J Virol 84(16): 8007-8020.

Bonner, W. M., C. E. Redon, et al. (2008). "GammaH2AX and cancer." Nat Rev Cancer 8(12): 957-967.

Boothman, D. A., E. Odegaard, et al. (1998). "Molecular analyses of adaptive survival responses (ASRs): role of ASRs in radiotherapy." Hum Exp Toxicol 17(8): 448-453.

Borrelli, M. J., L. L. Thompson, et al. (1989). "Evidence that the feeder effect in mammalian cells is mediated by a diffusible substance." Int J Hyperthermia 5(1): 99-103.

Boshart, M., L. Gissmann, et al. (1984). "A new type of papillomavirus DNA, its presence in genital cancer biopsies and in cell lines derived from cervical cancer." EMBO J 3(5): 1151-1157.

Brumbaugh, K. M., D. M. Otterness, et al. (2004). "The mRNA surveillance protein hSMG-1 functions in genotoxic stress response pathways in mammalian cells." Mol Cell 14(5): 585-598.

Burdak-Rothkamm, S., S. C. Short, et al. (2007). "ATR-dependent radiation-induced gamma H2AX foci in bystander primary human astrocytes and glioma cells." Oncogene 26(7): 993-1002.

Burdak-Rothkamm, S., K. Rothkamm, et al. (2008). "ATM acts downstream of ATR in the DNA damage response signaling of bystander cells." Cancer Res 68(17): 7059-7065.

Burdak-Rothkamm, S., K. Rothkamm, et al. (2009). "DNA and chromosomal damage in response to intermittent extremely low-frequency magnetic fields." Mutat Res 672(2): 82-89.

Burhans, W. C. and M. Weinberger (2007). "DNA replication stress, genome instability and aging." Nucleic Acids Res 35(22): 7545-7556.

Carrano, A. V. (1973). "Chromosome aberrations and radiation-induced cell death. II. Predicted and observed cell survival." Mutat Res 17(3): 355-366.

Chaudhry, M. A. (2006). "Bystander effect: biological endpoints and microarray analysis." Mutat Res 597(1-2): 98-112.

Chen, B., D. A. Simpson, et al. (2009). "Human papilloma virus type16 E6 deregulates CHK1 and sensitizes human fibroblasts to environmental carcinogens independently of its effect on p53." Cell Cycle 8(11): 1775-1787.

Chen, L., D. M. Gilkes, et al. (2005). "ATM and Chk2-dependent phosphorylation of MDMX contribute to p53 activation after DNA damage." EMBO J 24(19): 3411-3422.

Choi, V. W., D. M. McCarty, et al. (2006). "Host cell DNA repair pathways in adeno-associated viral genome processing." J Virol 80(21): 10346-10356.

Chow, L. T. and T. R. Broker (1994). "Papillomavirus DNA replication." Intervirology 37(3-4): 150-158.

Chow, L. T. and T. R. Broker (1997). "In vitro experimental systems for HPV: epithelial raft cultures for investigations of viral reproduction and pathogenesis and for genetic analyses of viral proteins and regulatory sequences." Clin Dermatol 15(2): 217-227.

Chowdhury, D., M. C. Keogh, et al. (2005). "gamma-H2AX dephosphorylation by protein phosphatase 2A facilitates DNA double-strand break repair." Mol Cell 20(5): 801-809.

Cimprich, K. A. and D. Cortez (2008). "ATR: an essential regulator of genome integrity." Nat Rev Mol Cell Biol 9(8): 616-627.

Collaco, R. F., J. M. Bevington, et al. (2009). "Adeno-associated virus and adenovirus coinfection induces a cellular DNA damage and repair response via redundant phosphatidylinositol 3-like kinase pathways." Virology 392(1): 24-33.

Collins, A. R., A. A. Oscoz, et al. (2008). "The comet assay: topical issues." Mutagenesis 23(3): 143-151.

Collis, S. J., T. L. DeWeese, et al. (2005). "The life and death of DNA-PK." Oncogene 24(6): 949-961.

Collis, S. J., J. M. Schwaninger, et al. (2004). "Evasion of early cellular response mechanisms following low level radiation-induced DNA damage." J Biol Chem 279(48): 49624-49632.

Contreras-Paredes, A., E. De la Cruz-Hernandez, et al. (2009). "E6 variants of human papillomavirus 18 differentially modulate the protein kinase B/phosphatidylinositol 3-kinase (akt/PI3K) signaling pathway." Virology 383(1): 78-85.

Cooke, M. S., M. D. Evans, et al. (2003). "Oxidative DNA damage: mechanisms, mutation, and disease." FASEB J 17(10): 1195-1214.

Cuadrado, M., B. Martinez-Pastor, et al. (2006). ""ATR activation in response to ionizing radiation: still ATM territory"." Cell Div 1(1): 7.

Dahl, J., J. You, et al. (2005). "Induction and utilization of an ATM signaling pathway by polyomavirus." J Virol 79(20): 13007-13017.

Dall, K. L., C. G. Scarpini, et al. (2008). "Characterization of naturally occurring HPV16 integration sites isolated from cervical keratinocytes under noncompetitive conditions." Cancer Res 68(20): 8249-8259.

Day, T. and C. Vaziri (2009). "HPV E6 oncoprotein prevents recovery of stalled replication forks independently of p53 degradation." Cell Cycle 8(14): 2138.

de Feraudy, S., I. Revet, et al. (2010). "A minority of foci or pan-nuclear apoptotic staining of gammaH2AX in the S phase after UV damage contain DNA double-strand breaks." Proc Natl Acad Sci U S A 107(15): 6870-6875.

de Villiers, E. M. (1994). "Human pathogenic papillomavirus types: an update." Curr Top Microbiol Immunol 186: 1-12.

de Villiers, E. M., C. Fauquet, et al. (2004). "Classification of papillomaviruses." Virology 324(1): 17-27.

Deschavanne, P. J. and B. Fertil (1996). "A review of human cell radiosensitivity in vitro." Int J Radiat Oncol Biol Phys 34(1): 251-266.

Deshpande, A., P. Sicinski, et al. (2005). "Cyclins and cdks in development and cancer: a perspective." Oncogene 24(17): 2909-2915.

Dickey, J. S., B. J. Baird, et al. (2009). "Intercellular communication of cellular stress monitored by gamma-H2AX induction." Carcinogenesis 30(10): 1686-1695.

Digweed, M., I. Demuth, et al. (2002). "SV40 large T-antigen disturbs the formation of nuclear DNA-repair foci containing MRE11." Oncogene 21(32): 4873-4878.

Dip, R. and H. Naegeli (2005). "More than just strand breaks: the recognition of structural DNA discontinuities by DNA-dependent protein kinase catalytic subunit." FASEB J 19(7): 704-715.

Djordjevic, B. and C. S. Lange (2006). "Cell-cell interactions in spheroids maintained in suspension." Acta Oncol 45(4): 412-420.

Doorbar, J. (2006). "Molecular biology of human papillomavirus infection and cervical cancer." Clin Sci (Lond) 110(5): 525-541.

Downward, J. (2004). "PI 3-kinase, Akt and cell survival." Semin Cell Dev Biol 15(2): 177-182.

Duan, D., P. Sharma, et al. (1998). "Circular intermediates of recombinant adeno-associated virus have defined structural characteristics responsible for long-term episomal persistence in muscle tissue." J Virol 72(11): 8568-8577.

Duensing, S., A. Duensing, et al. (2001). "Centrosome abnormalities and genomic instability by episomal expression of human papillomavirus type 16 in raft cultures of human keratinocytes." J Virol 75(16): 7712-7716.

Duensing, S. and K. Munger (2002). "The human papillomavirus type 16 E6 and E7 oncoproteins independently induce numerical and structural chromosome instability." Cancer Res 62(23): 7075-7082.

Duensing, S. and K. Munger (2004). "Mechanisms of genomic instability in human cancer: insights from studies with human papillomavirus oncoproteins." Int J Cancer 109(2): 157-162.

Durst, M., L. Gissmann, et al. (1983). "A papillomavirus DNA from a cervical carcinoma and its prevalence in cancer biopsy samples from different geographic regions." Proc Natl Acad Sci U S A 80(12): 3812-3815.

Eastham, A. M., J. Atkinson, et al. (2001). "Relationships between clonogenic cell survival, DNA damage and chromosomal radiosensitivity in nine human cervix carcinoma cell lines." Int J Radiat Biol 77(3): 295-302.

Eifel, P. J., K. Winter, et al. (2004). "Pelvic irradiation with concurrent chemotherapy versus pelvic and para-aortic irradiation for high-risk cervical cancer: an update of radiation therapy oncology group trial (RTOG) 90-01." J Clin Oncol 22(5): 872-880.

El-Deiry, W. S. (2003). "The role of p53 in chemosensitivity and radiosensitivity." Oncogene 22(47): 7486-7495.

Fakhry, C. and M. L. Gillison (2006). "Clinical implications of human papillomavirus in head and neck cancers." J Clin Oncol 24(17): 2606-2611.

Falk, M. H., L. Hultner, et al. (1993). "Irradiated fibroblasts protect Burkitt lymphoma cells from apoptosis by a mechanism independent of bcl-2." Int J Cancer 55(3): 485-491.

Fisher, H. W. and T. T. Puck (1956). "On the Functions of X-Irradiated "Feeder" Cells in Supporting Growth of Single Mammalian Cells." Proc Natl Acad Sci U S A 42(12): 900-906.

Flores, E. R., B. L. Allen-Hoffmann, et al. (2000). "The human papillomavirus type 16 E7 oncogene is required for the productive stage of the viral life cycle." J Virol 74(14): 6622-6631.

Flores, E. R., B. L. Allen-Hoffmann, et al. (1999). "Establishment of the human papillomavirus type 16 (HPV-16) life cycle in an immortalized human foreskin keratinocyte cell line." Virology 262(2): 344-354.

Flores, E. R. and P. F. Lambert (1997). "Evidence for a switch in the mode of human papillomavirus type 16 DNA replication during the viral life cycle." J Virol 71(10): 7167-7179.

Fragkos, M., M. Breuleux, et al. (2008). "Recombinant adeno-associated viral vectors are deficient in provoking a DNA damage response." J Virol 82(15): 7379-7387.

Fragkos, M., J. Jurvansuu, et al. (2009). "H2AX is required for cell cycle arrest via the p53/p21 pathway." Mol Cell Biol 29(10): 2828-2840.

Franken, N. A., H. M. Rodermond, et al. (2006). "Clonogenic assay of cells in vitro." Nat Protoc 1(5): 2315-2319.

Frattini, M. G., H. B. Lim, et al. (1997). "Induction of human papillomavirus type 18 late gene expression and genomic amplification in organotypic cultures from transfected DNA templates." J Virol 71(9): 7068-7072.

Frattini, M. G., H. B. Lim, et al. (1996). "In vitro synthesis of oncogenic human papillomaviruses requires episomal genomes for differentiation-dependent late expression." Proc Natl Acad Sci U S A 93(7): 3062-3067.

Friesner, J. D., B. Liu, et al. (2005). "Ionizing radiation-dependent gamma-H2AX focus formation requires ataxia telangiectasia mutated and ataxia telangiectasia mutated and Rad3-related." Mol Biol Cell 16(5): 2566-2576.

Fu, B., J. Quintero, et al. (2003). "Keratinocyte growth conditions modulate telomerase expression, senescence, and immortalization by human papillomavirus type 16 E6 and E7 oncogenes." Cancer Res 63(22): 7815-7824.

Fuhrman, C. B., J. Kilgore, et al. (2008). "Radiosensitization of cervical cancer cells via double-strand DNA break repair inhibition." Gynecol Oncol 110(1): 93-98.

Funk, J. O., S. Waga, et al. (1997). "Inhibition of CDK activity and PCNA-dependent DNA replication by p21 is blocked by interaction with the HPV-16 E7 oncoprotein." Genes Dev 11(16): 2090-2100.

Furuta, T., H. Takemura, et al. (2003). "Phosphorylation of histone H2AX and activation of Mre11, Rad50, and Nbs1 in response to replication-dependent DNA double-strand breaks induced by mammalian DNA topoisomerase I cleavage complexes." J Biol Chem 278(22): 20303-20312.

Fusenig, N. E., S. M. Amer, et al. (1978). "Characteristics of chemically transformed mouse epidermal cells in vitro and in vivo." Bull Cancer 65(3): 271-279.

Fusenig, N. E., A. Limat, et al. (1994). "Modulation of the differentiated phenotype of keratinocytes of the hair follicle and from epidermis." J Dermatol Sci 7 Suppl: S142-151.

Gagou, M. E., P. Zuazua-Villar, et al. (2010). "Enhanced H2AX phosphorylation, DNA replication fork arrest, and cell death in the absence of Chk1." Mol Biol Cell 21(5): 739-752.

Galloway, D. A. (2009). "Human papillomaviruses: a growing field." Genes Dev 23(2): 138-142.

Garner, E., F. Martinon, et al. (2007). "Cells with defective p53-p21-pRb pathway are susceptible to apoptosis induced by p84N5 via caspase-6." Cancer Res 67(16): 7631-7637.

Garner, E. and K. Raj (2008). "Protective mechanisms of p53-p21-pRb proteins against DNA damage-induced cell death." Cell Cycle 7(3): 277-282.

Garner-Hamrick, P. A., J. M. Fostel, et al. (2004). "Global effects of human papillomavirus type 18 E6/E7 in an organotypic keratinocyte culture system." J Virol 78(17): 9041-9050.

Gaspar, M. and T. Shenk (2006). "Human cytomegalovirus inhibits a DNA damage response by mislocalizing checkpoint proteins." Proc Natl Acad Sci U S A 103(8): 2821-2826.

Gebow, D., N. Miselis, et al. (2000). "Homologous and nonhomologous recombination resulting in deletion: effects of p53 status, microhomology, and repetitive DNA length and orientation." Mol Cell Biol 20(11): 4028-4035.

Gerashchenko, B. I. and R. W. Howell (2003). "Flow cytometry as a strategy to study radiation-induced bystander effects in co-culture systems." Cytometry A 54(1): 1-7.

Gerashchenko, B. I. and R. W. Howell (2003). "Cell proximity is a prerequisite for the proliferative response of bystander cells co-cultured with cells irradiated with gamma-rays." Cytometry A 56(2): 71-80.

Gey, G. O., Coffman, W. D. & Kubicek, M. T. (1952). "Tissue culture studies of the proliferative capacity of cervical carcinoma and normal epithelium." Cancer Res 12: 264–265.

Gilbert, D. M. and S. N. Cohen (1987). "Bovine papilloma virus plasmids replicate randomly in mouse fibroblasts throughout S phase of the cell cycle." Cell 50(1): 59-68.

Gottifredi, V. and C. Prives (2005). "The S phase checkpoint: when the crowd meets at the fork." Semin Cell Dev Biol 16(3): 355-368.

Green, H., O. Kehinde, et al. (1979). "Growth of cultured human epidermal cells into multiple epithelia suitable for grafting." Proc Natl Acad Sci U S A 76(11): 5665-5668.

Green, H., J. G. Rheinwald, et al. (1977). "Properties of an epithelial cell type in culture: the epidermal keratinocyte and its dependence on products of the fibroblast." Prog Clin Biol Res 17: 493-500.

Grm, H. S., M. Bergant, et al. (2009). "Human papillomavirus infection, cancer & therapy." Indian J Med Res 130(3): 277-285.

Gruhne, B., R. Sompallae, et al. (2009). "The Epstein-Barr virus nuclear antigen-1 promotes genomic instability via induction of reactive oxygen species." Proc Natl Acad Sci U S A 106(7): 2313-2318.

Gruhne, B., R. Sompallae, et al. (2009). "Three Epstein-Barr virus latency proteins independently promote genomic instability by inducing DNA damage, inhibiting DNA repair and inactivating cell cycle checkpoints." Oncogene 28(45): 3997-4008.

Gupta, A. K., J. H. Lee, et al. (2009). "Radiation response in two HPV-infected head-and-neck cancer cell lines in comparison to a non-HPV-infected cell line and relationship to signaling through AKT." Int J Radiat Oncol Biol Phys 74(3): 928-933.

Halbert, C. L., G. W. Demers, et al. (1992). "The E6 and E7 genes of human papillomavirus type 6 have weak immortalizing activity in human epithelial cells." J Virol 66(4): 2125-2134.

Hall-Jackson, C. A., D. A. Cross, et al. (1999). "ATR is a caffeine-sensitive, DNA-activated protein kinase with a substrate specificity distinct from DNA-PK." Oncogene 18(48): 6707-6713.

Hamada, N., H. Matsumoto, et al. (2007). "Intercellular and intracellular signaling pathways mediating ionizing radiation-induced bystander effects." J Radiat Res (Tokyo) 48(2): 87-95.

Hampson, L., E. S. El Hady, et al. (2001). "The HPV16 E6 and E7 proteins and the radiation resistance of cervical carcinoma." FASEB J 15(8): 1445-1447.

Hanasoge, S. and M. Ljungman (2007). "H2AX phosphorylation after UV irradiation is triggered by DNA repair intermediates and is mediated by the ATR kinase." Carcinogenesis 28(11): 2298-2304.

Hawley-Nelson, P., K. H. Vousden, et al. (1989). "HPV16 E6 and E7 proteins cooperate to immortalize human foreskin keratinocytes." EMBO J 8(12): 3905-3910.

Hei, T. K., H. Zhou, et al. (2008). "Mechanism of radiation-induced bystander effects: a unifying model." J Pharm Pharmacol 60(8): 943-950.

Hein, J., S. Boichuk, et al. (2009). "Simian virus 40 large T antigen disrupts genome integrity and activates a DNA damage response via Bub1 binding." J Virol 83(1): 117-127.

Hein, J., S. Boichuk, et al. (2009). "Simian virus 40 large T antigen disrupts genome integrity and activates a DNA damage response via Bub1 binding." J Virol 83(1): 117-127.

Henner, W. D., S. M. Grunberg, et al. (1982). "Sites and structure of gamma radiation-induced DNA strand breaks." J Biol Chem 257(19): 11750-11754.

Hill, H. Z., G. J. Hill, et al. (1979). "Radiation and melanoma: response of B16 mouse tumor cells and clonal lines to in vitro irradiation." Radiat Res 80(2): 259-276.

Hill, M. A., J. R. Ford, et al. (2005). "Bound PCNA in nuclei of primary rat tracheal epithelial cells after exposure to very low doses of plutonium-238 alpha particles." Radiat Res 163(1): 36-44.

Hoffmann, R., B. Hirt, et al. (2006). "Different modes of human papillomavirus DNA replication during maintenance." J Virol 80(9): 4431-4439.

Houtgraaf, J. H., J. Versmissen, et al. (2006). "A concise review of DNA damage checkpoints and repair in mammalian cells." Cardiovasc Revasc Med 7(3): 165-172.

Howie, H. L., R. A. Katzenellenbogen, et al. (2009). "Papillomavirus E6 proteins." Virology 384(2): 324-334.

Hu, B., L. Wu, et al. (2006). "The time and spatial effects of bystander response in mammalian cells induced by low dose radiation." Carcinogenesis 27(2): 245-251.

Huo, L., H. Nagasawa, et al. (2001). "HPRT mutants induced in bystander cells by very low fluences of alpha particles result primarily from point mutations." Radiat Res 156(5 Pt 1): 521-525.

Iftner, T., M. Elbel, et al. (2002). "Interference of papillomavirus E6 protein with single-strand break repair by interaction with XRCC1." EMBO J 21(17): 4741-4748.

Ingemarsdotter, C., D. Keller, et al. (2010). "The DNA damage response to non-replicating adeno-associated virus: Centriole overduplication and mitotic catastrophe independent of the spindle checkpoint." Virology 400(2): 271-286.

Ismail, I. H. and M. J. Hendzel (2008). "The gamma-H2A.X: is it just a surrogate marker of double-strand breaks or much more?" Environ Mol Mutagen 49(1): 73-82.

Ito, K., K. Takubo, et al. (2007). "Regulation of reactive oxygen species by Atm is essential for proper response to DNA double-strand breaks in lymphocytes." J Immunol 178(1): 103-110.

Iwahori, S., N. Shirata, et al. (2007). "Enhanced phosphorylation of transcription factor sp1 in response to herpes simplex virus type 1 infection is dependent on the ataxia telangiectasia-mutated protein." J Virol 81(18): 9653-9664.

Iyer, R., B. E. Lehnert, et al. (2000). "Factors underlying the cell growth-related bystander responses to alpha particles." Cancer Res 60(5): 1290-1298.

Jackson, S. P. (2002). "Sensing and repairing DNA double-strand breaks." Carcinogenesis 23(5): 687-696.

Jackson, S. P. (2009). "The DNA-damage response: new molecular insights and new approaches to cancer therapy." Biochem Soc Trans 37(Pt 3): 483-494.

Jazayeri, A., J. Falck, et al. (2006). "ATM- and cell cycle-dependent regulation of ATR in response to DNA double-strand breaks." Nat Cell Biol 8(1): 37-45.

Jeggo, P. and M. F. Lavin (2009). "Cellular radiosensitivity: how much better do we understand it?" Int J Radiat Biol 85(12): 1061-1081.

Jeon, S., B. L. Allen-Hoffmann, et al. (1995). "Integration of human papillomavirus type 16 into the human genome correlates with a selective growth advantage of cells." J Virol 69(5): 2989-2997.

Joiner, M. C., B. Marples, et al. (2001). "Low-dose hypersensitivity: current status and possible mechanisms." Int J Radiat Oncol Biol Phys 49(2): 379-389.

Jones, D. L., D. A. Thompson, et al. (1997). "Destabilization of the RB tumor suppressor protein and stabilization of p53 contribute to HPV type 16 E7-induced apoptosis." Virology 239(1): 97-107.

Jurvansuu, J., K. Raj, et al. (2005). "Viral transport of DNA damage that mimics a stalled replication fork." J Virol 79(1): 569-580.

Kadaja, M., H. Isok-Paas, et al. (2009). "Mechanism of genomic instability in cells infected with the high-risk human papillomaviruses." PLoS Pathog 5(4): e1000397.

Kadhim, M. A., S. R. Moore, et al. (2004). "Interrelationships amongst radiation-induced genomic instability, bystander effects, and the adaptive response." Mutat Res 568(1): 21-32.

Kalantari, M., E. Blennow, et al. (2001). "Physical state of HPV16 and chromosomal mapping of the integrated form in cervical carcinomas." Diagn Mol Pathol 10(1): 46-54.

Kamochi, N., M. Nakashima, et al. (2008). "Irradiated fibroblast-induced bystander effects on invasive growth of squamous cell carcinoma under cancer-stromal cell interaction." Cancer Sci 99(12): 2417-2427.

Kastan, M. B. and J. Bartek (2004). "Cell-cycle checkpoints and cancer." Nature 432(7015): 316-323.

Kastan, M. B. and E. Berkovich (2007). "p53: a two-faced cancer gene." Nat Cell Biol 9(5): 489-491.

Kaur, P. and J. K. McDougall (1989). "HPV-18 immortalization of human keratinocytes." Virology 173(1): 302-310.

Khanna, K. K. and S. P. Jackson (2001). "DNA double-strand breaks: signaling, repair and the cancer connection." Nat Genet 27(3): 247-254.

Kim, T. J., J. W. Lee, et al. (2006). "Increased expression of pAKT is associated with radiation resistance in cervical cancer." Br J Cancer 94(11): 1678-1682.

King, L. E., J. C. Fisk, et al. (2010). "Human papillomavirus E1 and E2 mediated DNA replication is not arrested by DNA damage signalling." Virology 406(1): 95-102.

Klumpp, D. J. and L. A. Laimins (1999). "Differentiation-induced changes in promoter usage for transcripts encoding the human papillomavirus type 31 replication protein E1." Virology 257(1): 239-246.

Komarova, E. A., R. V. Kondratov, et al. (2004). "Dual effect of p53 on radiation sensitivity in vivo: p53 promotes hematopoietic injury, but protects from gastro-intestinal syndrome in mice." Oncogene 23(19): 3265-3271.

Koturbash, I., R. E. Rugo, et al. (2006). "Irradiation induces DNA damage and modulates epigenetic effectors in distant bystander tissue in vivo." Oncogene 25(31): 4267-4275.

Koyama, S., S. Kodama, et al. (1998). "Radiation-induced long-lived radicals which cause mutation and transformation." Mutat Res 421(1): 45-54.

Kudoh, A., S. Iwahori, et al. (2009). "Homologous recombinational repair factors are recruited and loaded onto the viral DNA genome in Epstein-Barr virus replication compartments." J Virol 83(13): 6641-6651.

Kumagai, J., K. Masui, et al. (2003). "Long-lived mutagenic radicals induced in mammalian cells by ionizing radiation are mainly localized to proteins." Radiat Res 160(1): 95-102.

Kusumoto-Matsuo, R., T. Kanda, et al. (2010). "Rolling circle replication of human papillomavirus type 16 DNA in epithelial cell extracts." Genes Cells.

Lai, M., E. S. Zimmerman, et al. (2005). "Activation of the ATR pathway by human immunodeficiency virus type 1 Vpr involves its direct binding to chromatin in vivo." J Virol 79(24): 15443-15451.

Lambert, P. F., M. A. Ozbun, et al. (2005). "Using an immortalized cell line to study the HPV life cycle in organotypic "raft" cultures." Methods Mol Med 119: 141-155.

Lau, A., K. M. Swinbank, et al. (2005). "Suppression of HIV-1 infection by a small molecule inhibitor of the ATM kinase." Nat Cell Biol 7(5): 493-500.

Lavin, M. F. (1999). "ATM: the product of the gene mutated in ataxia-telangiectasia." Int J Biochem Cell Biol 31(7): 735-740.

Lavin, M. F. (2008). "Ataxia-telangiectasia: from a rare disorder to a paradigm for cell signalling and cancer." Nat Rev Mol Cell Biol 9(10): 759-769.

Lee, C. M., C. B. Fuhrman, et al. (2006). "Phosphatidylinositol 3-kinase inhibition by LY294002 radiosensitizes human cervical cancer cell lines." Clin Cancer Res 12(1): 250-256.

Lee, S., B. Elenbaas, et al. (1995). "p53 and its 14 kDa C-terminal domain recognize primary DNA damage in the form of insertion/deletion mismatches." Cell 81(7): 1013-1020.

Lee, S. H. and C. H. Kim (2002). "DNA-dependent protein kinase complex: a multifunctional protein in DNA repair and damage checkpoint." Mol Cells 13(2): 159-166.

Li, H. F., J. S. Kim, et al. (2009). "Radiation-induced Akt activation modulates radioresistance in human glioblastoma cells." Radiat Oncol 4: 43.

Li, L., L. A. Johnson, et al. (2008). "Hsc70 focus formation at the periphery of HSV-1 transcription sites requires ICP27." PLoS One 3(1): e1491.

Lilley, C. E., R. A. Schwartz, et al. (2007). "Using or abusing: viruses and the cellular DNA damage response." Trends Microbiol 15(3): 119-126.

Little, J. B. (2000). "Radiation carcinogenesis." Carcinogenesis 21(3): 397-404.

Little, J. B. (2006). "Cellular radiation effects and the bystander response." Mutat Res 597(1-2): 113-118.

Little, J. B., H. Nagasawa, et al. (2003). "Involvement of the nonhomologous end joining DNA repair pathway in the bystander effect for chromosomal aberrations." Radiat Res 159(2): 262-267.

Liu, S. S., K. Y. Chan, et al. (2006). "Enhancement of the radiosensitivity of cervical cancer cells by overexpressing p73alpha." Mol Cancer Ther 5(5): 1209-1215.

Liu, X., S. Han, et al. (1997). "HPV-16 oncogenes E6 and E7 are mutagenic in normal human oral keratinocytes." Oncogene 14(19): 2347-2353.

Liu, Y., J. A. Parry, et al. (2008). "Soluble histone H2AX is induced by DNA replication stress and sensitizes cells to undergo apoptosis." Mol Cancer 7: 61.

Ljungman, M. (2005). "Activation of DNA damage signaling." Mutat Res 577(1-2): 203-216.

Longworth, M. S. and L. A. Laimins (2004). "Pathogenesis of human papillomaviruses in differentiating epithelia." Microbiol Mol Biol Rev 68(2): 362-372.

Lorimore, S. A., P. J. Coates, et al. (2001). "Inflammatory-type responses after exposure to ionizing radiation in vivo: a mechanism for radiation-induced bystander effects?" Oncogene 20(48): 7085-7095.

Lorimore, S. A. and E. G. Wright (2003). "Radiation-induced genomic instability and bystander effects: related inflammatory-type responses to radiation-induced stress and injury? A review." Int J Radiat Biol 79(1): 15-25.

Lukas, J., C. Lukas, et al. (2004). "Mammalian cell cycle checkpoints: signalling pathways and their organization in space and time." DNA Repair (Amst) 3(8-9): 997-1007.

Luo, M. H., K. Rosenke, et al. (2007). "Human cytomegalovirus disrupts both ataxia telangiectasia mutated protein (ATM)- and ATM-Rad3-related kinase-mediated DNA damage responses during lytic infection." J Virol 81(4): 1934-1950.

Mah, L. J., A. El-Osta, et al. (2010). "gammaH2AX: a sensitive molecular marker of DNA damage and repair." Leukemia 24(4): 679-686.

Marples, B. and S. J. Collis (2008). "Low-dose hyper-radiosensitivity: past, present, and future." Int J Radiat Oncol Biol Phys 70(5): 1310-1318.

Marti, T. M., E. Hefner, et al. (2006). "H2AX phosphorylation within the G1 phase after UV irradiation depends on nucleotide excision repair and not DNA double-strand breaks." Proc Natl Acad Sci U S A 103(26): 9891-9896.

Masters, J. R. (2002). "HeLa cells 50 years on: the good, the bad and the ugly." Nat Rev Cancer 2(4): 315-319.

Matoltsy, AG (1960). "Epidermal cells in culture." Int Rev Cytol 10: 315–351.

Matsumoto, H., S. Hayashi, et al. (2001). "Induction of radioresistance by a nitric oxide-mediated bystander effect." Radiat Res 155(3): 387-396.

Matsumoto, H., A. Takahashi, et al. (2004). "Radiation-induced adaptive responses and bystander effects." Biol Sci Space 18(4): 247-254.

McLaughlin-Drubin, M. E., N. D. Christensen, et al. (2004). "Propagation, infection, and neutralization of authentic HPV16 virus." Virology 322(2): 213-219.

McLaughlin-Drubin, M. E. and K. Munger (2009). "The human papillomavirus E7 oncoprotein." Virology 384(2): 335-344.

Meyers, C., M. G. Frattini, et al. (1992). "Biosynthesis of human papillomavirus from a continuous cell line upon epithelial differentiation." Science 257(5072): 971-973.

Meyers, C., T. J. Mayer, et al. (1997). "Synthesis of infectious human papillomavirus type 18 in differentiating epithelium transfected with viral DNA." J Virol 71(10): 7381-7386.

Mistry, N., C. Wibom, et al. (2008). "Cutaneous and mucosal human papillomaviruses differ in net surface charge, potential impact on tropism." Virol J 5: 118.

Mohni, K. N., C. M. Livingston, et al. (2010). "ATR and ATRIP are recruited to Herpes Simplex Virus type 1 replication compartments even though ATR signaling is disabled." J Virol.

Moody, C. A., A. Fradet-Turcotte, et al. (2007). "Human papillomaviruses activate caspases upon epithelial differentiation to induce viral genome amplification." Proc Natl Acad Sci U S A 104(49): 19541-19546.

Moody, C. A. and L. A. Laimins (2009). "Human papillomaviruses activate the ATM DNA damage pathway for viral genome amplification upon differentiation." PLoS Pathog 5(10): e1000605.

Moody, C. A. and L. A. Laimins (2010). "Human papillomavirus oncoproteins: pathways to transformation." Nat Rev Cancer 10(8): 550-560.

Morgan, W. F. (2003). "Non-targeted and delayed effects of exposure to ionizing radiation: II. Radiation-induced genomic instability and bystander effects in vivo, clastogenic factors and transgenerational effects." Radiat Res 159(5): 581-596.

Mothersill, C. and C. Seymour (2001). "Radiation-induced bystander effects: past history and future directions." Radiat Res 155(6): 759-767.

Mothersill, C. and C. Seymour (2006). "Radiation-induced bystander effects: evidence for an adaptive response to low dose exposures?" Dose Response 4(4): 283-290.

Mothersill, C. and C. B. Seymour (2004). "Radiation-induced bystander effects--implications for cancer." Nat Rev Cancer 4(2): 158-164.

Mothersill, C., R. J. Seymour, et al. (2006). "Increased radiosensitivity in cells of two human cell lines treated with bystander medium from irradiated repair-deficient cells." Radiat Res 165(1): 26-34.

Munshi, A., M. Hobbs, et al. (2005). "Clonogenic cell survival assay." Methods Mol Med 110: 21-28.

Myers, J. S. and D. Cortez (2006). "Rapid activation of ATR by ionizing radiation requires ATM and Mre11." J Biol Chem 281(14): 9346-9350.

Nagasawa, H., A. Cremesti, et al. (2002). "Involvement of membrane signaling in the bystander effect in irradiated cells." Cancer Res 62(9): 2531-2534.

Nagasawa, H., Y. Peng, et al. (2005). "Role of homologous recombination in the alpha-particle-induced bystander effect for sister chromatid exchanges and chromosomal aberrations." Radiat Res 164(2): 141-147.

Natarajan, A. T. and F. Palitti (2008). "DNA repair and chromosomal alterations." Mutat Res 657(1): 3-7.

Nghiem, P., P. K. Park, et al. (2002). "ATR is not required for p53 activation but synergizes with p53 in the replication checkpoint." J Biol Chem 277(6): 4428-4434.

Nichols, G. J., J. Schaack, et al. (2009). "Widespread phosphorylation of histone H2AX by species C adenovirus infection requires viral DNA replication." J Virol 83(12): 5987-5998.

Nicholson, K. M. and N. G. Anderson (2002). "The protein kinase B/Akt signalling pathway in human malignancy." Cell Signal 14(5): 381-395.

Nyberg, K. A., R. J. Michelson, et al. (2002). "Toward maintaining the genome: DNA damage and replication checkpoints." Annu Rev Genet 36: 617-656.

Olive, P. L. (2009). "Impact of the comet assay in radiobiology." Mutat Res 681(1): 13-23.

Olive, P. L. and J. P. Banath (2006). "The comet assay: a method to measure DNA damage in individual cells." Nat Protoc 1(1): 23-29.

Park, E. J., D. W. Chan, et al. (2003). "DNA-PK is activated by nucleosomes and phosphorylates H2AX within the nucleosomes in an acetylation-dependent manner." Nucleic Acids Res 31(23): 6819-6827.

Park, R. B. and E. J. Androphy (2002). "Genetic analysis of high-risk e6 in episomal maintenance of human papillomavirus genomes in primary human keratinocytes." J Virol 76(22): 11359-11364.

Peehl, D. M. and R. G. Ham (1980). "Growth and differentiation of human keratinocytes without a feeder layer or conditioned medium." In Vitro 16(6): 516-525.

Peh, W. L., J. L. Brandsma, et al. (2004). "The viral E4 protein is required for the completion of the cottontail rabbit papillomavirus productive cycle in vivo." J Virol 78(4): 2142-2151.

Perfettini, J. L., R. Nardacci, et al. (2008). "Critical involvement of the ATM-dependent DNA damage response in the apoptotic demise of HIV-1-elicited syncytia." PLoS One 3(6): e2458.

Pett, M. R., W. O. Alazawi, et al. (2004). "Acquisition of high-level chromosomal instability is associated with integration of human papillomavirus type 16 in cervical keratinocytes." Cancer Res 64(4): 1359-1368.

Pietenpol, J. A., R. W. Stein, et al. (1990). "TGF-beta 1 inhibition of c-myc transcription and growth in keratinocytes is abrogated by viral transforming proteins with pRB binding domains." Cell 61(5): 777-785.

Piirsoo, M., E. Ustav, et al. (1996). "Cis and trans requirements for stable episomal maintenance of the BPV-1 replicator." EMBO J 15(1): 1-11.

Pim, D., P. Massimi, et al. (2005). "Activation of the protein kinase B pathway by the HPV-16 E7 oncoprotein occurs through a mechanism involving interaction with PP2A." Oncogene 24(53): 7830-7838.

Podhorecka, M., A. Skladanowski, et al. (2010). "H2AX Phosphorylation: Its Role in DNA Damage Response and Cancer Therapy." J Nucleic Acids 2010.

Polyak, K., Y. Xia, et al. (1997). "A model for p53-induced apoptosis." Nature 389(6648): 300-305.

Prise, K. M., Burdak-Rothkamma, et al. (2007). "New insights on radiation-induced bystander signalling and its relationship to DNA repair." International Congress Series 1299: 121-127.

Prise, K. M. and J. M. O'Sullivan (2009). "Radiation-induced bystander signalling in cancer therapy." Nat Rev Cancer 9(5): 351-360.

Prose, P. H., A. E. Friedman-Kien, et al. (1967). "Ultrastructural studies of organ cultures of adult human skin. In vitro growth and keratinization of epidermal cells." Lab Invest 17(6): 693-716.

Prunieras, M. (1979). "Recent advances in epidermal cell cultures." Arch Dermatol Res 264(2): 243-247.

Puck, T. T. and P. I. Marcus (1955). "A Rapid Method for Viable Cell Titration and Clone Production with Hela Cells in Tissue Culture: The Use of X-Irradiated Cells to Supply Conditioning Factors." Proc Natl Acad Sci U S A 41(7): 432-437.

Puck, T. T., P. I. Marcus, et al. (1956). "Clonal growth of mammalian cells in vitro; growth characteristics of colonies from single HeLa cells with and without a feeder layer." J Exp Med 103(2): 273-283.

Raj, K., P. Ogston, et al. (2001). "Virus-mediated killing of cells that lack p53 activity." Nature 412(6850): 914-917.

Raj, K. (2010) Personal communication.

Rantanen, V., S. Grenman, et al. (1998). "p53 mutations and presence of HPV DNA do not correlate with radiosensitivity of gynecological cancer cell lines." Gynecol Oncol 71(3): 352-358.

Redon, C., D. Pilch, et al. (2002). "Histone H2A variants H2AX and H2AZ." Curr Opin Genet Dev 12(2): 162-169.

Reed, M., B. Woelker, et al. (1995). "The C-terminal domain of p53 recognizes DNA damaged by ionizing radiation." Proc Natl Acad Sci U S A 92(21): 9455-9459.

Regulus, P., B. Duroux, et al. (2007). "Oxidation of the sugar moiety of DNA by ionizing radiation or bleomycin could induce the formation of a cluster DNA lesion." Proc Natl Acad Sci U S A 104(35): 14032-14037.

Restle, A., M. Farber, et al. (2008). "Dissecting the role of p53 phosphorylation in homologous recombination provides new clues for gain-of-function mutants." Nucleic Acids Res 36(16): 5362-5375.

Rheinwald, J. G. and H. Green (1975). "Serial cultivation of strains of human epidermal keratinocytes: the formation of keratinizing colonies from single cells." Cell 6(3): 331-343.

Rice, R. H., K. E. Steinmann, et al. (1993). "Elevation of cell cycle control proteins during spontaneous immortalization of human keratinocytes." Mol Biol Cell 4(2): 185-194.

Riley, P. A. (1994). "Free radicals in biology: oxidative stress and the effects of ionizing radiation." Int J Radiat Biol 65(1): 27-33.

Rogakou, E. P., C. Boon, et al. (1999). "Megabase chromatin domains involved in DNA double-strand breaks in vivo." J Cell Biol 146(5): 905-916.

Rogakou, E. P., D. R. Pilch, et al. (1998). "DNA double-stranded breaks induce histone H2AX phosphorylation on serine 139." J Biol Chem 273(10): 5858-5868.

Rohaly, G., K. Korf, et al. (2010). "Simian virus 40 activates ATR-Delta p53 signaling to override cell cycle and DNA replication control." J Virol 84(20): 10727-10747.

Romanczuk, H. and P. M. Howley (1992). "Disruption of either the E1 or the E2 regulatory gene of human papillomavirus type 16 increases viral immortalization capacity." Proc Natl Acad Sci U S A 89(7): 3159-3163.

Romanczuk, H., F. Thierry, et al. (1990). "Mutational analysis of cis elements involved in E2 modulation of human papillomavirus type 16 P97 and type 18 P105 promoters." J Virol 64(6): 2849-2859.

Roshal, M., B. Kim, et al. (2003). "Activation of the ATR-mediated DNA damage response by the HIV-1 viral protein R." J Biol Chem 278(28): 25879-25886.

Rothkamm, K. and S. Horn (2009). "gamma-H2AX as protein biomarker for radiation exposure." Ann Ist Super Sanita 45(3): 265-271.

Ruesch, M. N., F. Stubenrauch, et al. (1998). "Activation of papillomavirus late gene transcription and genome amplification upon differentiation in semisolid medium is coincident with expression of involucrin and transglutaminase but not keratin-10." J Virol 72(6): 5016-5024.

Salles, B., P. Calsou, et al. (2006). "The DNA repair complex DNA-PK, a pharmacological target in cancer chemotherapy and radiotherapy." Pathol Biol (Paris) 54(4): 185-193.

Sancar, A., L. A. Lindsey-Boltz, et al. (2004). "Molecular mechanisms of mammalian DNA repair and the DNA damage checkpoints." Annu Rev Biochem 73: 39-85.

Sanlioglu, S., P. Benson, et al. (2000). "Loss of ATM function enhances recombinant adeno-associated virus transduction and integration through pathways similar to UV irradiation." Virology 268(1): 68-78.

Sasaki, M. S. (1995). "On the reaction kinetics of the radioadaptive response in cultured mouse cells." Int J Radiat Biol 68(3): 281-291.

Sasaki, M. S., Y. Ejima, et al. (2002). "DNA damage response pathway in radioadaptive response." Mutat Res 504(1-2): 101-118.

Saxena, A., C. Yashar, et al. (2005). "Cellular response to chemotherapy and radiation in cervical cancer." Am J Obstet Gynecol 192(5): 1399-1403.

Schultz, L. B., N. H. Chehab, et al. (2000). "p53 binding protein 1 (53BP1) is an early participant in the cellular response to DNA double-strand breaks." J Cell Biol 151(7): 1381-1390.

Schwartz, R. A., C. T. Carson, et al. (2009). "Adeno-associated virus replication induces a DNA damage response coordinated by DNA-dependent protein kinase." J Virol 83(12): 6269-6278.

Schwartz, R. A., J. A. Palacios, et al. (2007). "The Mre11/Rad50/Nbs1 complex limits adeno-associated virus transduction and replication." J Virol 81(23): 12936-12945.

Seedorf, K., G. Krammer, et al. (1985). "Human papillomavirus type 16 DNA sequence." Virology 145(1): 181-185.

Settle, K., M. R. Posner, et al. (2009). "Racial survival disparity in head and neck cancer results from low prevalence of human papillomavirus infection in black oropharyngeal cancer patients." Cancer Prev Res (Phila) 2(9): 776-781.

Shechter, D., V. Costanzo, et al. (2004). "ATR and ATM regulate the timing of DNA replication origin firing." Nat Cell Biol 6(7): 648-655.

Shi, Y., G. E. Dodson, et al. (2005). "Ataxia-telangiectasia-mutated (ATM) is a T-antigen kinase that controls SV40 viral replication in vivo." J Biol Chem 280(48): 40195-40200.

Shin, H. J., J. Y. Kim, et al. (2010). "Human papillomavirus 16 E6 increases the radiosensitivity of p53-mutated cervical cancer cells, associated with up-regulation of aurora A." Int J Radiat Biol 86(9): 769-779.

Shin, K. H., J. H. Ahn, et al. (2006). "HPV-16 E6 oncoprotein impairs the fidelity of DNA end-joining via p53-dependent and -independent pathways." Int J Oncol 28(1): 209-215.

Shintani, S., M. Mihara, et al. (2003). "Up-regulation of DNA-dependent protein kinase correlates with radiation resistance in oral squamous cell carcinoma." Cancer Sci 94(10): 894-900.

Shrivastav, M., L. P. De Haro, et al. (2008). "Regulation of DNA double-strand break repair pathway choice." Cell Res 18(1): 134-147.

Sionov, R. V. and Y. Haupt (1999). "The cellular response to p53: the decision between life and death." Oncogene 18(45): 6145-6157.

Skalka, A. M. and R. A. Katz (2005). "Retroviral DNA integration and the DNA damage response." Cell Death Differ 12 Suppl 1: 971-978.

Sokolov, M. V., J. S. Dickey, et al. (2007). "gamma-H2AX in bystander cells: not just a radiation-triggered event, a cellular response to stress mediated by intercellular communication." Cell Cycle 6(18): 2210-2212.

Sokolov, M. V., L. B. Smilenov, et al. (2005). "Ionizing radiation induces DNA double-strand breaks in bystander primary human fibroblasts." Oncogene 24(49): 7257-7265.

Song, S., G. A. Gulliver, et al. (1998). "Human papillomavirus type 16 E6 and E7 oncogenes abrogate radiation-induced DNA damage responses in vivo through p53-dependent and p53-independent pathways." Proc Natl Acad Sci U S A 95(5): 2290-2295.

Spardy, N., K. Covella, et al. (2009). "Human papillomavirus 16 E7 oncoprotein attenuates DNA damage checkpoint control by increasing the proteolytic turnover of claspin." Cancer Res 69(17): 7022-7029.

Spardy, N., A. Duensing, et al. (2008). "HPV-16 E7 reveals a link between DNA replication stress, fanconi anemia D2 protein, and alternative lengthening of telomere-associated promyelocytic leukemia bodies." Cancer Res 68(23): 9954-9963.

Sprague, D. L., S. L. Phillips, et al. (2002). "Telomerase activation in cervical keratinocytes containing stably replicating human papillomavirus type 16 episomes." Virology 301(2): 247-254.

Stanley, M. A., H. M. Browne, et al. (1989). "Properties of a non-tumorigenic human cervical keratinocyte cell line." Int J Cancer 43(4): 672-676.

Stanley, M. (2002). Culture Of Human Cervical Epithelial Cells. 137-169. In Freshney, R., Freshney, M. (eds.), Culture of Epithelial Cells, Second Edition, Wiley-Liss, Inc. New York.

Stanley, M. A., M. R. Pett, et al. (2007). "HPV: from infection to cancer." Biochem Soc Trans 35(Pt 6): 1456-1460.

Stenerlow, B. (2006). "Radiation-induced bystander effects." Acta Oncol 45(4): 373-374.

Stiff, T., M. O'Driscoll, et al. (2004). "ATM and DNA-PK function redundantly to phosphorylate H2AX after exposure to ionizing radiation." Cancer Res 64(7): 2390-2396.

Stoker, M. G. and M. Sussman (1965). "Studies on the Action of Feeder Layers in Cell Culture." Exp Cell Res 38: 645-653.

Stoler, M. H. (2003). "Human papillomavirus biology and cervical neoplasia: implications for diagnostic criteria and testing." Arch Pathol Lab Med 127(8): 935-939.

Stoppler, H., D. P. Hartmann, et al. (1997). "The human papillomavirus type 16 E6 and E7 oncoproteins dissociate cellular telomerase activity from the maintenance of telomere length." J Biol Chem 272(20): 13332-13337.

Stracker, T. H., C. T. Carson, et al. (2002). "Adenovirus oncoproteins inactivate the Mre11-Rad50-NBS1 DNA repair complex." Nature 418(6895): 348-352.

Suzuki, K., M. Ojima, et al. (2003). "Radiation-induced DNA damage and delayed induced genomic instability." Oncogene 22(45): 6988-6993.

Szumiel, I. (2005). "Adaptive response: stimulated DNA repair or decreased damage fixation?" Int J Radiat Biol 81(3): 233-241.

Szumiel, I. (2008). "Intrinsic radiation sensitivity: cellular signaling is the key." Radiat Res 169(3): 249-258.

Tapio, S. and V. Jacob (2007). "Radioadaptive response revisited." Radiat Environ Biophys 46(1): 1-12.

Taylor, W. R. and G. R. Stark (2001). "Regulation of the G2/M transition by p53." Oncogene 20(15): 1803-1815.

Tenchini, M. L., C. Ranzati, et al. (1992). "Culture techniques for human keratinocytes." Burns 18 Suppl 1: S11-16.

Thomas, J. T., W. G. Hubert, et al. (1999). "Human papillomavirus type 31 oncoproteins E6 and E7 are required for the maintenance of episomes during the viral life cycle in normal human keratinocytes." Proc Natl Acad Sci U S A 96(15): 8449-8454.

Thompson, D. A., V. Zacny, et al. (2001). "The HPV E7 oncoprotein inhibits tumor necrosis factor alpha-mediated apoptosis in normal human fibroblasts." Oncogene 20(28): 3629-3640.

Todaro, G. J. and H. Green (1963). "Quantitative studies of the growth of mouse embryo cells in culture and their development into established lines." J Cell Biol 17: 299-313.

Toulany, M., U. Kasten-Pisula, et al. (2006). "Blockage of epidermal growth factor receptor-phosphatidylinositol 3-kinase-AKT signaling increases radiosensitivity of K-RAS mutated human tumor cells in vitro by affecting DNA repair." Clin Cancer Res 12(13): 4119-4126.

Tsang, N. M., H. Nagasawa, et al. (1995). "Abrogation of p53 function by transfection of HPV16 E6 gene enhances the resistance of human diploid fibroblasts to ionizing radiation." Oncogene 10(12): 2403-2408.

Valerie, K. and L. F. Povirk (2003). "Regulation and mechanisms of mammalian double-strand break repair." Oncogene 22(37): 5792-5812.

Valerie, K., A. Yacoub, et al. (2007). "Radiation-induced cell signaling: inside-out and outside-in." Mol Cancer Ther 6(3): 789-801.

Viniegra, J. G., N. Martinez, et al. (2005). "Full activation of PKB/Akt in response to insulin or ionizing radiation is mediated through ATM." J Biol Chem 280(6): 4029-4036.

Vozenin, M. C., H. K. Lord, et al. (2010). "Unravelling the biology of human papillomavirus (HPV) related tumours to enhance their radiosensitivity." Cancer Treat Rev.

Wahl, A. F., K. L. Donaldson, et al. (1996). "Loss of normal p53 function confers sensitization to Taxol by increasing G2/M arrest and apoptosis." Nat Med 2(1): 72-79.

Waldren, C. A. (2004). "Classical radiation biology dogma, bystander effects and paradigm shifts." Hum Exp Toxicol 23(2): 95-100.

Wang, H., M. Wang, et al. (2005). "Complex H2AX phosphorylation patterns by multiple kinases including ATM and DNA-PK in human cells exposed to ionizing radiation and treated with kinase inhibitors." J Cell Physiol 202(2): 492-502.

Wang, Q., S. Fan, et al. (1996). "UCN-01: a potent abrogator of G2 checkpoint function in cancer cells with disrupted p53." J Natl Cancer Inst 88(14): 956-965.

Wang, Y. (2008). "Bulky DNA lesions induced by reactive oxygen species." Chem Res Toxicol 21(2): 276-281.

Ward, I. M. and J. Chen (2001). "Histone H2AX is phosphorylated in an ATR-dependent manner in response to replicational stress." J Biol Chem 276(51): 47759-47762.

Ward, J. F. (1988). "DNA damage produced by ionizing radiation in mammalian cells: identities, mechanisms of formation, and reparability." Prog Nucleic Acid Res Mol Biol 35: 95-125.

Watson, G. E., S. A. Lorimore, et al. (2000). "Chromosomal instability in unirradiated cells induced in vivo by a bystander effect of ionizing radiation." Cancer Res 60(20): 5608-5611.

Weitzman, M. D., C. T. Carson, et al. (2004). "Interactions of viruses with the cellular DNA repair machinery." DNA Repair (Amst) 3(8-9): 1165-1173.

Weitzman, M. D., C. E. Lilley, et al. (2010). "Genomes in conflict: maintaining genome integrity during virus infection." Annu Rev Microbiol 64: 61-81.

Weizsaecker, M. and D. F. Deen (1980). "Effect of feeder cell-released substances on the survival of clonogenic 9L cells after treatment with antimetabolites." Cancer Res 40(9): 3202-3205.

Wells, J., R. J. Berry, et al. (1980). "The effect of irradiated feeder cells on the X-ray survival curve shape of freshly explanted human tumor cells and a standard human tumor cell line." Radiat Res 81(1): 150-156.

Williams, A. T., C. J. Sexton, et al. (1994). "Retention of low copy number human papillomavirus DNA in cultured cutaneous and mucosal wart keratinocytes." J Gen Virol 75 (Pt 3): 505-511.

Wilson, R. and L. A. Laimins (2005). "Differentiation of HPV-containing cells using organotypic "raft" culture or methylcellulose." Methods Mol Med 119: 157-169.

Wise-Draper, T. M., R. J. Morreale, et al. (2009). "DEK proto-oncogene expression interferes with the normal epithelial differentiation program." Am J Pathol 174(1): 71-81.

Wiseman, H. and B. Halliwell (1996). "Damage to DNA by reactive oxygen and nitrogen species: role in inflammatory disease and progression to cancer." Biochem J 313 (Pt 1): 17-29.

Wolff, S. (1992). "Failla Memorial Lecture. Is radiation all bad? The search for adaptation." Radiat Res 131(2): 117-123.

Wolff, S. (1998). "The adaptive response in radiobiology: evolving insights and implications." Environ Health Perspect 106 Suppl 1: 277-283.

Wright, E. G. and P. J. Coates (2006). "Untargeted effects of ionizing radiation: implications for radiation pathology." Mutat Res 597(1-2): 119-132.

Xu, B., S. Kim, et al. (2001). "Involvement of Brca1 in S-phase and G(2)-phase checkpoints after ionizing irradiation." Mol Cell Biol 21(10): 3445-3450.

Xu, C., W. Meikrantz, et al. (1995). "The human papilloma virus 16E6 gene sensitizes human mammary epithelial cells to apoptosis induced by DNA damage." Proc Natl Acad Sci U S A 92(17): 7829-7833.

Yang, J., Y. Yu, et al. (2003). "ATM, ATR and DNA-PK: initiators of the cellular genotoxic stress responses." Carcinogenesis 24(10): 1571-1580.

Zhao, X., R. J. Madden-Fuentes, et al. (2008). "Ataxia telangiectasia-mutated damage-signaling kinase- and proteasome-dependent destruction of Mre11-Rad50-Nbs1 subunits in Simian virus 40-infected primate cells." J Virol 82(11): 5316-5328.

Zheng, L., M. Zhou, et al. (2005). "Novel function of the flap endonuclease 1 complex in processing stalled DNA replication forks." EMBO Rep 6(1): 83-89.

Zhou, B. B. and J. Bartek (2004). "Targeting the checkpoint kinases: chemosensitization versus chemoprotection." Nat Rev Cancer 4(3): 216-225.

Zhou, H., V. N. Ivanov, et al. (2005). "Mechanism of radiation-induced bystander effect: role of the cyclooxygenase-2 signaling pathway." Proc Natl Acad Sci U S A 102(41): 14641-14646.

Zhou, H., G. Randers-Pehrson, et al. (2003). "Interaction between radiation-induced adaptive response and bystander mutagenesis in mammalian cells." Radiat Res 160(5): 512-516.

zur Hausen, H. (1977). "Human papillomaviruses and their possible role in squamous cell carcinomas." Curr Top Microbiol Immunol 78: 1-30.

zur Hausen, H. (2002). "Papillomaviruses and cancer: from basic studies to clinical application." Nat Rev Cancer 2(5): 342-350.

zur Hausen, H. (2009). "Papillomaviruses in the causation of human cancers - a brief historical account." Virology 384(2): 260-265.

Characterisation of the biological functions of *Mll*

Molecular Haematology and Cancer Biology
Institute of Child Health
University College London

Abstract

The *M*ixed *L*ineage *L*eukaemia (*MLL*) gene on chromosome 11q23 is frequently rearranged in infant leukaemia. Studies done on *Mll* knockout mice have shown that the lack of this protein impedes cell proliferation. This defect could be owed to increased cell death or senescence, both of which are typical cellular responses to DNA damage when the intensity of the damage is too great to be rectified. In this study, we used mouse embryonic fibroblasts (MEFs) that were isolated from E13.5 wild type or *Mll* knockout mice that were previously generated by McMahon et al. (2007). We report that $Mll^{-/-}$ MEFs have diminished replicative capacity, indicating a reduced potential of $Mll^{-/-}$ cells to divide until they senesce *in vitro*. A markedly reduced proliferation rate of $Mll^{-/-}$ MEFs, overtime, was also observed in comparison to the wild type cells. In contrast with early passage (p1) wild type and $Mll^{-/-}$ MEFs that have comparable cell cycle status (similar proportions of cells in G1, S and G2, M phases of the cell cycle), late passage (p8) $Mll^{-/-}$ MEFs exhibited a vast reduction of cells in S phase and accumulates in G1 and G2 phases. We showed that this pronounced proliferation defect in late passage MEFs was accompanied by accumulation of DNA damage through detection of γ-H2AX nuclear foci, with small contributions from cell death and senescence. We hypothesized that the DNA damage-associated phenotype might be attributed to oxidative stress and measured the ROS levels. The ROS levels in P1 $Mll^{-/-}$ MEFs were increased compared to $Mll^{+/+}$ MEFs, and a more profound increase was observed in p8 $Mll^{-/-}$ MEFs compared to wild type cells. The lines of evidence compiled from this study suggest that *Mll*-deficient cells accumulate more DNA damage owing to excessive ROS production. Central to the DNA damage checkpoint activation is ATM phosphorylation on serine 1987 (ATM-S1987-P) and p53 phosphorylation on serine 15 (p53-Ser15-P). We found that the levels of ATM-S-1987-P were only marginally decreased in $Mll^{-/-}$ MEFs. Interestingly, the level of p53-Ser 15-P is decreased in late passage $Mll^{-/-}$ MEFs, which suggests that Mll acts on p53 phosphorylation of serine 15 in a pathway independent of ATM. The decreased p53-Ser15-P levels upon induction of DNA damage could lead to the inability of p53 to elicit repair of damaged DNA, hence leading to cell death and senescence, and the acquisition of genomic instability.

Table of Contents

List of Figures and Tables

Abbreviation

γ-H2AX	Gamma-H2AX
7AAD	7-amino-actinomycin
ALL	Acute Lymphoblastic Leukaemia
AML	Acute Myeloblastic Leukaemia
ATM	Ataxia-Telangiectasia Mutated
ATR	Ataxia Telangiectasia and Rad3 Related
BrdU	Bromodeoxyuridine
BSA	Bovine Serum Albumin
CBP	CREB-Binding Protein
CDK	Cyclin-Dependent Kinase
CO_2	Carbon Dioxide
DAPI	4',6-diamidino-2-phenylindole
DCFDA	2'-7'-dichlorofluorescene diacetate
DCF	Dichlorofluorescene
dH2O	Distilled water
DMEM	Dulbeccos Modified Eagle Media
DMSO	Dimethylsulphoxide
DNA	Deoxyribonucleic Acid
DNase	Deoxyribonuclease
DSBs	Double-Strand Breaks
DTT	Dithiothreitol
E	Embryonic Day
EDTA	Ethylene-diamine-tetra-acetic Acid
e.g.	For example
FBS	Fetal Bovine Serum
FITC	Fluorescein
Fpc	Foci per cell
GAPDH	Glyceraldehyde 3-phosphate dehydrogenase
g	Grams

H3K4	Histone H3 Lysine 4
H3K4 HMT	Histone H3 Lysine 4 Histone Methyltransferase
HCl	Hydrochloric Acid
H_2O_2	Hydrogen Peroxide
Hox	Homeobox
HDAC	Histone De-acetylase
HSC	Haematopoietic Stem Cell
i.e.	That is
Kb	Kilobases
KDa	Kilodalton
LDH	Lactate Dehydrogenase
MEF	Mouse embryonic fibroblast
MLL	Mixed Lineage Leukaemia
mg	Milligrams
min	minutes
ml	Millilitres
mM	Milimolar
MT Domain	MethylTransferase Domain
µl	microlitres
NaCl	Sodium Chloride
NIMR	National Institute for Medical Research, Mill Hill
nm	nanometre
nM	nanomolar
O/N	OverNight
PAGE	PolyAcrylamide Gel Electrophoresis
PBS	Phosphate Buffered Saline
PCR	Polymerase Chain Reaction
PHD	Plant Homeodomain
Rpm	Revolutions per minute
ROS	Reactive Oxygen Species
RT	Room Temperature

s	Seconds
SA-β-gal	Senescence-Associated Beta Galactosidase
SD	Standard Deviation
SDS	Sodium Dodecyl-Sulphate
Ser	Serine
SET	Su(var)3-9, enchancer-of-zeste, trithorax
ST-HSC	Short Term Haematopoietic Stem Cell
TA	Transcriptional Activation
TE	Tris-EDTA solution
Tris	Tris(hydroxylmethyl)methylamine
U	Unit
V	Volts
WT	Wild Type

Chapter 1: Introduction

The *M*ixed *L*ineage *L*eukaemia (*MLL*) gene on chromosome 11q23 is involved in chromosomal rearrangements associated with more than 70% of infant leukaemias and 10% of overall human leukaemias (reviewed in Krivtsov and Armstrong, 2007). The prognostic implications of the disease resulting from *MLL* rearrangements depend on the immunophenotype of the leukaemia (reviewed in Aplan, 2006). Acute Myeloid Leukaemia (AML) patients with *MLL* translocation possess a similar prognosis as other AMLs, whereas B-lineage Acute Lymphoid Leukaemia (ALL) patients with *MLL* translocations tend to have poor outcome (reviewed in Mitterbauer-Hohendanner and Mannhalter, 2004). *MLL* translocations are also found in therapy-related leukaemias that develop in patients previously treated with topoisomerase II inhibitors for other malignancies (Sung *et al*., 2006). The growing interest in the biology of *MLL*-translocation-associated leukaemias is attributed to the young age at diagnosis, the presence of *MLL* translocations in both ALL and AML and the poor clinical outcome of patients with *MLL* translocations.

The *MLL* locus, which is approximately 80 kb long consists of 37 exons and encodes a 3969 amino acid nuclear protein with a molecular weight of 430 kDa (Hess, 2004; Li *et al*., 2005) (Figure 1). DNA-binding activity is found in AT hooks, which are thought to mediate binding to the minor groove of AT-rich genomic DNA sequences. The RD1 region contains a DNA methyltransferase (MT) domain that may recruit proteins such as HPC2 and the transcriptional repressor CtBP. The RD2 domain recruits histone deacetylase 1 and 2, and the plant homeodomain (PHD) finger domains are components of chromatin remodelling complexes that mediate the binding of the cyclophilin, CYP33, to facilitate protein folding. The transcriptional activation (TA) domain recruits the transcriptional co-activator CBP (CREB-binding protein) and precedes a C-terminal SET (Su(var)3-9, enchancer-of-zeste, trithorax) domain that possesses histone H3 lysine 4 (H3K4) methyltransferase activity and is structurally homologous to Drosophila melanogaster trithorax (Milne *et al*., 2005b). The MLL protein contains self-association motifs in the PHD fingers and SET domain,

suggesting that MLL normally functions as a dimer or oligomer. Besides these domains, MLL also has nuclear localization signals in its N-terminal region that determine a punctuate localization pattern of the proteins in the nucleus. The maturation of the MLL protein requires proteolytic cleavage by Taspase 1 (threonin aspartase) at two sites to generate the amino-terminal (MLL_{N320}) and carboxy-terminal (MLL_{C180}) subunits (Capotosti *et al.*, 2007). The two fragments generated by the cleavage re-associate non-covalently to form a heterodimer and this interaction confers stability to the N-terminal portion and its correct localization to the C-terminal part (Hsieh *et al*., 2003).

When *MLL* translocations occur, *MLL* is broken within an 8.3 kb breakpoint cluster region and exons encoding approximately 1400 amino acids are fused in-frame to a fusion partner gene (Popovic and Zeleznik-Le, 2005). To date, more than 50 different translocation fusion partners have been identified of which the five most prominent are *MLL -AF4*, *MLL-AF9*, *MLL-ENL*, *MLL-AF10* and *MLL-AF6* (Collins and Rabbitts, 2002; Daser and Rabbitts, 2004). Other rearrangements involving *MLL* are either chromosomal insertions, duplications, or jumping translocations that result from integration of an amplicon of chromosome 11 adjacent to the MLL locus on either one or more chromosomes, resulting in cells that have multiple additional copies of the *MLL* gene (Aplan, 2006). The possibility that *MLL* translocations occur as a result of a failure to appropriately repair double-stranded breaks of DNA during development of haematopoietic cells has been discussed previously (Richardson and Jasin, 2000; Lightfoot, 2005). The breakpoint cluster region between exons 8 and 13 is the target for most *MLL* rearrangements. It contains putative topoisomerase II cleavage sites and nuclear matrix attachment regions that may contribute to mechanisms by which translocations occur (Stanulla *et al*., 1997; Sung *et al*., 2006; Scharf *et al*., 2007).

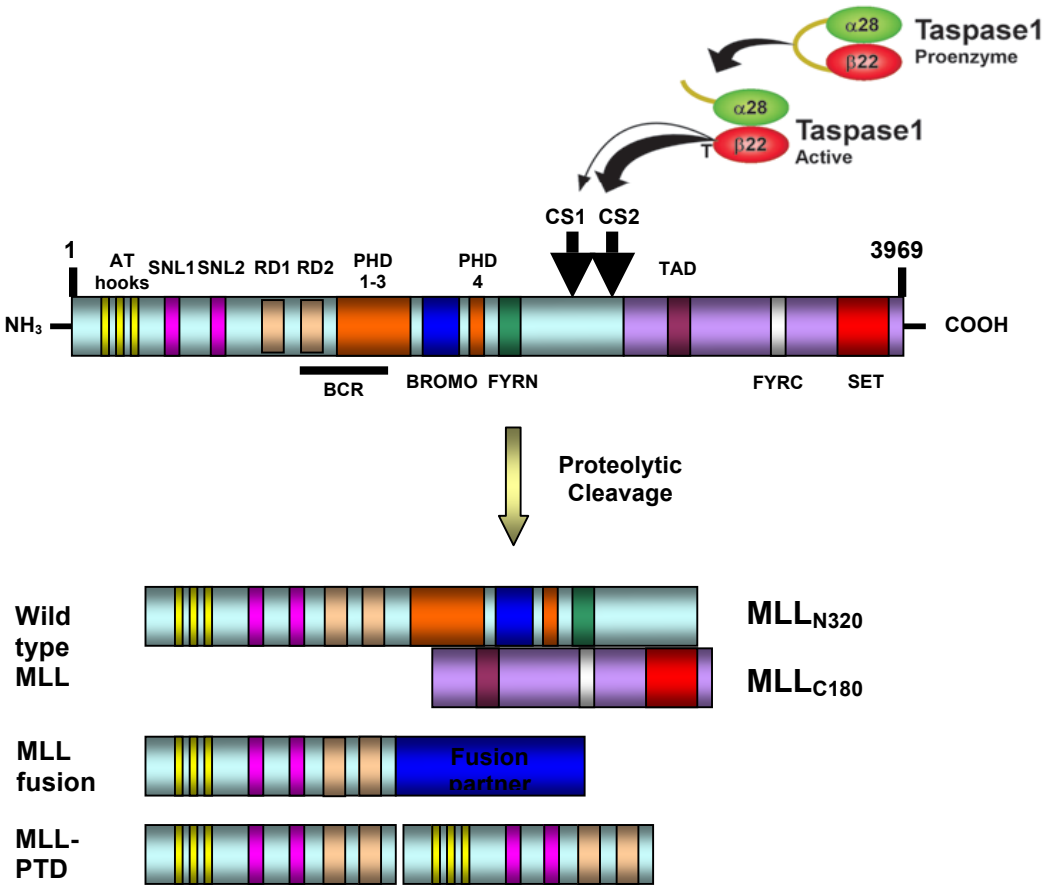

Figure 1. Schematic depictions of wild type and aberrant MLL proteins. Various putative functional domains are shown as coloured boxes and labelled as follows: AT hooks, AT hook DNA binding motifs; SNL 1 and 2, speckled nuclear localization signals 1 and 2; RD1 and RD2, transcriptional repression domain where RD1 contain CxxC (MT), cysteine-rich motif homologous to DNA methyltransferase and RD2 recruits histone deacetylase; PHD 1–3, PHD fingers 1, 2 and 3; BROMO, BROMO domain; FYRN, F/Y rich region, N-terminus; FYRC, F/Y-rich region, C-terminus; TAD, transactivation domain; SET, SET domain. The mature protein consist of two non-covalently associated subunits MLL_{N320} and MLL_{C180} produced by cleavage of nascent MLL by taspase 1 after amino acid residues 2,666 (cleavage site 1, CS1) and 2,718 (CS2) that associate through the FYRN and FYRC plus part of the SET domain.
[Adapted from Liu *et al.* (2008)]

A key feature of the MLL fusion proteins is their ability to transform haematopoietic cells into leukaemia stem cells (LSCs) (Krivtsov *et al*., 2006). MLL fusion proteins may do this via more than one mechanism (Krivtsov and Armstrong, 2007). The loss of the C-terminus fragment of MLL, which contains the H3K4 methylation activity, may perturb the chromatin structure of target promoters (Milne *et al.*, 2005b). The protein partners that are fused to the MLL protein are thought to stimulate expression of different cohorts of cellular genes (Bernard *et al*., 1994; Megonigal *et al*., 2000). The MLL-AF9, MLL-AF10, MLL-ENL and MLL-ELL fusion proteins associate with p53 through their respective fusion partners and suppress p53-mediated induction of p21, MDM2, and Bax in response to various types of DNA damage (Wiederschain *et al*., 2003; 2005).

In recent years, the biological functions of *MLL* have been made clearer from the studies that were designed to disrupt the *Mll* gene in mice. Consistently, all the knockout models have revealed that *Mll* sustains expression of multiple *Hox* genes, which are transcription factors that determine cell fate and body patterning in the developing embryo. The absence of *Mll* led to decrease of Hoxa7, Hoxa9, Hoxa10, Hoxb4, Hoxb5, Hoxb6, Hoxb8, and Hoxc6 in embryoid bodies (Ernst *et al.*, 2004b). *Mll* does not initiate but maintain *Hox* genes expression during development (Yu *et al.*, 1998). The expression of *Hox* genes are independent of *Mll* from the time of initiation until the period between E8.5 and E9, after which it becomes dependent on *Mll*; this stage in development may reflect a dynamic period of chromatin reorganization, which leads to either gene silencing or gene expression (Yu *et al*., 1998). Consistently, *Mll* knockout ($Mll^{-/-}$) mice exhibited severe developmental and haematopoietic abnormalities (Yu *et al.*, 1995; Yagi *et al*., 1998; Ayton *et al*., 2001; Ernst *et al*., 2004a; McMahon *et al*., 2007; Jude *et al*., 2007), and die at the embryonic stage. The developmental day at which it dies vary between different knockout experiments that utilised distinct knock-out targeting sites; Yu *et al*., (E10.5), Ayton *et al*., (pre-implantation), Yagi *et al*., (E12.5 – E14.5) and McMahon *et al*., (E14.5 – E16.5). Although the inability to maintain expression of *Hox* genes in the absence of *Mll* is likely to contribute to leukaemia stem cell (LSC) initiation and maintenance, this feature by itself is unable to recapitulate the phenotype and biology of *MLL* leukaemias (Guenther *et al*., 2005).

The *Mll* knockout mice used in this study were generated by Kathryn A. McMahon who used the Cre-lox system to induce haematopoietic-specific deletion of *Mll* in adult mice according to methods that were employed by de Boer *et al*. (2003). A full knockout was also established to enable analysis of fetal haematopoiesis where the $Mll^{-/-}$ mice die between embryonic days E12.5 to E16.5. Between E9.5 and E11.5, these haematopoietic stem cells (HSCs) transplant to the fetal liver, which becomes the primary site for haematopoiesis in the embryo (Cumano and Godin, 2007; Mikkola and Orkin, 2006). Until haematopoiesis transplants to the bone marrow at E15.5, the fetal liver is the main site of HSC expansion and differentiation. When the E13.5 $Mll^{-/-}$ fetal liver cells were transplanted into irradiated recipients, they are unable to compete with wild type cells and contribute to either long- or short-term haematopoiesis, suggesting a cell intrinsic defect in the long-term HSCs (LT-HSCs) and the short-term HSCs (ST-HSCs) for self-renewal (McMahon *et al*., 2007). The $Mll^{-/-}$ HSCs obtained from the fetal liver have reduced cellularity compared to its wild type counterpart, suggesting a cell proliferation defect as HSCs in the fetal liver must undergo large scale expansion to populate the fetal liver. As for the effect that *Mll* may have on the cell cycle, there have been contradictory reports of positive and negative impact of *MLL* and its fusion proteins on cell proliferation (Milne *et al*., 2005a; Xia *et al*., 2005; Takeda *et al*., 2006).

The first direct evidence for the association of *Mll* with components of the cell cycle came from the work of Milne and his colleagues, in which they found a striking decrease in the levels of cyclin-dependent kinase (CDK) inhibitors $p27^{Kip1}$ and $p18^{Ink4c}$ in *Mll*-deficient mouse embryonic fibroblast (MEF). As a result, the proliferation of these cells is accelerated (Milne *et al.*, 2005a). This study provided the groundwork for cell cycle studies that were previously thought to be difficult owing to the early lethality of *Mll* knockout embryos. However, the use of a spontaneously immortalised fibroblast cell line to evaluate the effect of *Mll* absence on the cell cycle raises some serious concerns as immortalised cell lines emerge largely as a result of mutations that prevent senescence and abrogate cell cycle checkpoints (Morgan, 2007). Xia *et al*. (2005) demonstrated that *Mll* stimulates the promoter of p27KIP1 by aiding the H3K4 methylation of the latter.

As a result, cellular proliferation is impeded. All previous studies to investigate cell growth in *Mll*$^{-/-}$ MEFs were performed on immortalized *Mll*$^{-/-}$ cell lines as early embryonic lethality following *Mll* homozygous disruption precludes detailed studies of its function in the cell cycle (Yu *et al*., 1995).

All eukaryotic cells have four phases within their cell cycle, G1, S, G2, and M, and one outside, G0 (Sancar *et al.*, 2004). Key regulatory components in each phase include E2Fs, Rbs, Cyclins, Cyclin-dependent kinases (CDKs), and CDK inhibitors (CDKIs), which form complex circuits that ensure accurate cell cycle progression (Murray, 2004). The G1-S and intra-S phase checkpoints respectively regulate transition into and progression through S phase, and the G2-M checkpoint regulates entry into mitosis (Sancar *et al*., 2004). The G1-S checkpoint ensures that the DNA to be replicated is not damaged (Cann and Hicks, 2007; Delaval and Birnbaum, 2007). Activated G2-M checkpoint triggers a rapid inhibition against cells entering mitosis (Delaval and Birnbaum, 2007).

Interestingly, *Mll* was implicated in the promotion of cell-cycle progression by interacting with E2F transcription factors to stimulate the expression of cell cycle genes (e.g., cyclins) (Takeda *et al.*, 2006). This significant finding was observed in a *Taspase1* knockout mouse. It is thought that proteolysis of MLL family proteins by Taspase1 is required to fully activate their histone methyl transferase (HMT) activity. The participation of MLL in inducing cell cycle progression was thought to occur at the G1-to-S phase transition (Tyagi *et al*., 2007). The herpes simplex virus *h*ost *c*ell *f*actor-1 (HCF-1) recruits MLL histone H3 lysine 4 methyltransferase (H3K4 HMT) complexes (WDR5, RbBP5, and ASH2) and target E2F to E2F-responsive promoters (i,e., Cyclins). HCF-1-MLL complex associates with E2F1 and by doing so, is recruited to E2F-responsive promoters, where this complex stimulates H3K4 trimethylation of histones at these promoters, therefore facilitate the activation of gene expression and increase of the levels of associated transcripts (Dou *et al.*, 2006; Ruthenburg *et al.*, 2007; Tyagi *et al.*, 2007). This finding opened up avenues for further investigation into the varied roles that *MLL* play in the cell cycle machinery. The mechanistic insight into these seemingly opposing *MLL* activities was further explored by Liu *et al.* (2007). They monitored the protein level of MLL through the cell cycle and

discovered a rigidly controlled biphasic expression of MLL in all cell types. Two prevalent expression peaks of MLL, corresponding G1/S transition and M phase progression were observed. This was attributed to the degradation of MLL at very specific periods within the cells cycle by SCF^{SKP92} and APC^{Cdc20}. Disruption of Mll expression by short hairpin RNA resulted in defects in G1/S entry and M phase progression. These findings indicate that MLL activity is needed for successful cell cycle progression.

From the current reports of experiments with *Mll* knockout mice, it appears that the lack of this protein impedes cell proliferation (Takeda *et al.*, 2006; McMahon *et al.*, 2007; Jude *et al.*, 2007). This defect could be due to increased cell death or senescence, both of which are typical cellular responses to DNA damage when the nature and intensity of the damage is too great to be rectified (Campisi and d'Adda di Fagagna, 2007). However, it is of interest to note that cells lacking *Taspase1* and bearing uncleaved (and hence inactive) Mll protein are delayed or prevented from transiting through the G1/S and G2/M checkpoint, and is reminiscent of activation of "DNA damage signalling" (Sancar *et al.*, 2004). The DNA damage response pathway encompasses multiple levels of reaction that begins with the sensing of the damage (sensors), the relaying of the damage signal (mediators and signal transducers), followed by activation of G1/S and / or G2/M checkpoints and repair of the DNA (effectors) (Figure 2) (Sancar *et al.*, 2004; Lou and Chen, 2006; Chen *et al*., 2007).

Two groups of proteins have been identified as checkpoint-specific damage sensors: the two phosphoinositide 3-kinase-like kinase (PIKK) family members, ATM (ataxia telangiectasia mutated) and ATR (ataxia telangiectasia and Rad3 related) and the RFC/PCNA (clamp loader/polymerase clamp)-related Rad17-RFC/9-1-1 complex. The major sensor of double-strand breaks (DSBs) is ATM. The Mre11-Rad50-Nbs1 (MRN) mediator complex, which is normally downstream of the ATM signalling, has recently been shown to act upstream of ATM to recruit ATM to the site of DNA lesion (Harper and Elledge, 2007). ATM is a 350 kDa oligomeric protein that exists as an inactive dimer that, when recruited to DSBs, dissociate and autophosphorylate the internal serine (Ser1981) thought to be important for maintaining ATM activation (Bakkenist and Kastan,

2003). Activated ATM phosphorylates many proteins, including Chk2, p53, NBS1, and BRCA1 at serines and threonines (Sancar *et al.*, 2004). Mediator proteins such as Mdc1, 53BP1, the MRN complex, Claspin, Brit1/Mcph1, and Brca1 act downstream of ATM and ATR as substrates that play various roles, acting both as recruiters of additional substrates and as scaffolds upon which to assemble complexes (Harper and Elledge, 2007). At the site of DNA damage, the histone H2A variant, H2AX, becomes phosphorylated on Ser139 by ATM, ATR, and DNA PK (Figure 3). The phosphorylated H2AX (γ-H2AX) encompasses a region of several thousand base pairs around the damage sites, forming foci within the nucleus that act as an attractant for the recruitment of the DNA repair machinery (Collis *et al.*, 2004).

In human cells, Chk1 and Chk2 are the effector proteins that receive signals following DNA damage caused by ionising irradiation or radiomimetic agents. Upon being activated, ATM phosphorylates p53 at the serine 15 residue and Chk2 at the threonine 68 residue. These phosphorylations results in the activation of two signal transduction pathways, one to initiate and one to maintain the G1/S arrest. Phosphorylated Chk2 phosphorylates CDC25A, causing it to be excluded from the nucleus and degraded, hence initiating a G1/S arrest. This rapid response is followed by the p53-mediated maintenance of G1/S arrest, which becomes fully operational several hours after the detection of DNA damage. In the maintenance stage, ATM phosphorylates Ser15 of p53 directly (Sancar *et al.*, 2004). Phosphorylated p53 stimulates expression of its target genes, including $p21^{WAF-1/Cip1}$, which binds to and inhibits the S-phase promoting Cdk2-CyclinE complex, thereby maintaining the G1/S arrest. The $p21^{WAF-1/Cip1}$ protein also binds to the Cdk4-CyclinD complex and prevents it from phosphorylating Rb, which will result in the release of E2F transcription factor that is required for the transcription of S-phase genes in order for S phase to proceed (Cann and Hicks, 2007). The balancing act between the kinases and phosphatases in regulating cellular responses to stress is important to maintain genomic stability of the cell (Bakkenist and Kastan, 2004).

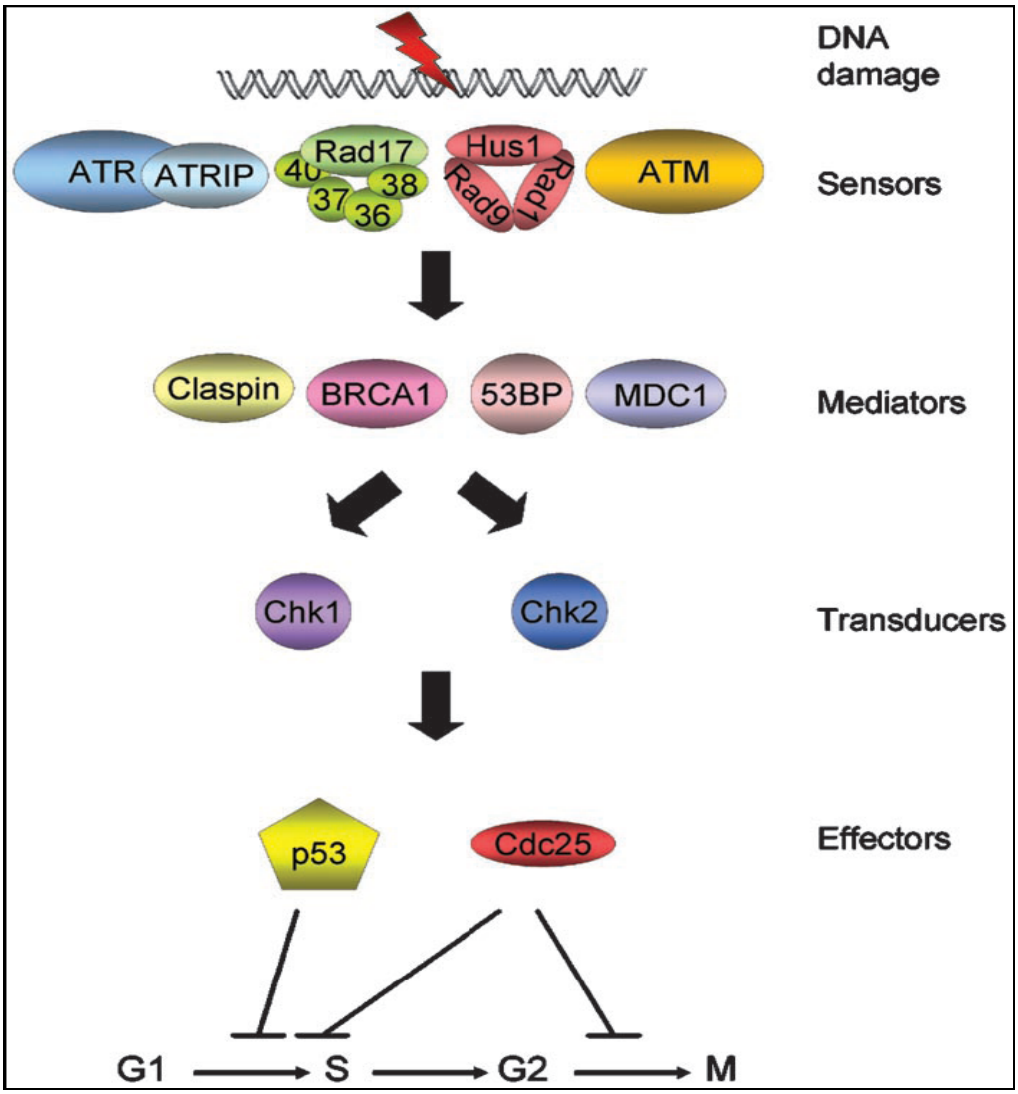

Figure 2. Components of the DNA damage checkpoints in human cells. DNA damage is detected by sensors that, with the aid of mediators, convey the signal to transducers. The transducers, in turn, activate or inactivate other proteins (effectors) that directly participate in inhibiting the G1/S transition, S-phase progression, or the G2/M transition. [Taken from Sancar *et al.* (2004)]

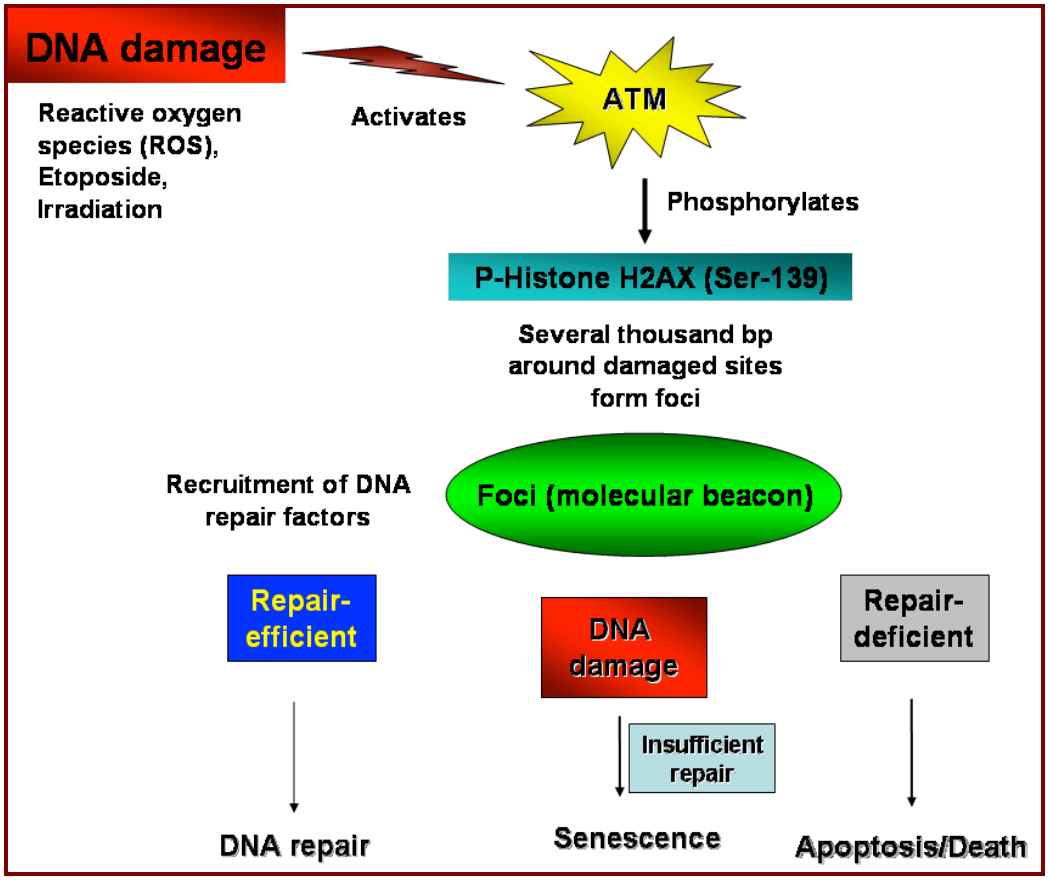

Figure 3. Schematic representations of H2AX phosphorylation in response to DNA damage.

Within minutes of incurring small amounts of DNA damage from the accumulation of ROS, etoposide or ionising irradiation, ATM is activated by an autophosphorylation event at Ser-1981, which may require the NBS1 protein. Once activated, ATM initiates several signalling cascades, which halt cell cycle progression and allows damaged DNA to be repaired. One of the earliest detectable downstream targets of ATM is the histone H2A variant, H2AX, localizing to a region of about 2 Mbp surrounding the site of the double-strand break. Gamma-H2AX appears to play an essential role in recruiting other repair proteins including Rad50, Rad51 and BRCA1 (Paull *et al*., 2000).

Damage to DNA induces several cellular responses that enable the cell to remove or cope with the damage by activating either the survival pathways consisting of double-stranded break repair, cell cycle checkpoints, stress response or cell death pathways, presumably to eliminate cells with potentially catastrophic mutations (Barzilai *et al*., 2002; Sancar *et al.*, 2004). The determinants of whether a cell undergoes growth arrest or cell death are cell type and intensity of the damage or stress (Campisi and d'Adda di Fagagna, 2007).

In recent years, compelling evidences demonstrated that cellular senescence, whether replicative or premature senescence occurs as a result of severe DNA damage (Chen *et al*., 2007). The senescent phenotype is characterised by functional or correlative assays. Functionally, senescent cells undergo distinctive morphological changes to become enlarged, flattened and granular, a permanent arrest of cell proliferation, development of resistance to apoptosis (in some cells), an altered pattern of gene expression and remain metabolically active for long periods of time in culture (Campisi and d'Adda di Fagagna, 2007; Chen *et al*., 2007). Correlative assays that can distinguish senescent cells from their normal counterparts are the staining of the biomarker-senescence-associated beta-galactosidase (SA-β-gal), which is detectable at pH 6, cytological markers of senescence-associated heterochromatic foci (SAHFs) by preferential binding of DNA dyes 4',6-diamidino-2-phenylindole (DAPI) and senescence-associated DNA damage foci (SDFs) that are present in senescent cells from mice and humans and contain proteins that are associated with DNA damage (e.g., γ-H2AX and 53BP1). These damage foci may contain the site of irreparable DNA damage and may provide constitutive signals to p53 to maintain senescence (Campisi and d'Adda di Fagagna, 2007).

Cellular senescence may occur as a consequence of accumulation of DNA damage foci caused by deregulated oncogene expression or alterations in the cellular redox state leading to constant oxidative stress (Heman and Narita, 2007; Mallette *et al*., 2007). The over-expression of oncogenes can cause hyperproliferation and DNA hyper-replication whereby the replicons re-fire or premature termination of replication; generating DNA breaks that initiate a DNA damage response (Bartkova *et al*., 2006; Di Mocco *et al.*, 2006). Another

mechanism by which deregulated oncogenes, such as *Ras*, induce DNA damage involves an increase in cellular levels of reactive oxygen species (ROS), which are normally the by-product of cellular metabolism (Hemann and Narita, 2007). The production of ROS that exceeds the capacity for detoxification may contribute to oxidative base damage and DNA single- and double-strand breaks (Barzilai and Yamamoto, 2004). The evidence discussed above thus suggests that cellular senescence that is induced by different stressors, share a common aetiology, that is, DNA damage. ROS are the major agents responsible for endogenous oxidative DNA damage in the cells. Therefore, any disturbance of biological systems that increase intracellular ROS levels, whether from oncogenic or oxidative stress, would be expected to ultimately induce senescence. It is also worth mentioning that mouse embryonic fibroblasts, which are used in this study, senesce after fewer population doublings than human fibroblasts when cultured under standard conditions which include atmospheric (20%) oxygen (Parinello *et al.*, 2003). The extensive damage inflicted by high levels of ROS on cellular macromolecules leaves the cell with the same options posed by DNA damage alone: repair the damage while arresting the cell cycle, undergo senescence, or execute programmed cell death (Barzilai *et al.*, 2002).

The p53 tumour suppressor protein is the key regulator of cell fate decisions that is often referred to as "the cellular gatekeeper for growth and division" (Levine, 1997). Under mild, physiological stress, the activity of p53 is directed to restore homeostasis, to mobilize adequate repair, to choose the optimal balance of energy sources and to protect the genome from mutagenic influences of ROS (Chumakov, 2007). When exposed to various intracellular and extracellular stresses such as damage to DNA integrity, hypoxia or oncogene expression, p53 is rapidly stabilised and activated through extensive post-translational modifications to function as a transcription factor that regulate a large number of genes to mediate cell cycle arrest, apoptosis, senescence, differentiation, DNA repair, antioxidant activity, angiogenesis and metastasis (Chumakov, 2007; Das *et al.*, 2008). At high levels of damage that exceed the physiologically tolerable threshold, p53 stimulates apoptosis or other kinds of genetic death that will lead to terminal exit of the cells from further cell division (Chumakov, 2007; Garner and Raj, 2008).

Many different proteins are able to bind to p53 and change its quantity as well as to create covalent modifications on the molecule. These proteins are kinases, phosphatases, ubiquitin ligases, factors that regulate interaction of p53 with the protein degradation machinery, methylases, deubiquitinylating enzymes, acetyltransferases, deacetylating enzymes, and proteins that participate in coupling p53 to ubiquitin-like proteins (Chumakov, 2007). The eukaryotic strategy to deal with damaged DNA can be split to three components: recognition of injured DNA, a period of damage assessment, and the implementation of appropriate response, whether it is cell survival via DNA repair or cell death pathway (Fei and El-Deiry, 2003). P53 selectively transactivate its target genes, such as p21, GADD45, members of the 14-3-3 family and others that are cell cycle regulators, as well as BAX, CD95, DR5 and others that are members of the core apoptotic pathways (Figure 4). The changes to the activity of p53 via different modifications, its interactions with other proteins, oncogenic composition and the type of extracellular stimulus determine the ultimate fate of an altered cell, which depends significantly on the tissue origin or the cell type, as different cell types display individual range of parameters that is recognised as normal or optimal (Fei and El-Deiry, 2003; Chumakov, 2007; Das *et al.*, 2008).

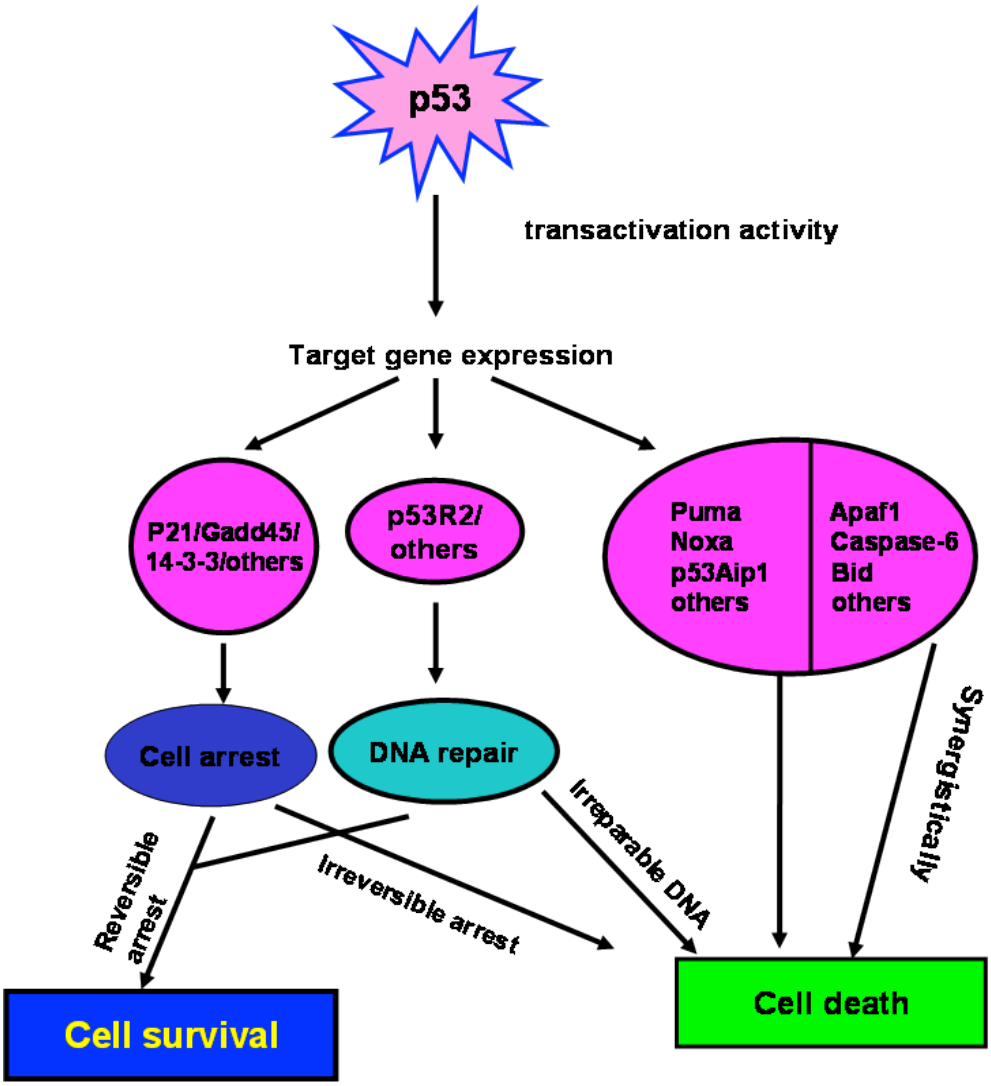

Figure 4. Schematic presentation of the influence of p53 in the event of DNA damage.

P53-dependent effects in response to ionising radiation /DNA damage are mediated either through transactivating its target genes. The target gene expressions may result in reversible arrest coupled DNA repair, which leads to the fate of cell survival, cell death or result in synergy apoptosis, which attributes to the fate of cell death [Adapted from Fei and El-Deiry (2003)]

The *Mll* knockout model established by Kathryn McMahon was studied extensively in the haematopoietic compartment and provided us with important foresights. The failure of HSCs lacking *Mll* to reconstitute lethally-irradiated recipients point towards a self-renewal defect of these cells, as the lack of repopulating stem cells in the recipient was not due to defective homing ability (McMahon *et al.*, 2007). As no studies have thoroughly examined the proliferation defect of cells devoid of *Mll*, we sought to investigate whether the *Mll* knockout mouse embryonic fibroblasts (MEFs) have deregulated cell cycle machinery. We were interested to find out if *Mll* have a role to play in determining cell fate and given the lack of it, may impede cellular proliferation. We carried out assays to measure apoptosis and senescence *in vitro*. Owing to the fact that mouse embryonic fibroblasts have the propensity to senesce after several population doublings earlier than human fibroblasts (Parinello *et al.*, 2003), we measured the levels of ROS because its accumulation is thought to cause continuous low level of DNA damage in cells. This is believed to be the major cause of premature senescence in MEFs. Hence we also examined some components of the DNA damage checkpoints, such as ATM, the accumulation of histone H2AX (γ-H2AX) and the phosphorylation of p53 (Ser15).

Chapter 2: Materials and Methods

2.1 Generation, culture, and cryo-preservation of primary MEFs

The mice used in this study were derived from *Mll*-knockout mice that were generated by Kathryn McMahon using the Cre-lox system to induce deletion of this gene in the whole mice according to the method described by de Boer *et al.* (2003). *Mll* heterozygous ($Mll^{+/-}$) mice were mated, and pregnant females were sacrificed on day 13.5. The embryos were surgically removed and the embryonic tissue prepared for culture. Primary MEFs were grown in Dulbecco's Modified Eagle's Medium (DMEM, Invitrogen) supplemented with 10% heat-inactivated foetal calf serum (FCS, Sigma-Aldrich), 100 U/ml Penicillin (Invitrogen), 100 µg/ml Streptomycin (Invitrogen) and 2 mM L-glutamine (Invitrogen) (complete medium) at 37°C in a humidified atmosphere containing 5% CO_2. Each embryo was cultured separately, and during the 4 days necessary to amplify the MEFs in mass culture, they were genotyped. *Mll* wild-type ($Mll^{+/+}$), heterozygous ($Mll^{+/-}$), and knockout ($Mll^{-/-}$) cells were available in a single litter, which averaged 5 to 12 viable embryos with average yields from an embryo of approx. 1 x 10^7 cells. However, the appearance of $Mll^{-/-}$ embryos in a litter is unpredictable as the absence of *Mll* causes death of the embryo. The cells were expanded over 12 passages and more in T75 flasks. Whenever necessary, MEFs were also trysinised, centrifuged and frozen in 50% complete medium, 40% FCS, and 10% dimethylsulfoxide (DMSO) (Sigma).

2.2 Genotyping

All the wild type ($Mll^{+/+}$) and heterozygote ($Mll^{+/-}$) mice used for breeding were housed at the National Institute for Medical Research (NIMR). Animal husbandry, re-derivations (necessary for transferral of the mice to clean animal facilities) and tail tipping were taken care of by the staff at NIMR. DNA samples for genotyping were prepared from tail tips. Briefly, tips were digested O/N in 500 µl TNES lysis buffer plus 0.5 mg/ml proteinase K at 37°C or 55°C. The following day samples were centrifuged and the supernatant transferred to a fresh microcentrifuge tube. 500 µl isopropanol was added to each tube and the DNA spooled out using an

inoculating loop. DNA was washed once in 70% ethanol, resuspended in 1 x TE and shaken O/N at 37°C. PCR analysis was carried out using 2 combinations of primers. E2/F2 and E2/G2 primers were used to genotype the wild type and knockout alleles, respectively. PCR reactions for genotyping the Mll allele were set up using the Advantage GC2 PCR kit according to manufacturer's instructions (BD-Biosciences). All primer combinations and the programmes used are shown in Table 1.

A

Primer Name	Primer Sequence
E2	5′ GCCAGTCAGTCCGAAAGTAC 3′
F2	5′ AGGATGTTCAAAGTGCCTGC 3′
G2	5′ GCTCTAGAACTAGTGGATCCC 3′

B

PCR	Primers	Programme
Genotyping of the wild type and knock out alleles	E2 F2 G2	97°C 3 min, (97°C 30s, 62°C 1 min, 72°C 2 min) ×3 cycles, (96°C 30s, 62°C 1 min, 72°C 2 min) ×7 cycles, (96°C 30s, 61°C 1 min, 72°C 2 min) ×10 cycles, (96°C 30s, 60°C 1 min, 72°C 2 min) ×10 cycles, 72°C 10 min

Table 1: All primer combinations and the PCR programmes used for genotyping.

(A) Primers used for cloning and genotyping.

(B) PCR programmes used for cloning and genotyping

2.3 Preparation of cellular extracts for Western blot analysis

Whole-cell lysates for Western blotting were prepared using 60 μl 2 x Dithiothreitol (DTT) sample buffer [0.31 g DTT, 1 ml 20% sodium dodecyl sulphate (SDS), 1 ml Glycerol, 0.1 ml 10% Bromophenol blue, 1.25 ml Tris-HCL (tris(hydroxymethyl)aminomethane) (pH 6.8), 6.65 ml H_2O] per 1 x 10^6 cells. Another method of preparing cell lysates was using RIPA lysis buffer [1.5 ml of 5 M sodium chloride (NaCl), 0.5 ml Triton X-100, 0.25g sodium deoxycholate, 0.5 ml 10% SDS, 2.5 ml of 1 M Tris-HCL (pH 8.0), 0.5 ml of 0.5 mM EDTA (pH 8.0), 44.5 ml water and added with a protease inhibitor cocktail].

2.4 Western blotting

When cells were lysed by 2 x DTT sample buffer, lysates were sonicated for 1 min with a 50% pulse, boiled for 5 min and centrifuged. Cells that were lysed by RIPA buffer were resuspended with lysis buffer approx. 5 x the pellet volume, left on ice for 20 min, centrifuged at 13,000 rpm in 4ºC for 10 min. The supernatant that contained the total cell lysate was transferred into a new microcentrifuge tube and the protein concentration was measured by the Bio-Rad Protein Assay kit. The samples were mixed with 5 x DTT sample buffer and boiled at 100ºC for 5 min. In every SDS-Polyacrylamide gel electrophoresis (SDS-PAGE) gel lane, protein lysates that were prepared from either sample buffer or RIPA lysis were loaded and electrophoresed. The proteins were transferred to PVDF membranes and blocked for an hour in 5% (w/v) non-fat dry milk in Tris buffered saline (TBS). Membranes were incubated with primary antibody at 4ºC overnight in 5% (w/v) non-fat dry milk. Horseradish peroxidase (HRP) conjugated secondary antibodies (GE Healthcare) were used at 1:2000 dilution and incubated at room temperature for one hour. Membranes were washed in TBS containing 0.05% Tween 20 and protein bands visualised by enhanced chemiluminescence (ECL, Amersham Biosciences, Bucks, UK) and exposed to light sensitive film (Kodak, New Haven, USA). Primary antibodies used for Western analysis of the Mll protein include anti-MLL N- and C-terminal mouse monoclonal antibodies (Upstate) that were raised against maltose-binding protein (MBP) fused to human MLL protein from amino acids 161-356 (clone N4.4) and 3084-3959 (clone 9-12). Primary antibodies used for Western analysis of ATM and p53 are anti-ATM 2C1 mouse monoclonal antibody (Santa Cruz), anti-Phospho-ATM (Ser 1981)

10H11.E12 mouse monoclonal antibody (Cell Signaling Technology), anti-p53 DO-1 mouse monoclonal antibody (Santa Cruz), and anti-Phospho-p53 (Ser 15) rabbit polyclonal antibody. Anti-Hsp90 rabbit polyclonal antibody (Cell Signaling Technology) was used to control the loading of the gel.

2.5 Assays for cell proliferation capacity and cell proliferation rate

Primary MEFs were derived and genotyped as described previously. The proliferation properties of the MEFs were determined by performing two separate assays. The first of which measures the capacity (or extent in time) of the cells to divide and the other measures the speed at which these cells proliferate. In the assay to determine proliferation capacity, early passage MEFs were seeded into 100 mm dishes at 2×10^5 cells/ dish. Every 3 days, cells from each dish were trypsinised, counted and re-seeded at 1×10^5 cells per well. The replicative capacity of MEFs was illustrated by plotting the increase (more than 1.0) or decrease (less than 1.0) in fold change of cell number from cell populations plated at identical densities and then trypsinised and replated every 3 days at identical density. In the second assay, the proliferation capacities of MEFs were determined by plating replicate cultures of 10^5 cells per 6 cm dish on day 0. The cells were counted each day for eight consecutive days.

2.6 Cell cycle analysis

All the reagents used in this analysis were part of the BD Pharmingen™ BrdU Flow Kit. Primary MEFs were pulsed with 1 mM bromodeoxyuridine (BrdU) for 3 hr, after which the cells were trypsinised and harvested by centrifugation at 1,200 rpm for 5 min. The cells were then fixed, permeabilised and treated with DNase to expose incorporated BrdU that marks synthesised DNA. The cells were then stained with FITC-conjugated anti-BrdU antibody and 7-amino-actinomycin D (7AAD) was added to bind total DNA. The levels of cell-associated BrdU are then measured by flow cytometry on the flow cytometer (Beckman-Coulter XL). With this combination, two-color flow cytometric analysis permits the enumeration and characterisation of cells that were synthesising DNA (BrdU incorporation) in terms of their cell cycle position (i.e., G0/1, S, or G2/M phases defined by 7-AAD staining intensities).

2.7 LDH leakage assay for cell death

Cell death in culture as indicated by lactate dehydrogenase (LDH) leakage (Roche Diagnostics) was determined in a time-dependent manner. For a time course of LDH leakage, cells were plated at 1 x 10^5 cells per well in a 6 well plate and passaged every 3 days. A day before LDH leakage analysis, the medium was changed with 1 ml DMEM containing 1% FBS (assay medium). Media was collected from cultures and centrifuged to remove cell debris, and immediately subjected to the testing protocol recommended by the manufacturer. Absorbances at 490 nm, with a reference reading at a wavelength above 600 nm, were measured. As a positive control, cells were treated with 75 μM etoposide (a concentration that is capable of inducing cell death) for 24 hr.

2.8 Annexin V staining and FACS analysis

Cells were plated at 2 x 10^5 per 60 mm dish. At the time of test, the media was first collected and floating cells were harvested. The adherent cells were washed with PBS, trypsinised and then gently resuspended with an equal amount of fresh growth media; Floating and adherent cells were combined and centrifuged at low speed (1,500 rpm, 5 min). The supernatant was aspirated, and the cell pellet was washed once in 1× Annexin V binding buffer (Annexin V-PE apoptosis detection kit 1, BD Pharmingen), then re-centrifuged and resuspended in 1 x Annexin V binding buffer containing Annexin V-PE. A plate of wild-type cells was always used as control for instrument calibration. Data were collected on a flow cytometer (Beckman-Coulter XL) and analysed using Summit v4.3 software.

2.9 Senescence-associated beta galactosidase staining

To enumerate the proportion of cells that undergo senescence, senescence-associated beta galactosidase staining (SA-β-gal) was performed. Growth media was removed from cells, and the cell monolayer washed 3 times with PBS, and fixed with 3% formaldehyde in PBS (or in DMEM) for 5 min at room temperature. The cells were washed 3 times with PBS and 5 to 6 ml of SA-β-gal (pH 6.0) staining solution [40 mM Citric Acid - 12mM sodium Phosphate (Na2HPO4) (pH 6.0), 5 mM $K_3Fe(CN)_6$, 5 mM $K_4Fe(CN)_6$, 150 mM NaCl, 2 mM $MgCl_2$, and 1 mg/ml X-Gal)] (pre-warmed 37°C) was added per 100 mm culture dish and incubated at 37°C O/N.

2.10 Immunofluorescence labelling of γ-H2AX foci

Cells were plated at densities of 3 to 5 x 10^4 cells per coverslip per dish on a 6 well plate. MEFs were grown to 70-80% confluency before staining with an anti-Phospho-Histone H2A.X (Ser 139) (clone JBW301) antibody. The cells were first fixed with cold methanol for 10 min at RT and permeabilised with ice-cold acetone for 1 min. Coverslips were blocked with 10% foetal bovine serum (FBS) in TBS-0.1% Tween-20 for 15 minutes at RT. Cells were then washed with TBS-0.1% Tween 20, 3 times for 5mins each. The cells were then incubated with anti-γ-H2AX antibody in a 1:200 dilution in TBS-0.1% Tween-20 2% BSA for 2 hr. Next, cells were washed three times with TBS-0.1% Tween-20, and then incubate for 1 hr with 1:200 dilution of fluorescein (FITC)-conjugated AffiniPure donkey anti-mouse IgG (Jackson ImmunoResearch Laboratories, Inc.) in TBS-0.1% Tween-20 2% BSA. Cells were washed three times with TBS-0.1% Tween-20. DNA was stained with 1% ug/ml DAPI/Antifade (Chemicon) for 10 min. Cells were washed three times with TBS-T. The coverslips were mounted with a 90% solution of glycerol in TBS. At least 10 images of cells were randomly collected at each time point and the number of foci was determined optically under a fluorescent microscope at 400 x magnification.

2.11 Analysis of intracellular ROS

The day before ROS analysis, the cells were seeded at equal densities of 2.5 x 10^5 per T25 flasks. Cells were fed with 5 μM 2'-7'-dichlorofluorescene diacetate (DCFDA) (Sigma-Aldrich) in DMEM without FCS for 30 min at 37°C, 5% CO_2. After that, cells were trypsinised, washed once with PBS, and resuspended in PBS before measurement of ROS levels by flow cytometric analysis. DCFDA is a cell-permeant and non-fluorescent compound until it is oxidized in the cytoplasm of live cells. After entering live cells, the diacetate groups are cleaved by intracellular esterases. Oxidation of the reduced dyes can then occur in the presence of ROS, causing the dyes to fluoresce. The peak excitation wavelength for oxidized DCF is fluorescein (FITC) that is typically excited by 488 nm line of an argon laser, and the emission is collected at 525 nm. As a positive control for increased ROS level, we increased free radicals in cells by adding 300 μM H_2O_2 for 15 min, after prior incubation of MEFs with DCFDA as described above. The samples should be read within 30 min as the DCFDA fluorescence is not stable.

2.12 RNA extraction

Total RNA from MEFs was isolated using the reagents from the RNeasy Mini Kit (Qiagen) according to the manufacturer's instructions. The RNA purity was examined using the Bioanalyser 2100 (Agilent Technologies, Palo Alto, CA).

2.13 cDNA preparation

3 to 4 µg total RNA was DNase-treated at RT for 15 min. The reaction was stopped by heating to 65ºC for 5 min with 25 mM EDTA. RNA was converted into cDNA by adding 10 µl of Reverse Transcriptase (RT) reaction mix [(4 µl first strand buffer, 2 µl of 0.1 M DTT and 1 µl Moloney Murine Leukaemia Virus-Reverse Transcriptase (MMLV-RT), 1 µl of 200 ng random hexamer primer, 1 µl of 10 mM dNTP, and 1 µl RNase Out)] that were purchased Invitrogen. The reverse transcription reaction was incubated at 37ºC for 2 hours and stopped by heating the reaction mixture at 70ºC for 15 min. cDNA was aliquoted into 4 tubes.

2.14 Quantitative PCR (qPCR)

qPCR was performed with the Applied Biosystems ABI 7900HT Fast Real-time PCR system using TaqMan® . The ATM (Mm00431917_m1) and GAPDH (Mm99999915_g1) primer/probe sets were purchased from ABI. 1µl cDNA (5 ng) was used with 900 nM forward primer, 900 nM reverse primer, 150 nM probe and 1 x Taqman universal master mix. Levels of the target genes were normalized against those of GAPDH and a standard curve was generated for each primer/probe set to ensure that the target PCR efficiency was equivalent to the GAPDH PCR efficiency.

2.15 Affymetrix gene chip analysis

Total RNA was prepared as described in Section 2.12. The rest of the procedures leading up to data analysis, which include conversion of total RNA to cDNA using reagents from the Microarray cDNA synthesis kit (Roche Diagnostics), preparation of biotinylated cRNA target by *in vitro* transcription, target cRNA fragmentation and hybridization, and fluidics protocol for microarray staining were carried out by Miss Nipurna Jina at the Institute of Child Health (ICH) Gene Microarray Centre.

2.1.6 Gene Array Data Analysis

Quality control was carried out using GCOS software. Signal values were calculated using MAS 5.0, scaled to 100 and normalised to the median. Downstream analysis was done using Genespring 7.3.1. Statistical analysis was carried out using a two-tailed students t-test with Welsh correction and genes were considered to be differentially expressed where there was a fold change ≥ 3 with a P value <0.01. To analyse the data sets as whole and confirm differential expression between individual chips, a volcano plot was drawn.

Chapter 3: Results

3.1 Generation of *Mll*$^{-/-}$ mice

To assess the biological functions of *Mll*, our former colleague, Kathryn McMahon, generated conditional *Mll* knockout (*Mll*$^{-/-}$) mice. A cre-lox gene-targeting strategy was employed to delete exons 9 and 10 of the *Mll* locus. The *Mll*$^{-/-}$ mice were not viable from developmental day E12.5 to 16.5. Lethality at the embryonic stage is often caused by deregulation of signaling pathways that control cell growth and/or cell proliferation (Takeda *et al.*, 2006). In this study, the biological functions of *Mll* were examined in mouse embryonic fibroblasts (MEFs) that were derived from E13.5 *Mll* embryos and cultured *in vitro*.

3.2 Determination of the status of Mll protein in *Mll*$^{-/-}$ mice

To ascertain the status of the N- and C-terminus portions of Mll protein in the absence of exons 9 and 10, protein lysates were made from mouse embryonic fibroblasts (MEFs) obtained from E13.5 *Mll*$^{+/+}$, *Mll*$^{+/-}$ and *Mll*$^{-/-}$ embryos. A human erythroleukemia cell line (K562), known to express Mll, was used as positive control for Mll expression. Figure 5 shows the status of Mll N-terminus portion (320 kDa) and the smaller C-terminus portion (180 kDa). Deletion of these exons unexpectedly resulted in the complete loss of Mll protein expression. The Mll proteins were present in *Mll*$^{+/+}$, reduced in *Mll*$^{+/-}$ and absent in *Mll*$^{-/-}$ MEFs, suggesting that the exons 9 and 10 encode domains that confer stability of the Mll protein. Two cysteine residues belonging to one of the putative zinc binding sites of PHD finger 1 of MLL are removed following deletion of exons 9 and 10 (Aasland *et al*., 1995). It is possible that the removal of these residues and probable loss of zinc binding in this location may have gross consequences for protein folding and maturation. This may then lead to degradation of the protein. The death of *Mll*$^{-/-}$ embryos suggests that either the 1st PHD finger was integral to the function of Mll or that the levels of Mll were decreased.

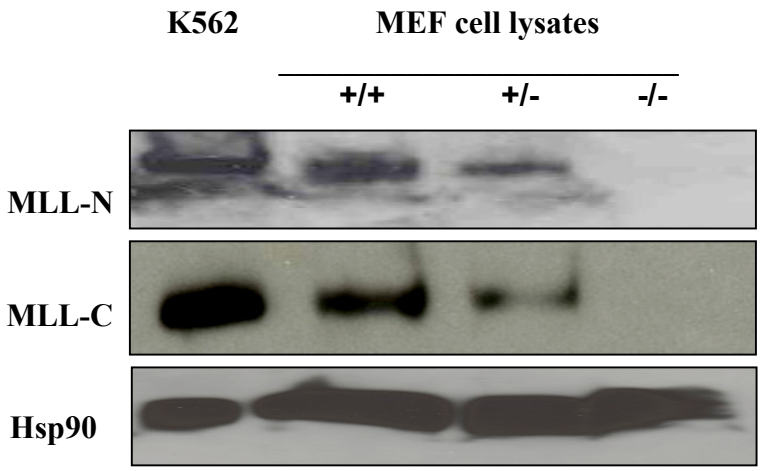

Figure 5. Western blot analysis for Mll expression in whole cell lysates. Western blots for Mll expression in whole-mouse embryonic fibroblasts (MEFs) lysates shows the absence of Mll in knockout (-/-) MEFs. Primary MEF cells were derived from E13.5 embryos with wild type (+/+), heterozygote (+/-), and knock out (-/-) genetic background. A human erythroleukemia cell line (K562), known to express MLL, was used as positive control for MLL expression.

The antibodies used were anti-MLL N- and C- terminal monoclonal antibodies that detected the MLL-N terminus (approx. 300 kDa) and MLL-C terminus (approx.180 kDa) proteins. An Hsp90 Western blot is shown as loading control.

3.3 Growth characteristics of the *Mll*$^{-/-}$ mouse embryonic fibroblasts

In our system of cultivating MEFs, the cells were passed every 2.5 days (two population doublings). Freshly isolated MEFs were seeded into flasks and labelled as P0. Two and a half days later, they were passed and labelled as passage 1 (P1) MEFs, with subsequent passaging every 2.5 days. Cells were harvested at various time points between P1 to P12 for analyses. After P1, three independent sets of *Mll*$^{+/+}$ and *Mll*$^{-/-}$ MEFs were seeded at equal numbers. At each passaging, the cells were trypsinised and counted. A change of 1.0 fold or less of the number of cells plated would indicate lack of cell growth while a change of more than a fold would indicate growth from the time that they were plated. *Mll*$^{+/+}$ MEFs proliferated robustly and lived up to twelve passages (30 days) when cultivated in optimal culture condition. Initially, at passage 1 (P1), the *Mll*$^{-/-}$ MEFs have comparable growth rate as *Mll*$^{+/+}$ MEFs. However from passage 5 (P5) onwards, the *Mll*$^{-/-}$ MEFs gradually lost the capacity to regenerate upon passaging in culture (Figure 6).

In another independent experiment, we assessed the proliferation rates of *Mll*$^{+/+}$ and *Mll*$^{-/-}$ MEFs at different passages. MEFs from either passage 0 or passage 3 were harvested and seeded in 8 flasks. Every day for 8 consecutive days, cells from a flask were harvested and counted (Figure 7A). While there was already a visible difference in the proliferation rate between *Mll*$^{+/+}$ and *Mll*$^{-/-}$ MEFs at passage 1, this difference is greatly amplified in passage 4 (Figure 7B). Although passage 1 *Mll*$^{-/-}$ MEFs were still proliferating, they were clearly proliferating at a slower rate than the wild-type MEFs. Interestingly, the *Mll*$^{-/-}$ MEFs at passage 4 did not grow at all. Instead, they exhibited a decrease in cell number. These experiments, which were carried out in triplicates revealed defects in proliferation of MEFs devoid of *Mll*.

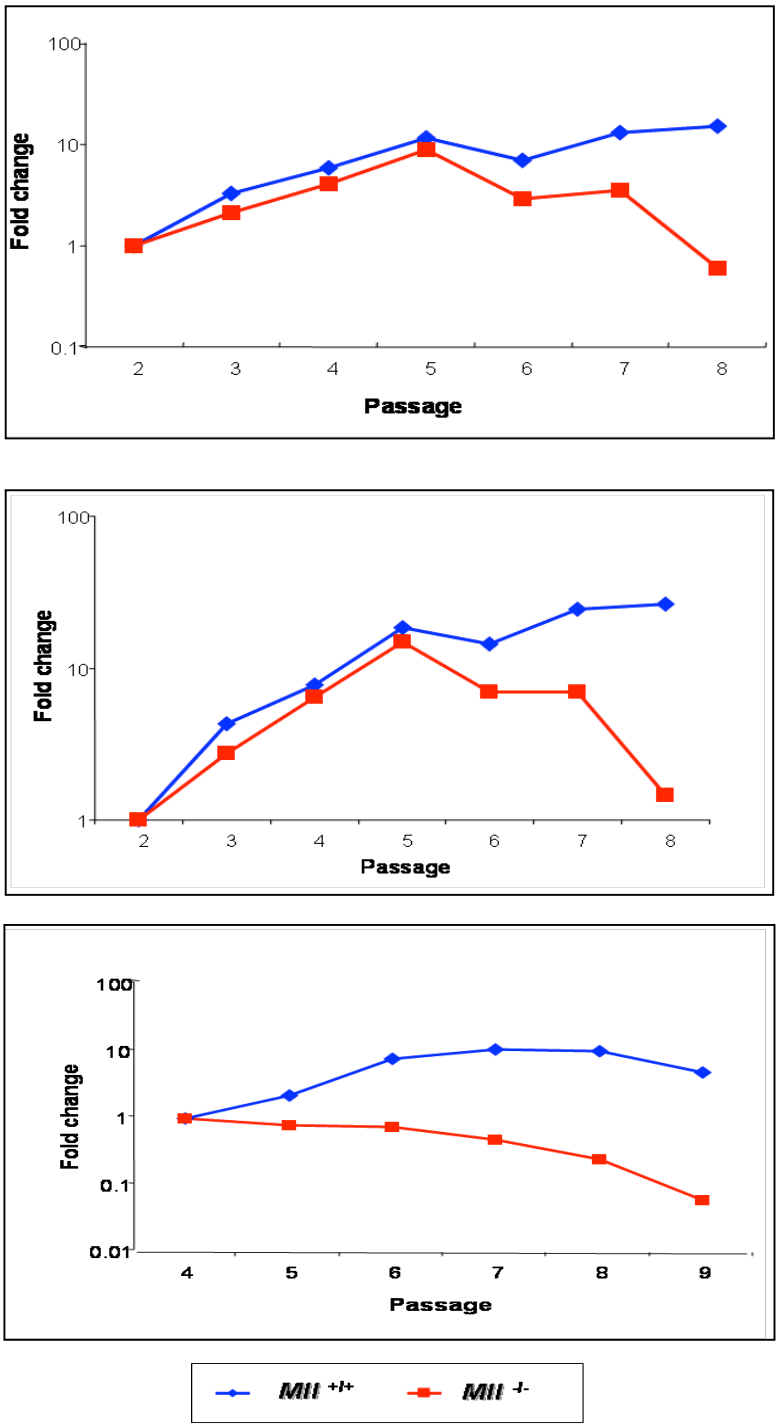

Figure 6. The replicative capacity of three independent sets of *Mll*$^{+/+}$ and *Mll*$^{-/-}$ MEFs.

The replicative capacities of the respective MEFs were illustrated by plotting fold change in cell number every 2.5 days from the previous passage.

A

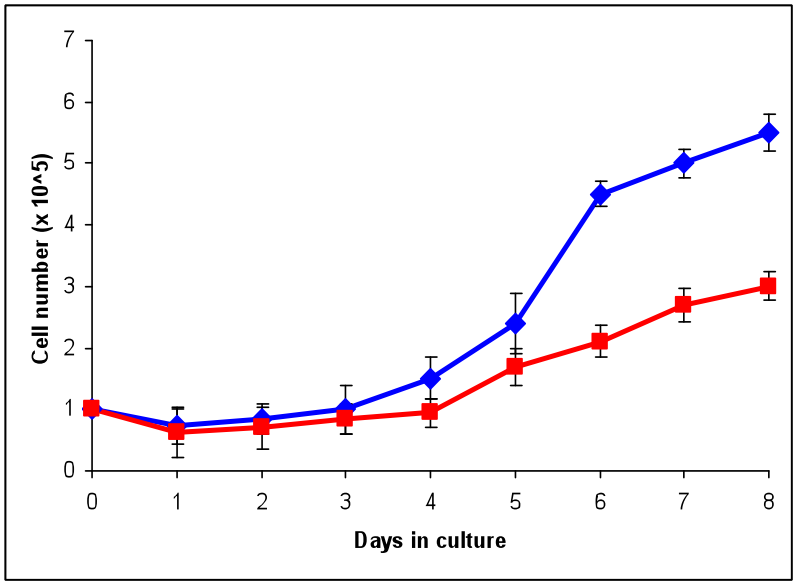

B

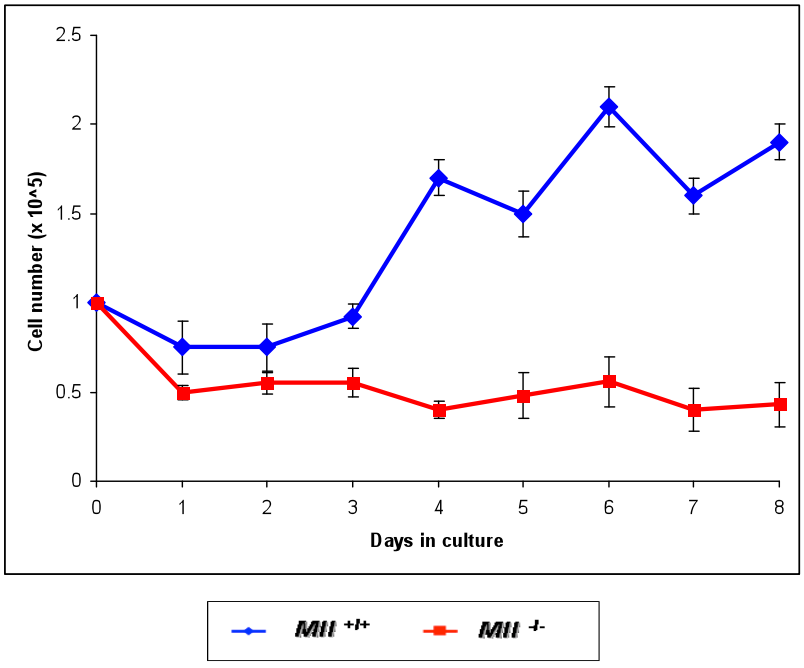

Figure 7. Growth curves showing the proliferative rate of *Mll*$^{+/+}$ and *Mll*$^{-/-}$ MEFs at Passage 1 and 4.

Replicate cultures of 1 x 10^5 cells per 6cm dish were plated on day 0 and cells were counted each day for 8 consecutive days. Data shown was obtained by *Mll*$^{+/+}$ and *Mll*$^{-/-}$ primary MEFs at (A) Passage 1 (B) Passage 4 at the start of the experiment.

3.4 Alteration of cell cycle status

The reduction in the replicative potential and also the rate of proliferation in later passages of *Mll*$^{-/-}$ MEFs prompted us to consider the possibility of defects in the cell cycle checkpoints. To examine whether the lack of Mll affects the cell cycle, we performed a 2-dimensional flow cytometric cell cycle analysis. Cells were fed with the thymidine analogue, bromodeoxyuridine (BrdU), to label those that were replicating their DNA. Together with the use of 7-amino-actinomycin D (7-AAD) to stain and measure DNA content in each cell, we were able to identify and measure the proportion of cells that were in G1, S and G2/M phases of the cell cycle. The cell cycle profile of passage 1 (p1) *Mll*$^{+/+}$ and *Mll*$^{-/-}$ MEFs were similar, with comparable proportion of cells in G1, S and G2/M phases (Figure 8A). However passage 8 *Mll*$^{-/-}$ MEFs exhibited a drastic decrease in the number of cells that incorporated BrdU and an increase in the number of cells within the G2/M compartment. Together, these features point to a cell cycle block at the G2/M transition (Figure 8B).

Such a pattern of cell cycle block is often exhibited in the event of DNA damage. In response to DNA damage, cells often arrest at (a) the G1/S transition to prevent replication of damaged DNA and also at (b) the G2/M transition to prevent mitosis. Failure of cells to arrest at these checkpoints results in them undergoing mitosis with un-repaired DNA. If the damage is substantial, the resulting daughter cells may become genomically unstable and this may lead to cell death.

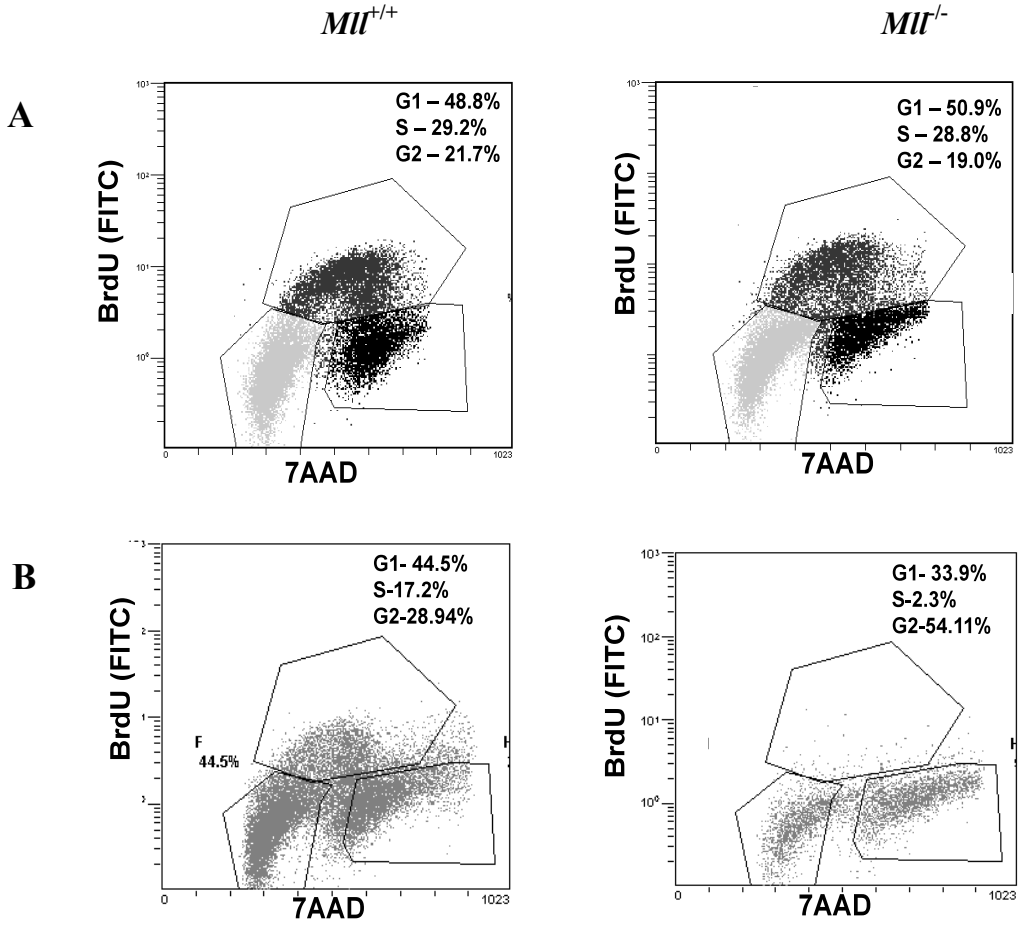

Figure 8: Cell cycle analyses to evaluate the cell cycle status of *Mll*$^{+/+}$ and *Mll*$^{-/-}$ MEFs.

Three hours after BrdU was added in culture medium, cells were trypsinised, washed and stained with anti-BrdU (FITC) antibody and 7AAD.

(Insets) Percentages of cells in G1, S and G2/M phase.

Results shown are representative data of three independent experiments.

(A) Cell cycle status of passage 1 (P1) *Mll*$^{+/+}$ and *Mll*$^{-/-}$ MEFs.

(B) Cell cycle status of passage 8 (P8) *Mll*$^{+/+}$ and *Mll*$^{-/-}$ MEFs.

3.5 Assessment of cell death

Apart from cell cycle blockade, the apparent reduction in replicative potential of the *Mll*$^{-/-}$ MEFs may be also contributed to by cell death and or cellular senescence. To assess the level of cell death in these cells, we measured lactate dehydrogenase (LDH) activity from these cells at passage 5. An LDH leakage kit (Roche) was used to assay LDH that was released from the cytosol of damaged cells. A high level of cell death was induced when MEFs were treated with high concentrations of etoposide (as positive control for cell death). The application of this assay on samples from *Mll*$^{+/+}$ and *Mll*$^{-/-}$ MEFs from passage 5 to passage 8 revealed a marginal and gradual increase of LDH activity in *Mll*$^{-/-}$ MEF cells.(Figure 9). This increase of cell death was also observed when Annexin V staining was used to ascertain percentage of dead/dying cell in passage 8 of these two types of MEFs (Figure 10). The percentage of Annexin V-positive *Mll*$^{+/+}$ and *Mll*$^{-/-}$ MEFs were 17.6 ± 0.32 and 25.3 ± 1.11, respectively (Figure 10B), showing that passage 8 *Mll*$^{-/-}$ MEFs have 1.4 fold more dead/dying cells than their wild type counterpart. Together, these assays reveal that although *Mll*$^{-/-}$ MEFs populations experienced more cell death at later passages, the magnitude of this difference is somewhat modest and statistically insignificant. While this can contribute to the diminished replicative potential of the *Mll*$^{-/-}$ MEFs it is unlikely to be the major cause.

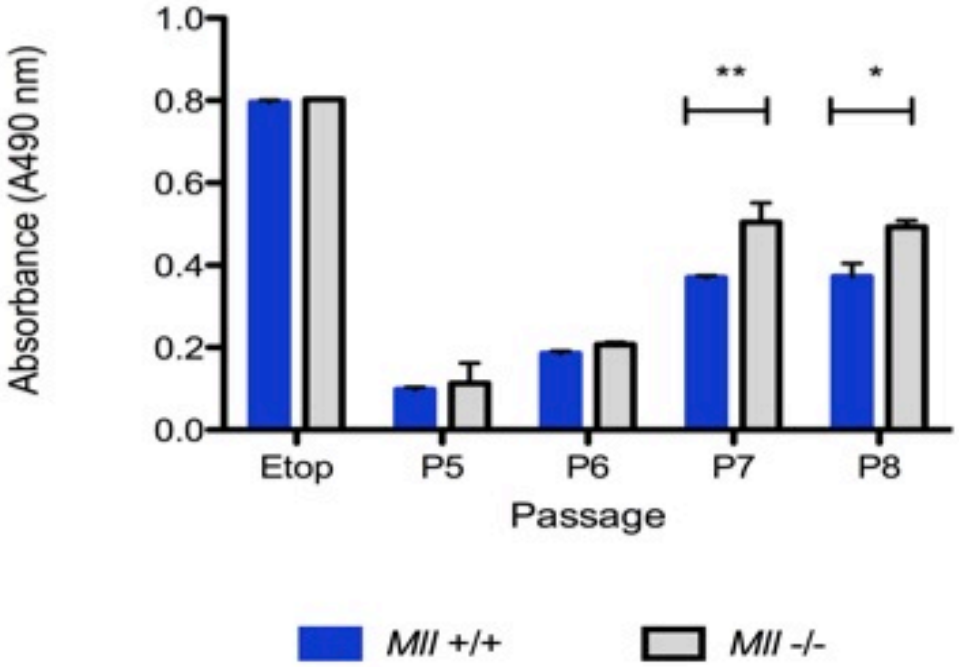

Figure 9: Cell death as measured by LDH activity.

Cell death in MEFs populations from passage 5 to 8 was quantitated by measuring the activity of LDH in the medium of the cells. The positive control for this experiment was cells that were treated with etoposide at 75 μM, a concentration that was sufficient to induce cell death in MEFs. Standard deviation shown was calculated from results obtained from triplicate of experiments.

A

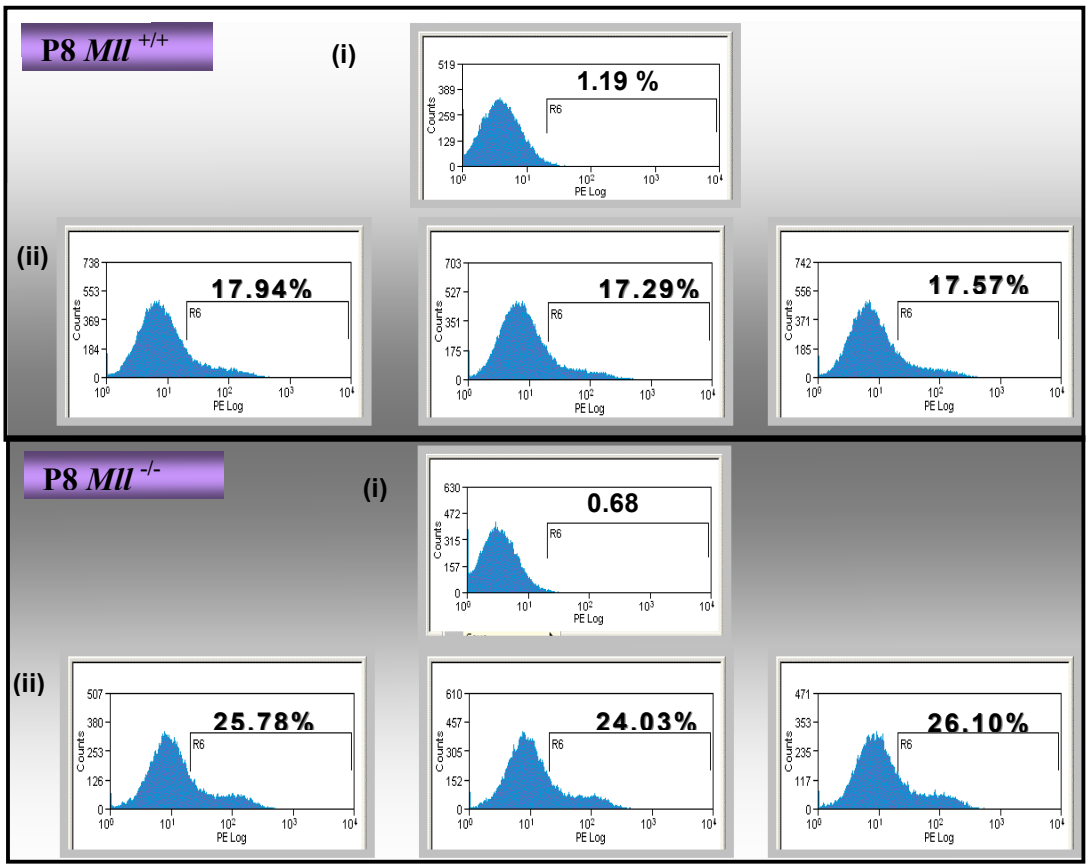

B

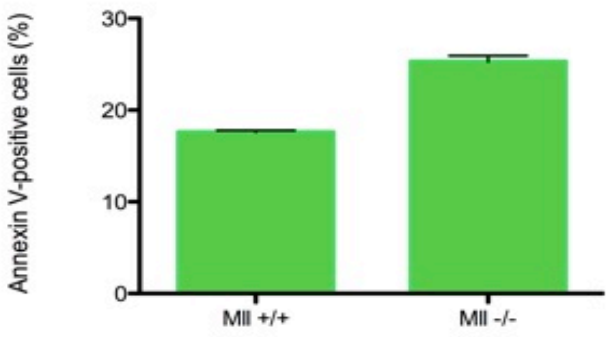

Figure 10: Annexin V staining of passage 8 *Mll*$^{+/+}$ and *Mll*$^{-/-}$ MEFs.

(A) Flow cytometric analyses showing histogram of (i) Annexin V-PE negative and (ii) Annexin V-PE-positive cells from three independent experiments.

(B) Data shown as mean ± SD in a graph.

3.6 Enumeration of cells that undergo premature senescence in culture

From the time they are plated onto culture flasks, primary MEFs undergo an intrinsically defined number of divisions *in vitro* that result in replicative senescence (Mathon and Lloyd, 2001). Under abnormal circumstances, MEFs undergo premature senescence, i.e., oncogene- or culture-induced senescence, as a consequence of accumulation of DNA damage or stress-causing signals (Dimri, 2005). We were interested to ascertain if the reduced proliferation potential of *Mll*$^{-/-}$ MEFs could be attributed to increased premature senescence. To assess the rate of senescence in *Mll*$^{+/+}$ and *Mll*$^{-/-}$ MEFs, we performed a well-characterised correlative assay to detect senescence-associated *β*-galactosidase (SA-*β*-gal) activity that is optimally active at pH 6.0 (Dimri *et al.*, 1995). MEFs from passage 2, 4, 6, 8, 10 to 12, were trypsinised and re-plated at equal numbers; after which SA-*β*-gal activity was measured. The percentage of SA-*β*-gal-positive cells was determined by counting the number of cells that exhibited intense blue staining against the total number of cells in every field and the average was obtained from ten independent fields (An example of SA-*β*-gal-positive cells is shown in Figure 11A).

The starting cultures of both *Mll*$^{+/+}$ and *Mll*$^{-/-}$ MEFs (P1) consisted of small, vigorously proliferating cells of rather uniform size. With increasing passage, the wild-type cultures gradually became enriched for large, often bi-nucleated cells, and stained blue for SA-*β*-gal activity. A significant proportion of senescent cells appeared in *Mll*$^{+/+}$ MEFs from P4 onwards and the appearance of senescent cells remained at a constant kinetics throughout P4 to P12, but a vast majority of cells continued to proliferate even after p12 (Figure 11B). In comparison, the *Mll*$^{-/-}$ MEF cultures from P4 to P8 contained a mixed population of cells that acquired the senescent morphology (enlarged and flattened) but lacked the SA-*β*-gal activity seen in wild type cells, and some cells that were stained blue with SA-*β*-gal. Interestingly, P12 *Mll*$^{-/-}$ MEFs exhibited a marked increase in SA-*β*-gal-positive cells, indicating increased senescence (Figure 8B). Although there was an increase in senescent cells in the *Mll*$^{-/-}$ MEFs population, it is not possible to ascribe this as the cause for the reduction in proliferative capacity of these cells because up until passage 12 the difference in the proportion of senescent cells

between the *Mll*$^{-/-}$ MEFS and the wild-type cells was marginal.

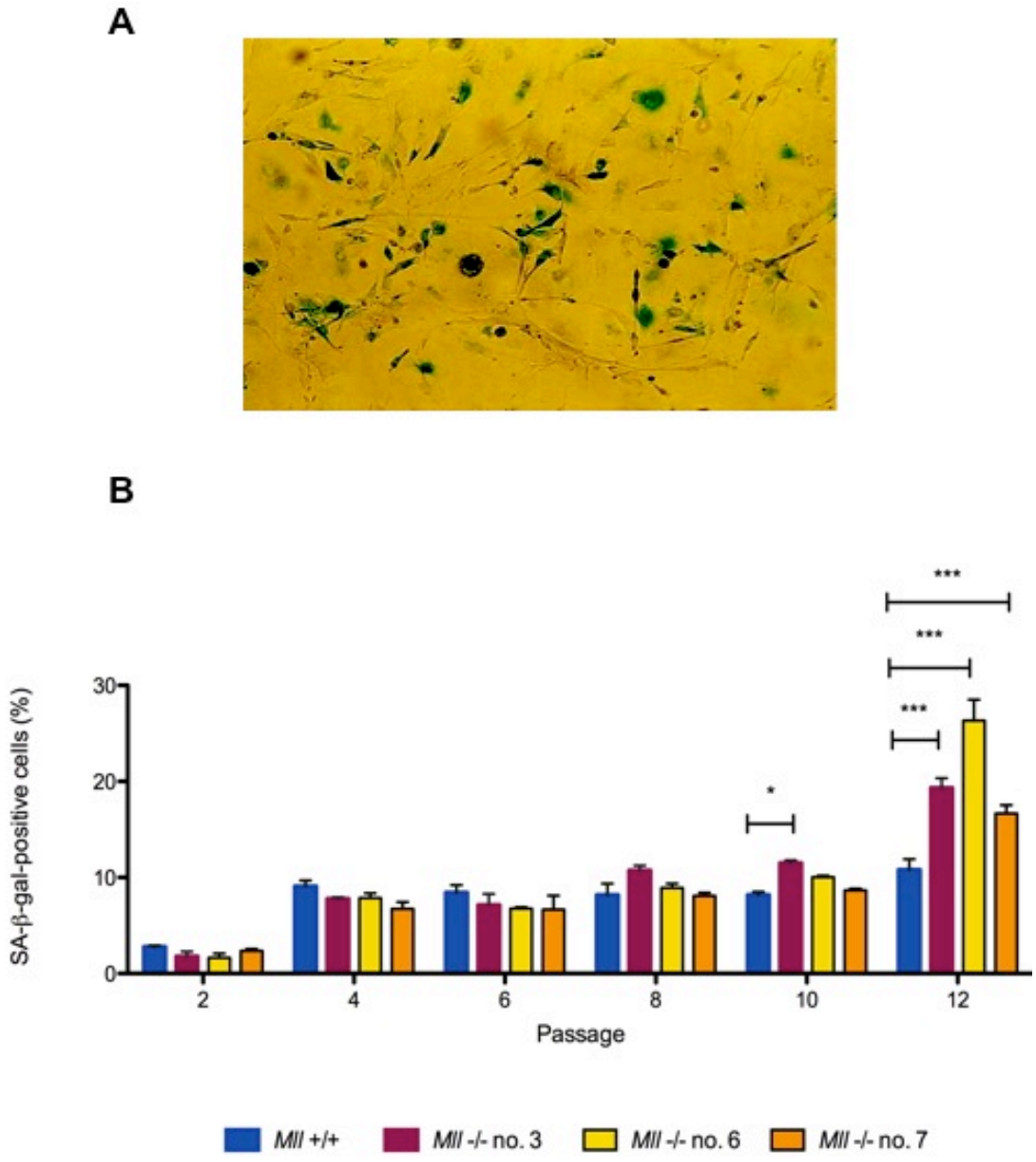

Figure 11: Assessment of cellular senescence in MEFs population using SA-*β*-gal staining. Cultures of *Mll*$^{+/+}$ and *Mll*$^{-/-}$ MEFs were scored at passage 2, 4, 6, 8, 10 and 12 for SA-*β*-gal activity (indicating senescence).

(A) MEFs that were stained an intense blue colour with SA-*β*-gal (pH 6.0).

(B) SA-*β*-gal-positive *Mll*$^{-/-}$ and *Mll*$^{+/+}$ MEFs from passage 2 to12. Experiments repeated in triplicate, statistical analysis was carried out using a 2-way ANOVA with a Bonferroni post test, * $p<0.05$ and *** $p<0.001$.

3.7 Quantitation of MEFs that undergo spontaneous DNA damage in culture

From the assays above, it appears that the major cause of proliferation defect in *Mll*$^{-/-}$ MEFs may be cell cycle arrest. As mentioned above, the pattern of this arrest is reminiscent of DNA damage-induced arrest. Hence we went on to investigate whether cells lacking Mll acquire more damage to their DNA than wild type cells during culture. The site of DNA breakages is often marked by phosphorylated H2AX (γ-H2AX) and the number of γ-H2AX foci increases linearly with the severity of the damage (Fernandez-Capetillo *et al*., 2004). Therefore, we quantitated the γ-H2AX foci in MEF cells by immunofluorescence microscopy (refer to Figure 12A for example of cells that were stained with antibody that marks γ-H2AX, a DNA dye DAPI, and a merged profile indicating the formation of γ-H2AX in the nucleus). To assess the rate of DNA damage that occur spontaneously in culture, we counted γ-H2AX foci that appeared in cells at passage 2, 4, 6, 8, 10,12, and 14. The percentages of cells with damaged DNA i.e. cells that contained more than four foci per cell (> 4fpc), were calculated in each field and the average was obtained from ten independent fields.

At passage 2, *Mll*$^{-/-}$ MEFs contained approximately 20% more damaged cells than in wild type MEFs and the proportion of cells with > 4fpc in both *Mll*$^{+/+}$ and *Mll*$^{-/-}$ MEFs increased at passage 4 (Figure 12B). In these experiments where the magnitude of DNA damage peaked around passage 4, there were significant proportion of cells that contained more than 20 foci per cell (> 20 fpc) (data not shown). In normal wild type cells, the reduction of the (1) number of foci per cell (from more than 20 fpc to 10 to 20 fpc or less than 10 fpc) and (2) the number of cells containing > 4fpc were observed steadily from P4 to P14. Surprisingly, the *Mll*$^{-/-}$ MEFs exhibited a decrease in damaged cells from P4 to P10 but its proportion rose again at P12, whilst the wild type cells remained at a low level of damage. Consistently in every passage, *Mll*$^{-/-}$ MEFs contained more damaged cells than wild type MEFs. At passage 12 when *Mll*$^{-/-}$ MEFs exhibited the highest level of damage, one of the *Mll*$^{-/-}$ MEFs (*Mll*$^{-/-}$ #3) had 40% more damaged cells than wild type MEFs. Together, we hypothesize that the phenotypes we observed in late passage *Mll*$^{-/-}$ MEFs - which are; cell cycle arrest, increased cell death and premature senescence - could be the effect of elevated DNA damage.

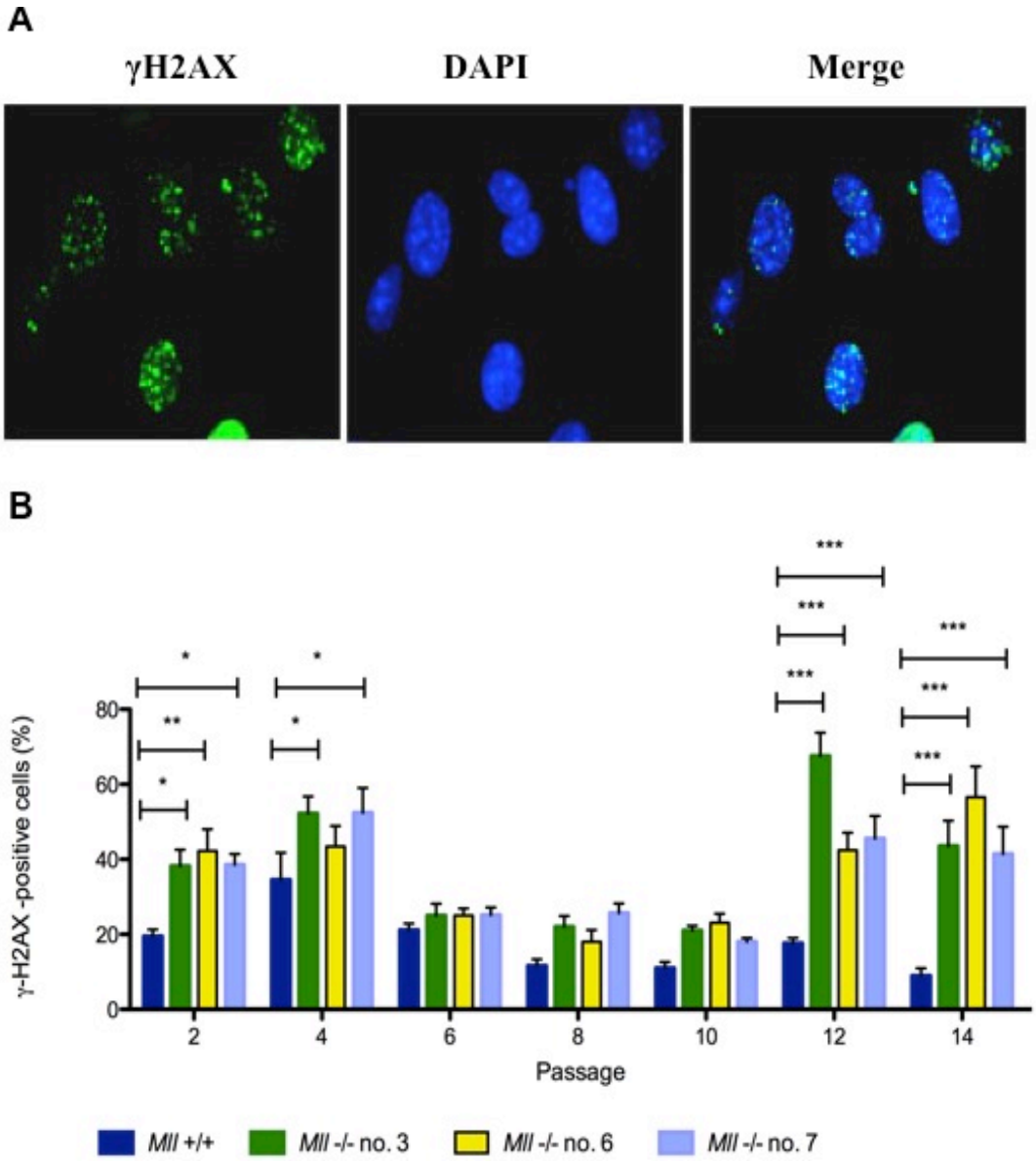

Figure 12: Frequency of γ-H2AX foci in MEFs as a marker of DNA damage.
Cultures of *Mll*$^{+/+}$ and *Mll*$^{-/-}$ MEFs were stained at passage 2, 4, 6, 8, 10, 12, and 14 with an antibody against histone H2AX to trace the formation of γ-H2AX foci in MEFs (indicating spontaneously damaged cells). (A) MEFs were stained with an antibody that marks γ-H2AX, a DNA dye DAPI, and a merge profile indicating the formation of γ-H2AX in the nucleus. (B) Quantitation of data obtained from culturing one *Mll*$^{+/+}$ MEFs and three independent *Mll*$^{-/-}$ MEFs from passage 2 to passage 14. Statistical analysis was carried out using a 2-way ANOVA with a Bonferroni post test, * $p<0.05$, ** $p<0.01$ and *** $p<0.001$.

3.8 Measurement of oxidative DNA damage in MEFs during culture

When primary MEFs are repeatedly passaged *in vitro* under standard laboratory conditions of approximately 20% oxygen, excessive amount of oxidative DNA damage occurs, and this is thought to be the driving force behind premature senescence (Parinello *et al*., 2003). Such accumulation of damaged DNA is largely attributed to the elevation of reactive oxygen species (ROS) molecules. As we passaged the MEFs in standard culture conditions, we observed increased senescence and decreased viability in late passage $Mll^{-/-}$ MEFs. This prompted us to examine whether the ROS level might be altered in these cells. To evaluate basal levels of ROS in $Mll^{-/-}$ MEFs, we measured the hydrogen peroxide (H_2O_2) concentrations of one set of $Mll^{+/+}$ and $Mll^{-/-}$ MEFs at passage 2. Using 5 μM DCFDA (2',7'-dichlorofluorescein diacetate), a cell permeable peroxide-sensitive probe that will only fluoresce upon oxidation in the cytoplasm, the ROS level was found to be marginally higher in $Mll^{-/-}$ MEFs compared to wild type MEFs. Exogenous H_2O_2 was introduced into cells as a positive control and an increase in ROS levels from the basal levels in $Mll^{+/+}$ and $Mll^{-/-}$ MEFs was observed (Figure 13A).

We repeated the experiment and this time compared the ROS levels in $Mll^{+/+}$ and $Mll^{-/-}$ MEFs at passage 2 and passage 8. Again, at passage 2 only a minor increase in basal ROS levels was observed in $Mll^{-/-}$ MEFs (Figure 13B). Interestingly, at passage 8 a significant increase of ROS level was seen in $Mll^{-/-}$ MEFs. Hence, ROS is increased in $Mll^{-/-}$ MEFs, as they grow older (in function of cell division). Our findings suggest that the increase in ROS levels may increase DNA damage in $Mll^{-/-}$ cells, which in turn may lead to cell cycle arrest, cell death and senescence; all of which can reduce the proliferative potential of the $Mll^{-/-}$ MEFs population.

A

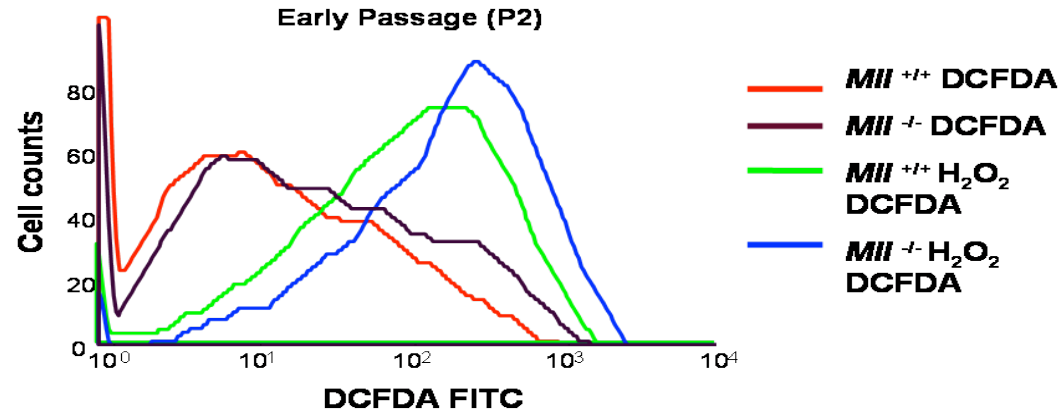

B

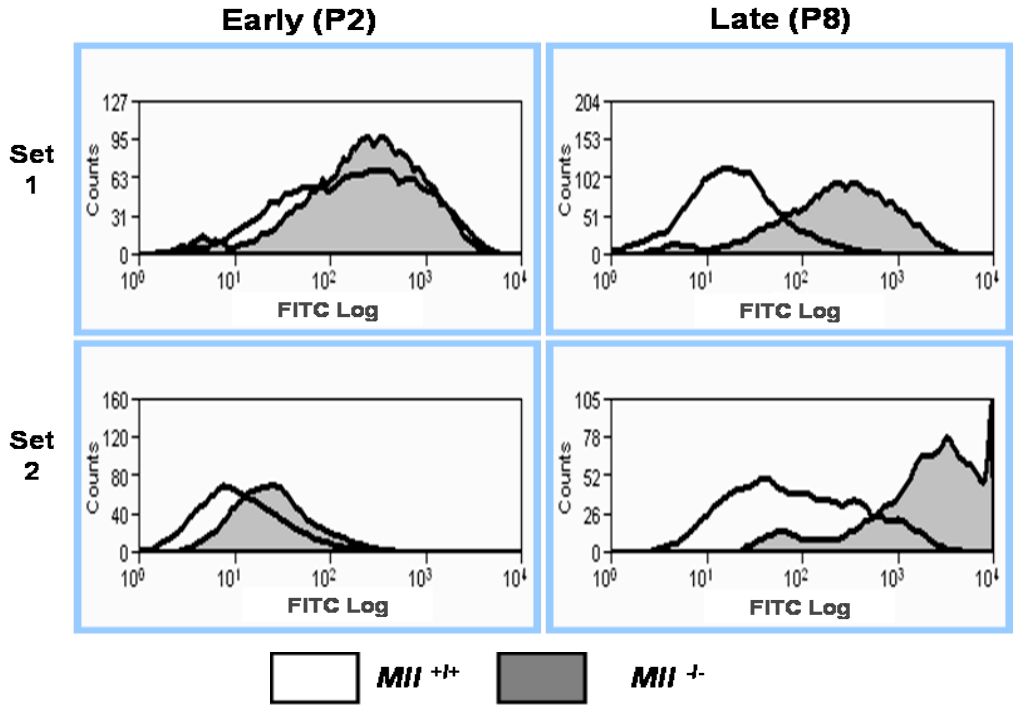

Figure 13: ROS generation in passage 2 and passage 8 *Mll*$^{+/+}$ and *Mll*$^{-/-}$ MEFs under atmospheric (20%) oxygen.

ROS production was estimated by oxidation of the fluorescent probe, DCFDA-FITC.

(A) Passage 2 *Mll*$^{-/-}$ MEFs produced marginally higher ROS after treatment with DCFDA. Prior treatment with H_2O_2 increased ROS levels further in *Mll*$^{+/+}$ and *Mll*$^{-/-}$ MEFs.

(B) ROS production in *Mll*$^{-/-}$ MEFs increased significantly from passage 2 to passage 8 cells and exceeds the ROS levels of wild type MEFs in both Set 1 and Set 2.

3.9 DNA microarray analysis of genes differentially expressed in *Mll*$^{-/-}$ MEFs

We have determined that the high ROS levels increased DNA damage in *Mll*$^{-/-}$ MEFs as they grow older which may result in cell cycle arrest and ultimately cellular senescence or cell death, if DNA was too severely damaged to be repaired. As an aid to elucidating how this may come about, we sought to identify genes whose expressions are altered in the absence of the Mll protein. Toward this aim, we performed DNA micro-array analyses of RNA expressed in *Mll*$^{-/-}$ and *Mll*$^{+/+}$ MEFs.

Total RNA was extracted from three independent pairs of MEF that were in passage 0 (P0), converted to cRNA and subjected to microarray on the Affymetrix GeneChip® Mouse Genome 430 2.0 Array (an oligonucleotide array). The gene expression analysis was carried out using GeneSpring GX 7.3.1 software. The raw data were filtered on the basis of including genes whose expression were significantly changes when the p value was < 0.05. Subsequently, the data were further filtered on a change of 3.0 fold and p value (< 0.01). A volcano plot was drawn for *Mll*$^{-/-}$ MEFs that were normalized to *Mll*$^{+/+}$ MEFs. Statistical analysis was done with Welch "t" test on the three pairs of MEF cells. We narrowed down a total of 270 genes to be differentially regulated in *Mll*$^{-/-}$ MEF cells (Appendix). From this list, expression from a total of twelve different *Hox* genes were found to be diminished (Table 2A). *Hox* genes are well-characterised targets of *Mll*. Some of these genes were further classified based on interest on their biological functions. Some of the genes that were found to be regulators of cell cycle and play an important role in signalling pathway in response to stress are depicted in Table 2B. The genes that could be potential target genes of *Mll* were analysed using DAVID bioinformatics resources and classified into their functional annotations and respective biochemical pathways. Amongst these genes, the *Ataxia Telangiectasia Mutated homolog (human) ATM* gene was selected for further characterisation.

A

Gene	Fold change (decrease)
Hoxa7	19.9
Hoxc5	10.94
Hoxc8	8.098
Hoxb6	5.487
Hoxc10	4.149
Hoxc9	3.822
Hoxc5	3.268
Hoxc6	2.669
Hoxb9	2.595
Hoxb3	2.398
Hoxd13	1.773
Hoxd9	1.588

B

Gene title	Gene	Fold change (decrease)
ataxia telangiectasia mutated homolog (human)	ATM	2.343
signal transducer and activator of transcription 5A	Stat5a	2.242
c-fos induced growth factor	Figf	2.024
growth arrest specific 2	Gas2	1.85
fyn-related kinase	Frk	1.654
feline sarcoma oncogene	Fes	1.845

Table 2: The list of genes that showed at least one-fold reduction in the absence of Mll compared to wild type MEFs.

(A) Expression of *Hox* genes in *Mll*$^{-/-}$ MEFs from three independent set of DNA microarray experiments.

(B) Some of the genes that were involved in regulating cell cycle progression and response to stress were differentially regulated in *Mll*$^{-/-}$ MEFs.

3.10 Investigating the role of *ATM* in *Mll*-deficient fibroblasts

The characteristics displayed by MEFs lacking *Mll* such as delayed onset of senescence, decreased viability in late passage cells, cell cycle alteration and accumulation of DNA damage owing to ROS may also indicate deficiencies in the cellular DNA damage machinery. One of the potential targets of *Mll* that were deregulated in $Mll^{-/-}$ MEFs from our affymetrix gene chip array analysis was the main sensor kinase in the DNA damage signaling pathway, *ATM*.

We performed a real time quantitative-PCR analysis of ATM whereby total RNA was isolated from three independent sets of passage 1 and 8 $Mll^{+/+}$ and $Mll^{-/-}$ MEFs. The relative mRNA expression levels of *ATM* were measured by quantitative-PCR analysis. In passage 1 MEFs, we found that the *ATM* expression levels were comparable between $Mll^{+/+}$ and $Mll^{-/-}$ MEFs (Figure 14). However, passage 8 $Mll^{-/-}$ MEFs exhibited a minor decrease in ATM expression in comparison to wild type MEFs of the same passage (Figure 15). We also performed western blotting of ATM on these passages of MEFs. ATM is activated by autophosphorylation at a single, conserved serine residue (Ser 1981 in humans; Ser 1987 in mouse) in response to double-stranded breaks and other forms of damage to DNA (Bakkenist and Kastan, 2003). To assess the levels of phosphorylated ATM protein in $Mll^{-/-}$ MEFs, we induced DNA double-stranded breaks in these cells by treatment with etoposide (ETOP). Etoposide is a topoisomerase II inhibitor that prevents ligation of cleaved DNA molecules. Etoposide treatment would result in accumulation of single- or double-strand DNA breaks, the inhibition of DNA replication and transcription, and apoptotic cell death. Surprisingly, the expression of ATM was unchanged in $Mll^{-/-}$ MEFs compared to $Mll^{+/+}$ MEFs, whether in early or late passage cells (Figure 16). We speculate that this was due to the small decrease in the ATM RNA levels (2.343) in $Mll^{-/-}$ MEFs that may not be significant enough to affect expression of the ATM protein. We also checked the levels of ATM-ser 1987-P because previous literatures have highlighted the importance of phosphorylation of ATM for its functional activation.

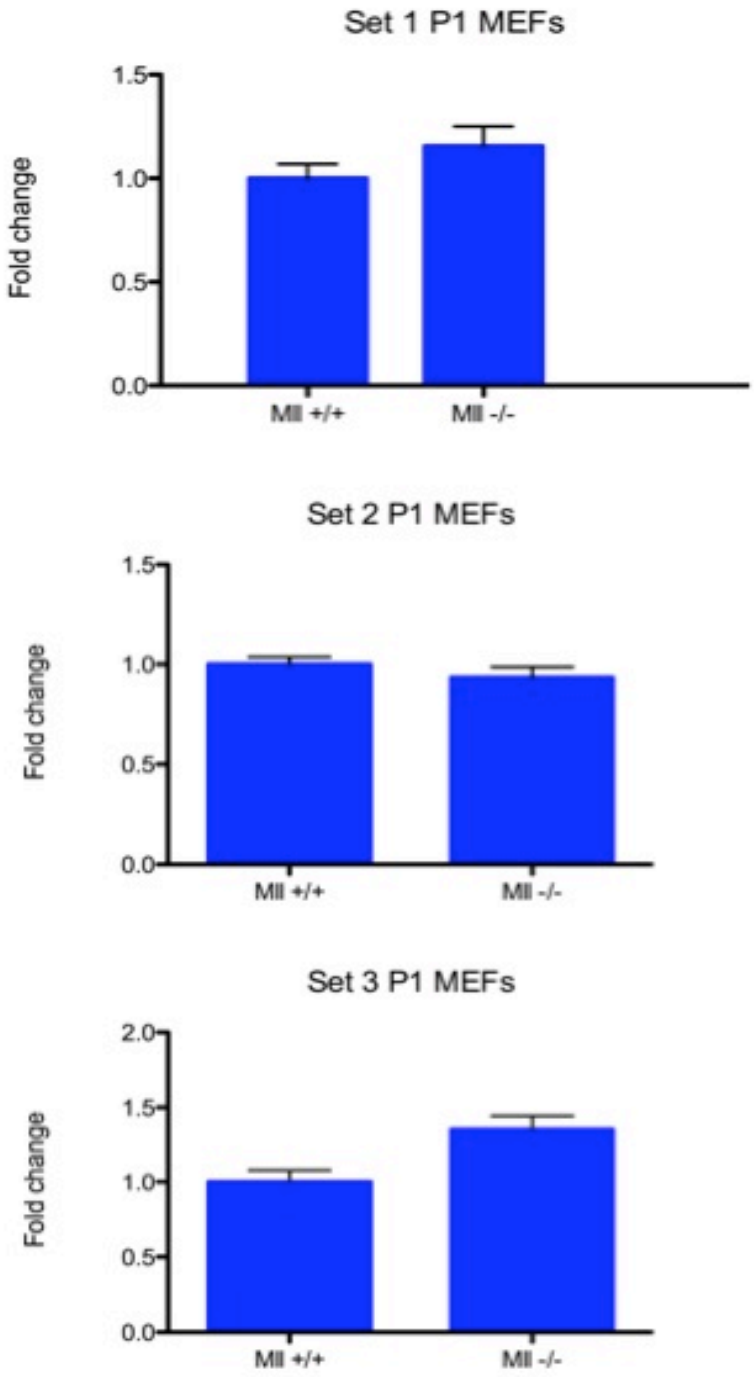

Figure 14: Comparable ATM expression in three independent passage 1 *Mll*$^{+/+}$ and *Mll*$^{-/-}$ MEFs.

The relative mRNA expression levels of ATM in *Mll*$^{+/+}$ and *Mll*$^{-/-}$ MEFs were evaluated by quantitative-PCR and normalized to GAPDH expression. Data shown are the mean ± SD of transcript levels over GAPDH.

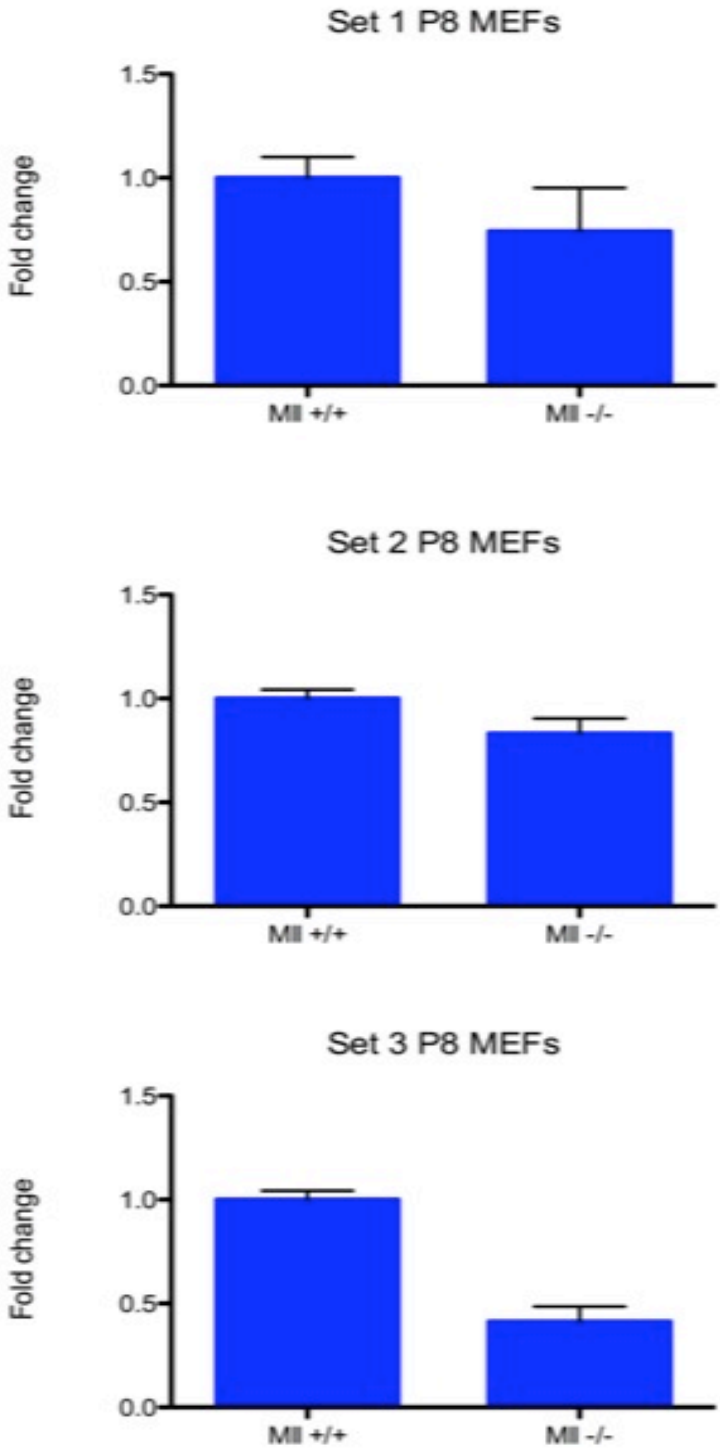

Figure 15: Decreased *ATM* expression in three independent passage 8 *Mll*$^{+/+}$ and *Mll*$^{-/-}$ MEFs. The relative mRNA expression levels of ATM in *Mll*$^{+/+}$ and *Mll*$^{-/-}$ MEFs were evaluated by quantitative-PCR and normalized to *GAPDH* expression. Results shown are the mean ± SD of transcript levels over *GAPDH*.

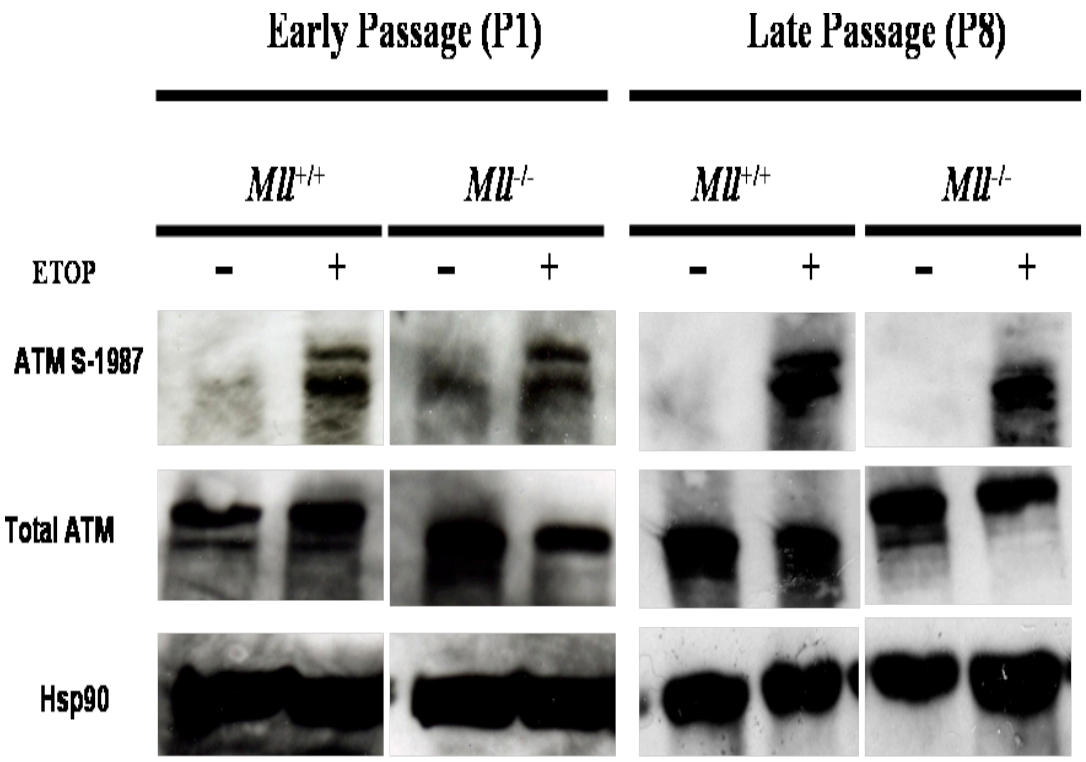

Figure 16: Western blot analysis of ATM-ser 1987-P and total ATM expression in RIPA cell lysates prepared from passage 1 and passage 8 MEFs.

Western blots for ATM-ser 1987-P expression in RIPA cell lysates. Comparable protein levels of ATM-ser 1987-P between early (P1) and late (P8) passage *Mll*$^{+/+}$ and *Mll*$^{-/-}$ MEFs upon treatment with 20 μM etoposide for 6 hours (ETOP). As expected, no phosphorylation was seen in MEFs that were not subjected to any treatment (untreated). The total ATM was unchanged in all these cells, regardless of the presence of treatment and there was no difference in ATM protein levels between early and late passage *Mll*$^{+/+}$ and *Mll*$^{-/-}$ MEFs. An Hsp90 Western blot is shown as loading control.

3.11 Examining the phosphorylation level of p53 on Serine 15 residue

The western blot for ATM showed that ATM is not altered in *Mll*-deficient fibroblasts, indicating that the signalling network for sensing damaged DNA is intact. We next sought to investigate whether one of the effector of DNA damage response pathway, p53, is active. We decided to check the levels of phosphorylated p53 at the serine 15 residue (p53-Ser15-P), which is activated downstream of the ATM signaling pathway. We performed western blotting on MEF cells that were retrieved from passage 1 and passage 8. The induction of double-stranded DNA break was by etoposide in the culture for 6 hours before preparing lysates from these cells.

In *Mll* WT cells, p53 (ser15) phosphorylation increased 6 hours following treatment with etoposide in passage 1 and it was similarly seen in passage 8 cells (Figure 17). While p53 (ser15) phosphorylation and abundance also increased in passage 1 $Mll^{-/-}$ MEFs when etoposide was added to cells, it was not maintained in passage 8 cells. Late passage $Mll^{-/-}$ MEFs exhibited the inability to phosphorylate p53 on Ser 15 residue without etoposide treatment, where the contributing stress factor is the high levels of ROS in passage 8 $Mll^{-/-}$ MEFs (Figure 13B). However, when passage 8 $Mll^{-/-}$ MEFs were treated with etoposide the phosphorylation level of p53 (ser 15) was nearly similar to that seen in wild type cells without any treatment (Figure 17). This observation led us to extrapolate that the lack of p53 (ser15) phosphorylation may compromise the DNA damage signalling pathway. The lack of effector activity that will activate the DNA repair circuit in cells may lead to an abnormal accumulation of DNA damage in $Mll^{-/-}$ MEFs.

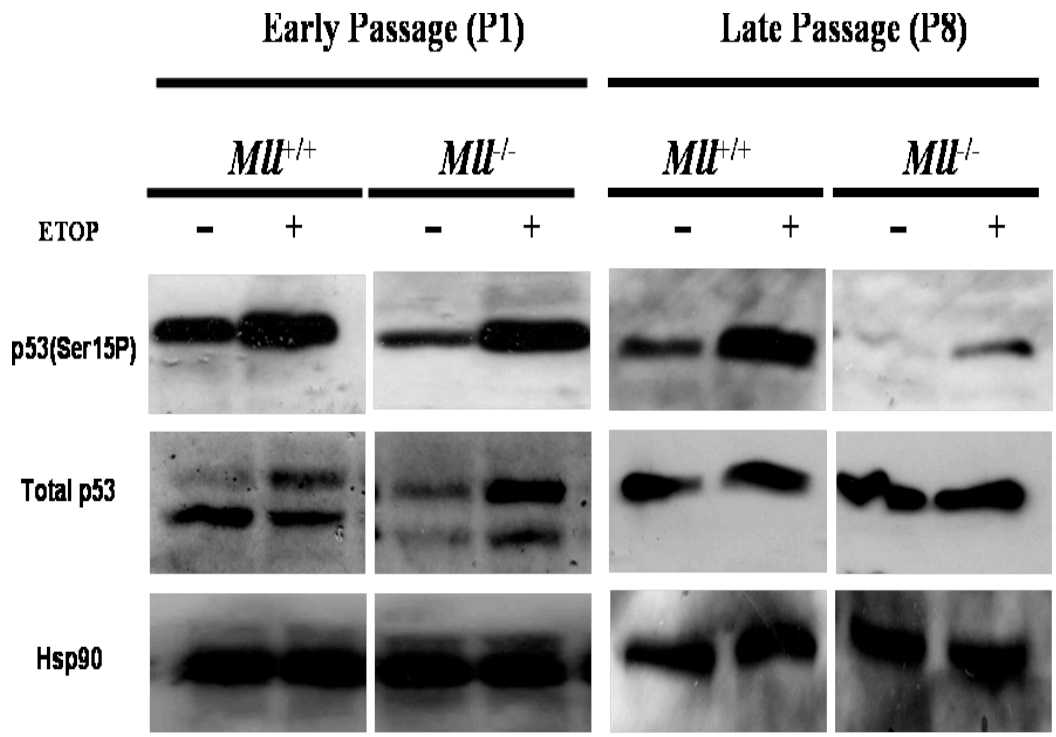

Figure 17: Western blot analysis for p53-Ser 15-P and total p53 expressions in RIPA cell lysates prepared from early and late passage MEFs.
Comparable protein levels of p53-ser 15-P between early (P1) and late (P8) passage *Mll*$^{+/+}$ and *Mll*$^{-/-}$ MEFs upon treatment with 20 μM etoposide for 6 hours (ETOP). There was a small level of phosphorylation of p53 in MEFs that were not subjected to any treatment (untreated). Early passage *Mll*$^{+/+}$ and *Mll*$^{-/-}$ MEFs showed no difference in the p53-ser15-P before and after etoposide treatment (ETOP). In the P8 *Mll*$^{-/-}$ MEFs that were not treated with etoposide, an insufficient level of p53-ser 15-P in comparison to wild type MEFs was observed. The total p53 was unchanged in all these cells, regardless of the presence of treatment. An Hsp90 Western blot is shown as loading control.

Chapter 4: Discussion and Conclusion

The *Mll* knockout (*Mll*$^{-/-}$) mice that were generated in the laboratory died in utero at developmental day 12.5 to 16.5. This is largely consistent with attempts by other groups to produce such mutant mice. This notwithstanding, the generation of these mice are still of immense value as the embryos are sufficiently mature to allow for the extraction of fibroblasts, and their subsequent culture in vitro. The deletion of exons 9 and 10 of the *Mll*$^{-/-}$ loci would in theory result in the production of a shortened Mll protein that lacked the first PHD zinc finger domain. However western blots of the Mll-/- embryos unexpectedly failed to reveal MLL protein of any size. It is possible that the removal of the PHD domain (which resides within the excised exons) lead to the failure of MLL proteins to homodimerise; an act that is important for MLL stability (Fair *et al*., 2000; Bienz, 2006). As such, these mice could be considered virtual MLL knockout mice and the cells from them provide us with the resource to study the consequence of MLL absence on various aspects of cell biology including the cell cycle. In recent years, initial characterisations of *Mll*$^{-/-}$ mice have revealed that *Mll* may have a role in proliferation in addition to differentiation. For example, *Mll*$^{-/-}$ fetal liver or yolk sac haematopoietic cells grow more slowly and form smaller colonies in methyl cellulose assays (Hess *et al*., 1997; McMahon *et al*., 2007).

In our study, we were interested in knowing whether *Mll* is involved in regulating the cell cycle. We derived wild type and *Mll*$^{-/-}$ MEFs from E13.5 embryos and studied their replicative capacity and proliferation rate. *Mll*$^{-/-}$ MEFs exhibited a diminished replicative capacity, indicating a reduced potential of *Mll*$^{-/-}$ cells to divide until they senesce *in vitro*. We also observed a significant reduction in proliferation rate of *Mll*$^{-/-}$ MEFs, overtime in comparison to the wild type cells during their growth in culture. A recent report has shown that MEFs derived from *Taspase1* knockout mice that lack functional Mll protein and also exhibited reduced proliferation rate (Takeda *et al.*, 2006). These observations are consistent with reports that show MLL to couple with HCF-1 to target E2F to E2F-responsive promoters (e.g. cyclins) to activate transcription of genes whose

protein products are necessary for G1/S transition and cell cycle progression (Takeda *et al*., 2006; Tyagi *et al.*, 2006). We hypothesised that the lack of *Mll* predisposes a cell to execute cell cycle block, undergo premature senescence or apoptosis, all of which can account for the decreased replicative capacity and slower rate of cell proliferation observed *in vitro*.

We sought to test these possibilities by first performing a cell proliferation assay [5-bromo-2-deoxyuridine (BrdU) and 7-amino-actinomycin (7-AAD) staining] of early (P1) and late (P8) passages of wild type and *Mll*$^{-/-}$ MEFs. The cell cycle status of passage 1 wild type and *Mll*$^{-/-}$ MEFs were comparable, with similar proportions of cells in G1, S and G2, M phases of the cell cycle. However, in passage 8 *Mll*$^{-/-}$ MEF cells, a vast reduction of cells in S phase was observed. These cells were being restrained from traversing the G1/S and G2/M checkpoints. The G1/S checkpoint ensures that the DNA to be replicated is not damaged whilst the G2/M checkpoint then verifies that DNA replication has been completed correctly and that damaged DNA is not segregated (Skorski, 2002). This cell cycle perturbation observed in *Mll*$^{-/-}$ cells could be explained by the recent work of James Hsieh's group in which it was revealed that MLL is expressed in a biphasic pattern throughout the cell cycle, wherein the expression of MLL was decreased in S and late M phases following respective peaks at G1/S and G2/M transitions (Liu *et al.*, 2007). The bimodal expression of MLL throughout the cell cycle may be a reflection of points within the cell cycle at which MLL functions (Liu *et al.*, 2007). Therefore, in the absence of *Mll*, the temporal regulation of gene expression by *Mll* would be disrupted, resulting in perturbation of the cell cycle. Furthermore, the cell cycle arrest in late passage *Mll*$^{-/-}$ cells is reminiscent of a pattern of cell cycle block often seen in the event of DNA damage.

When we plated wild type and *Mll*$^{-/-}$ MEFs, the latter grew normally from P1 to P4, after which they progressively grew more sparsely compared to the growth of wild type MEFs. This prompted us to enumerate dead cells in culture from passage 5, 6, 7, and 8 using the LDH leakage assay. Wild type and *Mll*$^{-/-}$ MEF cells that were harvested from passage 5 onwards showed marginal increase in LDH. Annexin V staining was also performed on these MEFs to further examine

the levels of cell death in passage 8; the time point at which the proliferation defect was clearly evident in *Mll*$^{-/-}$ MEF. The marginal increase in annexin V-positive P8 *Mll*$^{-/-}$ MEF cells suggested that although more cell death was observed in *Mll*$^{-/-}$ MEFs, this could not be the major factor that causes the pronounced proliferation defect.

In our assay to measure replicative capacity, we observed that *Mll*$^{-/-}$ MEFs began to exhibit a decreased efficiency to re-plate from passage 5, which could indicate the occurrence of premature senescence. This prompted us to measure the rate of cellular senescence from passage 2 to passage 12. The *Mll*$^{-/-}$ MEFs did not exhibit an increase in senescence-associated-*β*-gal-positive cells in early passage (P2, P4), intermediate passage (P6), up to late passage (P8 and P10). Although the proportion of SA-*β*-gal-positive cells were similar between *Mll*$^{-/-}$ and wild type MEFs up to passage 10, it was surprising to see that at passage 12, there was a sudden increase in SA-*β*-gal-positive cells in *Mll*$^{-/-}$ MEFs. It is plausible that *Mll*$^{-/-}$ cells may not undergo senescence up until a time point where they have accumulated severe DNA damage, when the extent of the damage is too great to be repaired (Campisi and d'Adda di Fagagna, 2007).

The onset for cellular proliferation defects occurred from the intermediate passage (from passage 5), whilst senescent cells only appeared in the later passages (from passage 12). As the rate of senescence between passage 5 and 10 in these cells was similar to those in the wild type MEFs, we speculated that senescence could not have contributed to the cellular proliferation deficiencies in *Mll*$^{-/-}$ MEFs. Instead, the cell cycle arrest as a consequence of accumulation of DNA damage may be the major contributing factor. To examine the rate of spontaneous DNA damage, we decided to employ the method for detection of a sensitive and selective signal for the existence of a DNA double-stranded breaks (DSBs) i.e. the formation of phosphorylated H2AX (gamma H2AX or γ-H2AX) nuclear foci (Fernandez-Capetillo *et al*., 2004). Phosphorylated histone H2AX (gamma-H2AX) forms foci over large chromatin domains surrounding double-stranded DNA breaks (DSB) (Chowdhury *et al*., 2005). It has been demonstrated that each γ-H2AX focus is equivalent to one DSB (Rogakou *et al.,* 1999), and disappearance of γ-H2AX is a reliable indicator of double-stranded break repair

(DSBR) in mammalian cells (Rothkamm and Löbrich, 2003; Chowdhury *et al*., 2005). A role for H2AX phosphorylation has been demonstrated in DNA repair, cell cycle checkpoints, regulated gene recombination events, and tumour suppression (Fernandez-Capetillo *et al*., 2004). When the cells were first plated at passage 2, the number of cells with γ-H2AX foci formation was higher in *Mll*$^{-/-}$ MEFs, indicating that *Mll*$^{-/-}$ MEFs may have a higher level of DNA damage. We speculated that P2 and P4 *Mll*$^{-/-}$ MEFs have more damage owing to culture stress inflicted by the need for these cells to adapt to the culture conditions whilst trying to kick start cell division to progress into the cell cycle. At P6 to P10, the wild type and *Mll*$^{-/-}$ MEF cells seemed to have adjusted to culture selection and there is no evidence of increasing levels of damage. However, a slightly higher percentage of *Mll*$^{-/-}$ MEFs exhibited γ-H2AX over control wild type MEFs. Upon further analyses, we observed that the number of foci per *Mll*$^{-/-}$ MEF was greater than per wild type MEFs. Furthermore, the number of γ-H2AX foci per cell in *Mll*$^{-/-}$ MEFs was higher than those found in the wild type. This observation indicates that *Mll*$^{-/-}$ MEFs may have much more than wild-type control. Interestingly at passage 12 and 14, *Mll*$^{-/-}$ MEFs seem to have strikingly elevated levels of DNA damage in comparison to wild type cells. As there is no evidence of a steady increase of H2AX positive *Mll*$^{-/-}$ cells from passage 6 to 10, the sudden increase in DNA damage in passage 10-12 cannot be due to a gradual build up of DNA damage accrued during the previous passages. Such a clear demarcation of DNA damage increase at these very late passages may be owed instead to the exposure of chromosome telomeres of the *Mll*$^{-/-}$ cells. Telomeres, which shorten upon each cell division, when exposed or are un-capped (when they are critically short) will appear as damaged DNA to the cell, which will duly initiate an arrest of the cell cycle. The ongoing work conducted by Dr. Yali Dou (University of Michigan Medical School) to examine this reveals that *Mll* regulates the telomere transcript levels (personal communication). Telomeres were long thought to be transcriptionally-silent non-coding DNAs at the ends of chromosomes. However, it has now been reported that the telomere repeats TTAGGG are transcribed by DNA-dependent RNA polymerase II, giving rise to telomeric RNAs (TelRNAs) that contain UUAGGG repeats containing telomere transcripts (Schoeftner and Blasco, 2008). Telomere length and TelRNA levels showed a positive correlation, cells having long telomeres display higher levels

of TelRNA trancripts than cells with short telomeres. It is also possible that *Mll* may be involved in capping telomeres. The DNA damage response resulting from telomere attrition consists of the execution of DNA repair and inadvertently creating end-to-end fusion of unprotected chromosomes (Maser and DePinho, 2004; Viscardi *et al*., 2005; Deng and Chang, 2007; Longhese, 2008). The existence of multiple critically short telomeres generates the potential for chromosomal instability (Cheung and Deng, 2008).

We sought to explore the factors that contribute to the DNA-damage-associated characteristics observed in the cells lacking *Mll*. In general, the main cause of lifespan-limitation in murine fibroblasts cultured in vitro is thought to be excess level of oxygen (Parinello *et al.*, 2003). Mouse embryonic fibroblasts senesce after fewer population doublings than human fibroblasts when cultured *in vitro* under similar conditions, which is at an unusually high concentration of oxygen (20%). This concentration is distinctly higher than the concentration of oxygen in the physiological setting *in vivo*. It is clear that senescence of MEFs under this culture condition is due to their sensitivity to the high levels of oxidative damage in 20% oxygen (Busuttil *et al.*, 2004). This culture condition was also used for the fibroblasts in our study, which could cause cells to accumulate reactive oxygen species (ROS) as a consequence of cellular metabolism. We hypothesized that the DNA damage-associated phenotype might be attributed to oxidative stress; therefore we were interested in examining the levels of ROS in these MEFs. Our study showed that the early passage $Mll^{-/-}$ MEFs displayed a higher level of ROS when compared to $Mll^{+/+}$ MEFs. Interestingly, the late passage $Mll^{-/-}$ MEFs displayed a markedly higher level of ROS when compared to the wild type cells. It is plausible that the primary fibroblasts lacking *Mll* accumulated a lethal-dosage of ROS that resulted in oxidative damage. The *Mll*-deficient MEFs may be incapable of scavenging free-radicals and when combined with an inability to repair this damage correctly led to an increase in cell death. The occurrence and accumulation of DNA damage is largely determined by the levels of ROS produced and how efficiently the antioxidant defence systems remove ROS and DNA repair mechanisms operate (Barzilai and Yamamoto, 2004; Chen *et al*., 2007). The increase of ROS may correlate with an increase of DNA damage with age, and may therefore be due to an imbalance

between ROS generation and clearance, and decline of DNA repair mechanisms (Hornsby, 2003; Busuttil *et al*., 2004).

From DNA microarray analyses, it appeared that the virtual absence of Mll protein in MEFs changed the expression of some genes compared to the wild type cells (Appendix). Notably, expressions of several genes of the Mitogen-Activated Protein Kinase (MAPK) signalling pathway (*e.g., Efna1, PpM1L, and Smad1*) were decreased. The MAPK pathways play important regulatory roles for a variety of downstream molecules such as transcription and translation factors, cell cycle molecules, kinases, or scaffold proteins, and thus exert an influence on a variety of cellular activities, including cell proliferation, cycle arrest, migration, differentiation, senescence, and apoptosis (Dhillon *et al.*, 2007). The involvement of Ataxia-Telangiectasia Mutated (*ATM*), whereby its gene expression level was decreased in *Mll*-deficient cells, was considered as we assessed the level of *ATM* transcription and protein in $Mll^{-/-}$ MEFs. *ATM* transcripts were marginally decreased in $Mll^{-/-}$ MEFs but the changes were insignificant. Similarly, the ATM protein and its active phosphorylated form (upon induction of DNA damage by etoposide) was present in early and late passage $Mll^{-/-}$ MEFs at a comparable level to those of the wild type cells. These results reveal that, the lack of *Mll* does not affect ATM at the level of either transcript or protein and thus ATM cannot be responsible for the accumulation of DNA damage in $Mll^{-/-}$ MEFs.

The lines of evidence compiled from this study suggest that *Mll*-deficient cells accumulate more DNA damage owing to excessive ROS production. The accumulation of DNA damage in these cells resulted in activation of DNA damage checkpoint and of particular importance in this checkpoint activation is p53 phosphorylation on serine 15. Depending on the severity of damage to the genome, p53 can activate pathways that halt cell proliferation transiently (G_1 and G_2 cell cycle arrest), permanently (senescence), or eliminate the cell altogether (apoptosis) (Rosso *et al.*, 2006). Stabilised p53 regulates many cellular pathways that are components of the DNA damage response (Harper and Elledge, 2007), DNA repair (Garner and Raj, 2008), cell cycle arrest (Fei and El-Deiry, 2003), and cell survival in response to oxidative stress (Chumakov, 2007). Western

blotting of p53 and p53-Ser 15-P showed that the level of p53-Ser 15-P is decreased in late passage *Mll*$^{-/-}$ MEFs, which suggests that Mll acts on p53 phosphorylation of serine 15 in a pathway independent of ATM. It is possible that Mll might regulate a kinase or phosphatase that acts on p53 to decrease the levels of p53-Ser 15-P. Recently, p53 was found to be phosphorylated on its serine 15 residue by a non-ATM kinase, which is a phosphatidylinositol 3-kinase-like kinase (PIKK) family member known as human suppressor of morphogenesis in genitalia-1 (hSMG-1) or autotoxin (ATX) (Gehen *et al.*, 2008). Therefore, it is plausible that *Mll* acts on a pathway (either upstream or downstream) of hSMG-1 to phosphorylate p53, thus affecting the level of phosphorylated p53 protein. hSMG-1 was shown to be a mediator of checkpoint signalling in response to chronic oxidative DNA damage caused by the elevated levels of ROS (Gehen *et al.*, 2008)

In *Mll*-deficient cells, when p53 phosphorylation was intact (in the early passages of the cells), the cells did not exhibit any abnormality in respect to cellular senescence, cell death, or altered cell cycle distribution, compared to the wild-type control MEFs. However, the lack of p53 phosphorylation in late passage *Mll*$^{-/-}$ MEFs was associated with increased levels of the above-mentioned features. Hence it is possible that failure to repair DNA efficiently (as indicated indirectly by the reduced ability of p53 to be activated) led to cell cycle arrest, senescence and cell death, all which could contribute to the acquisition of genomic instability.

Conclusion and Future Work

In this study, we have established that the *Mll*-deficient MEFs derived from E13.5 embryos display abnormalities in later passage (after passage 5) of growth. Early passage $Mll^{-/-}$ MEFs appeared phenotypically normal. Late passage $Mll^{-/-}$ MEFs displayed:

1) Cell proliferation defect that is observed as cells were passaged *in vitro*.
2) Cell cycle alteration in late passage when cells were blocked at the G1/S and G2/M transitions of the cell cycle.
3) Marginal increase in dead and senescent cells compared to wild type MEFs.
4) Accumulation of damaged DNA that was markedly higher at much later passage (10-12).
5) Vast ROS production that could lead to increase oxidative DNA damage in cells.
6) Decreased phosphorylation of p53 on serine 15 upon induction of DNA damage.

In conclusion, the high levels of DNA damage induced by ROS production could lead to activation of the G1 and G2 arrest in the cell cycle machinery. The inefficient phosphorylation of p53 on serine 15 could lead to the inability of p53 to elicit repair of damaged DNA, hence leading to cell death and senescence, and the acquisition of genomic instability. Although this study was performed in mouse embryonic fibroblasts, it has provided us with the basis for molecular mechanisms that occur in the absence of Mll. Further study should be carried out in haematopoietic cells to assess the consequences of *Mll*-deficiency on the DNA damage response of these cells, which would provide us with more accurate understanding on genomic instability and leukaemia.

Previous work done by McMahon et al. (2007) has shown that *Mll* knockout mice lack severe self-renewal capacity. Therefore, it would be interesting to examine if this defect is due to an inability in mediating a response to replicative stress. On this note, future work could be carried out to:

1) Characterise the DNA damage response defect in fetal liver stem cells by analysis of the genes (ATM, ATR, or p53) that are involved in mounting a DNA damage response in the absence of Mll.

2) Compare the ability of WT and *Mll*$^{-/-}$ MEFs fetal liver cells to respond to replicative stress-induced by hydroxyurea, by subjecting them to analysis of cell death and cell cycle content thereafter.

3) Analyse the effects of induction of DNA replicative stress (using mitomycin C) on chromosomal breaks or other cytogenetics defect.

4) Further analyses (Point 1 to 3) on the effects of *Mll*-deficiency on adult haematopoiesis in heterozygotes or *Mll* conditional knockout mice. This is to determine if the possible defect in response to replicative stress is a dominant-negative effect.

Appendix

The gene list from DNA microarray analysis showing genes that were differentially regulated in *Mll*$^{-/-}$ MEFs. Only genes with a *P* value of 0.05 or less were included in the list. For each gene, the fold change (FC), probe set I.D., and gene title are shown.

FC	Probe Set ID	Gene Title	Gene Symbol
19.9	1449499_at	homeo box A7	Hoxa7
17.54	1456033_at	T-box 4	Tbx4
13.74	1455224_at	angiopoietin-like 1	Angptl1
10.95	1418317_at	LIM homeobox protein 2	Lhx2
10.94	1450832_at	homeo box C5	Hoxc5
10.24	1416236_a_at	epithelial V-like antigen 1	Eva1
9.995	1455946_x_at	thymosin, beta 10	Tmsb10
8.834	1426155_a_at	odd-skipped related 2 (Drosophila)	Osr2
8.487	1453044_at	RIKEN cDNA C030014I23 gene	C030014I23Rik
8.388	1448265_x_at	epithelial V-like antigen 1	Eva1
8.098	1452412_at	homeo box C8	Hoxc8
7.602	1424098_at	ELOVL family member 7, elongation of long cha	Elovl7
7.25	1458453_at	LIM domain only 7	Lmo7
7.237	1424067_at	intercellular adhesion molecule	Icam1
6.549	1450906_at	plexin C1	Plxnc1
6.147	1436086_at	RIKEN cDNA 4921526F01 gene	4921526F01Rik
5.998	1446557_at	RIKEN cDNA E130309F12 gene	E130309F12Rik
5.809	1459790_x_at	aristaless 3	Alx3
5.713	1434601_at	adhesion molecule with Ig like domain 2	Amigo2
5.655	1456903_at	pentraxin related gene	Ptx3
5.637	1455416_at	hypothetical protein C130021I20	C130021I20
5.487	1451660_a_at	homeo box B6	Hoxb6
5.355	1423874_at	WD repeat domain 33	Wdr33
5.308	1426766_at	RIKEN cDNA 6330403K07 gene	6330403K07Rik
5.287	1450533_a_at	pleiomorphic adenoma gene-like 1	Plagl1
5.165	1449488_at	paired-like homeodomain transcription factor 1	Pitx1
5.126	1457642_at	RIKEN cDNA 5730507N06 gene	5730507N06Rik
4.996	1460187_at	secreted frizzled-related sequence protein 1	Sfrp1
4.965	1415832_at	angiotensin II receptor, type 2	Agtr2
4.766	1429448_s_at	CXXC finger 6	Cxxc6
4.541	1438350_at	G protein-coupled receptor 64	Gpr64
4.533	1422941_at	wingless-related MMTV integration site 16	Wnt16
4.526	1457429_s_at	gene model 106, (NCBI)	Gm106
4.489	1450272_at	tumor necrosis factor (ligand) superfamily, memb	Tnfsf8
4.452	1441729_at	Transcribed locus	---
4.338	1460382_at	cDNA sequence BC020535	BC020535
4.268	1441607_at	expressed sequence AU015603	AU015603
4.164	1421882_a_at	ELAV (embryonic lethal, abnormal vision, Droso	Elavl2
4.149	1439798_at	homeo box C10	Hoxc10
4.096	1433919_at	ankyrin repeat and SOCS box-containing protein	Asb4
4.074	1437276_at	Transcribed locus	---
3.92	1443002_at	zinc finger RNA binding protein	Zfr
3.822	1449867_at	homeo box C9	Hoxc9
3.785	1457275_at	desmuslin	Dmn
3.719	1427369_at	NACHT, leucine rich repeat and PYD containing	Nalp6
3.627	1450990_at	glypican 3	Gpc3
3.501	1437600_at	Atpase, class VI, type 11C	Atp11c
3.311	1453285_at	transmembrane protein 88	Tmem88
3.268	1439885_at	homeo box C5	Hoxc5
3.068	1417127_at	homeo box, msh-like 1	Msx1

FC	Probe Set ID	Gene Title	Gene Symbol
2.859	1448601_s_at	homeo box, msh-like 1	Msx1
2.845	1435987_x_at	RIKEN cDNA 1110059G02 gene	1110059G02Rik
2.762	1453913_a_at	transporter 2, ATP-binding cassette, sub-family B	Tap2
2.669	1427362_x_at	homeo box C6	Hoxc6
2.639	1422868_s_at	guanine deaminase	Gda
2.595	1452317_at	Homeo box B9	Hoxb9
2.505	1457367_at	Amylase 2, pancreatic	Amy2
2.433	1446812_at	Heart and neural crest derivatives expressed tra	Hand2
2.426	1424367_a_at	homer homolog 2 (Drosophila)	Homer2
2.426	1448301_s_at	serine (or cysteine) peptidase inhibitor, clade B,	Serpinb1a
2.398	1427605_at	homeo box B3	Hoxb3
2.388	1419527_at	cartilage oligomeric matrix protein	Comp
2.343	1421205_at	ataxia telangiectasia mutated homolog (human)	Atm
2.325	1441408_at	expressed sequence AU044856	AU044856
2.318	1421365_at	follistatin	Fst
2.315	1452426_x_at	Zinc finger protein 236 /// CDNA clone IMAGE:40	Zfp236
2.308	1444760_at	nuclear receptor co-repressor 1	Ncor1
2.3	1436467_at	RIKEN cDNA D230004N17 gene	D230004N17Rik
2.296	1421028_a_at	myocyte enhancer factor 2C	Mef2c
2.242	1450259_a_at	signal transducer and activator of transcription 5	Stat5a
2.23	1417282_at	matrix metallopeptidase 23	Mmp23
2.218	1435385_at	teashirt zinc finger family member 2	Tshz2
2.197	1438083_at	Hedgehog-interacting protein	Hhip
2.167	1443108_at	15 days embryo head cDNA, RIKEN full-length e	---
2.161	1430978_at	ribosomal protein S25	Rps25
2.158	1426970_a_at	ubiquitin-activating enzyme E1-like /// RIKEN cD	Ube1l /// D330022A01Rik
2.149	1440355_at	potassium channel tetramerisation domain conta	Kctd12b
2.109	1429197_s_at	RAB GTPase activating protein 1-like	Rabgap1l
2.103	1450036_at	serum/glucocorticoid regulated kinase 3	Sgk3
2.099	1460062_at	pleckstrin homology domain containing, family H	Plekhh2
2.095	1435676_at	centrosomal protein 164	Cep164
2.074	1430762_at	RIKEN cDNA 4833427G06 gene	4833427G06Rik
2.043	1416895_at	ephrin A1	Efna1
2.043	1431362_a_at	SPARC related modular calcium binding 2	Smoc2
2.031	1422479_at	acyl-CoA synthetase short-chain family member	Acss2
2.024	1449528_at	c-fos induced growth factor	Figf
2.022	1438884_at	RIKEN cDNA D830007B15 gene	D830007B15Rik
1.999	1439552_at	triple functional domain (PTPRF interacting)	Trio
1.993	1418186_at	glutathione S-transferase, theta 1	Gstt1
1.98	1427982_s_at	synaptic nuclear envelope 2	Syne2
1.949	1431530_a_at	tetraspanin 5	Tspan5
1.945	1425336_x_at	histocompatibility 2, K1, K region	H2-K1
1.94	1454783_at	interleukin 13 receptor, alpha 1	Il13ra1
1.93	1435499_at	RIKEN cDNA D030041N04 gene	D030041N04Rik
1.9	1458515_at	zinc finger protein 128	Zfp128
1.885	1431512_at	RIKEN cDNA 4933437F24 gene	4933437F24Rik
1.883	1423493_a_at	nuclear factor I/X	Nfix
1.878	1442331_at	Aminolevulinic acid synthase 1	Alas1
1.87	1434380_at	RIKEN cDNA 9830147J24 gene	9830147J24Rik
1.863	1447505_at	RIKEN cDNA 1700020G03 gene	1700020G03Rik
1.862	1435787_at	protein phosphatase 1 (formerly 2C)-like	Ppm1l

FC	Probe Set ID	Gene Title	Gene Symbol
1.855	1433615_at	transmembrane protein 117	Tmem117
1.85	1450112_a_at	growth arrest specific 2	Gas2
1.845	1452410_a_at	feline sarcoma oncogene	Fes
1.822	1417179_at	tetraspanin 5	Tspan5
1.81	1434980_at	phosphoinositide-3-kinase, regulatory subunit 5,	Pik3r5
1.8	1442402_at	SH3 domain containing ring finger 1	Sh3rf1
1.798	1460666_a_at	early B-cell factor 3	Ebf3
1.786	1418618_at	engrailed 1	En1
1.773	1422239_at	homeo box D13	Hoxd13
1.768	1426267_at	zinc finger and BTB domain containing 8 opposit	Zbtb8os
1.745	1429159_at	RIKEN cDNA 4631408O11 gene	4631408O11Rik
1.733	1417312_at	dickkopf homolog 3 (Xenopus laevis)	Dkk3
1.732	1422784_at	keratin complex 2, basic, gene 6a	Krt2-6a
1.73	1450231_a_at	baculoviral IAP repeat-containing 4	Birc4
1.727	1418535_at	ral guanine nucleotide dissociation stimulator,-lik	Rgl1
1.72	1439129_at	RIKEN cDNA 1110060D06 gene /// dedicator of	1110060D06Rik /// Dock5
1.696	1448676_at	calcium/calmodulin-dependent protein kinase II,	Camk2b
1.69	1418517_at	Iroquois related homeobox 3 (Drosophila)	Irx3
1.684	1439788_at	cDNA sequence BC065112	BC065112
1.681	1458213_at	Nuclear factor of activated T-cells 5	Nfat5
1.676	1456687_at	Retinitis pigmentosa 9 homolog (human)	Rp9h
1.669	1424148_a_at	expressed sequence AW049765	AW049765
1.664	1434697_at	RIKEN cDNA 1110001P04 gene	1110001P04Rik
1.657	1429988_at	zinc finger protein 235	Zfp235
1.654	1426570_a_at	fyn-related kinase	Frk
1.654	1458117_at	GTPase activating RANGAP domain-like 1	Garnl1
1.645	1436364_x_at	nuclear factor I/X	Nfix
1.644	1418755_at	T-box 15	Tbx15
1.638	1437261_at	RIKEN cDNA 2900024O10 gene	2900024O10Rik
1.624	1434025_at	Transcribed locus	---
1.599	1455462_at	adenylate cyclase 2	Adcy2
1.596	1432268_at	RIKEN cDNA 2310068J16 gene	2310068J16Rik
1.594	1441162_at	Rho-associated coiled-coil forming kinase 1	Rock1
1.588	1419126_at	homeo box D9	Hoxd9
1.585	1445461_at	Transcribed locus	---
1.579	1456401_at	calcium channel, voltage-dependent, beta 2 sub	Cacnb2
1.572	1451784_x_at	histocompatibility 2, D region locus 1 /// histocom	H2-D1 /// H2-L /// LOC547343
1.566	1438012_at	protein phosphatase 1 (formerly 2C)-like	Ppm1l
1.559	1436244_a_at	transducin-like enhancer of split 2, homolog of D	Tle2
1.534	1425416_s_at	proline/serine-rich coiled-coil 1	Psrc1
1.533	1422465_a_at	nucleoredoxin	Nxn
1.532	1428695_at	RIKEN cDNA 2310014G06 gene	2310014G06Rik
1.531	1425362_at	HIV-1 Rev binding protein-like	Hrbl
1.529	1432011_at	RIKEN cDNA 2900052L18 gene	2900052L18Rik
1.511	1418057_at	T-cell lymphoma invasion and metastasis 1	Tiam1
1.51	1433672_at	RIKEN cDNA 4732479N06 gene	4732479N06Rik
1.505	1451544_at	TAP binding protein-like	Tapbpl
1.5	1449314_at	zinc finger protein, multitype 2	Zfpm2
1.499	1423428_at	receptor tyrosine kinase-like orphan receptor 2	Ror2
1.495	1450687_at	insulin-like growth factor 2 mRNA binding protein	Igf2bp3

FC	Probe Set ID	Gene Title	Gene Symbol
1.49	1451430_at	slit homolog 2 (Drosophila)	Slit2
1.489	1451021_a_at	Kruppel-like factor 5	Klf5
1.485	1456388_at	ATPase, class VI, type 11A	Atp11a
1.483	1424693_at	RIKEN cDNA 4933407N01 gene	4933407N01Rik
1.483	1429683_at	RIKEN cDNA 5830472M02 gene	5830472M02Rik
1.481	1436363_a_at	nuclear factor I/X	Nfix
1.474	1416081_at	MAD homolog 1 (Drosophila)	Smad1
1.47	1442285_at	synaptic nuclear envelope 2	Syne2
1.458	1427178_at	transmembrane channel-like gene family 4	Tmc4
1.455	1417043_at	lecithin cholesterol acyltransferase	Lcat
1.453	1455073_at	cytidine and dCMP deaminase domain containin	Cdadc1
1.452	1456859_at	limb and neural patterns	Lnp
1.439	1429886_at	zinc finger protein 294	Zfp294
1.439	1449047_at	phytanoyl-CoA 2-hydroxylase 2	Phyh2
1.437	1428289_at	Kruppel-like factor 9	Klf9
1.431	1443160_at	SET binding factor 2	Sbf2
1.431	1453368_at	RIKEN cDNA 2310003H01 gene	2310003H01Rik
1.429	1438328_at	host cell factor C2	Hcfc2
1.423	1417211_a_at	RIKEN cDNA 1110032A03 gene	1110032A03Rik
1.416	1444089_at	spectrin beta 2	Spnb2
1.414	1434193_at	zinc finger, MYM-type 6	Zmym6
1.412	1449014_at	lactamase, beta	Lactb
1.404	1436104_a_at	RIKEN cDNA 2310015A05 gene	2310015A05Rik
0.701	1432269_a_at	SH3-domain kinase binding protein 1	Sh3kbp1
0.698	1425175_at	C1q-like 3	C1ql3
0.689	1446558_at	RIKEN cDNA F730015K02 gene	F730015K02Rik
0.688	1425055_at	SAPS domain family, member 2	Saps2
0.68	1418980_a_at	cyclic nucleotide phosphodiesterase 1	Cnp1
0.68	1453629_at	RIKEN cDNA 4930478L05 gene	4930478L05Rik
0.676	1456287_at	expressed sequence BB236558	BB236558
0.675	1425511_at	MAP/microtubule affinity-regulating kinase 1	Mark1
0.669	1416674_at	protein tyrosine phosphatase, receptor type, U	Ptpru
0.656	1450166_at	iduronate 2-sulfatase	Ids
0.652	1424231_s_at	exocyst complex component 6	Exoc6
0.649	1430662_at	RIKEN cDNA 9430091E24 gene	9430091E24Rik
0.645	1423693_at	elastase 1, pancreatic	Ela1
0.643	1428417_at	RIKEN cDNA 3110050N22 gene	3110050N22Rik
0.639	1437965_at	HEAT repeat containing 1	Heatr1
0.639	1453478_at	POU domain, class 3, transcription factor 2	Pou3f2
0.635	1423946_at	PDZ and LIM domain 2	Pdlim2
0.632	1418318_at	ring finger protein 128	Rnf128
0.63	1457430_at	Sparc/osteonectin, cwcv and kazal-like domains	Spock2
0.623	1452523_a_at	RIKEN cDNA 4930527D15 gene	4930527D15Rik
0.617	1458426_at	Kinesin family member 1B	Kif1b
0.614	1454572_at	RIKEN cDNA 2810414N06 gene	2810414N06Rik
0.611	1429696_at	G protein-coupled receptor 123	Gpr123
0.597	1429946_at	RIKEN cDNA 2610301F02 gene	2610301F02Rik
0.589	1455137_at	Rap guanine nucleotide exchange factor (GEF) 5	Rapgef5
0.587	1450702_at	hemochromatosis	Hfe
0.587	1451924_a_at	endothelin 1	Edn1
0.584	1435994_at	potassium voltage-gated channel, subfamily H (e	Kcnh1

FC	Probe Set ID	Gene Title	Gene Symbol
0.583	1436930_x_at	hydroxymethylbilane synthase /// similar to hydr	Hmbs /// LOC623818
0.581	1418498_at	fibroblast growth factor 13	Fgf13
0.577	1456380_x_at	calponin 3, acidic	Cnn3
0.576	1439760_x_at	uroplakin 1B	Upk1b
0.574	1450065_at	adenylate cyclase 7	Adcy7
0.574	1455116_at	tumor necrosis factor receptor superfamily, mem	Tnfrsf19l /// LOC671976
0.568	1440933_at	RIKEN cDNA 4732460I02 gene	4732460I02Rik
0.566	1458474_at	DNA segment, Chr 10, Brigham & Women's Ger	D10Bwg1364e
0.56	1442492_at	DNA segment, Chr X, ERATO Doi 11, expressed	DXErtd11e
0.555	1435282_at	gene model 967, (NCBI)	Gm967
0.547	1431671_at	RIKEN cDNA 4930447A16 gene	4930447A16Rik
0.547	1433465_a_at	expressed sequence AI467606	AI467606
0.542	1422800_at	HLA-B associated transcript 2	Bat2
0.535	1431234_at	RIKEN cDNA 1700041B20 gene	1700041B20Rik
0.53	1451813_at	opioid receptor, kappa 1	Oprk1
0.526	1453466_at	ribosomal protein S6	Rps6
0.517	1456893_at	Adult male liver tumor cDNA, RIKEN full-length e	---
0.516	1457219_at	rho/rac guanine nucleotide exchange factor (GE	Arhgef18
0.508	1448289_at	collapsin response mediator protein 1	Crmp1
0.503	1446241_at	Adult male thymus cDNA, RIKEN full-length enri	---
0.502	1460104_at	vacuolar protein sorting 4b (yeast)	Vps4b
0.496	1439892_at	BR serine/threonine kinase 1	Brsk1
0.491	1419708_at	wingless-related MMTV integration site 6	Wnt6
0.485	1419425_at	cannabinoid receptor 1 (brain)	Cnr1
0.48	1457232_at	F-box and leucine-rich repeat protein 21	Fbxl21
0.471	1452369_at	membrane associated guanylate kinase, WW an	Magi1
0.467	1454833_at	ribosomal protein L35	Rpl35
0.459	1445259_at	sodium channel, voltage-gated, type II, alpha 1	Scn2a1
0.449	1419613_at	procollagen, type VII, alpha 1	Col7a1
0.446	1435191_at	corneodesmosin	Cdsn
0.445	1452650_at	tripartite motif-containing 62	Trim62
0.435	1440899_at	flavin containing monooxygenase 5	Fmo5
0.421	1431554_a_at	annexin A9	Anxa9
0.414	1441059_at	RIKEN cDNA 1700049G17 gene	1700049G17Rik
0.409	1446037_at	RIKEN cDNA C230081A13 gene	C230081A13Rik
0.406	1431611_a_at	immunoglobulin superfamily, member 4A	Igsf4a
0.402	1455771_at	benzodiazapine receptor associated protein 1	Bzrap1
0.395	1437727_at	Odd Oz/ten-m homolog 3 (Drosophila)	Odz3
0.391	1442621_at	expressed sequence C77798	C77798
0.385	1443657_at	RIKEN cDNA 6330505N24 gene	6330505N24Rik
0.377	1445346_at	Ankyrin 2, brain	Ank2
0.371	1457526_at	growth factor receptor bound protein 14	Grb14
0.369	1447605_at	Zinc finger protein 457	Zfp457
0.362	1441784_at	Adult male hypothalamus cDNA, RIKEN full-leng	---
0.325	1439018_at	RIKEN cDNA 6330505N24 gene	6330505N24Rik
0.316	1458624_at	similar to RNA binding motif protein 24 /// similar	LOC380843 /// LOC666794
0.313	1435895_at	RIKEN cDNA D930023J12 gene	D930023J12Rik
0.306	1448891_at	macrophage scavenger receptor 2	Msr2
0.302	1457098_at	DNA segment, Chr 2, ERATO Doi 624, expresse	D2Ertd624e
0.262	1449133_at	small proline-rich protein 1A	Sprr1a
0.249	1421921_at	serine (or cysteine) peptidase inhibitor, clade A,	Serpina3m

FC	Probe Set ID	Gene Title	Gene Symbol
0.198	1422048_at	transient receptor potential cation channel, subfa	Trpc5
0.186	1420344_x_at	granzyme D	Gzmd
0.152	1455449_at	gene model 468, (NCBI)	Gm468
0.117	1431805_a_at	rhophilin, Rho GTPase binding protein 2	Rhpn2
0.0826	1441502_at	Leucine rich repeat and fibronectin type III doma	Lrfn5

References

Aasland, R., Gibson, T.J., Stewart, A.F. (1995). The PHD finger: implications for chromatin-mediated transcriptional regulation. Trends Biochem Sci. *20(2)*, 56-59.

Aplan, P.D. (2006). Chromosomal translocations involving the *MLL* gene: Molecular mechanisms. DNA repair. *5(9-10)*, 1265-1272.

Ayton, P., Sneddon, S.F., Palmer, D.B., Rosewell, I.R., Owen, M.J., Young, B., Presley, R., Subramanian, V. (2001). Truncation of the Mll gene in exon 5 by gene targeting leads to early preimplantation lethality of homozygous embryos. Genesis. 30(4):201-12.

Bakkenist, C.J., Kastan, M.B. (2003). DNA damage activates ATM through intermolecular autophosphorylation and dimer dissociation. Nature. *421(6922)*, 499-506.

Bakkenist, C.J., Kastan, M.B. (2004). Phosphatases join kinases in DNA-damage response pathways. Trends Cell Biol. *14(7)*, 339-41.

Bartkova, J., Rezaei, N., Liontos, M., Karakaidos, P., Kletsas, D., Issaeva, N., Vassiliou, L.V., Kolettas, E., Niforou, K., Zoumpourlis, V.C., Takaoka, M., Nakagawa, H., Tort, F., Fugger, K., Johansson, F., Sehested, M., Andersen, C.L., Dyrskjot, L., Orntoft, T., Lukas, J., Kittas, C., Helleday, T., Halazonetis, T.D., Bartek, J., Gorgoulis, V.G. (2006). Oncogene-induced senescence is part of the tumorigenesis barrier imposed by DNA damage checkpoints. Nature. *444(7119)*, 633-7.

Barzilai, A., Rotman, G., Shiloh, Y. (2002). ATM deficiency and oxidative stress: a new dimension of defective response to DNA damage. DNA Repair. *1(1)*, 3-25.

Barzilai, A., Yamamoto, K. (2004). DNA damage responses to oxidative stress. DNA repair. *3*, 1109-1115.

Bernard, O.A., Mauchauffe, M., Mecucci, C., Van den Berghe, H., Berger, R. (1994). A novel gene, AF-1p, fused to HRX in t (1; 11)(p32;q23), is not related to AF-4, AF-9 nor ENL. Oncogene. *9(4)*,1039-45.

Bienz M. (2006). The PHD finger, a nuclear protein-interaction domain. Trends Biochem Sci. *31(1)*, 35-40.

Busuttil, R.A., Dollé, M., Campisi, J., Vijga, J. (2004). Genomic instability, aging, and cellular senescence. Ann N Y Acad Sci. *1019*, 245-55.

Cann, K.L., Hicks, G.G. (2007). Regulation of the cellular DNA double-strand break response. Biochemistry and Cell Biology. *85(6)*, 663-674.

Campisi, J., d'Adda di Fagagna, F. (2007). Cellular senescence: when bad things happen to good cells. Nature Reviews Molecular Cell Biology. *8*, 729-740.

Capotosti, F., Hsieh, J.J.D., Herr, W. 2007. Species Selectivity of Mixed-Lineage Leukemia/ Trithorax and HCF Proteolytic Maturation Pathways. Mol. Cell. Biol. *27*, 7063-7072.

Chen, J.H., Hales, C.N., Ozanne, S.E. (2007). DNA damage, cellular senescence and organismal ageing: causal or correlative? Nucleic Acids Res. *35(22)*, 7417-28.

Cheung, A.L., Deng, W. (2008). Telomere dysfunction, genome instability and cancer. Front Biosci. *13*, 2075-90.

Chowdhury, D., Keogh, M.C., Ishii, H., Peterson, C.L., Buratowski, S., Lieberman, J. (2005). Gamma-H2AX dephosphorylation by protein phosphatase 2A facilitates DNA double-strand break. Mol Cell. *20*, 801-9.

Chumakov, P.M. (2007). Versatile function s of p53 protein in multicellular organism. Biochemistry (Moscow). *72(13)*, 1399-1421.
Collins, E.C., Rabbitts, T.H. (2002). The promiscuous MLL gene links chromosomal translocations to cellular differentiation and tumour tropism. Trends Mol Med. *8(9)*:436-42.

Collis, S.J., Schwaninger, J.M., Ntambi, A.J., Keller, T.W., Nelson, W.G., Dillehay, L.E., DeWeese, T.L. (2004). Evasion of Early Cellular Response Mechanisms following Low Level Radiation-induced DNA Damage. Biol. Chem. *279(48)*, 49624-49632.

Cumano, A., Godin, I. (2007). Ontogeny of the Hematopoietic system. Annual Review of Immunology. *25*, 745-785.

Das, S., Boswell, S.A., Aaronson, S.A., Lee, S.W. (2008). P53 promoter selection: choosing between life and death. Cell Cycle. *7(2)*, 154-7.

Daser, A., Rabbitts, T.H. (2004). Extending the repertoire of the mixed-lineage leukemia gene *MLL* in leukemogenesis. Genes & Development. *18*,965-974.

de Boer, J., Williams, A., Skavdis, G., Harker, N., Coles, M., Tolaini, M., Norton, T., Williams, K., Roderick, K., Potocnik, A.J., Kioussis, D. (2003). Transgenic mice with hematopoietic and lymphoid specific expression of Cre. Eur J Immunol. *33(2)*, 314-25.

Delaval, B., Birnbaum, D. (2007). A cell cycle hypothesis of cooperative oncogenesis (Review). Int J Oncol. *30(5)*, 1051-8.

Deng, Y., Chang, S. (2007). Role of telomeres and telomerase in genomic instability, senescence and cancer. Lab Invest. *87(11)*, 1071-6.

Dhillon, A.S., Hagan, S., Rath, O., Kolch, W. (2007). MAP kinase signalling pathways in cancer. Oncogene. *26(22)*, 3279-90.

Di Micco, R., Fumagalli, M., Cicalese, A., Piccinin, S., Gasparini, P., Luise, C., Schurra, C., Garre, M., Nuciforo, P.G., Bensimon, A., Maestro, R., Peliccim P.G., d'Adda di Fagagna, F. (2006). Nature *444*, 638–642.

Dimri, G.P., Lee, X., Basile, G., Acosta, M., Scott, G., Roskelley, C., Medrano, E.E., Linskens, M., Rubelj, I., Pereira-Smith, O., *et al.* (1995). A biomarker that identifies senescent human cells in culture and in aging skin in vivo. Proc. Natl. Acad. Sci. U. S. A. *92(20)*, 9363-7.

Dimri, G.P. (2005). What has senescence got to do with cancer? Cancer Cell. *7(6)*, 505-12.

Dobson, C.L., Warren, A.J., Pannell, R., Forster, A., Rabbitts, T.H. (2000). Tumorigenesis in mice with a fusion of the leukaemia oncogene *Mll* and the bacterial *lacZ* gene. The EMBO Journal. 19**,** 843–851.

Dou, Y., Milne, T.A., Ruthenburg, A.J., Lee, S., Lee, J.L., Verdine, G.L. (2006). Regulation of MLL1 H3K4 methyltransferase activity by its core components. Nat Struct Mol Biol. *13(8)*,713-9.

Ernst, P., Fisher, J.K., Avery, W., Wade, S., Foy, D., Korsmeyer, S.J. (2004a). Definitive hematopoiesis requires the mixed-lineage leukemia gene. Dev Cell. *6(3)*, 437-43.

Ernst, P., Mabon, M., Davidson, A.J., Zon, L.I., Korsmeyer, S.J. (2004b). An *Mll*-dependent Hox program drives hematopoietic progenitor expansion. Curr Biol. *14(22)*, 2063-9.

Fair, K., Anderson, M., Bulanova, E., Mi, H., Tropschug, M., Diaz, M.O. (2001). Protein interactions of the MLL PHD fingers modulate MLL target gene regulation in human cells. Mol Cell Biol. *21(10)*, 3589-97.

Fei, P., El-Deiry, W.S. (2003). P53 and radiation responses. Oncogene. *22(37)*, 5774-83.

Fernandez-Capetillo, O., Lee, A., Nussenzweig, M., Nussenzweig, A. (2004). H2AX: the histone guardian of the genome. DNA Repair. *3(8-9)*, 959-67.

Garner, E., Raj, K. (2008). Protective mechanisms of p53-p21-pRb proteins against DNA damage-induced cell death. Cell Cycle. *7(3)*, 277-82.

Gehen, S.C., Staversky, R.J., Bambara, R.A., Keng, P.C., O'Reilly, M.A. (2008). hSMG-1 and ATM sequentially and independently regulate the G1 checkpoint during oxidative stress. Oncogene. [Epub ahead of print].

Guenther, M.G., Jenner, R.G., Chevalier, B., Nakamura, T., Croce, C.M., Canaani, E., Young, R.A. (2005). Global and Hox-specific roles for the MLL1 methyltransferase. Proc. Natl. Acad. Sci. U. S. A. *102(24)*, 8603-8.

Harper, J.W., Elledge, S.J. (2007). The DNA damage response: ten years after.

Mol Cell. *28(5)*, 739-45.

Hemann, M.T., Narita, M. (2007). Oncogenes and senescence: breaking down in the fast lane. Genes & Dev. *21*, 1-5.

Hess, J.L., Yu, B.D., Li, B., Hanson, R., Korsmeyer, S.J. (1997). Defects in yolk sac hematopoiesis in Mll-null embryos. Blood. *90(5)*, 1799-806.

Hess, J.L. (2004). MLL: a histone methyltransferase disrupted in leukemia. Trends Mol Med. *10*, 500-7.

Hsieh, J.J, Ernst, P., Erdjument-Bromage, H., Tempst, P., Korsmeyer, S.J. (2003) Proteolytic cleavage of MLL generates a complex of N- and C-terminal fragments that confers protein stability and subnuclear localization. Mol Cell Biol. *23(1)*,186-94.

Hornsby, P.J. (2003). Mouse and human cells versus oxygen. Sci Aging Knowledge Environ. *2003(30)*, PE21.

Jude, C.D., Climer, L., Xu, D., Artinger, E., Fisher, J.K., Ernst, P. (2007). Unique and independent roles for MLL in adult hematopoietic stem cells and progenitors. Cell Stem Cell. *1(3)*,324-37.

Krivtsov, A.V., Twomey, D., Feng, Z., Stubbs, M.C., Wang, Y., Faber, J., Levine, J.E., Wang, J., Hahn, W.C., Gilliland, D.G., Golub, T.R., Armstrong, S.A. (2006).Transformation from committed progenitor to leukaemia stem cell initiated by MLL-AF9. Nature. *442(7104)*: 818-22.

Krivtsov, A.V., Armstrong, S.A. (2007). *MLL* translocations, histone modifications and leukaemia stem-cell development. Nature Reviews Cancer. *7*, 828-833.

Levine AJ. (1997). p53, the cellular gatekeeper for growth and division. Cell. *88(3)*, 323-31.

Lin, W.C., Lin, F.T., Nevins, J.R. (2001). Selective induction of E2F1 in response to DNA damage, mediated by ATM-dependent phosphorylation. Genes Dev. *15(14)*, 1833-44.

Li, Z.Y, Liu, D.P., Liang, C.C. (2005). New insight into the molecular mechanisms of *MLL*-associated leukemia. Leukaemia. *19*, 183–190.

Lightfoot, T. (2005). Aetiology of childhood leukemia. Bioelectromagnetics. *7*: 5-11.

Liu, H., Cheng, E.H., Hsieh, J.J. (2007). Bimodal degradation of MLL by SCFSkp2 and APCCdc20 assures cell cycle execution: a critical regulatory circuit lost in leukemogenic MLL fusions. Genes Dev. *21(19)*, 2385-98.

Liu, H., Takeda, S., Cheng, E.H., Hsieh, J.J. (2008). Biphasic MLL takes helm at cell cycle control: implications in human mixed lineage leukemia. Cell Cycle. *7(4)*:428-35.

Longhese, M.P. (2008). DNA damage response at functional and dysfunctional telomeres. Genes Dev. *22(2)*, 125-40.
Lou Z, Chen J. (2006). Cellular senescence and DNA repair. Exp. Cell Res. *312*, 2641–2646.

Mallette, F.A., Gaumont-Leclerc, M.F., Ferbeyre, G. (2007). The DNA damage signaling pathway is a critical mediator of oncogene-induced senescence. Genes Dev. *21*, 43–48.

Maser, R.S., DePinho, R.A. (2004). Telomeres and the DNA damage response: why the fox is guarding the henhouse. DNA Repair (Amst). *3(8-9)*, 979-88.

McMahon, K.A., Hiew, S.Y., Hadjur, S., Veiga-Fernandes, H., Menzel, U., Price, A.J., Kioussis, D., Williams, O., Brady, H.J. (2007). *Mll* has a critical role in fetal and adult hematopoietic stem cell self-renewal. Cell Stem Cell. *1(3)*, 338-45.

Megonigal, M.D., Cheung, N.K., Rappaport, E.F., Nowell, P.C., Wilson, R.B., Jones, D.H., Addya, K., Leonard, D.G., Kushner, B.H., Williams, T.M., Lange, B.J., Felix, C.A. (2000). Detection of leukemia-associated MLL-GAS7 translocation early during chemotherapy with DNA topoisomerase II inhibitors. Proc. Natl. Acad. Sci. U. S. A. *97(6)*, 2814-9.

Mikkola, H.K.A., Orkin, S.H. (2006). The journey of developing hematopoietic stem cells. Development. *133*, 3733-3744.

Milne, T.A., Hughes, C.M., Lloyd, R., Yang, Z., Rozenblatt-Rosen, O., Dou, Y., Schnepp, R.W., Krankel, C., LiVolsi, V.A., Gibbs, D., Hua, X., Roeder, R.G., Meyerson, M., Hess, J.L. (2005a). Menin and MLL cooperatively regulate expression of cyclin-dependent kinase inhibitors. Proc. Natl. Acad. Sci. U.S.A. *102(3)*, 749-754.

Milne, T.A., Martin, M.E., Brock, H.W., Slany, R.K., Hess, J.L. (2005b). Leukemogenic MLL Fusion Proteins Bind across a Broad Region of the *Hox a9* Locus, Promoting Transcription and Multiple Histone Modifications. Cancer Res. *65,* 11367-11374.

Mitterbauer-Hohendanner, G., Mannhalter, C. (2004). The biological and clinical significance of *MLL* abnormalities in haematological malignancies. European Journal of Clinical Investigation. *34*, 12-24.

Morgan, D.O. (2007). Model Organisms in Cell-Cycle Analysis. Pg. 22. The Cell cycle, Principles of control. Primers In Biology series, New Science Press Ltd. Oxford University Press.

Murray, A.W. (2004). Recycling the cell cycle: Cyclins revisited. Cell. *116*, 221-234.

Parrinello, S., Samper, E., Krtolica, A., Goldstein, J., Melov, S., Campisi, J. (2003). Oxygen sensitivity severely limits the replicative lifespan of murine fibroblasts. Nat Cell Biol. *5(8)*, 741-7.

Paull, T.T., Rogakou, E.P., Yamazaki, V., Kirchgessner, C.U., Gellert, M., Bonner, W.M. (2000). A critical role for histone H2AX in recruitment of repair factors to nuclear foci after DNA damage. Curr Biol. *10(15)*, 886-95.

Popovic, R., Zeleznik-Le, N.J. (2005). MLL: how complex does it get? J. Cell Biochem. *95(2)*:234-42.

Richardson, C., Jasin, M. (2000). Frequent chromosomal translocations induced by DNA double-strand breaks. Nature. *405(6787)*, 697-700.

Rogakou, E.P., Boon, C., Redon, C., and Bonner, W.M. (1999). Megabase chromatin domains involved in DNA double-strand breaks in vivo. J. Cell Biol. *146*, 905-915.

Rosso, A., Balsamo, A., Gambino, R., Dentelli, P., Falcioni, R., Cassader, M., Pegoraro, L., Pagano, G., Brizzi, M.F. (2006). p53 Mediates the accelerated onset of senescence of endothelial progenitor cells in diabetes. J Biol Chem. *281(7)*, 4339-47.

Rothkamm, K., Löbrich, M. (2003). Evidence for a lack of DNA double-strand break repair in human cells exposed to very low x-ray doses. Proc. Natl. Acad. Sci. U. S. A. *100(9)*, 5057-62.

Ruthenburg, A.J., Allis, D., Wysocka, J. (2007). Methylation of Lysine 4 on Histone H3: Intricacy of Writing and Reading a Single Epigenetic Mark. Molecular Cell. *25(1)*, 15-30.

Sancar, A., Lindsey-Boltz, L.A., Unsal-Kaçmaz, K., Linn, S. (2004). Molecular mechanisms of mammalian DNA repair and the DNA damage checkpoints. Annu. Rev. Biochem. *73*, 39-85.

Scharf, S., Zech, J., Bursen, A., Schraets, D., Oliver, P.L., Kliem, S., Pfitzner, E., Gillert, E., Dingermann, T., Marschalek, R. (2007) Transcription linked to recombination: a gene-internal promoter coincides with the recombination hot spot II of the human MLL gene. Oncogene. *26(10)*,1361-71.

Schoeftner, S., Blasco, M.A. (2007). Developmentally regulated transcription of mammalian telomeres by DNA-dependent RNA polymerase II. Nat Cell Biol. *10(2)*, 228-36.

Skorski T. (2002). Oncogenic tyrosine kinases and the DNA-damage response. Nat Rev Cancer. *2(5)*, 351-60.

Stanulla, M., Wang, J., Chervinsky, D.S., Thandla, S., Aplan, P.D. (1997). DNA cleavage within the MLL breakpoint cluster region is a specific event which occurs as part of higher-order chromatin fragmentation during the initial stages of apoptosis. Mol. Cell. Biol. *17(7)*, 4070-4079.

Sung, P.A., Libura, J., Richardson, C. (2006). Etoposide and illegitimate DNA double-strand break repair in the generation of MLL translocations: New insights and new questions. DNA repair. *5(9-10)*, 1109-1118.

Takeda, S., Chen, D.Y., Westergard, T.D., Fisher, J.K., Rubens, J.A., Sasagawa, S., Kan, J.T., Korsmeyer, S.J., Cheng, E.H., Hsieh, J.J. (2006). Proteolysis of MLL family proteins is essential for taspase1-orchestrated cell cycle progression. Genes Dev. *20(17)*, 2397-409.

Tyagi, S., Chabes,A.L., Wysocka, J., Herr, W. (2007). E2F Activation of S Phase Promoters via Association with HCF-1 and the MLL Family of Histone H3K4 Methyltransferases. Cell Molecular Cell. *27(1)*, 107-119.

Viscardi, V., Clerici, M., Cartagena-Lirola, H., Longhese, M.P. (2005). Telomeres and DNA damage checkpoints. Biochimie. *87(7)*, 613-24.

Wiederschain, D., Kawai, H., Gu, J., Shilatifard, A., Yuan, Z.M. (2003). Molecular basis of p53 functional inactivation by the leukemic protein MLL-ELL. Mol Cell Biol. *23(12)*:4230-46.

Wiederschain, D., Kawai, H., Shilatifard, A., Yuan, Z.M. (2005). Multiple mixed lineage leukemia (MLL) fusion proteins suppress p53-mediated response to DNA damage. J Biol Chem. 280(26), 24315-21.

Xia, Z.B., Popovic, R., Chen, J., Theisler, C., Stuart, T., Santillan, D.A., Erfurth, F., Diaz, M.O., Zeleznik-Le, N.J. (2005). The MLL fusion gene, MLL-AF4, regulates cyclin-dependent kinase inhibitor CDKN1B (p27kip1) expression. Proc. Natl. Acad. Sci. U. S. A. *102(39)*, 14028-33.

Yagi, H., Deguchi, K., Aono, A., Tani, Y., Kishimoto, T., Komori, T. (1998). Growth disturbance in fetal liver hematopoiesis of Mll-mutant mice. Blood. *92(1)*, 108-17.
Yu, B.D., Hanson, R.D., Hess, J.L., Horning, S.E., Korsmeyer, S.J. (1998). *MLL*, a mammalian trithorax-group gene, functions as a transcriptional maintenance factor in morphogenesis. Proc. Natl. Acad. Sci. U. S. A. *95(18)*, 10632-6.

Yu, B.D., Hess, J.L., Horning, S.E., Brown, G.A., Korsmeyer, S.J. (1995). Altered Hox expression and segmental identity in *Mll*-mutant mice. Nature. *378(6556)*, 505-8.